8-2013

Discrete Geometric Based Stress Analysis of the Lumbar Soft Tissues From In Vivo Kinematics

Joseph W. Mitchell
jmitch24@utk.edu

To the Graduate Council:

I am submitting herewith a dissertation written by Joseph W. Mitchell entitled "Discrete Geometric Based Stress Analysis of the Lumbar Soft Tissues From In Vivo Kinematics." I have examined the final electronic copy of this dissertation for form and content and recommend that it be accepted in partial fulfillment of the requirements for the degree of Doctor of Philosophy, with a major in Biomedical Engineering.

Mohamed R. Mahfouz, Major Professor

We have read this dissertation and recommend its acceptance:

Richard D. Komistek, William R. Hamel, Aly E. Fathy, Adrija Sharma

Accepted for the Council:

Carolyn R. Hodges

Vice Provost and Dean of the Graduate School

(Original signatures are on file with official student records.)

Discrete Geometric Based Stress Analysis of the Lumbar Soft Tissues from In Vivo Kinematics

A Dissertation Presented for the

Doctor of Philosophy

Degree

The University of Tennessee, Knoxville

Joseph W. Mitchell

August 2013

To my friends and family without whom I would not have been able to make it this far

Acknowledgements

First I would like to thank my advisor Dr. Mohamed Mahfouz for allowing me the opportunity to pursue my goals and be able to work in an orthopedic research lab. He provided me the chance to work on this NIH grant as well as gave me opportunities to provide help for others in many different areas of orthopedic research. His foresight and willingness to take risks within the context of his research provided for an incredible working and learning environment. Next I would like to thank Dr. Richard Komistek and Dr. Adrija Sharma for all their expertise and insight during the NIH grant process as well as my dissertation. Also thank you to Dr. William Hamel and Dr. Aly Fathy for agreeing to be on my committee and their support and patience during my time as a candidate. From Vanderbilt I would like to thank Dr. Joseph Cheng and Christy Hagewood for their time and patience during data collection phase.

To my fellow graduate student, I would like to thank Chris Carr for his work alongside me during the NIH grant and for agreeing to drive most times to and from Nashville. Next I would like to thank Dr. Emam Fatah for providing me with the surface models and allowing me to use the lumbar atlas in my work. Gary To thank you for your words of wisdom, always helping me with adobe, and being an overall great friend. Thank you to Rebecca Robertson, Lyndsay Bowers, Sumesh Zingde, Dr. Filip Leszko, Hatem El Dakhakhni, Nicholas Battaglia, Michael Johnson, and anyone else not mentioned for their support over the past few years.

Finally, I would like to thank my mom and dad, Renee and Raymond, as well as my sister, Aimee, for their support, encouragements, and affording me the opportunities I have had in life. I would like to thank my girlfriend, Stephanie, for putting her life on hold to spend time with me in Knoxville, and supporting me over the last few years especially through the last few grueling months.

Abstract

Back pain in the region of the lumbar spine has become an increasingly significant problem among individuals in the United States and is a leading cause of disability and missed work days. At present, efforts focused on treating both the symptoms and causes of low back pain have proven to be difficult, and researchers and clinicians still do not fully understand the most effective means for treating the symptoms. Utilizing a biomechanics approach, it is assumed that lower back pain is, at least in part, associated with an increased localized stress.

Current models used to determine stresses are typically based from a spine simulator data where pre-prescribed motion or forces are used; however, this does not allow for patient specific motions. The muscles in the back responsible for the motion or force are either neglected due to imputed forces or optimized out with the input of motion. The objective of this study was to determine the stresses in the intervertebral discs using the 3D motion with computed tomography bone models. This allows for patient specific stress to be calculated using material properties of the disc and the motion of the disc space. Furthermore, motion of the vertebra during this in vivo motion will allow for stress calculations of the ligaments as well. The materials prescribed to the soft tissues will be a combination of existing techniques in order to represent the tissue as close to how it actually is. From these stress results, correlations can be made between the different groups collected: normal, low back pain, degenerative, and surgical patients. This will hopefully provide insight into why people have low back pain without sign of degeneration, how degenerative discs effect stress, and if stress is higher at the adjacent disc after surgery.

Table of Contents

List of Tables

List of Figures

List of Attachments

1. SectionedStress.xlsx - The average stress and average changes from neutral for all groups within the nine sections of the intervertebral disc.

Chapter 1. Background and Significance

Back pain is a serious problem that costs Americans billions in medical bills, disability, and loses of productivity. The lumbar spine is attributed with providing the location for the most debilitating pain. The estimated cost in terms of treatments and missed work days is billions of dollars annually[1-7]. The U.S. spine market was a $3.3 billion business in 2005 with a compounded annual growth rate at 19%. This makes the spine the fastest growing area in the orthopedic market. Patient demographics are fueling dramatic market growth. Fourteen million Americans suffer from spinal stenosis, facet arthritis and spondylolisthesis. Spondylolisthesis may not cause any symptoms for years after disc slippage has occurred, but the symptoms include low back and buttocks pain, numbness, muscle tightness or weakness in the leg, increased sway back, or a limp. Once symptoms begin, patients usually have constant low grade back discomfort that is aggravated by standing, walking and other activities, while rest will provide temporary relief[8]. At present, it is difficult to treat both the symptoms and the causes of lower back pain, and effective means of treating the symptoms are not fully understood by researchers and clinicians.

1.1. Soft Tissue Structure and Function

The lumbar spine consists of five lumbar vertebral bodies, the sacrum, and the coccyx. The vertebrae provide the anterior support and structure of the spine. Each vertebra is connected to each adjacent vertebral body by three joints, one anterior (vertebral disc) and two posterior (facet joints). The soft tissues associated with the lumbar spine are the intervertebral discs, the facet joint capsules, ligaments, and muscles. The roles of the spine are to support weight, maintain balance, control movement, counter the numerous daily strains that are exerted on it during normal

recreational and working activities, and to protect the neural elements[9]. Although the local movement at a single motion segment is limited, considerable global motion can be achieved since the motion segments are stacked one on top of another.

1.1.1 Intervertebral Disc

The intervertebral disc consists of the nucleus pulpous, the annulus fibrosus, and the hyaline cartilage endplates. The nucleus pulpous is surrounded by the annulus fibrosus which both are sandwiched inferiorly and superiorly between the two hyaline cartilage endplates (Fig. 1). The intervertebral disc functions as a shock absorber for the compressive forces as well as to maintain the area between vertebral bodies which provides flexibility. The amplitude of motion between adjacent vertebrae is partially determined by the disc thickness[10]. The fibrosus tissue of the disc can accommodate the flexibility needed for the motion; however, the tissue reacts poorly to compressive forces. This limitation is partially eliminated by the presence of the hydraulic zone within the disc. The volume of the area must stay constant which transfers the pressure to the fibrous walls[11]. Markolf and Morris[12] discovered that the concept of the nucleus pulpous as a rigid sphere maintaining the correct spacing is actually false. The entire disc is a self-stabilizing unit which absorbs the deformations in three directions and redistributed the strain in order to ensure stability.

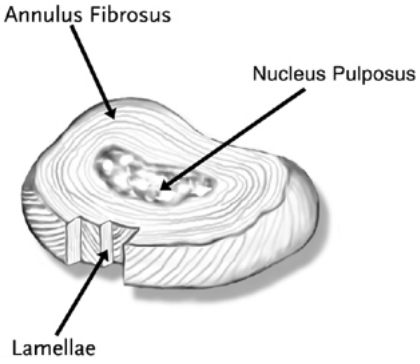

Figure 1. A diagram of a typical intervertebral disc[13]

1.1.1.1 Nucleus Pulpous (Nucleus)

The central zone of the intervertebral disc is a soft substance consisting of a heterogeneous structure composed of gylcosaminoglycans, collagen fibers, mineral salts, water and cellular elements. Early research noted that at early stages of life the water content is 80-88% with that amount dropping to 70% near the age of 40[14, 15]. The loss of water content continues with age. Furthermore within a shorter time scale, the water content changes over the course of the day with the disc thicker in the morning.

1.1.1.2 Annulus Fibrosus (Annulus)

The outer region is a series of fibrocartilage bands which surround the nucleus pulpous. The geometry varies with vertebral level and intradiscal region. The directional alignment of the bands of collagen fibers in each layer of the annulus alternate in subsequent bands. Generally, the fibers lie at about 30° to the horizontal, but the angle may be as high as 70° at some locations[16,17]. The amount of collagen fibers also varies radially with the outer layers having a higher concentration which lessens the closer the band is to the nucleus pulpous[18].

1.1.2 Ligaments

Ligaments in the spine connect one vertebra to another. The composition of ligaments is that 60% of the content is water. The remaining material is collagen fibrils, elastin, and proteoglycan. The collagen fibrils are arranged into crimped fibers. The ligaments in the spine are there to aid in joint stability. They provide this stability when nonhabitual functional loads are encountered during normal range of motion activities[19]. In the lumbar spine there are six ligaments which are: anterior longitudinal ligament, posterior longitudinal ligament, intertransverse ligament, supraspinous ligament, interspinous ligament, and ligamentum flavum (Fig. 2). The anterior longitudinal ligament and the posterior ligament are the two primary spine stabilizers. The ligamentum flavum is the strongest ligament with its main task to protect the spinal cord.

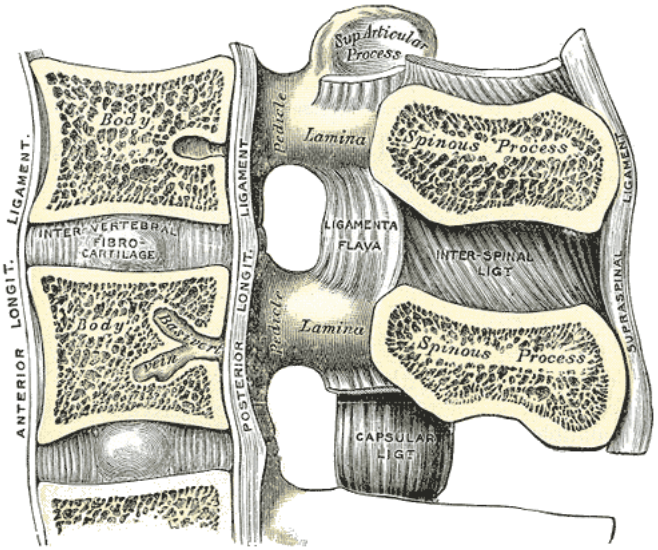

Figure 2. Diagram of some of the major ligaments in the lumbar spine[13].

1.1.3 Muscles

Muscle is the largest tissue amount in the body with over 700 muscles in the human body making up to 50% of the body weight. The muscles which the body uses for motion and control are done so with voluntary contractions. A single muscle consists of a collection of muscles cells, connective tissue, nerves, and blood vessels. In this study three of the muscles were chosen for their ability to be viewed within the MRI as well as their functional influence on the motion activities researched. These muscles are the psoas major, the multifidus, and the erector spinae (Fig. 3).

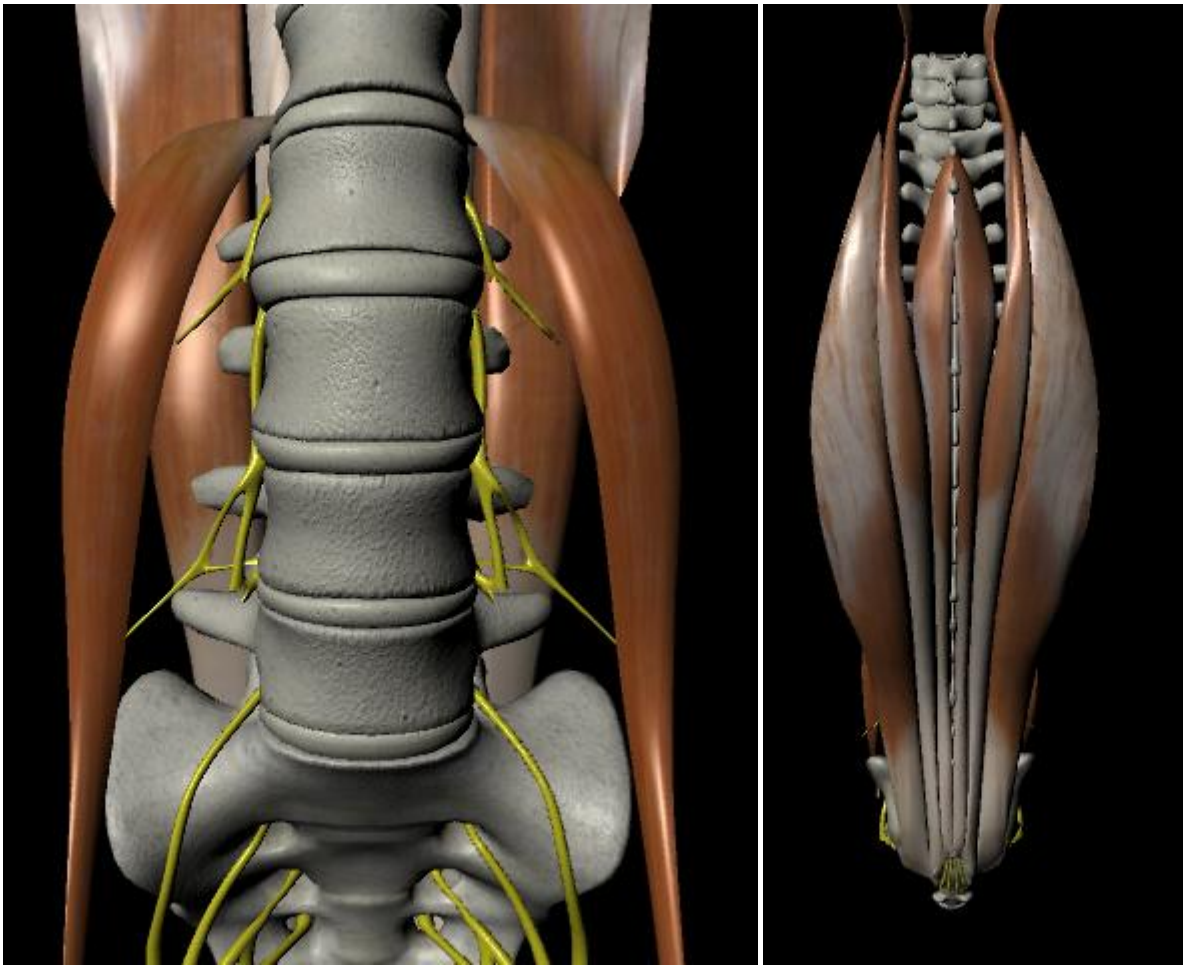

Figure 3. Generic model of the muscles of the spine highlighting the muscles for this study.

1.1.3.1 *Psoas Major*

The psoas major is a long fusiform muscle which occurs from the transverse processes of the vertebral bodies, the vertebral bodies, and intervertebral discs from T12 to L5. The psoas major then inserts on the femur. While it is well known that the psoas major is a primary flexor for the hip joint, there is conflicting studies of its influence on the motion of the spine. Bogduk et al.[20] studied the effect of psoas major on the spine and concluded it had no substantial role as a flexor or extensor of the spine. They also noted it would not be suitable as a lateral flexor either. This is disputed by Farfan[21] and Anderson et al.[22] whom both concluded the psoas major was ideal for lateral flexion of the spine. Gracovestky[23, 24] and Penning[25] both concluded that the role of the psoas major was to act as a controller used to stabilize the spine posture.

1.1.3.2 Multifidus

The multifidus muscle consists of a number of fleshy and tendinous fasciculi which fill the grooves of the spinous processes of the vertebrae and spans from the sacrum to the axis. In the lumbar region there a 5 separate bands emanating from each spinous process spreading caudally and laterally[26]. Gray[13] noted they are capable of producing extension, lateral flexion, and rotation. Several electromyography studies done concluded the multifidus play a role in intersegmental motion with one study concluding the individual muscles of the multifidus act more as stabilizers.

1.1.3.3 Erector Spinae

The erector spinae is not just one muscle, but a bundle of muscles and tendons. The erector spinae occurs from the anterior surface of the erector spinae aponeurosis. It extends throughout the lumbar, thoracic and cervical regions, and lies in the groove to the side of the vertebral column. It is covered in the lumbar region by the thoracolumbar fascia. In the lumbar region, this muscle is large,

and forms a thick fleshy mass which, on being followed upward, is subdivided into three columns: spinalis, longissimus, and the iliocostalis. These gradually diminish in size as they ascend to be inserted into the vertebrae and ribs (Fig. 4). The erector spinae function as an extensor for the vertebral column while also working as a lateral flexion mover if they are unilaterally contracted. They also work in conjunction with the multifidus to resist the flexion effect of the abdominal muscles [27].

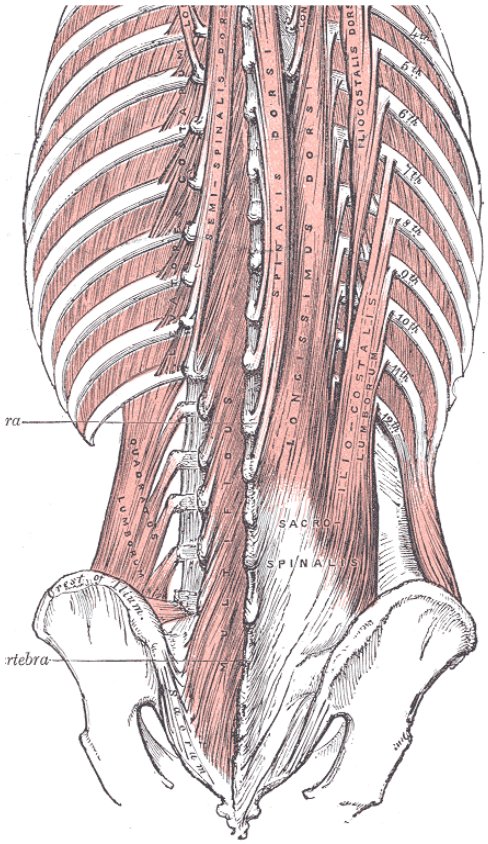

Figure 4. Diagram of the erector spinae muscle as it breaks into 3 branches[13].

1.2. In Vivo and In Vitro Testing

While in vivo testing is the gold standard, when working with human subjects the testing may be too invasive and most of the time in vitro tests are the only possibility. Within vitro testing of human tissues one of the large questions is whether or not any negative effects exist from freezing and storage of the cadaver spines. Panjabi et al.[28] studied the changes in the biomechanical properties of fresh cadaveric spinal specimens due to long-term freeze storage and long test periods. Fresh cadaveric specimens were divided into three groups: Group A specimens were tested fresh on the 1st day and 13 subsequent days; Group B specimens were tested on the 1st day, frozen in sealed bags at - 18°C for21 days, and tested for 13 consecutive days after thawing; and Group C specimens were frozen for up to 232 days and tested for 14 consecutive days after thawing. No significant differences in response were found in any of the three groups. The only major factor ever discovered was by Galante[29] who stated the need to prepare and test specimens in an atmosphere of 100% relative humidity.

1.2.1 Intervertebral Disc

In 1960's and 70's Nachemson et al.[30-33] studied the pressure in the lumbar spine using a needle-based transducer. The design consisted of a 1.1 mm diameter needle with a sealed end and a small opening on the side. The needle was filled with water and polyethylene was used as a diaphragm. This was connected to electromanometer (Fig. 5). Nachemson performed this both in vitro on cadavers and in vivo on volunteers. The in vitro tests were performed to develop the pressure transducer and the relationship between compression and intradiscal pressure. For the in vivo studies the volunteers had the device was inserted into the L3 or L4 intervertebral disc, and volunteers were asked to perform various tasks. Nachemson reported that there was a proportional

relationship of force to intradiscal pressure. That the pressures in the disc were 1.5 times the vertical load applied per unit area.

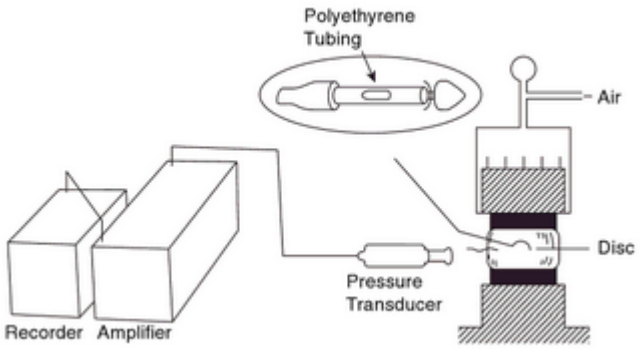

Figure 5. Diagram of Nachemson's intradiscal pressure testing apparatus[30].

Since Nachemson there have been other in vitro studies such as Cunningham et al.[34] studied spinal stability versus intradiscal pressure with their pressure needle transducer. They tested under four conditions of spinal stability: intact, destabilized, laminar hook and pedicle screw reconstructions. In response to destabilization and instrumentation, proximal disc pressures increased as much as 45%, and operative pressure levels decreased 41-55% depending on the instrumentation technique. McNally et al.[35, 36] created a needle-based device with a strain gauge on the end in order to determine the intradiscal pressure. This group further extended the research to examine the stress profiles between normal and degenerative discs in vivo. The stress profiles were found by removing the needle at a controlled rate. They found that age-related degenerative were greater at L4/L5 than at L2/L3, and the posterior annulus was affected more than the anterior. Degeneration reduced the diameter of the central hydrostatic region of each disc by approximately 50%, and the pressure within this region fell by 30%. The width of the functional annulus was increased by 80% and the height of compressive stress peaks within it by 160%. More recently Wilke et al.[37, 38] used a pressure transducer in vivo to corroborate with Nachemson's results. This study measured the results from one volunteer over the course of 24 hours. The pressure for lying prone was 0.1 MPa, standing was 0.5 MPa, flexed forward was 1.1 MPa, flexed backwards was 0.6 MPa, maximum during lateral bending was 0.6 MPa, and maximum during axial rotation was 0.7 MPa. The volunteer preformed many of the same activities and good correlation was found between the two studies[30, 37] (Fig. 6).

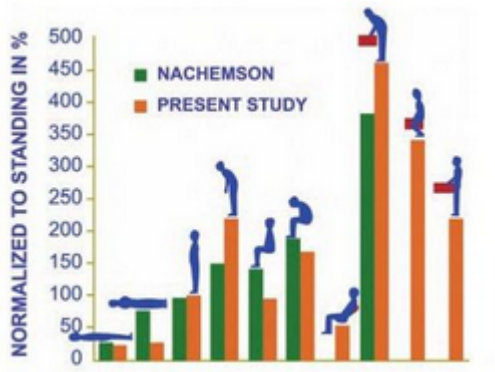

Figure 6. Comparison of disc pressure from Wilke to research conducted by Nachemson[37].

The tensile properties of the disc have also been studied to determine the biomechanical properties of the annulus fibers. Green et al.[39] did one such study where the one functional spinal unit was cut into an anterior and a posterior slice. The vertical slices were 5mm in width and 15 mm in length. The bony ends of the spinal unit were mounted onto a hydraulic testing machine. Specimens were stretched vertically using a linear ramped force. This studied determined estimated in situ strength in the vertical direction was 3.9 MPa for the anterior annulus and 8.6 MPa for the posterior annulus. Furthermore, fatigue failure can occur in less than 10,000 cycles if the tensile force on the annulus exceeds 45% of the ultimate tensile strength. It was also found that annulus stretches around 2mm before starting to oppose the tension. This was attributed to the crinkle effect of the fibers.

While compression and tensile tests are quite common shear tests have also been completed on the disc. Iatridis et al.[40-42] has published multiple shear tests. The first test was on the nucleus, testing it for torsional shear in a mechanical spectrometer. Under their dynamic conditions, the nucleus pulposus exhibited predominantly 'solid-like' behavior with values for dynamic modulus, (G*), ranging from 7 to 20 kPa. The group furthered there shear testing by also studying the annulus. They concluded that the annulus fibrosus material was less stiff and more dissipative at larger shear

strain amplitudes, stiffer at higher frequencies of oscillation, and stiffer and less dissipative at larger axial compressive stresses. The dynamic shear modulus, (G*), had values ranging from 100 to 400 kPa, depending on the experimental condition and degenerative level.

1.2.2 Ligaments

In vitro testing of the ligaments by Pintar et al.[43] was done to determine the biomechanical properties of the six major lumbar ligaments. This study is one of the few which broke the ligaments into not on type but lumbar level. For this study 132 samples were collected and tested. Table 1 provides the stiffness of the ligaments, the stress at failure, and the strain at failure for all six ligaments at the various levels of the lumbar. These values provide more realistic and consistent input for modeling. For most ligaments in the body, there exists an in situ tensile strain which is evident by the immediate retraction observed when the ligament is cut. Within the lumbar spine there is disagreement as to whether or not in situ strain does or does not exist[44, 45]. From the literature it appears the strain is relatively small and in most simulations it is ignored.

Table 1. Biomechanical parameters of the human lumbar ligaments [43]

Parameter	Ligament	L1 -- L2	L2--L3	L3--L4	L4--L5
Stiffness (N/mm)	**ALL**	32.4 ± 13.0	20.8 ± 14.0	39.5 ± 20.3	40.5 ± 14.3
	PLL	17.1 ± 9.6	36.6 ± 15.2	10.6 ± 8.5	25.8 ± 15.8
	JC	42.5 ± 0.8	33.9 ± 19.2	32.3 ± 3.3	30.6 ± 1.5
	LF	23.0 ± 7.8	25.1 ± 10.9	34.5 ± 6.2	27.2 ± 12.2
	ISL	10.0 ± 5.0	9.6 ± 4.8	18.1 ± 15.9	8.7 ± 6.5
	SSL	23.0 ± 17.3	24.8 ± 14.5	34.8 ± 11.7	18.0 ± 6.9
Stress at Failure (MPa)	**ALL**	13.4 ± 3.9	16.1 ± 6.2	12.8 ± 7.0	15.8 ± 1.9
	PLL	11.5 ± 10.0	28.4 ± 11.3	12.2 ± 1.9	20.6 ± 7.3
	JC	10.3 ± 2.9	14.4 ± 1.4	7.7 ± 1.6	3.5 ± 1.2
	LF	2.5 ± 0.8	1.3 ± 0.4	2.9 ± 1.7	2.9 ± 1.4
	ISL	5.9 ± 1.8	1.8 ± 0.1	1.8 ± 0.3	2.9 ± 1.9
	SSL	15.5 ± 5.1	9.9 ± 5.8	12.6 ± 7.1	12.7 ± 7.1
Strain at Failure (%)	**ALL**	44.0 ± 23.7	49.0 ± 31.7	32.8 ± 23.5	44.7 ± 27.4
	PLL	15.7 ± 7.4	11.3 ± 0.2	15.8 ± 3.7	12.7 ± 6.3
	JC	90.4 ± 17.7	70.0 ± 27.5	52.7 ± 7.2	47.9 ± 5.4
	LF	78.6 ± 6.7	28.8 ± 8.2	70.6 ± 13.6	102.0 ± 12.9
	ISL	119.7 ± 14.7	51.5 ± 2.9	96.5 ± 35.8	87.4 ± 6.7
	SSL	83.4 ± 21.4	70.6 ± 45.0	109.4 ± 2.5	106.3 ± 9.7

1.2.3 Muscles

While the testing of ligaments can be done in vitro, the muscles are not studied this way. Typical studies will report physiological changes in muscles. Belavy et al.[46] studied the effects of bed rest on the lumbar. The cross-sectional areas of all muscles changed with the rate of atrophy greatest for multifidus at L4/L5 and in the erector spinae at L1/L2. Atrophy of the quadratus lumborum was consistent throughout the muscle, but cross-sectional area of psoas muscle increased. Subjects who reported LBP after bed-rest showed greater increases in posterior disc height, and greater losses of multifidus cross-sectional area at L4 and L5 than subjects who did not report pain. Lifting exercise research has shown that in volunteers with low back pain their erector spinae activated for longer periods of time than normal volunteers[47]. A study done on cyclists explained that subjects with pain experienced a loss of co-contraction of the lower lumbar multifidus [48]. Other mathematical models

have been created to simulate muscle forces on the lumbar; however the results are highly reliant on the line of action of the muscle[49].

1.3. Spine Disorders: Intervertebral Disc Degeneration

The lumbar spine is a highly complex system which relies on a large number of interactions to function. Age, trauma, spinal disorders, or other parameters can negatively impact this system. Although the spine has a tremendous ability to withstand most mechanical stresses, failure of some tissues can occur. Degeneration in the intervertebral disc is a broad term used to describe the biomechanical changes that happen to the disc's properties. Once the disc begins to degenerate, the composition of the tissue begins to change. There is a structural disorganization of the disc with the loss in proteogylcans which in turn causes failure in the hydrostatic mechanism. Degeneration can occur in the nucleus or annulus, and depending on where it does occur, different issues will lead to pain.

A degenerated annulus can result in microscopic fragmentations of annulus fibers called fissures. Annular tears may result at the corners separating the annulus from the endplates. Furthermore, concentric cracks, cavities, and radiating ruptures can occur. Videman and Nurminen[50] found that annular tears risk increases with age and were almost unavoidable at 65+. Finally a decrease in radial tensile strength of the annulus may result in disc bulging. A degenerated nucleus will result in loss of water content. As the nucleus losses water collagenation occurs in the nucleus. This will result in the nucleus becoming stiffer thus increasing the elastic modulus. At a point the nucleus material property will react similar to the annulus. If the entire disc degenerates, disc herniation into the spinal canal is highly likely. This will result in low back pain due to pinched nerves.

Diagnosis of degenerative disc disease shows one of the issues as disc space narrowing which has been shown to be an indicator for pain[51]. This narrows the space between adjacent segments and increases the loading of the facet joint causing impingement[52]. Spinal stenosis is a possibility as the disc space is narrowed. The Thompson grading scale[53] is a five-category grading scheme for accessing the gross morphology of the intervertebral disc. While this method does provide a decent amount of information the grading is subject to observer error. The agreement between the assigned and average grades was 85, 92, 68, 90, and 76% for Grades I through V.

1.4. Treatment: Fusion

While hip and knee joint replacement surgery or anthroplasty has grown increasingly common with a high degree of patient satisfaction, spine anthroplasty (or artificial disc replacement) has not been a viable option in the U.S. The current strategy to tackle the problem of low back pain is mechanical treatments and has made spinal fusion the most common treatment of severe degeneration of the spine in the United States[1, 8]. A fusion is performed to prevent or correct a deformity, to stabilize the spine, or to relieve chronic pain[54]. The spinal disc or discs between the vertebrae levels are removed and the adjacent vertebrae are fused using donor bone grafts or bone grafts from the patient's hip. Metal devices secured by screws are sometimes used for better fixation of the fused vertebrae[55]. Spinal fusion results in some loss of flexibility and range of motion in the spine and requires a long recovery period to allow the bone grafts to grow and fuse the vertebrae together. This may cause further problems to develop at other levels, thereby increasing the chances of additional back surgery[55-57]. Spinal fusion is therefore more of a treatment for current pain and does not stop the progression of degeneration in the spine.

1.4.1 Adjacent Segment Degeneration

Many long term clinical studies have been conducted to reveal that while patients acquire adjacent segment degeneration, there was no clinical correlation. Lehmann et al.[58] studied 32 patients over a 30 year period. Nearly half of the patients developed instability at the segment superiorly adjacent, but there was no clinical correlation between the patients. Luk et al.[59] found that hypermobility at the adjacent level increased with follow-up time; however the mobility did not correlate with the clinical symptoms. Penta et al.[60] conducted a 10 year study where two similar groups of patients were compared. One group received a fusion and the other group received a different treatment. They concluded that there was no significant difference in rates of adjacent segment disease with approximately one-third of patients developed degeneration at the adjacent levels. While clinical follow-up haven't shown correlation, stress analysis has been conducted on simulated spinal fusions which report that the adjacent levels has an increased intradiscal pressures which increases with the number of levels fused [61].

1.5. Treatment: Motion Preserving

While fusions are the most common type of treatment for degenerative discs one of the major downfalls is that as discussed above that it removes all motion from the affected area and may cause adjacent issues in other discs. Total disc replacement (TDR) surgery has been a relatively new and active place for orthopedic companies to develop a device which will restore pain free motion. One of the driving reasons for this technology is the treatment of younger patients and their dissatisfaction of fusion. One of the first major issues with this technique is the long list of contraindications which would cause patients to not be suitable for the surgery. Huang et al.[62] found that out of 100 candidates receiving fusion and non-fusion spine surgery only 5% would meet the

strict inclusion/exclusion requirements. The study also noted that 100% of the fusion candidates had at least one contraindication which leads them to conclude that TDR would not eliminate the need for fusions. One of the pioneering artificial disc replacements was the Charité artificial disc which was designed at the Center of Musculoskeletal Surgery at the Medical University of Berlin. However in the United States this disc did not demonstrate, in the short-term, a clear superiority over an anterior lumbar interbody fusion with a standalone cage during the IDE trial[63]. With limited data demonstrating cost effectiveness of the Charité over fusions, insurance companies and Medicare and Medicaid have stopped authorizing or reimbursing for the procedure in the United States[64].

Another motion preserving technologies to come out is the Scient'x rod. Currently in the United States this technology may be used as an adjunct to fusions. The dynamic rod allows decompression of the stenotic motion segment and controlled movement of the functional spine unit, simultaneously unloading and protecting it from excessive forces or motion. In a ten year follow-up study, clinical outcomes all showed improves and radiographic results were all good as well with no loss in adjacent disc height[65]. While the company does provide supporting clinical support no in vivo kinematic studies could be found. A finite element model by Castellvi et al.[66] did show however the reduced-stiffness component of the dynamic instrumentation was associated with a 1% to 2% reduction in peak compressive stresses in the adjacent-level disc, and the increased axial motion component of this instrumentation reduced peak disc stress by 8% to 9%. They concluded that cumulative effect of this stress reduction over many cycles may be substantial in alleviating the problem of adjacent disc degeneration.

1.6. Deformable Modeling

Deformable models are typically broken in to broad categories. Interactive models have speed and low latency with physical accuracy secondary. Typical examples include mass-spring models and spline surfaces used as deformable models. Physical models start with the constitutive laws of the material and solve the resulting boundary value PDE's numerically using, for instance, Finite Element Method (FEM). To date, all research for the deformation in the lumbar spine has been completed using the finite element technique. Interactive models have a long history in computer graphics but have some uses in modeling of the human body.

1.6.1 Finite Element Modeling

Three dimensional finite element models of the spine have been created to simulate the response to various loading conditions. Current modeling techniques fall into four categories: linear elastic, non-linear elastic, viscoelastic, and poroelastic. Computed tomography images are used to create three dimensional models of the vertebrae and intervertebral discs. For computational purposes the intervertebral disc is separated into the nucleus and the annulus. In all types of models the annulus collagen fibers and ligaments are modeled as tension only cable elements with either linear or non-linear elastic properties. The location of the ligaments is not subject specific but rather locations as well as geometry will be taken from literature. Forces are applied to model so all muscles are neglected.

1.6.1.1 *Linear Elastic Modeling*

In linear elastic models stress, σ, acting on the nucleus pulposus and annulus fibrosus is linearly proportional to the strain, ε, by the Young's Modulus, E, of the various materials. For small-strain simulations of a single vertebral body this method may be appropriate. Recently Tsouknidas et

al.[67] introduced a linear elastic model which has various layers of annulus fibrosus which demonstrates the varying properties of an in vivo disc (Fig. 7). Validation was done to show that the range of motion for the segment as the moment was increased followed reported data from Panjabi and White[68].

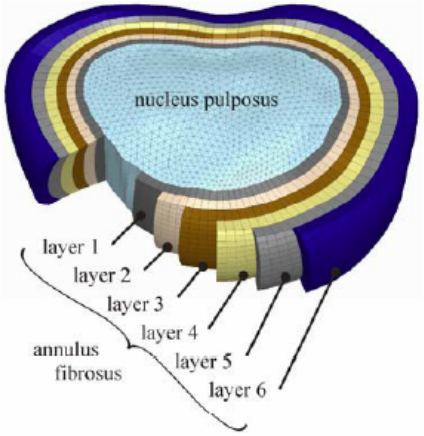

Figure 7. Intervertebral disc model with the six layers for the annulus used by Tsouknidas et al.

1.6.1.2 *Non-Linear Elastic Modeling*

Non-linear models are required when doing multisegmental simulations. In non-linear models such as Remner et al[69], the annulus fibrosus is described by a Mooney-Rivlin hyperelastic model where stress, σ, is based on constants C_{pq} which are material constants related to the distortional response and D_m are material constants related to the volumetric response. For their model a moment was applied with or without a preloading force. The results were compared with a cadaveric simulation testing apparatus results which were subjected to the same conditions. In vitro disc height ranged from 1.2 ± 0.3 mm to 1.6 ± 0.5 mm while the FEM varied from 1.4 to 2.0 mm which is within one standard deviation. Furthermore, the range of motion tests also compared well between the two models.

1.6.1.3 *Viscoelastic Modeling*

Lu et al.[70] created a model in which the annulus fibers and all ligaments were modeled as viscoelastic. The diurnal fluid change was modeled by reducing water content of the nucleus. Combined with bending and twisting, a compressive load was applied at different loading rates. Their model was able to determine that the maximum tensile stress in the annulus fibers always occurred in the fibers at the inner posterior annulus at the junction of the disc and the endplate. Of the three models tested, the first to fail was the saturated disc subjected to compression and bending and twisting. An increasing compressive load applied to a flexed, twisted, and saturated disc resulted in progressive failure, or fissure propagation, starting at the posterior inner annulus at the junction of the disc and the endplate. The key factors involved in the initiation and propagation of annulus failure were axial compressive load, bending and twisting, and disc saturation. Annulus failure was harder to achieve if one factor was absent.

1.6.1.4 *Poroelastic Modeling*

Poroelastic models were created to understand disc biomechanics under complex loading conditions. These models will include strain-dependent permeability and osmotic potential. The poroelastic model created by Natarajan et al.[71] also modeled the regional differences of the disc. For their study three activities were performed on the model: 1) Lift involving trunk flexion-extension 2) Lift involving axial rotation 3) Lift involving lateral bending. There results were that the highest von Mises of 4.5 MPa for task 1, 3.0 MPa for task 2, and 6.5 MPa for task 3. The analyses also showed that largest fluid exchange between the nucleus and the end plates occurred during asymmetric lifting. They hypothesize that if the fluid exchange is restricted due to end plate calcification or sclerosis of the subchondral bone, high intradiscal pressure might develop, leading to higher disc bulge causing back pain.

1.6.1.5 *Treatment Modeling*

One advantage to the finite element modeling technique is the ability to make quick changes to determine the outcome on that specific model. Typically, groups will create and validate a model for a "normal" case. By varying material properties, boundary conditions, and constraints that model is able to be tested on degenerative effects or changed to act as an instrumented lumbar spine. Chen et al.[72] simulated fusion in their model by removing the disc for a bone graft material. They studied the effect different fusions had on the stress of the adjacent disc both superiorly and inferiorly. They concluded that stress was highest with fusion at a lower site or with multilevel fusions under flexion, torsion and lateral bending. Larger stress increase was estimated at the superior disc adjacent to fusion; however the superior disc adjacent to fusion had a little alteration under torsion. For dynamic stabilization of the A finite element model by Castellvi et al.[66] did show however the reduced-stiffness

component of the dynamic instrumentation was associated with a 1% to 2% reduction in peak compressive stresses in the adjacent-level disc, and the increased axial motion component of this instrumentation reduced peak disc stress by 8% to 9%. They concluded that cumulative effect of this stress reduction over many cycles may be substantial in alleviating the problem of adjacent disc degeneration.

1.7. Fundamental Contributions

The specific original contribution of this dissertation to the medical field is the ability to determine in vivo intervertebral stresses for the lumbar spine:

- Creation of a multibody discrete stress analysis model for the intervertebral discs of the lumbar spine from in vivo kinematics with the inclusion of patient specific models.
- Overall determination of in vivo disc stress for normal, low back pain, degenerative, and surgical patients. Including in vivo stress analysis of adjacent segment stresses postoperatively
- Determining the stress change resulting from disc degeneration for in vivo subjects.
- Calculation of un-deformed disc heights in vivo which will allow for a neutral stress field of the disc. This would replace the generic preloading done in deformable models currently.

While the originality of the following items may not be new to deformable modeling, changing the way in which they are used:

- Improving ligament stress determination with patient specific geometry and motion.
- Creation of a discrete model to be used for the deformable modeling that is both fast and accurate for a biological system.

Chapter 2. Research Design and Methods

The purpose of this research is to provide a new fast and efficient stress model of the soft tissues during in vivo activities using the material properties, patient specific bone models, and the motion of the disc space taken from fluoroscopy in a discrete model. The soft tissues included in these calculations were the intervertebral discs and a preliminary study on some of the ligaments. The end goal was to provide a technique that can be used which is accurate like the finite element models with the increased speed provide by the discrete method that will provide overall better understanding of the lumbar soft tissue stresses during in vivo conditions.

Forty-four subjects participated in this study and were recruited from the patients and staff at Vanderbilt University and the University of Tennessee. All people participating in this study signed an informed consent which was obtained from the Institutional Review Board (IRB #7393). Four groups consisting of ten subjects each were defined as healthy, healthy with low back pain, degenerative and fusion. The remaining four subjects were two post-operative disc replacement, and two subjects with dynamic stabilization. Patient data can be found in Table 2. The healthy were asymptomatic subjects who had never been treated for low back pain and exhibited no limitation in daily activities. Furthermore, no radiological evidence of degeneration or defects was found. Healthy with low back pain group were healthy without radiological evidence of degeneration or defects in the lumbar spine but were symptomatic for acute low back pain. Of the subjects, eight were experiencing pain in the low back region at the time of evaluation. The degenerative subjects were determined to have one or more of the following conditions: Schmorl's Nodes, disc bulging both with and without canal or foraminal stenosis, disc osteophyte complexes, decreased height and fluid signal in the intervertebral disc, or facet hypertrophy. The degenerations were found at a single level for six of the subjects while

the rest experienced problems at multiple levels. This degeneration was determined to not be so severe as to require surgery. The ten subjects who were scheduled to receive a lumbar fusion with nine of the subjects also analyzed post-operatively. Most subjects received a fusion at either L5/S1 or L4/L5 spinal unit; however two patients did receive multilevel fusions. The subjects receiving the disc replacement were brought in from another study and were only able to obtain post-operatively with a follow-up time around 5 years. The dynamic stabilization group was also subjects from another study. This group received a scient`x rod at L4/L5 and a fusion at L5/S1 as required. Only two could tested, but both were imaged both pre and post-operatively.

Table 2. Study Subject Demographics

Group Classification	Subjects	Age (yrs)	Sex	Surgical Location	Postoperative Time (Months)
Healthy	10	40.8 ± 13.5	5 M 5 F	--	--
Low Back Pain	10	46.6 ± 9.7	5 M 5 F	--	--
Degenerative	10	40.1 ± 3.4	6 M 4 F	--	--
Pre-Operative Fusion	10	48.5 ± 10.3	6 M 4 F	--	--
Post-operative Fusion	9	49.1 ± 10.3	5 M 4 F	4 L4/L5 3 L5/S1 1 L3/L4, L4/L5 1 L4/L5, L5/S1	7.6
Post-operative Disc Replacement	2	49.64 ± 10.3	2 F	2 L5/S1	119.3
Pre-Operative Dynamical Stabilization	2	38.3 ± 4.6	2 M	--	--
Post-Operative Dynamical Stabilization	2	39.1 ± 4.6	2 M	2 -Scient`x Rod L4-L5 Fusion L5-S1	8.7

All subjects were analyzed with a high-frequency pulsated video fluoroscopy unit. The subject was positioned so the motion occurred on the sagittal plane as shown in Figure 8. Each subject was asked to perform a standing flexion-extension trial, an axial rotation trial, and a lateral bending trial while under fluoroscopic surveillance. For the flexion-extension activity all subjects began in a neutral standing position. They were then asked to flex to their maximum without moving at their hips, and then to travel back through neutral standing position into a maximum extension. The fluoroscopy was then positioned in the anterior-posterior plane for the lateral bending and axial rotation activities. The lateral bending activity also started in the neutral position. Subjects then flexed to their maximum left position before returning to the neutral and continuing to the maximum right position.

Finally the axial rotation again started in neutral position and subjects were asked to twist to their maximum left before returning to neutral and continuing to their maximum right position. During all activities, the subjects were asked to keep their hip from moving. The fluoroscopic video captured at a rate of 30 frames per second and was outputted to a camera in order to tape the motions for future analysis.

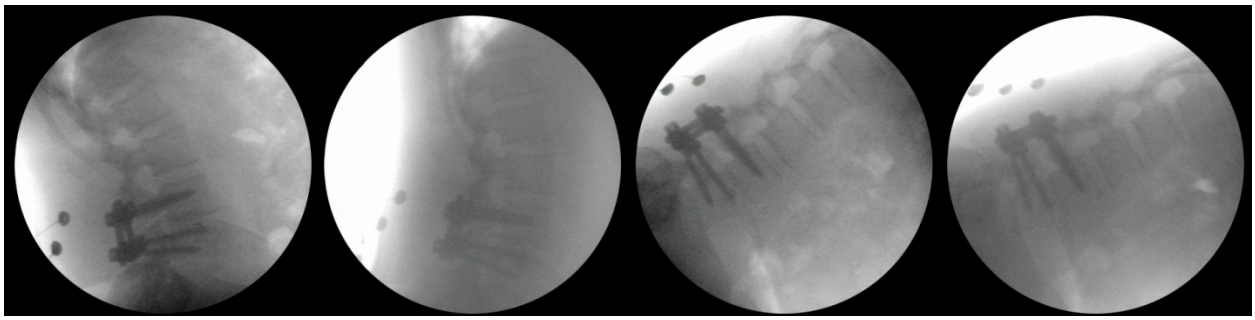

Figure 8. Sample patient preforming flexion-extention activity under flouroscopic surveillance.

Computed tomography (CT) and magnetic resonance imaging (MRI) scans of all subjects were made to include all lumbar vertebras (L1-L5) (Fig. 9). Each subject's stack of CT scans was manually segmented by applying a thresholding filter to isolate the bone from the soft tissue. Once all slices for a subject were accurately segmented, separate 3D polygon surface models were generated for each vertebra from L5 through L1 (Fig. 10). Segmented bones were then added to statistical atlas for each vertebra. A statistical atlas is a powerful tool for skeletal analyses because it allows for point correspondences and ensures that the surface points on each bone are homologous across the entire population of bones in the atlas[73, 74]. To add a bone to atlas a template mesh with a known point distribution across the surface undergoes an iterative deformation process to match all training sets of bones to be added to the atlas.

Figure 9. The CT image (left) and MRI image (right) for a sample subject.

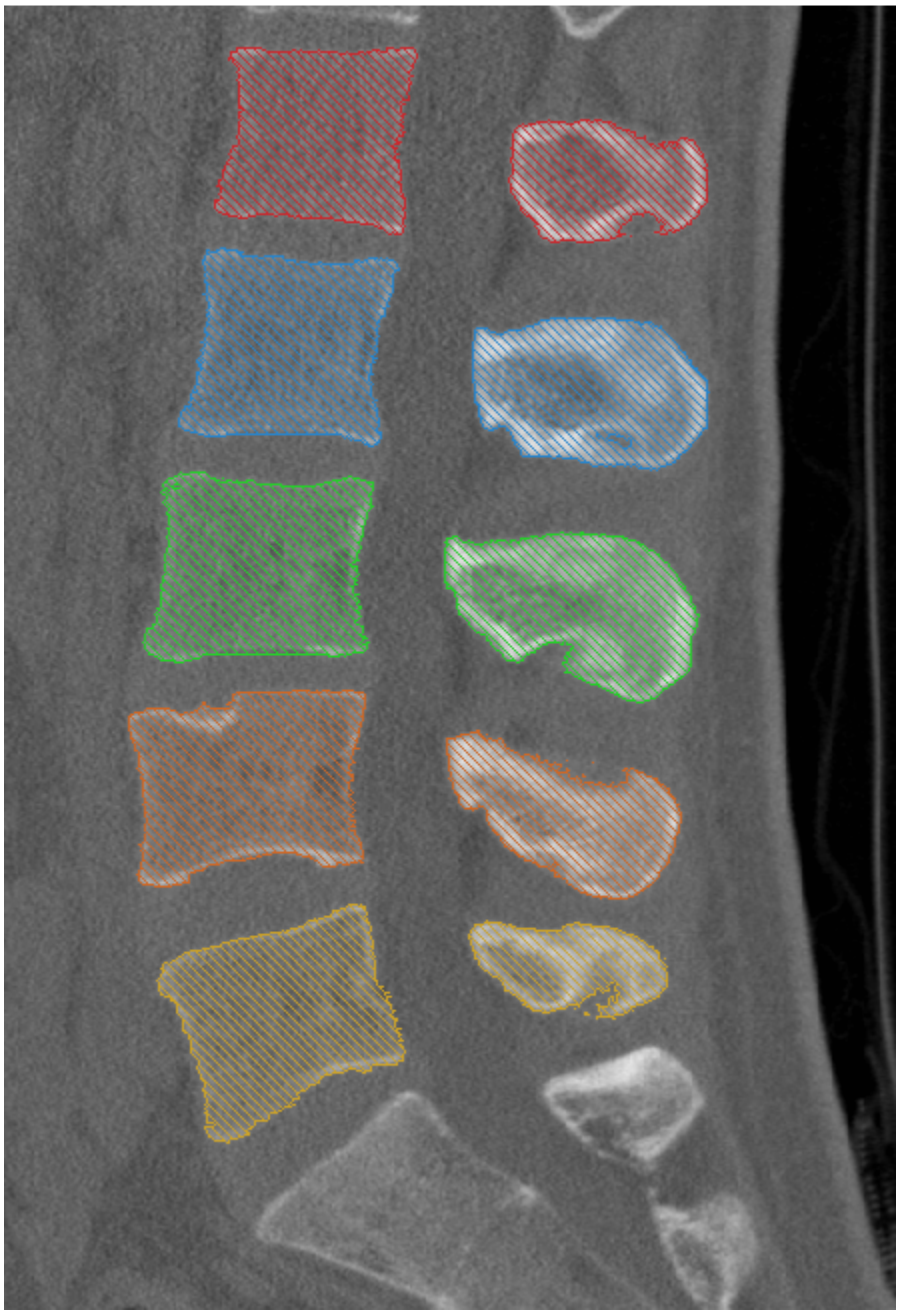

Figure 10. Individual segmented vertebraes for a sample subject on the corresponding CT scan.

Next step was 2D to 3D registration process[75] which registers the surface model of the bone to the single-plane fluoroscopic images using a direct image-to-image similarity measurement[75]. For the flexion extension trial, the fluoroscopic video was broken into 4 single frames at: Maximum Flexion, Mid-Flexion, Neutral, Max-Extension positions. For the flexion-extension activity all subjects began in a neutral standing position. They were then asked to flex to their maximum without moving at their hips, and then to travel back through neutral standing position into a maximum extension. The fluoroscopy was then positioned in the anterior-posterior plane for the lateral bending and axial rotation activities. The lateral bending activity also started in the neutral position. Subjects then flexed to their maximum left position before returning to the neutral and continuing to the maximum right position. Finally the axial rotation again started in neutral position and subjects were asked to twist to their maximum left before returning to neutral and continuing to their maximum right position. During all activities, the subjects were asked to keep their hip from moving. The lateral bending and axial rotation was broken into only 3 frames: Maximum Left, Neutral, and Maximum Right. The patient's individual 3D models were then manipulated within the space of each single-perspective fluoroscopic frame (Fig. 11).

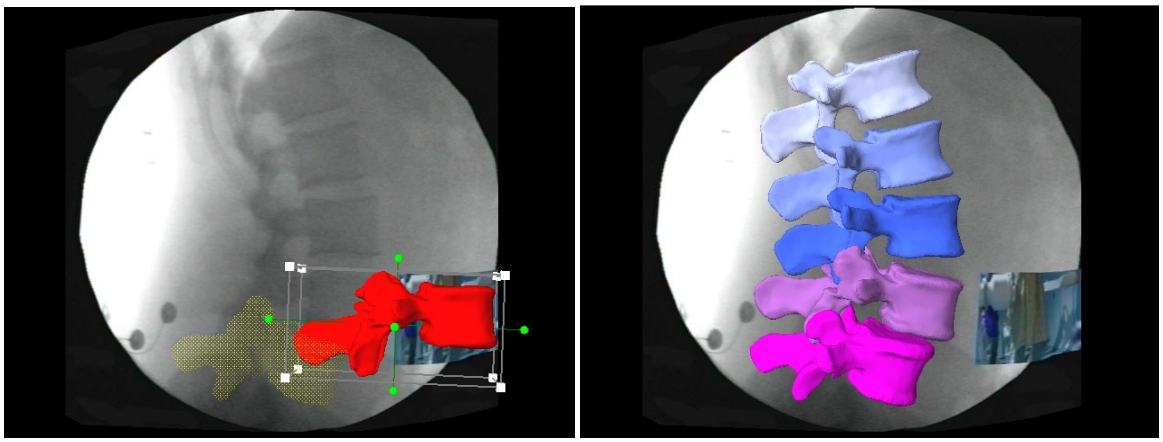

Figure 11. The process of overlaying: starting to fit (right) and finished spinal frame(left).

From the relative positions of the bone models within the 3D space, the kinematics were found for the rotations and translations of the superior vertebra to inferior vertebra. Once the kinematics were known for the bones the areas can be classified for the superior and inferior disc surface as well as occurances of the ligaments. These areas were found by picking an area of vertices on the bones (Fig. 12). Utlizing the atlas created, this area can then be propagated through all subjects. Furthermore, the areas can be tracked as the bones are rotated and translated through the captured motion. This gave an accurate description of the motion of the soft tissue from the rigid boundaries to which it connects. Using the changes in the contact areas as well as the material properties it was possible to determine stress.

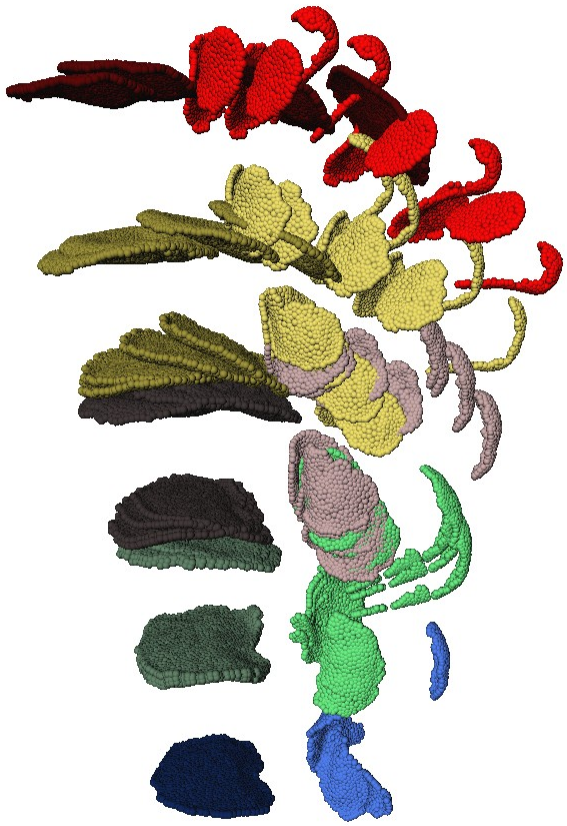

Figure 12. Sample patient with points selected during motion.

2.1. Intervertebral Disc Modeling

With this new discrete model a better understanding of intervertebral disc stresses from in vivo motion can be obtain. The following section will go through the steps required to successfully determine the stress within the intervertebral disc (Fig. 13).

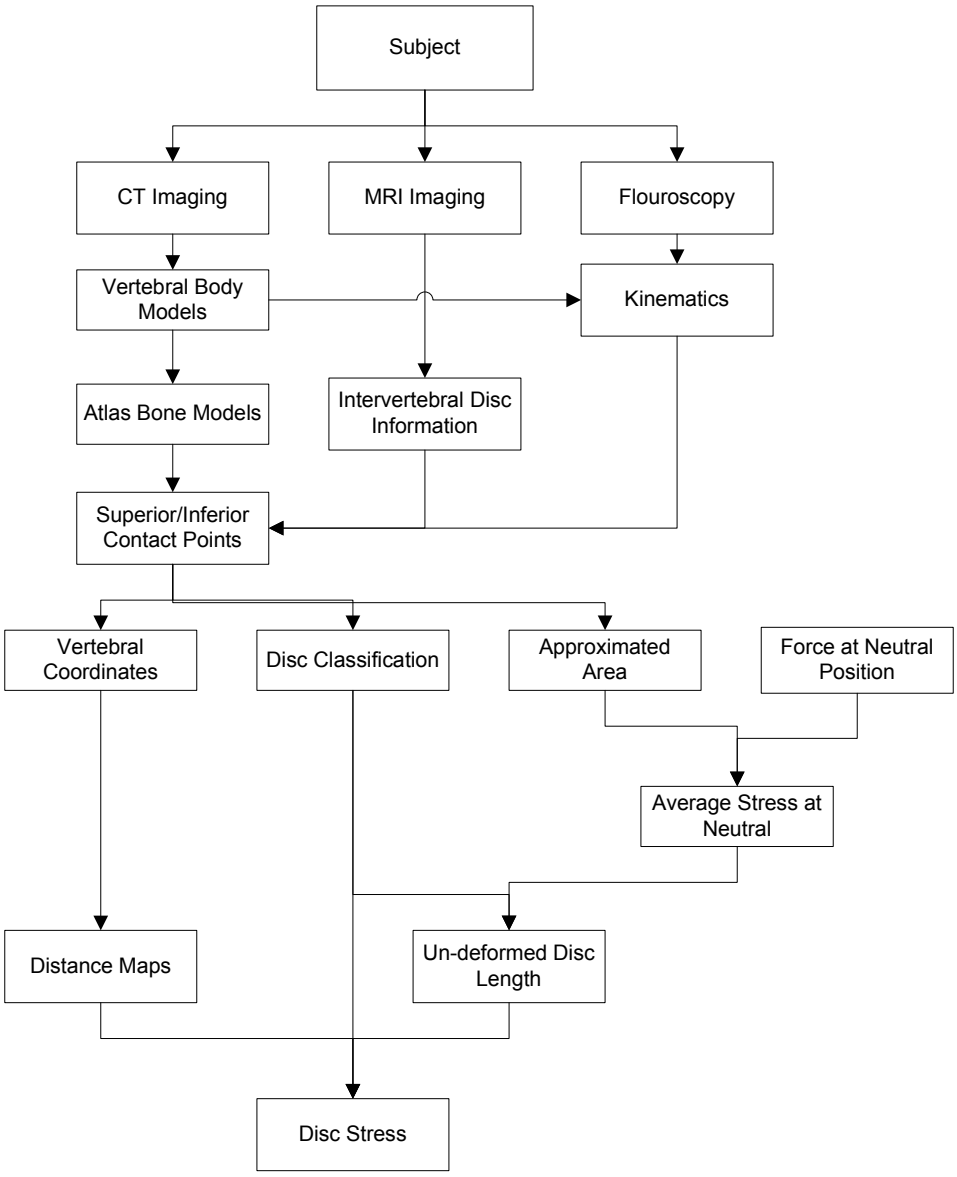

Figure 13. The flow chart used to determine the individual's disc stress.

2.1. 1 Vertebral Coordinates and Distance Maps

Given the contact areas from the kinematic data the first step was to determine the coordinate frame for the disc space. This was accomplished by finding the centroids for both collections of contact points. The vector between the centroids was defined as the normal (strain/stress) direction. Using the Gram-Schmidt orthogonalization process, another vector was found using the global x direction and the new normal direction vector. This was defined as one of the shear (stress/strain) directions. Finally the cross product of the new normal and new shear direction vectors was calculated to define the other shear (stress/strain) direction (Fig. 14). The contact points from both the inferior and superior boundary of the disc correspond between the surfaces. At each corresponding vertex of the contact areas, the distances at each point were measured in the 3 principal directions along the new unit vectors defining the disc space coordinate frame.

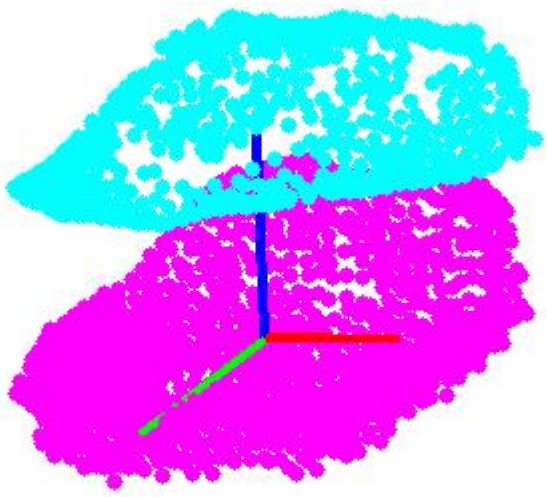

Figure 14. The new disc coordinate frame calculated.

(Superior Face = cyan, Inferior Face = magenta, X-direction = red, Y direction = blue, Z direction = green)

2.1. 2 Disc Classification

The inferior contact area for L5-L2 was used to classify the disc into annulus vertices and nucleus vertices. This was done by using the centroid of the full contact area then measuring the X and Z distances of each vertex from it. The disc was defined as an ellipse with the major and minor axis determined from these maximum distances. A pointType variable was returned so in any frame the vertex can be defined as whether it is part of the nucleus or annulus. Figure 15 shows a normal disc which was separated into the nucleus and annulus. Furthermore, figure 15 demonstrates the ability of the classification to change if degeneration is noticed in the disc. In vivo analysis has determined that as the disc degenerates the hydraulic area shrinks which in the case of the model was a decrease in the radius defining the nucleus points. For the model the levels of degeneration were: no degeneration (normal), mild, moderate, severe, and complete degeneration. One other additional function added to the classification was the determining if the point was anterior or posterior. This was done because the collagen fiber material is based on its location. The position of the point was based on the z position of the point relative to the centroid. Positive points meant the point was on the anterior and negative points meant it was posterior. Figure 16 showcases a sample subject's disc broken into the two regions.

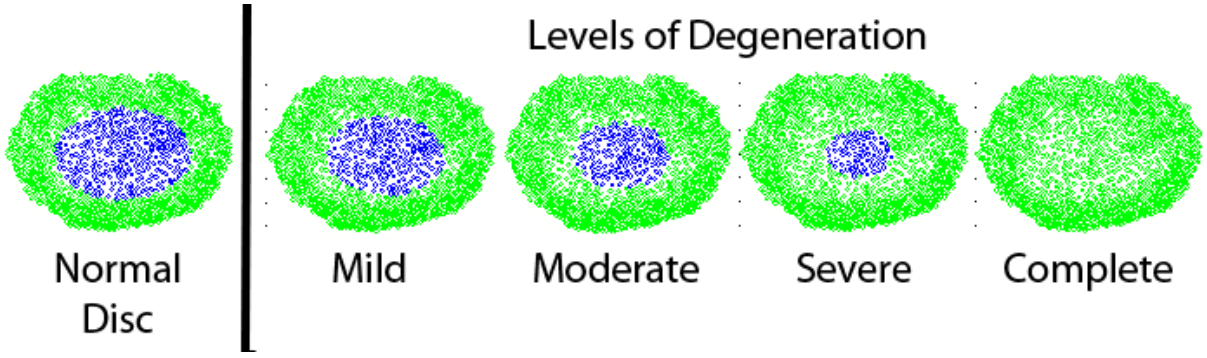

Figure 15. The levels of degeneration currently in the code which represent the loss of the hydraulic zone of the disc.

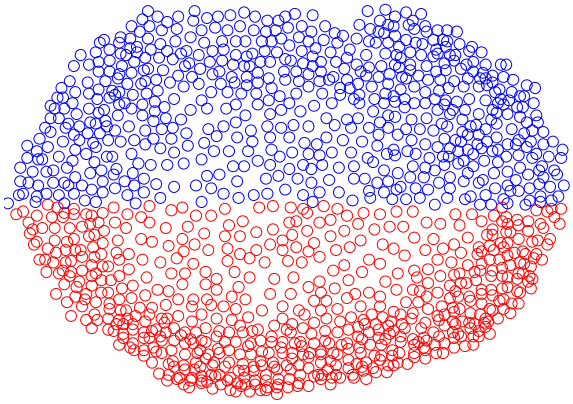

Figure 16. Sample disc broken into anterior (red) and posterior (blue) vertices.

2.1. 3 Disc Material Modeling

The annulus was assumed to be a Mooney-Rivlin hyperelastic material model with C1 = 0.2 and C2 = 0.05, and the nucleus was assumed to be linear elastic with a Young's modulus of 1 MPa and a Poisson's ratio of 0.4999. While the disc is under tension there exists collagen fibers throughout the annulus which will oppose that stress; therefore, in the tension our annulus was changed to a linear elastic model with an anterior Young's Modulus of 3.9 MPa and a posterior Young's Modulus of 8.6 MPa. Furthermore this change in Young's Modulus from compression to tension has a 2mm "crinkle" zone before changing material types as per the results from Green et al[39]. For any motion within the "crinkle" zone the disc was kept as hyperelastic material.

2.1. 4 Un-deformed Length

In order to find the strains within the vertebral disc, the original location of the vertices must be calculated. Since the *in vivo* disc is never under zero stress an approximation needed to be found by optimizing at the neutral position. This involves finding a length which creates a stress equal to the

assumed neutral stress. For our modeled disc there are two materials. First the linear elastic nucleus which has a stress, σ, to strain, ε, relationship given by Hooke's Law

$$\sigma_n = E\varepsilon$$

where E is defined as Young's Modulus. Over a discrete set of points the average stress, σ_{ave}, is therefore

$$\sigma_{n\,ave} = \frac{\sum_{i=1}^{n} E_i \varepsilon_i}{n}$$

where n is the number of nucleus vertices, E_i is the Young's Modulus at each vertex, and ε_i is the strain at each vertex. Several different techniques can be used to find average stress such as literature or use of a mathematical force calculated from the same subjects. Substituting for the strain

$$\sigma_{n\,ave} = \frac{\sum_{i=1}^{n} \left(E_i \left(\frac{L_i - L}{L} \right) \right)}{n}$$

where L_i is the distance of vertex i, and the only remaining unknown is the original length, L. Next the annulus material was non-linear elastic. Using the Mooney-Rivlin material type compressive stress, σ, is related to strain, ε, by

$$\sigma_a = 2\left(C_1 + \frac{C_2}{\gamma}\right)\left(\gamma^2 - \frac{1}{\gamma}\right)$$

where γ is the stretch ratio (L_i/L) and C1 and C2 are known material constants. Over a discrete set of points

$$\sigma_{a\ ave} = \frac{\sum_{i=1}^{m} 2\left(C_1 + \frac{C_2 L}{L_i}\right)\left(\left(\frac{L_i}{L}\right)^2 - \frac{L}{L_i}\right)}{m}$$

where m is the number of annulus vertices. Combining the two set of points the average stress for the entire disc becomes

$$\sigma_{ave} = \frac{\sum_{i=1}^{m} 2\left(C_1 + \frac{C_2 L}{L_i}\right)\left(\left(\frac{L_i}{L}\right)^2 - \frac{L}{L_i}\right) + \sum_{i=1}^{n}\left(E_i\left(\frac{L_i - L}{L}\right)\right)}{(m+n)}$$

The resulting stress equation has only one unknown which is the un-deformed length, L. By iterating through values of L, the optimized length was found when the stress calculated was within $\sigma_{ave} \pm$ 0.001.

2.1.4.1 *Sensitivity Analysis*

A sensitivity analysis was also performed on the un-deformed length measurement because it relies heavily on the number of points, and the initial length is crucial in calculating stresses at subsequent frames. This sensitivity analysis was done by changing the mesh size for the contact areas from 2mm spacing to 0.25mm spacing for one patient; which in turn changes the number of vertices in the un-deformed length calculation thus showing how the initial length is affected.

2.1.4.2 *Un-deformed Length Analysis*

The lengths for each level were recorded for each subject within the groups (Appendix A.3). This length was then averaged to determine if any differences could be found between the different group types as well as between the spinal levels.

2.1. 5 Disc Stress

The stress at each vertex becomes a mathematical problem with use of the changes in the location of the contact vertices, the material model, and the calculated un-deformed length of the disc. Hooke's law for linear elastic model can be defined as the stresses, σ_x, σ_y, σ_z which are the normal stress in the three principal directions, and τ_x, τ_y, τ_z which represent the shear stresses in the three principal directions. The intervertebral contact is only subjected to three of the six stresses which in our model would be σ_y, τ_x, and τ_z. For the linear elastic nucleus those stresses are

$$\sigma_y = E\varepsilon_y$$

$$\tau_x = G\varepsilon_{xy}$$

$$\tau_z = G\varepsilon_{yz}$$

where E is the Young's Modulus, G is the shear modulus, and ε is the strain in the subscripted direction. The discrete model used the Mooney-Rivlin hyperelastic material model. That means for the annulus the stress was equal to

$$\sigma_y = \left(2C_1 + \frac{2C_2}{\alpha_y}\right)\left({\alpha_y}^2 - \frac{1}{\alpha_y}\right)$$

$$\tau_x = 2(C_1 + C_2)\left({\gamma_{xy}}^2 - \frac{1}{{\gamma_{xy}}^2}\right)$$

$$\tau_z = 2(C_1 + C_2)\left({\gamma_{yz}}^2 - \frac{1}{{\gamma_{yz}}^2}\right)$$

where C_1 and C_2 are experimental constants, α is the stretch (L/L_{intial}) in the subscripted direction, and γ is the shear strain stretch ratio in the subscripted directions. When the disc experienced tension

and passes through the 2mm "crinkle" zone the annulus vertex was treated as linear elastic utilizing Hooke's Law to find those resulting stresses.

2.1.5.1 *Disc Stress Analysis*

The stresses at each disc vertex for each level were recorded. Several different analyses were performed to determine how the motion patterns effects the disc stress. First an average stress was determined for the entire disc at each major frame. The changes in the average stress were compared to determine if there was any difference between the group types. Next visual inspection of the individual discs was compared to the motion patterns to determine how the motion affects the disc stress field. Finally, the disc was sectioned to determine how the different areas of the intervertebral disc differ among the groups.

2.1.5.2 *Adjacent Segment Comparison*

Following a fusion surgery, some spinal models have shown that the adjacent segment from the surgical location will have increased motion which in turn will increase the stress of the disc. Given that no clinical data has been able to back up the claims, the stresses from the nine fusion subjects was compared to determine if the adjacent segment stresses in the discrete model were found to increase or decrease.

2.2. Ligaments

In most mathematical models the ligaments are chosen to be linear elastic. The ligaments in this model were modeled using a neo-Hookean material model which is Hooke's Law modified into a non-linear elastic model. For ligaments, the stress can only be unidirectional along the vector connecting the vertices, and the stress can only be tensile. Therefore the stress in the ligaments was

$$\sigma_y = \frac{E}{3}\left(\alpha_y - \frac{1}{{\alpha_y}^2}\right)$$

where E is the Young's Modulus and α is the stretch (L/L_{intial}) in the subscripted direction. The initial length used in our model was the distance at the neutral position. The lengths were the measured distance between the points selected for the insertions of the ligaments. Using data from Pintar et al.[43] the Young's Modulus constants were obtained. The length changes measured for each subject were found at the all vertices giving a stress profiles for the ligaments. The ligaments analyzed in this study were the intertransverse ligaments (ITL), both left and right, the supraspinous ligament (SSL), and the interspinal ligament (ISL). These ligaments stresses were found for all three activities at each major frame.

2.3. Validation

The main question in the validation is whether or not the model created is an accurate representation of what occurs in vivo. All parts of the code were tested with simulations to determine if the results were as expected. A simulation code was written for the disc spacing coordinate frame code to make sure no matter the orientation of the disc that the code would keep the coordinate frame consistent. This simulation consisted of 2 rigid plates which were rotated into different orientations. The code was then run to determine if it could reorient the plates. This code was also used to determine if the un-deformed length measurement was working as intended. For this simulation once the plates had been rotated an average stress was applied and the un-deformed length was calculated. For ease of calculation, this code was done with linear elastic material modeling with a Young's Modulus of 1 MPa. For the stress validation the first step was to create a finite element simulator. This simulator allowed for the manipulation of a disc model between two rigid plates. By displacing the top rigid plate a stress was found in the disc. This was compared to the

stress calculated from the displacement when inputted into the discrete code. Further stress validation was done comparing with in vivo, in vitro tests, and finite element models with the results of from our data.

Chapter 3. Results

3.1. Kinematic Results

3.1.1. Healthy Group

During the flexion extension activity the healthy group achieved rotations of 11.83°, 9.55°, 12.16°, and 13.05° of in-plane motion at L1/L2, L2/L3, L3/L4, and L4/L5 respectively. This is quite a bit larger than the 2.32°, 2.47°, 1.96°, and 2.09° degrees of combined out-of-plane rotations at L1/L2, L2/L3, L3/L4, and L4/L5 respectively (Fig. 17). It can be seen that the flexion extension activity, while complex, the healthy group had majority of the rotations happen in plane.

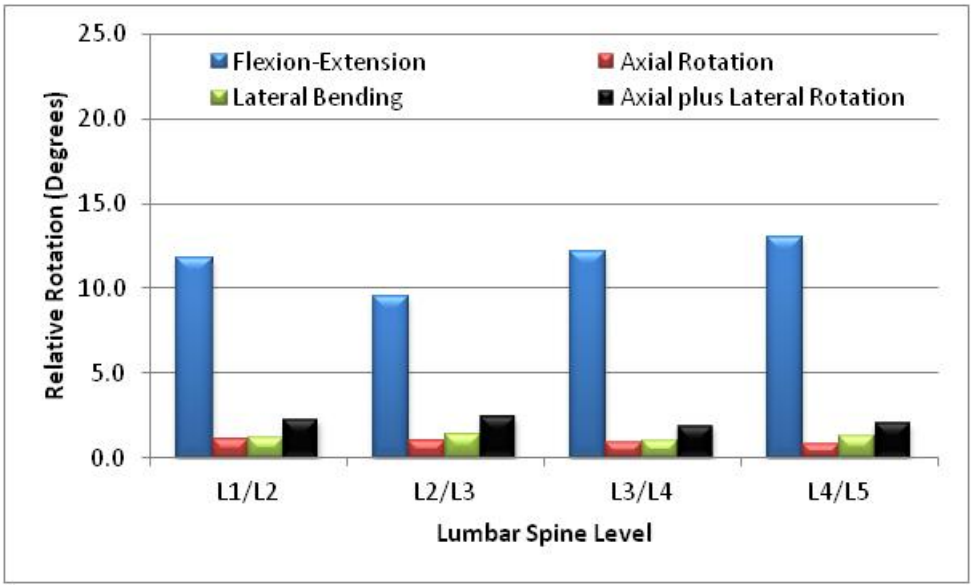

Figure 17. The overall amount of rotation achieved for each spinal level during the flexion extension activity.

The complexity of motion increased during the lateral bending activity for the healthy group. During this activity the group had 9.69°, 10.27°, 10.12°, and 10.53° of in-plane rotations and 8.95°, 9.75°, 9.03°, and 9.37° of out-of-plane rotations at L1/L2, L2/L3, L3/L4, and L4/L5 respectively (Fig. 18). Much different from flexion-extension activity, lateral bending has nearly equal overall rotation amounts between in-plane and out-of-plane rotations.

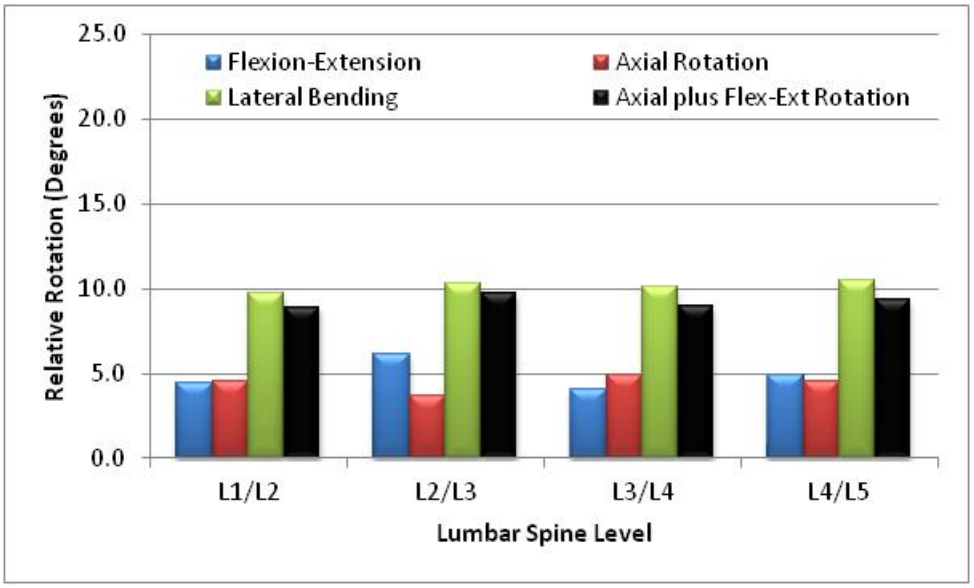

Figure 18. The overall amount of rotation achieved for each spinal level during the lateral bending activity.

Axial rotation was the most complex activity with out-of-plane rotations of 8.8°, 8°, 8.18°, and 8.25° at L1/L2, L2/L3, L3/L4, and L4/L5 respectively. This is more than double the in-plane rotations of 3.21°, 3.42°, 3.77°, and 3.17° at the same levels (Fig. 19). It would appear that a simple twist even for normal lumbar spine is not a simple motion but rather complicated.

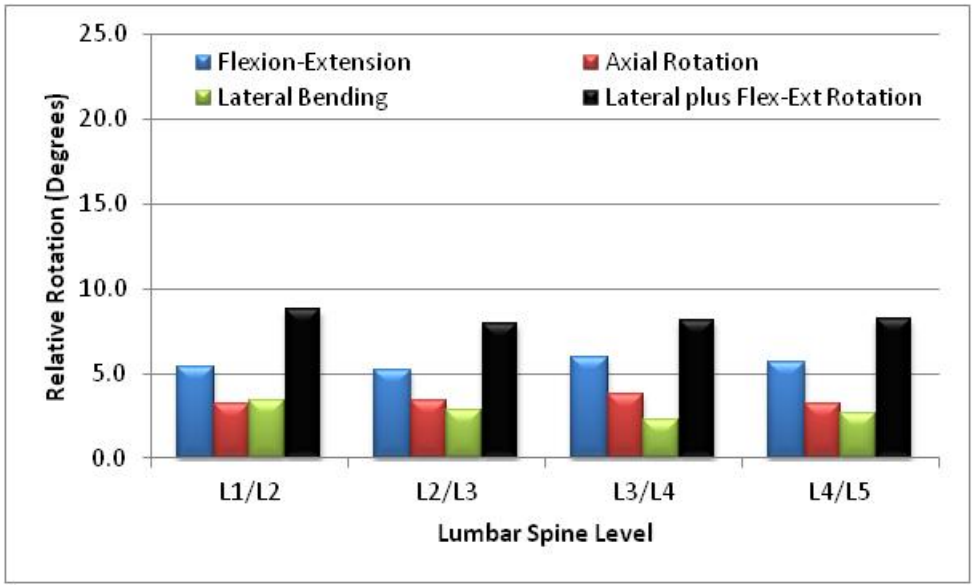

Figure 19. The overall amount of rotation achieved for each spinal level during the axial rotation activity.

3.1.2. Low Back Pain Group

Once the subjects start to experience pain the flexion-extension activity becomes increasingly more complex. For the low back pain subjects it can be seen that over all levels the out-of-plane rotations were anywhere from 50% to almost equal to that of in-plane rotations. The worst level was L1/L2 which had in-plane 11.7° compared to 10.7° of out-of-plane rotation. Next would be L2/L3 level which experienced 11.52° in-plane and 7.89° out-of-plane. This was followed by the L3/L4 level with 11.67° and 6.18° of in-plane and out-of-plane rotations respectively. Finally was L4/L5 level which had the highest amount of in-plane rotation of all levels at 15.78° and 9.08° of out-of-plane rotation (Fig. 20).

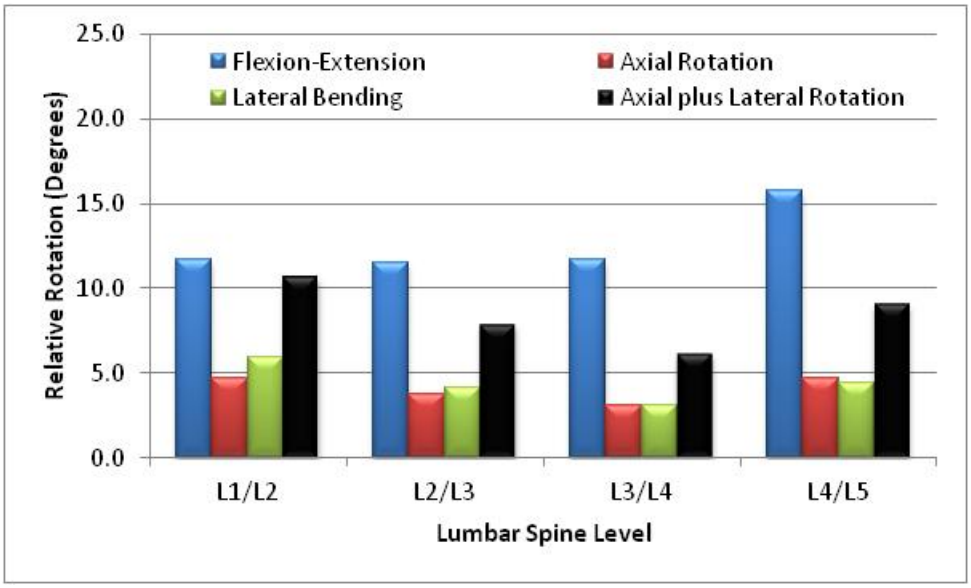

Figure 20. The overall amount of rotation achieved for each spinal level during the flexion extension activity.

While the healthy group had nearly equal amounts of in-plane to out-of-plane rotations for the lateral bending activity, the low back pain group showed a slightly more out-of-plane in all levels besides L1/L2 which had nearly twice as much out-of-plane to in-plane rotation. During this activity the group had 8.20°, 11.15°, 8.87°, and 8.52° of in-plane rotations and 14.35°, 11.33°, 10.57°, and 11° of out-of-plane rotations at L1/L2, L2/L3, L3/L4, and L4/L5 respectively (Fig. 21).

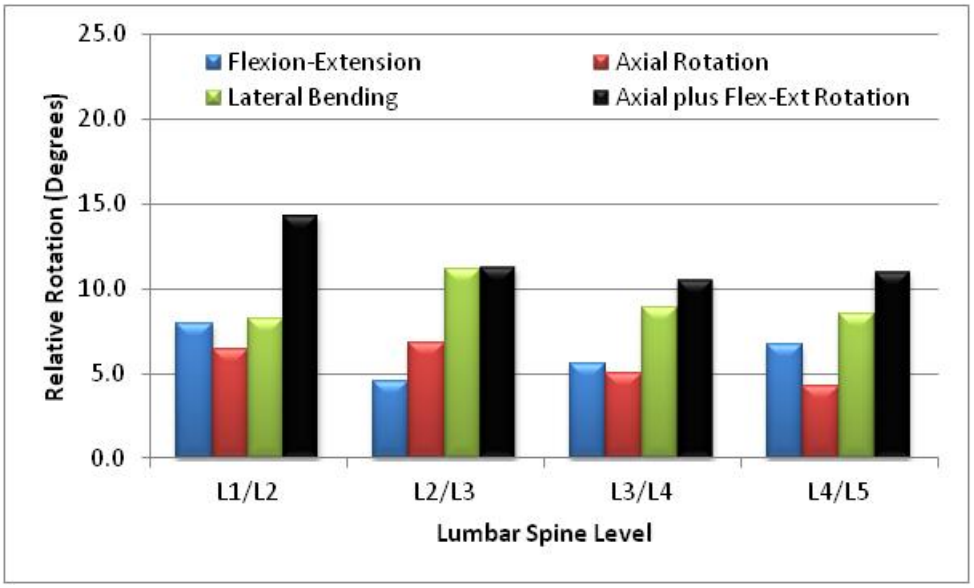

Figure 21. The overall amount of rotation achieved for each spinal level during the lateral bending activity.

Axial rotation activity had out-of-plane rotations of 11.51°, 11.42°, 7.55°, and 9.37° at L1/L2, L2/L3, L3/L4, and L4/L5 respectively. This was anywhere between two to four times the in-plane rotations of 4.36°, 2.59°, 3.73°, and 4.47° at the same levels (Fig. 22). Spinal unit L2/L3 showed the greatest change when compared to healthy.

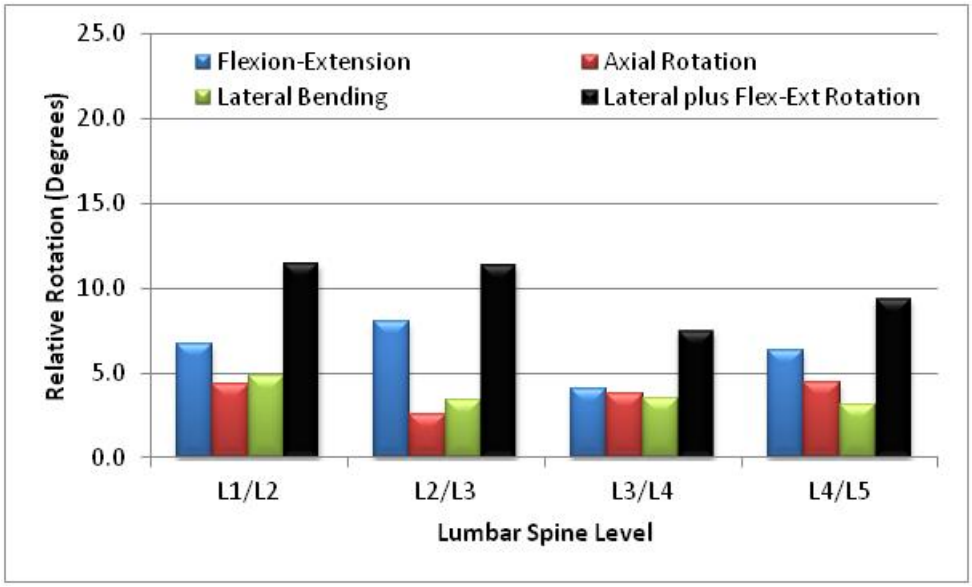

Figure 22. The overall amount of rotation achieved for each spinal level during the axial rotation activity.

3.1.3. Degenerative Group

The degenerative group showed a nearly equal amount of in-plane and out-of-plane rotation during the flexion-extension activity over all levels. During this activity the group had 10.52°, 9.85°, 10.96°, and 9.13° of in-plane rotations and 9.64°, 10.17°, 8.74°, and 9° of out-of-plane rotations at L1/L2, L2/L3, L3/L4, and L4/L5 respectively (Fig. 23). The greatest change from low back pain was at the L2/L3, L3/L4, and L4/L5 levels which have had increased out-of-plane rotations that nearly equal the in-plane rotations now.

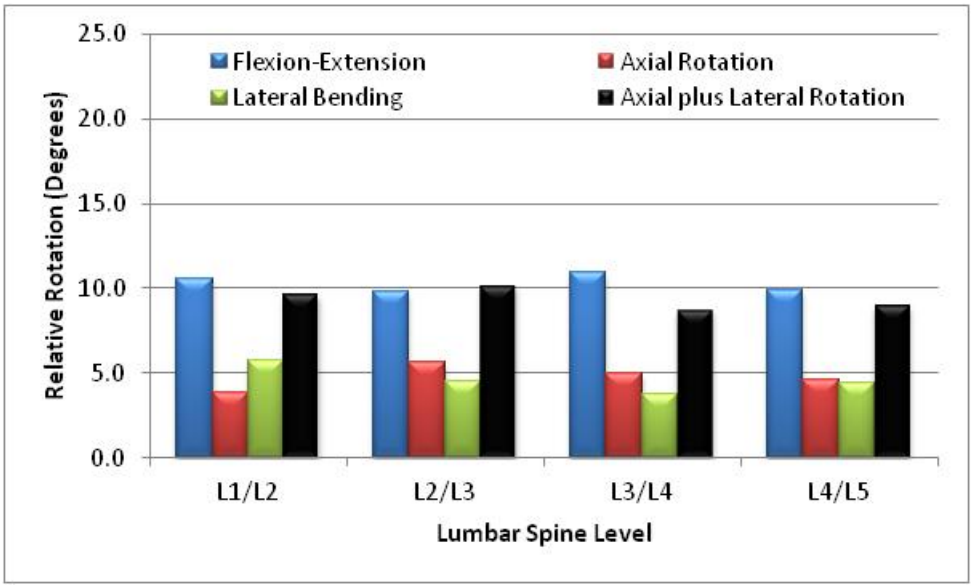

Figure 23. The overall amount of rotation achieved for each spinal level during the flexion extension activity.

For the lateral bending activity, the degenerative group had at least one and half times the amount of out-of-plane rotation to in-plane. During this activity the group had 12.69°, 11.69°, 12.99°, and 9.86° of in-plane rotations and 25.12°, 21.89°, 19.51°, and 22.27° of out-of-plane rotations at L1/L2, L2/L3, L3/L4, and L4/L5 respectively. The degenerative group also was the first group to have more flexion-extension overall than lateral bending (Fig. 24).

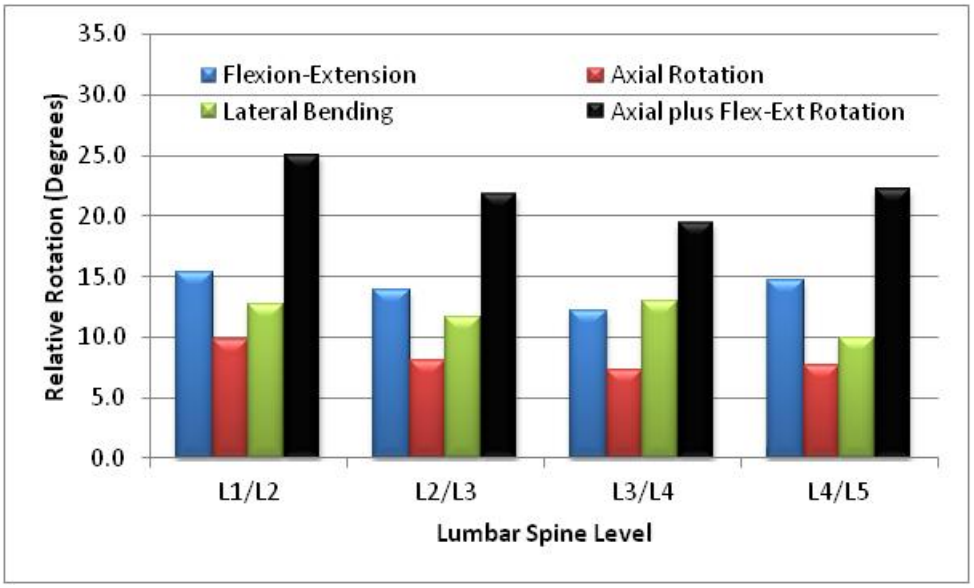

Figure 24. The overall amount of rotation achieved for each spinal level during the lateral bending activity.

The axial rotation activity saw similar results between the low back pain and degenerative group with the out-of-plane rotations being anywhere between two to four times higher. The degenerative group experienced 5.03°, 4.46°, 4.42°, and 5.09° of in-plane rotations and 12.36°, 10.75°, 16.19°, and 12.33° of out-of-plane rotations at L1/L2, L2/L3, L3/L4, and L4/L5 respectively during this activity (Fig. 25).

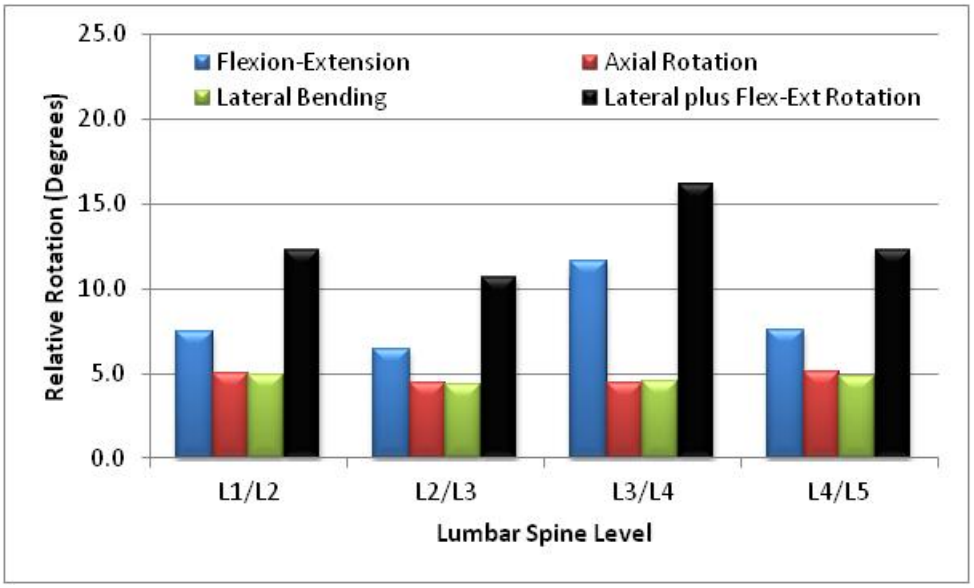

Figure 25. The overall amount of rotation achieved for each spinal level during the axial rotation activity.

3.1.4. Preoperative Fusion

The fusion group preoperatively had similar results to the degenerative group with the out-of-plane being slightly more than the in-plane with the highest difference being one and half times at L3/L4 and L4/L5 levels during flexion-extension. The rotations for this group was 8.54° in-plane and 8.69° out-of-plane at L1/L2 level, 8.56° in-plane and 9.93° out-of-plane at L2/L3 level, 7.49° in-plane and 11.66° out-of-plane at L3/L4 level, and 6.74° in-plane and 10.4° out-of-plane at L4/L5 level (Fig. 26).

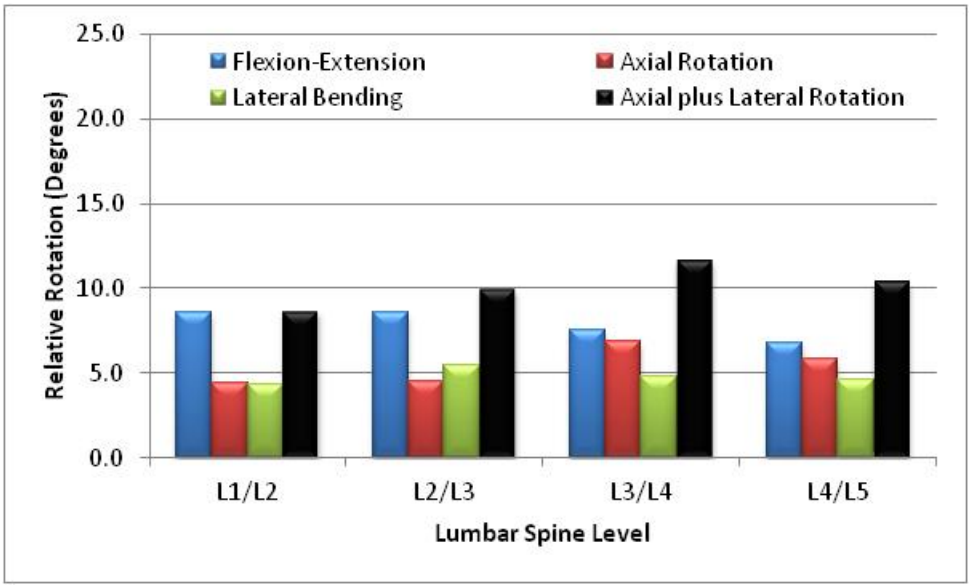

Figure 26. The overall amount of rotation achieved for each spinal level during the flexion extension activity.

The preoperative fusion group had increased out-of-plane rotations similar to the low back pain group with all but one level having slightly higher amounts for the lateral bending activity. The highest level was L1/L2 which had 8.2° of in-plane rotation and 14.36° of out-of-plane rotation. The rest of the levels had 11.13°, 8.87°, and 8.52° of in-plane rotations and 11.33°, 10.57°, and 11° of out-of-plane rotations at L2/L3, L3/L4, and L4/L5 respectively (Fig. 27).

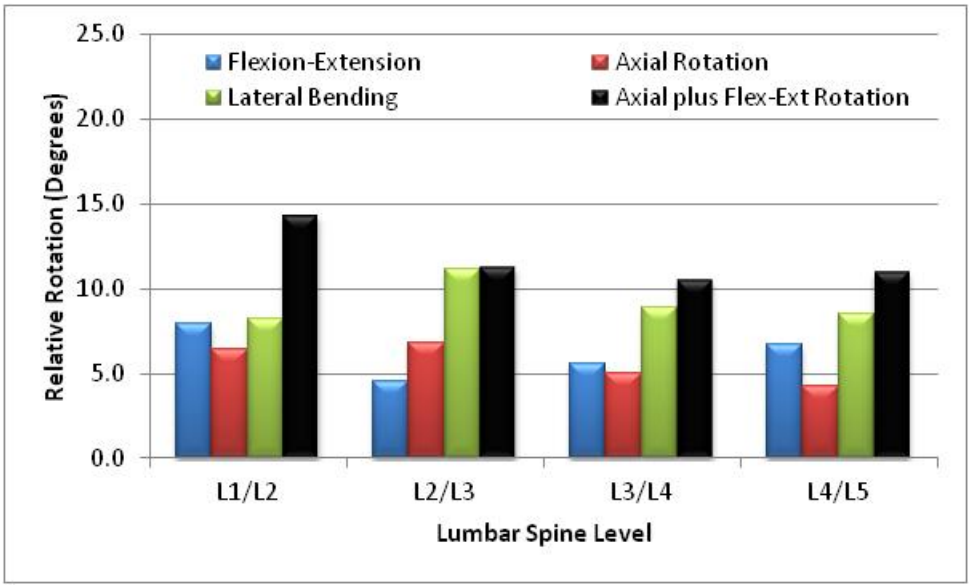

Figure 27. The overall amount of rotation achieved for each spinal level during the lateral bending activity.

During axial rotation activity, the preoperative fusion group had about twice as much out-of-plane rotations as in-plane with 4.35°, 3.73°, and 4.47° of in-plane rotations and 11.51°, 7.55°, and 9.38° of out-of-plane rotations at L1/L2, L3/L4, and L4/L5 respectively. The L2/L3 level was significantly higher with the out-of-plane rotation of 11.41° and only 2.59° of in-plane rotation (Fig. 28).

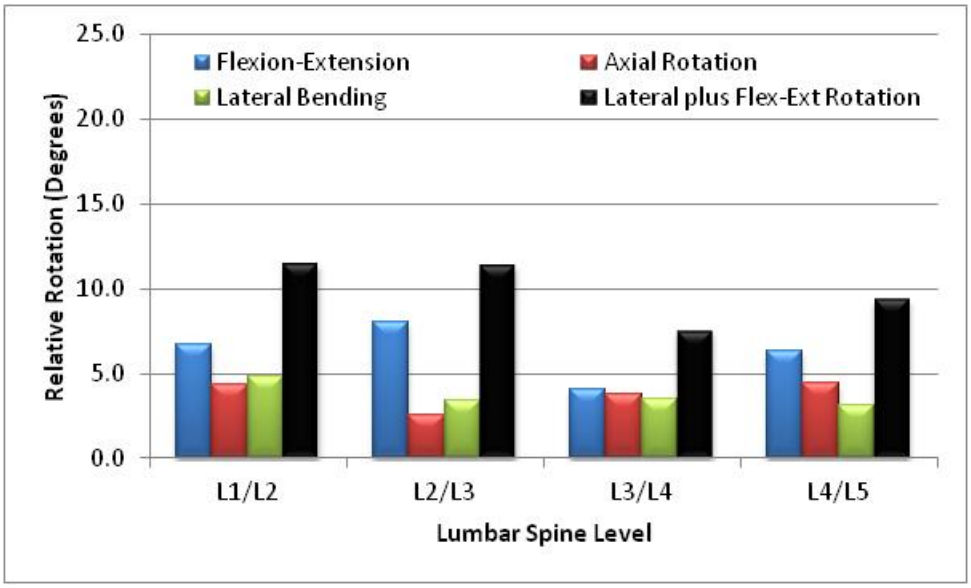

Figure 28. The overall amount of rotation achieved for each spinal level during the axial rotation activity.

3.1.5. Postoperative Fusion

Following the fusion surgery all of the in-plane rotations during flexion-extension activity were slightly less. Furthermore the out-of-plane rotations were found to have decreased at all levels with higher changes at L3/L4 and L4/L5 levels. The in-plane rotations were 8.19°, 7.67°, 7.39°, and 6.63° at L1/L2, L2/L3, L3/L4, and L4/L5 respectively. The out-of-plane rotations were 7.99°, 7.33°, 6.26°, and 4.72° at L1/L2, L2/L3, L3/L4, and L4/L5 respectively (Fig 29). While the decrease in out-of-plane rotations is desired outcome from fusion surgery, the group did experience a decrease in-plane and did not return to more healthy amounts at the non-fused levels.

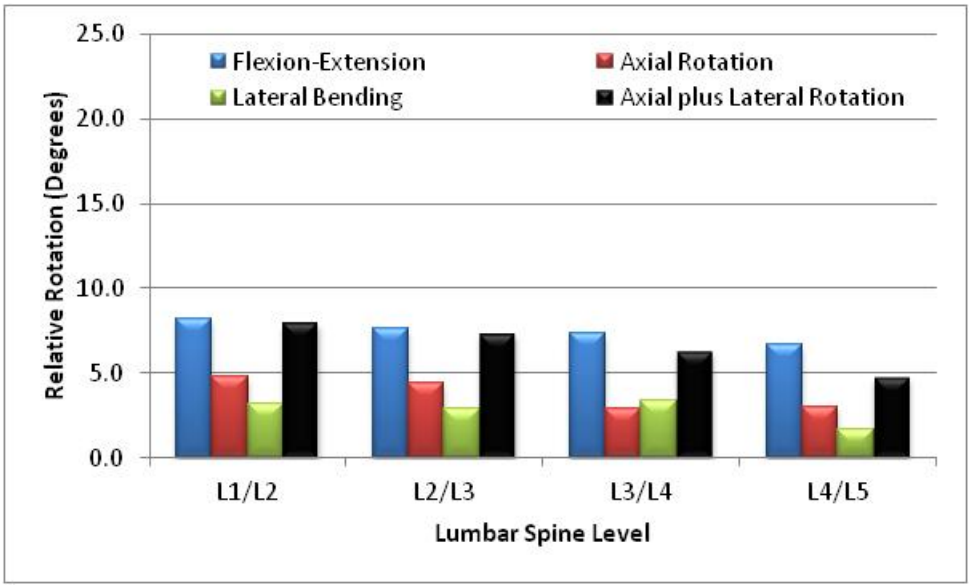

Figure 29. The overall amount of rotation achieved for each spinal level during the flexion extension activity.

During lateral bending the postoperative fusion subjects had three levels return to a more normal motion with in-plane rotations of 9.22°, 11.61°, and 6.89° and out-of-plane rotations of 8.30°, 9.02°, and 6.34° at L1/L2, L2/L3, and L4/L5 respectively. The L3/L4 level was the only one to have shown greater out-of-plane rotations of 9.89° to the in-plane rotation of 9.07° (Fig. 30). It would appear that the fusion subjects returned to a more normal motion pattern after surgery for this activity at the three levels given that all out-of-plane rotations decreased after surgical intervention.

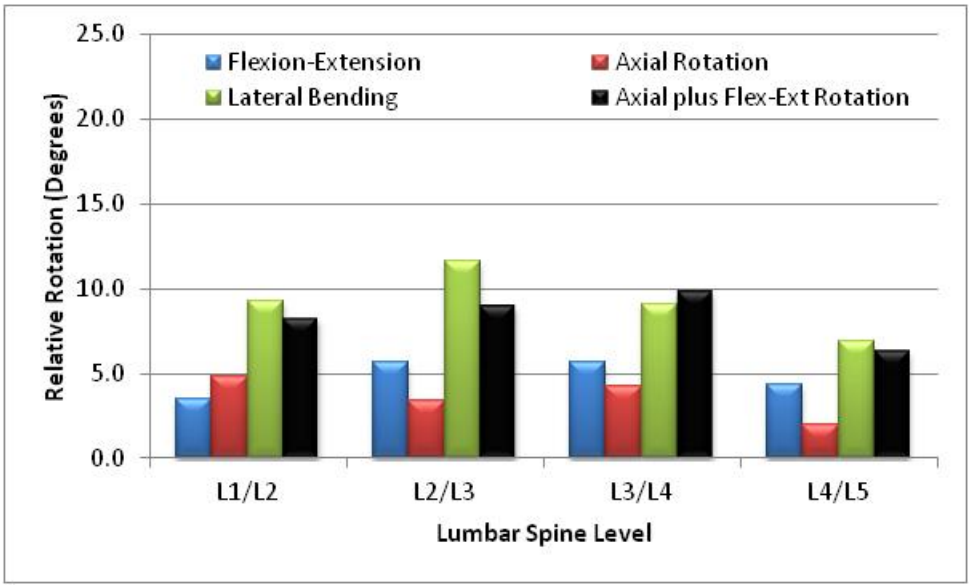

Figure 30. The overall amount of rotation achieved for each spinal level during the lateral bending activity.

During axial rotation activity, the postoperative fusion group had about twice as much out-of-plane rotations as in-plane with 3.99°, 4.86°, 3.19, and 3.27° of in-plane rotations and 8.36°, 9.16°, 7.84, and 6.51° of out-of-plane rotations at L1/L2, L2/L3, L3/L4, and L4/L5 respectively (Fig. 31). The L2/L3 level which had significantly higher preoperative rotations had decrease in both rotations causing it to be more in line with the other levels.

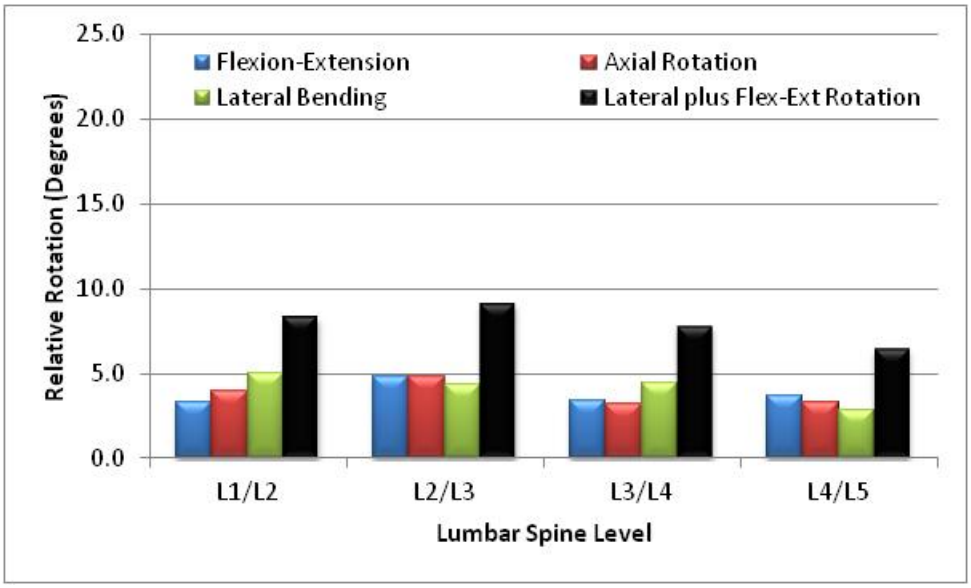

Figure 31. The overall amount of rotation achieved for each spinal level during the axial rotation activity.

3.1.6. Preoperative Facet

The preoperative facet subjects were a small sample size of only two; however, they had much different kinematics than the other groups during flexion-extension. The in-plane rotations were 6.33°, 5.03°, 4.20°, and 5.6° at L1/L2, L2/L3, L3/L4, and L4/L5 respectively which was relatively low. All out-of-plane rotations were less with 5.01°, 2.74°, 3.5°, and 2.87° at L1/L2, L2/L3, L3/L4, and L4/L5 respectively (Fig. 32). Overall it appeared that this group had trouble with this activity.

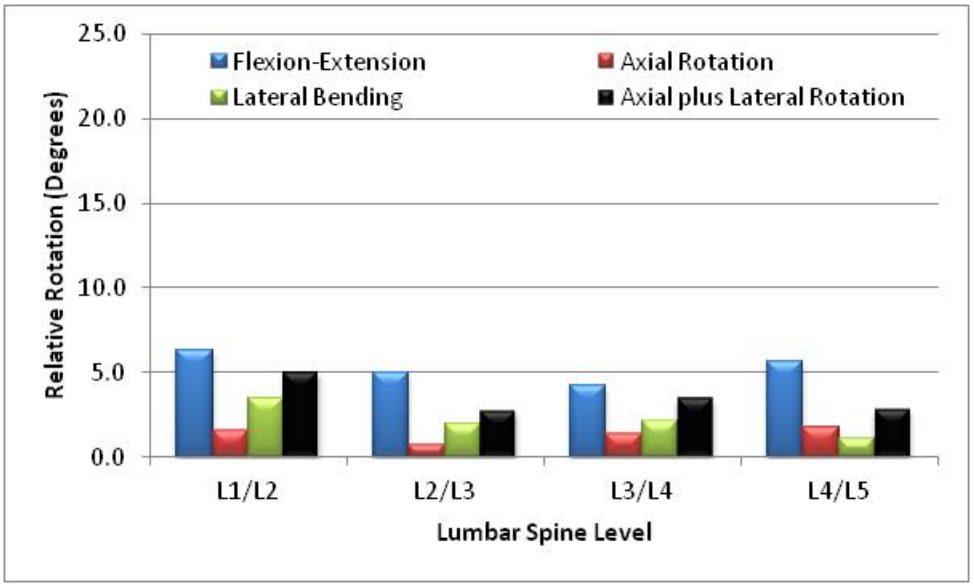

Figure 32. The overall amount of rotation achieved for each spinal level during the flexion extension activity.

During lateral bending the preoperative facet group showed similar lower rotations amounts compared to the other groups. During this activity the out-of-plane rotations were more than in-plane at all levels except L4/L5. The in-plane rotations were 6.2°, 7.58°, 5.04°, and 5.28° with out-of-plane rotation amounts of 7.41°, 9.41°, 8.53°, and 4.1° at L1/L2, L2/L3, L3/L4, and L4/L5 respectively (Fig. 33).

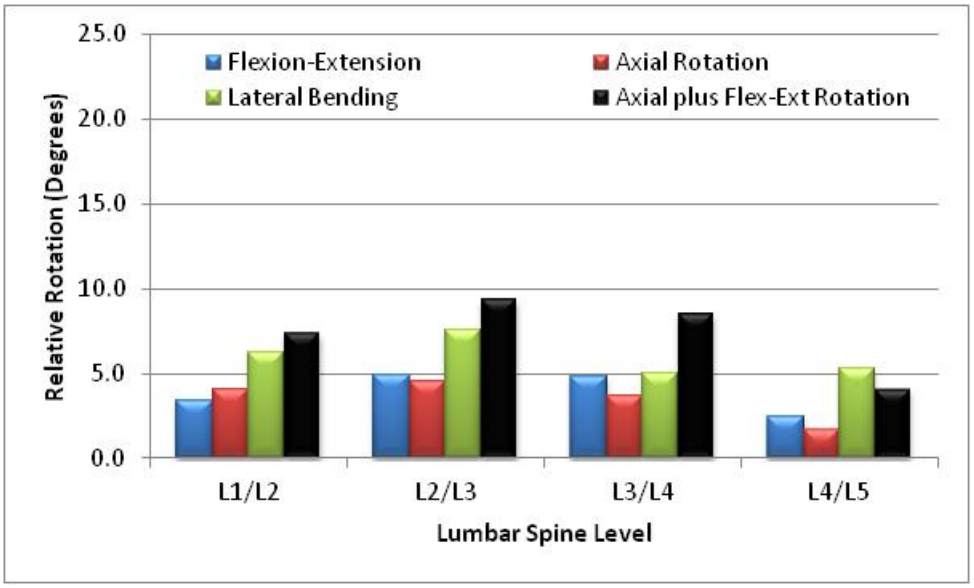

Figure 33. The overall amount of rotation achieved for each spinal level during the lateral bending activity.

The rotations during axial rotation activity were similar to the degenerative and low back pain groups for the preoperative facet subjects. The out-of-plane rotations of 5.98°, 7.45°, 10.93°, and 5° were anywhere from two to four times higher than the in-plane rotations of 3.03°, 3.06°, 2.79°, and 1.4° at L1/L2, L2/L3, L3/L4, and L4/L5 respectively (Fig. 34). While the activities which required more compressive motion had fewer rotation amounts, it appeared that this motion was unaffected.

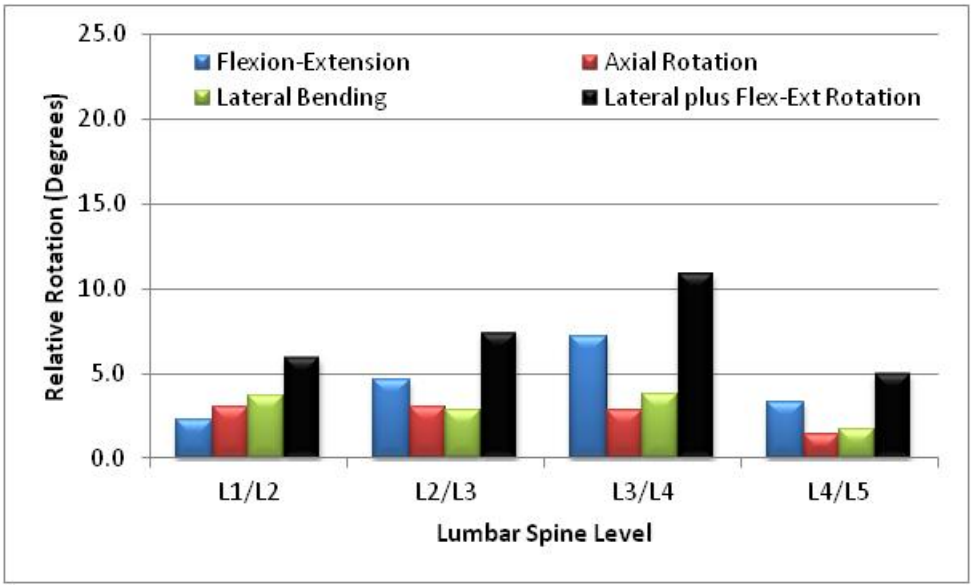

Figure 34. The overall amount of rotation achieved for each spinal level during the axial rotation activity.

3.1.7. Postoperative Facet

Following surgical intervention, the postoperative facet group had varying kinematic results for the flexion-extension activity. The L1/L2 level had an in-plane rotation of 10.44° with only 2.04° of out-of-plane rotations. This result has improved to the point that it is similar to the healthy group. At the adjacent lower levels the rotations show diminishing in-plane rotations with amounts of 7.32°, 5.59°, and 3.1°. The out-of-plane rotations remain rather constant over all levels with amounts of 1.92°, 2.08°, and 2.27° at L2/L3, L3/L4, and L4/L5 respectively (Fig. 35). The instrumentation was implanted at the L4/L5 level and while preoperatively the values were rather low it can be seen that this level is more constrained postoperatively.

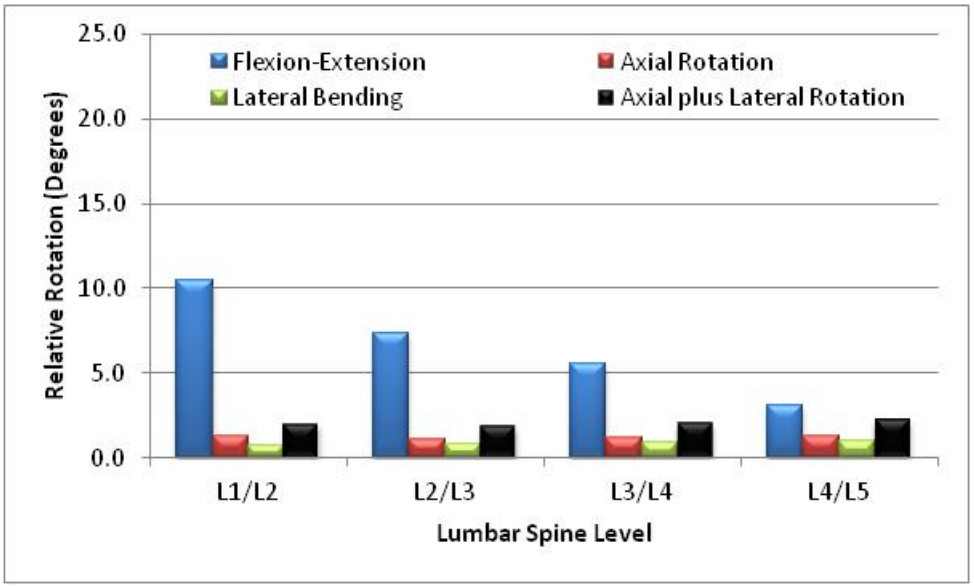

Figure 35. The overall amount of rotation achieved for each spinal level during the flexion extension activity.

Following surgical intervention, the postoperative facet group had increased motion at all levels except L4/L5. The L1/L2 level and L2/L3 level have improved to the point that it is similar to the healthy group. These levels experienced in-plane rotations of 12.07° and 10.94° respectively with lower out-of-plane rotations of 11.62° and 9.01° respectively. The L3/L4 level had higher out-of-plane rotation of 15.21° and only 11.06° in-plane which is similar to the low back pain, degenerative, and preoperative fusion groups. The instrumented L4/L5 level again had constrained motion with that level experiencing 3.64° in-plane rotation and 2.46° out-of-plane rotation (Fig. 36).

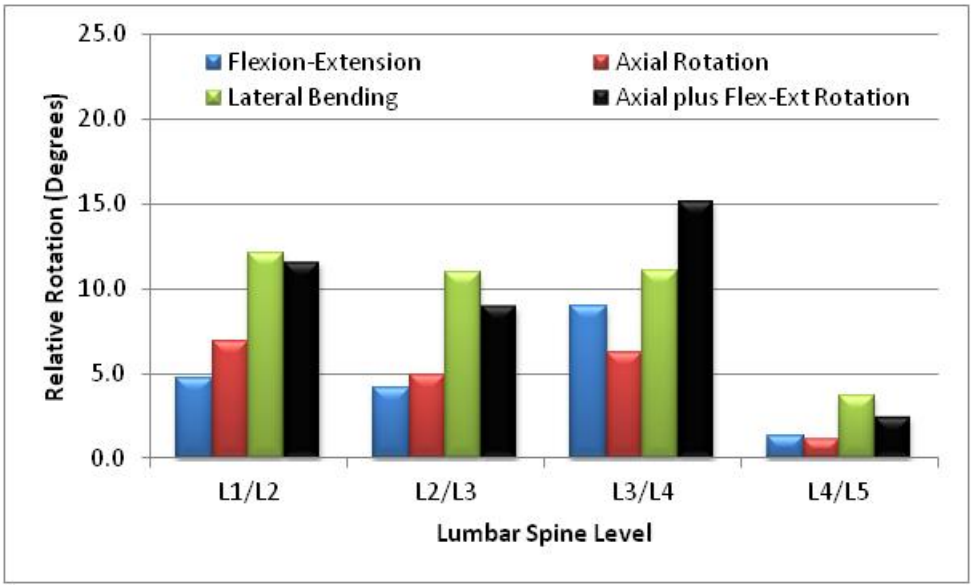

Figure 36. The overall amount of rotation achieved for each spinal level during the lateral bending activity.

The rotations during axial rotation activity were found to be slightly less after surgery at all non-instrumented levels. The out-of-plane rotations of 8.82°, 5.17°, and 6.05° were anywhere from 1.5 to 3.5 times higher than the in-plane rotations of 2.45°, 3.02°, and 3.64°at L1/L2, L2/L3, and L3/L4 respectively. The L4/L5 level had decreased in-plane motion of only 0.81°, and the out-of-plane rotations actually increased to 5.79° (Fig. 37).

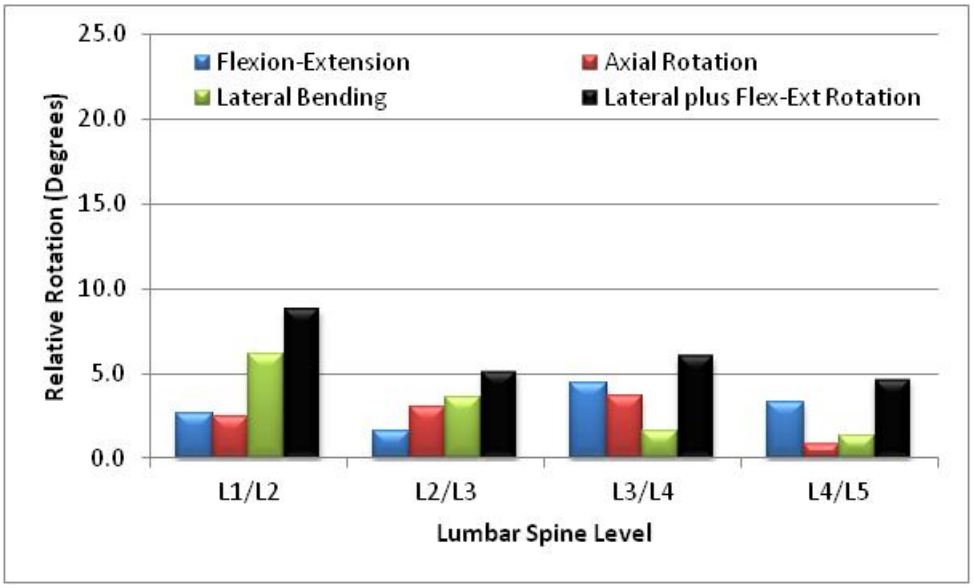

Figure 37. The overall amount of rotation achieved for each spinal level during the axial rotation activity.

3.1.8. Postoperative Disc

The final group was postoperative disc which like facet only had two subjects. During flexion-extension activity this group ended up having out-of-plane rotations similar to healthy group of 2.47°, 3.16°, 1.82°, and 2.16° at L1/L2, L2/L3, L3/L4, and L4/L5 respectively. They did however have lower amount of in-plane rotations with acquired rotations of 4.37°, 6.28°, 6.31°, and 7.19° at L1/L2, L2/L3, L3/L4, and L4/L5 respectively (Fig. 38). While the preoperative amounts are unknown for this group it was promising to see the level adjacent to the instrumentation, L4/L5, had results similar to healthy group.

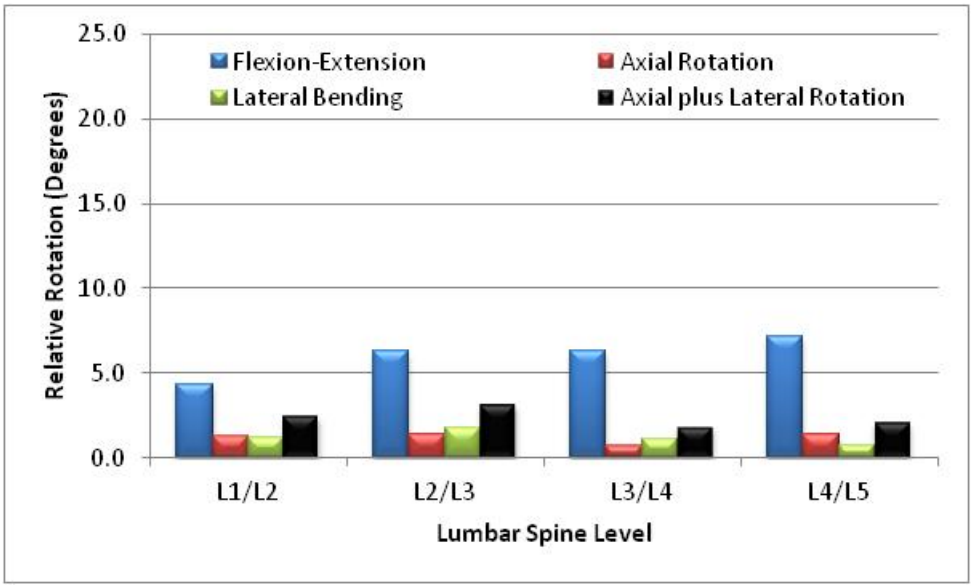

Figure 38. The overall amount of rotation achieved for each spinal level during the flexion extension activity.

During lateral bending activity this group ended up with two levels, L2/L3 and L3/L4, with more healthy results, and two levels, L1/L2 and L4/L5, with more degenerative results. The L2/L3 and L3/L4 levels had 8.33° and 8.6° of in-plane rotation and 4.47° and 7.23° of out-of-plane rotation respectively. While L1/L2 and L4/L5 had 7.06° and 5.75° of in-plane rotation and 8.63° and 8.37° of out-of-plane rotation respectively (Fig. 39). While the preoperative amounts are unknown for this group it appeared the level adjacent to the instrumentation, L4/L5, had not returned to a more normal motion for this activity.

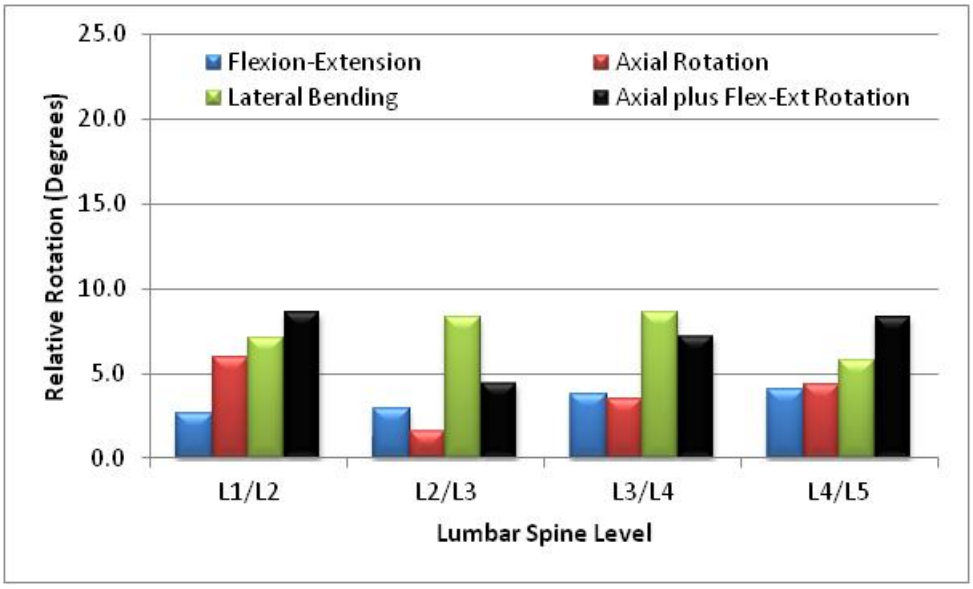

Figure 39. The overall amount of rotation achieved for each spinal level during the lateral bending activity.

Finally, for the axial rotation activity this group had from 1.5 to nearly 6 times as much out-of-plane rotation as in-plane rotation. The worst level was L2/L3 which only had 0.96° of in-plane rotation and 5.56° of out-of-plane rotation. The other three levels had values of 2.69°, 3.31°, and 2.67° in-plane rotations and 5.59°, 4.92°, and 8.22° out-of-plane rotations at L1/L2, L3/L4, and L4/L5 respectively (Fig. 40).

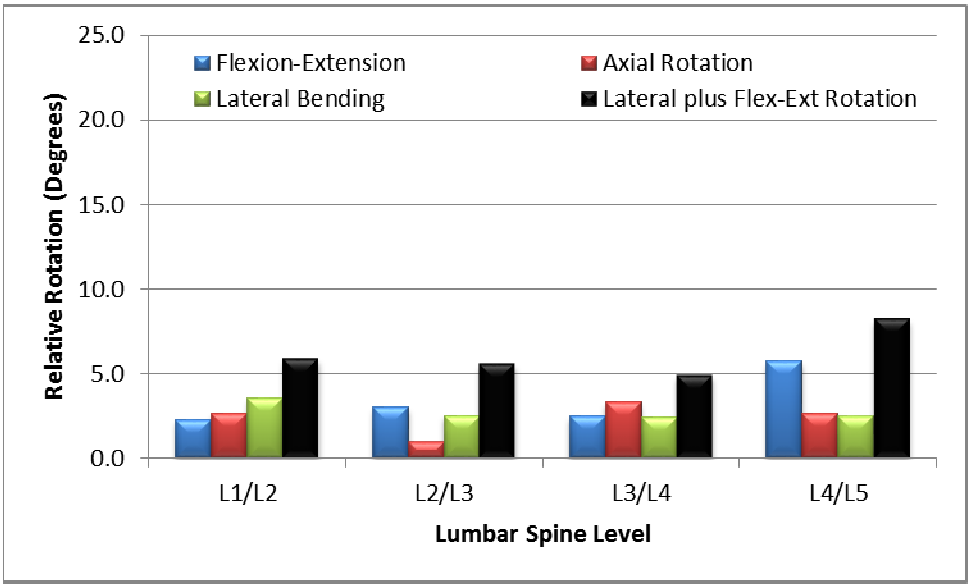

Figure 40. The overall amount of rotation achieved for each spinal level during the axial rotation activity.

3.2. Intervertebral Disc

3.2.1 Un-deformed Length

For the subjects that participated in this study the average lengths can be found in table 3. There were no significant differences in any of the groups when the means were compared with all pairs using Tukey-Kramer method. Overall the lengths were consistent through the lumbar spine with the only noticeable measurement that L4/L5 has the greatest average length with the rest of the levels having relatively similar lengths. Two of the major trends was that the lengths postoperatively increased from the preoperative lengths in most cases, and the L4/L5 lengths for the preoperative group with surgery happening at that location had smaller average length than healthy groups while the three subjects not having surgery actually were found to have a higher average length. One of the concerns was that some of the groups had higher un-deformed lengths then that of our healthy group. Typically as the disc degenerates the disc height will narrow. While this does not always occur, it is one of the major signs of degeneration. Therefore, the distance between the surfaces at neutral was found, and it was discovered the same groups actually have a higher distances at neutral as well (Table 4). This would hypothesize that while some of the subjects may have disc narrowing the average neutral height was not. Interestingly this was not the case for fusion group when compared preoperative lengths to postoperative lengths. The neutral lengths decreased after fusion while the un-deformed lengths increased. The reason for this phenomenon was that the subjects' weights also increased. This increased the stress over the same area to the point that the un-deformed length increased postoperatively. Appendix A.3 shows all of the lengths for the subjects. One of the interesting outliers for the un-deformed length was Fusion subject 4 with an average length at L4/L5 measured at 5.9 mm preoperatively. This person was much lower than the rest of subjects which

ranged from 8.63 to 20.58 mm. The interesting phenomenon was that this subject's surgery was at the L4/L5 level. While this measured height cannot be proved as the explanation warranting the surgery at this level, it was quite a fascinating coincidence.

Table 3. Average Un-deformed Lengths for Subject Groups

Identifier	Surgical Location	Average Lengths (mm)			
		L4/L5	L3/L4	L2/L3	L1/L2
Healthy	N/A	13.798	11.061	11.170	10.942
Low Back Pain	N/A	14.379	11.599	11.903	11.656
Degenerative	N/A	11.920	10.999	11.181	10.580
Preoperative Fusion	L5/S1	16.943	13.28	13.42	13.37
	L4/L5	11.025	12.018	11.758	10.368
	L3/L4 and L4/L5	13.53	14.29	13.84	12.61
	L4/L5 and L5/S1	12.12	13.11	7	8.7
Postoperative Fusion	L5/S1	17.033	13.323	13.547	13.463
	L4/L5	N/A	12.228	11.943	10.568
	L3/L4 and L4/L5	N/A	N/A	13.93	12.7
	L4/L5 and L5/S1	N/A	13.36	7	9
Postoperative Disc Replacement	L5/S1	8.630	9.860	7.000	8.390
Preoperative Facet	L4/L5 and L5/S1	14.140	13.145	12.780	12.195
Postoperative Facet	L4/L5 and L5/S1	N/A	15.190	12.410	12.325

Table 4. Neutral Lengths for Subject Groups

Identifier	Surgical Location	Average Lengths (mm)			
		L4/L5	L3/L4	L2/L3	L1/L2
Healthy	N/A	9.599	8.111	8.17	7.7
Low Back Pain	N/A	9.982	8.69	8.749	8.432
Degenerative	N/A	8.183	8.061	8.129	7.423
Preoperative Fusion	L5/S1	10.87	8.918	8.886	8.474
	L4/L5	7.632	8.191	7.863	6.969
	L3/L4 and L4/L5	9.266	10.469	10.158	9.161
	L4/L5 and L5/S1	8.844	7.581	3.923	6.781
Postoperative Fusion	L5/S1	10.589	8.573	8.588	8.089
	L4/L5	N/A	8.381	7.829	6.745
	L3/L4 and L4/L5	N/A	N/A	14.637	10.161
	L4/L5 and L5/S1	N/A	10.087	3.058	6.281
Postoperative Disc Replacement	L5/S1	6.244	6.818	4.717	5.775
Preoperative Facet	L4/L5 and L5/S1	10.015	9.433	9.163	8.315
Postoperative Facet	L4/L5 and L5/S1	N/A	10.8	9.046	8.287

3.2.2 Stress

The following sections will cover the stresses found in intervertebral discs. For the average stress over the entire disc all subjects in this study were found to have a higher normal stress than shear stress. The shear stress was found to be around 100 times smaller than the normal stress therefore all results center on the normal stress paths.

3.2.2.1 *Flexion-Extension*

In the healthy group this normal stress tended to get less compressive as the subject travels from maximum flexion to maximum extension. The normal average stresses for the disc at maximum flexion were -0.61 ± 0.22 MPa at L1/L2, -0.47 ± 0.15 MPa at L2/L3, -0.52 ± 0.24 MPa at L3/L4, and -0.84 ± 0.17 MPa at L4/L5. The L2/L3 spinal unit was the only location which has a lower stress at maximum flexion than mid flexion which was -0.52 ± 0.14 MPa. The rest of the levels L1/L2, L3/L4, and L4/L5 had increasing overall stress to -0.59 ± 0.24 MPa, -0.54 ± 0.22 MPa, and -0.80 ± 0.2 MPa respectively. At neutral the stress increased at all levels to -0.56 ± 0.08 MPa at L1/L2, -0.5 ± 0.03 MPa at L2/L3, -0.5 ± 0.06 MPa at L3/L4, and -0.65 ± 0.09 MPa at L4/L5. Finally at maximum extension, L1/L2 remained rather constant at -0.56 ± 0.21 MPa, L2/L3 increased to -0.43 ± 0.23 MPa, L3/L4 increased to -0.43 ± 0.2 MPa, and L4/L5 increased to -0.55 ± 0.24 MPa (Fig. 41). The decrease from neutral to extension was believed to be two-fold. First in some subjects the anterior portion of the disc went into tension which lowers the overall average. Second as the subject lean back the

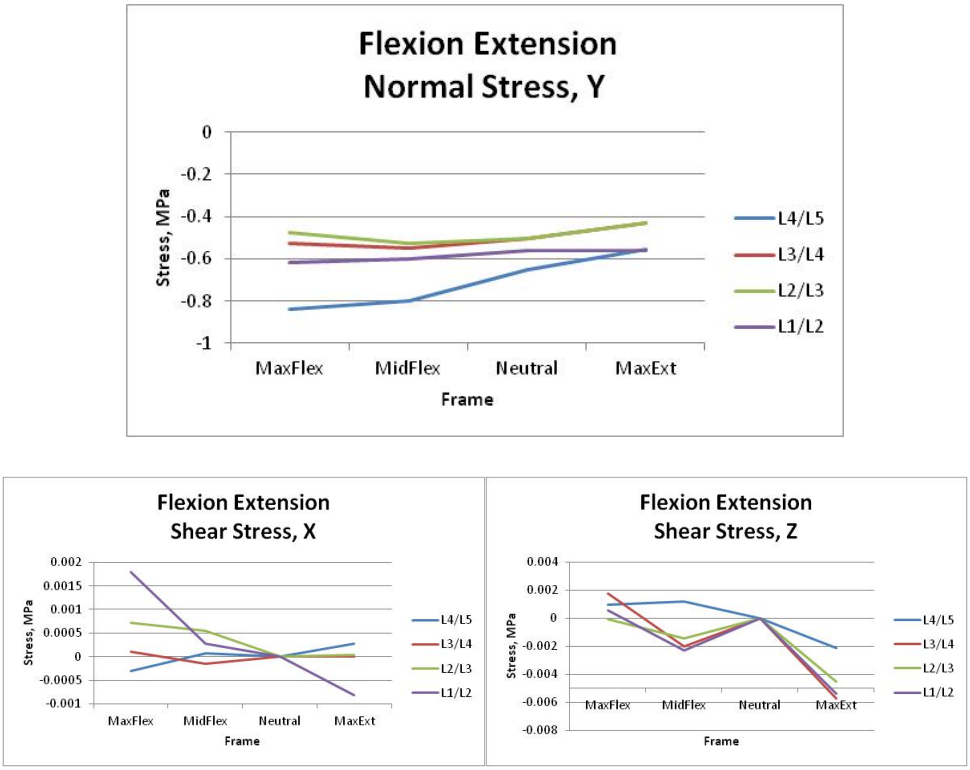

Figure 41. The average stress in the three principal directions for the normal subjects during flexion-extension.

stress was offloaded to the facets. The overall average stress did remain compressive throughout the entire activity. Figure 42 is a healthy subject's disc taken at all the frames besides neutral with each of the atlas vertices plotted with its corresponding stress color. This subject had only 1.5° of out-of-plane rotation during the activity, and it can be seen that the stresses follow with the in-plane rotation. Appendix A.4 contains the visualized magnitude stress profiles for all subjects it can be seen that the healthy subjects stress profile follows in the direction of the in-plane motion.

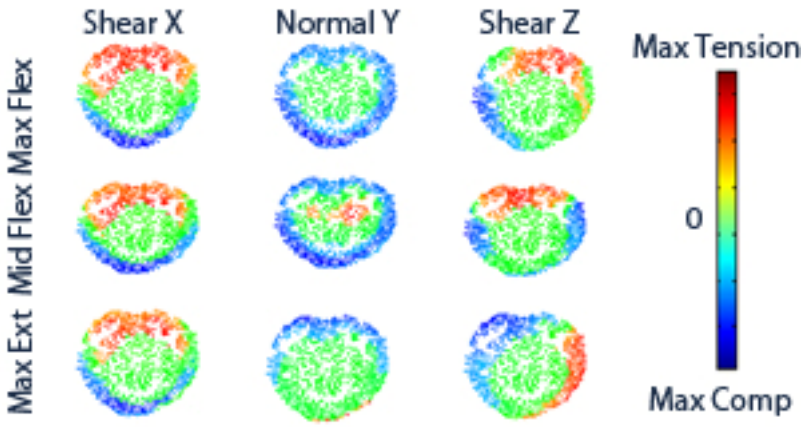

Figure 42. Stress profile for a healthy subject at a single level during the flexion-extension activity.

The normal stress at all spinal units besides the L4/L5 unit experienced little overall change from maximum flexion to maximum extension. The stresses at L1/L2 were found to be -0.56 ± 0.14 MPa, -0.49 ± 0.17 MPa, -0.54 ± 0.06 MPa, and -0.43 ± 0.22 MPa at maximum flexion, mid flexion, neutral, and maximum extension respectively. The stresses at L2/L3 were found to be -0.49 ± 0.09 MPa, -0.52 ± 0.11 MPa, -0.45 ± 0.12 MPa, and -0.43 ± 0.14 MPa at maximum flexion, mid flexion, neutral, and maximum extension respectively. The stresses at L3/L4 were found to be -0.43 ± 0.25 MPa, -0.45 ± 0.14, -0.49 ± 0.06 MPa, and -0.41 ± 0.12 MPa at maximum flexion, mid flexion, neutral, and maximum extension respectively. The L4/L5 spinal unit tended to follow a more normal pattern with stresses of -0.85 ± 0.17 MPa at maximum flexion, -0.78 ± 0.11 MPa at mid flexion, and -0.69 ± 0.1 MPa at neutral. The only difference was at maximum extension stress had increased compressive to -0.74 ± 0.24 MPa (Fig. 43). Figure 44 is a low back pain subject's disc and this subject had 2.6° of out-of-plane rotation during the activity of which majority was lateral bending. From the stress field it can be seen that the stress at the maximums tended to drift from center edge of the disc following with the increased lateral out-of-plane rotation for this subject. Appendix A.4 has all the subjects and

shows varying results throughout; however, all subjects have stress patterns that follow with the kinematic motion.

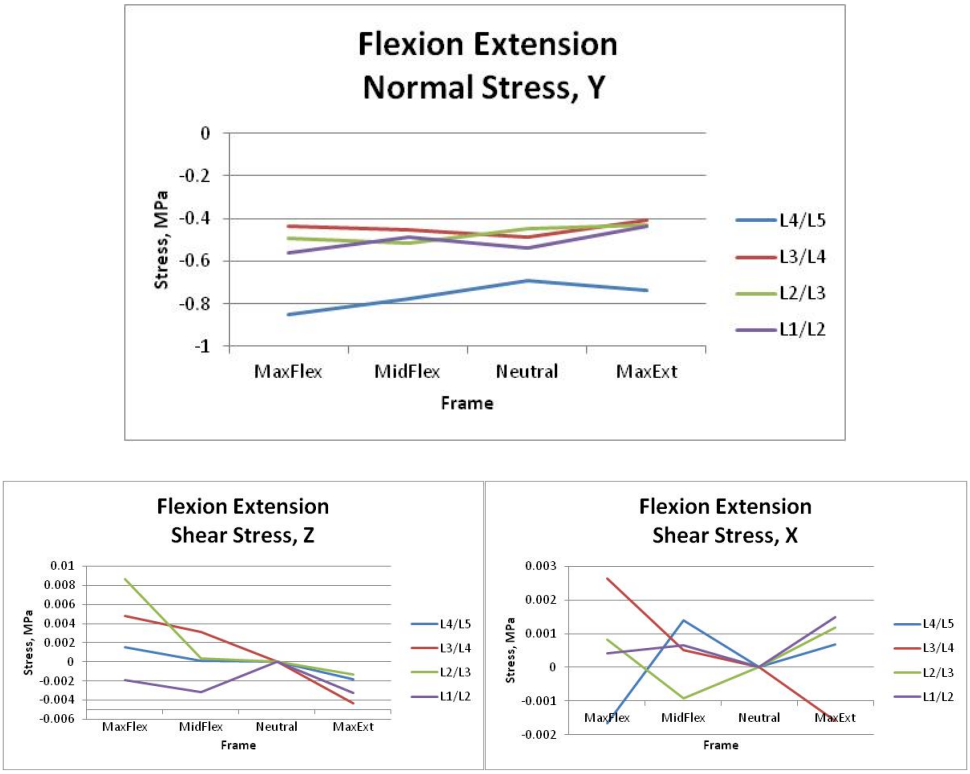

Figure 43. The average stress in the three principal directions for the low back pain subjects during flexion-extension.

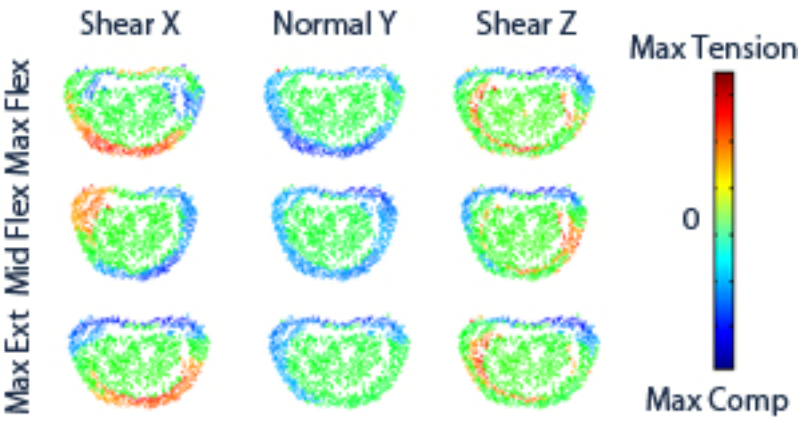

Figure 44. Stress profile for a low back pain subject at a single level during the flexion-extension activity.

The degenerative subjects' average normal stress at the L4/L5 spinal unit followed the normal pattern of the stress of decreasing stress from maximum flexion to maximum extension; however the rate of change from neutral to maximum extension was greater. For L4/L5 level the stress at maximum flexion was -0.73 ± 0.19 MPa, mid flexion was -0.71 ± 0.31 MPa, neutral was -0.68 ± 0.14 MPa, and maximum extension was -0.52 ± 0.19 MPa. The L2/L3 spinal unit had stress at maximum flexion was -0.57 ± 0.3 MPa, mid flexion was -0.5 ± 0.19 MPa, neutral was -0.51 ± 0.08 MPa, and maximum extension was -0.5 ± 0.17 MPa. This was a similar pattern to the low back pain subjects where the average stress throughout the motion was relatively the same. One major difference in this group from the previous two was that at the L1/L2 and L3/L4 spinal units the compressive stress decreased as the motion went to mid flexion from neutral and increased from mid flexion to maximum flexion. The stresses at L1/L2 were found to be -0.58 ± 0.25 MPa, -0.47 ± 0.15 MPa, -0.57 ± 0.11 MPa, and -0.46 ± 0.18 MPa at maximum flexion, mid flexion, neutral, and maximum extension respectively. The stresses at L3/L4 were found to be -0.57 ± 0.19 MPa, -0.47 ± 0.17 MPa, -0.68 ± 0.08 MPa, and -0.39 ± 0.17 MPa at maximum flexion, mid flexion, neutral, and maximum extension respectively (Fig. 45). The disc stress profile in Figure 46 shows that the degenerative subject had stress in areas of the disc which were unexpected such as compressive posterior stress at mid flexion. This subject had 12.12° degrees of out-of-plane rotation and it is evident at maximum flexion where the maximum stress had traveled towards the outer portion of the disc. Appendix A.4 has all the subjects and it can be seen that the degenerative group has shown signs of abnormal disc loading with areas of the disc under greater stress than in the normal subjects.

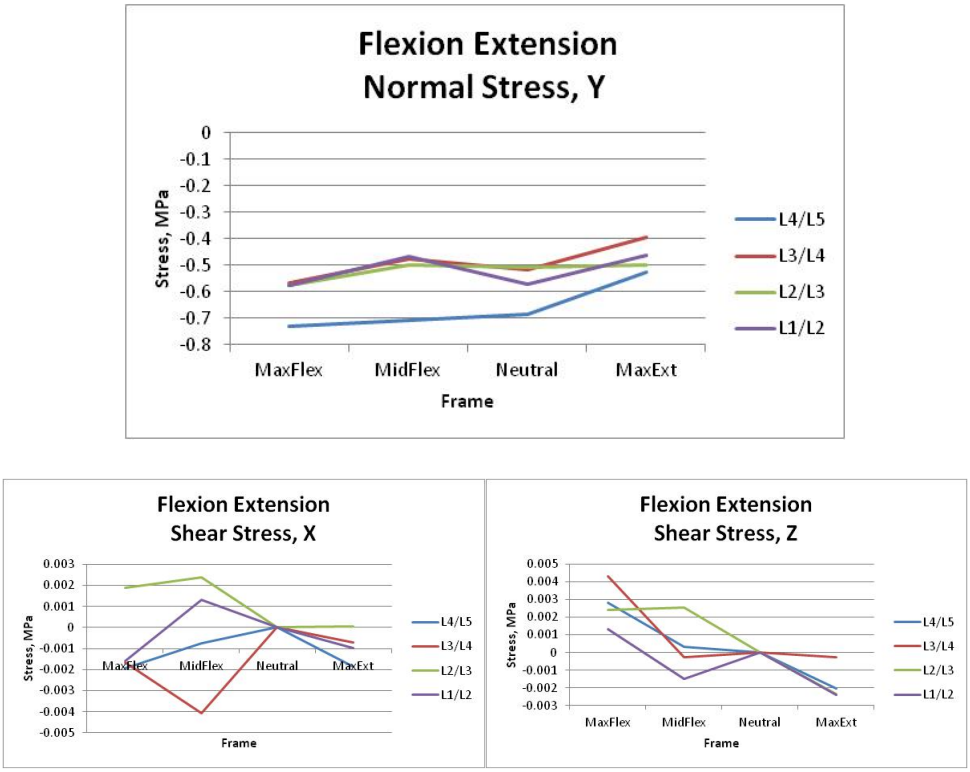

Figure 45. The average stress in the three principal directions for the degenerative subjects during flexion-extension.

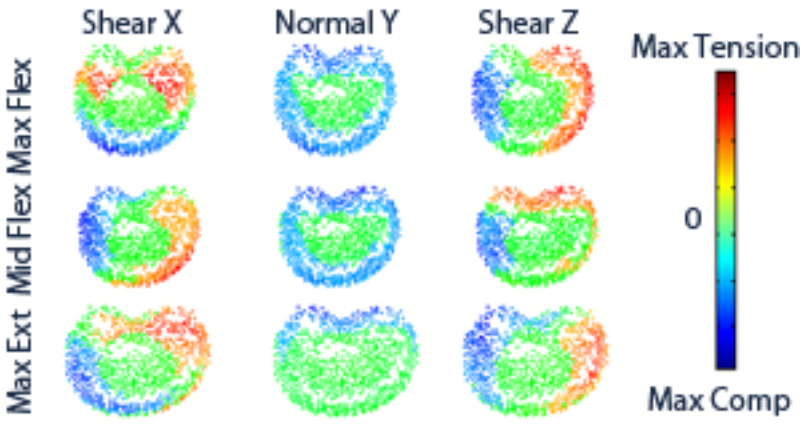

Figure 46. Stress profile for a degenerative subject at a single level during the flexion-extension activity.

The preoperative fusion group was found to have different normal average stress profiles for all four spinal units. The L4/L5 spinal unit has an unusual path where the mid flexion normal average stress, -0.57 ± 0.64 MPa is around half the magnitude when compared to neutral, -1.08 ± 0.46 MPa, and maximum flexion, -1.07 ± 0.4 MPa. The L3/L4 spinal unit increased from neutral, -0.68 ± 0.23 MPa, to mid flexion, -0.94 ± 0.43 MPa, and maximum extension, -0.71 ± 0.28 MPa. The stress decreased from mid flexion, -0.94 ± 0.43 MPa to maximum flexion, -0.85 ± 0.57 MPa. The L2/L3 spinal unit followed a more normal path from mid flexion to maximum extension going from -0.81 ± 0.33 MPa, to -0.71 ± 0.18 MPa, and to -0.63 ± 0.19 MPa. The average stress decreased the mid flexion, -0.81 ± 0.33 MPa, to maximum flexion -0.71 ± 0.41 MPa. Finally the L1/L2 spinal unit has decreasing stress from neutral, -0.86 ± 0.33 MPa, to maximum flexion, -0.79 ± 0.42 MPa, or extension, -0.74 ± 0.27 MPa (Fig. 47). The individual disc stress profile in Figure 48 shows how the abnormal disc loading in this group. This subject had 9.89° of out-of-plane rotation and had only 5.23° of in-plane rotation. From the figure it is evident that during the rotation areas of the disc which should have been loaded are experiencing lower stress and this stress has migrated to the outer portions of the disc as well as the posterior section of the disc. Appendix A.4 has all the subjects and it can be seen that the preoperative group has signs of major abnormal disc loading with areas of the disc under greater stress than in the normal subjects and less portions of the disc unloaded during the motion.

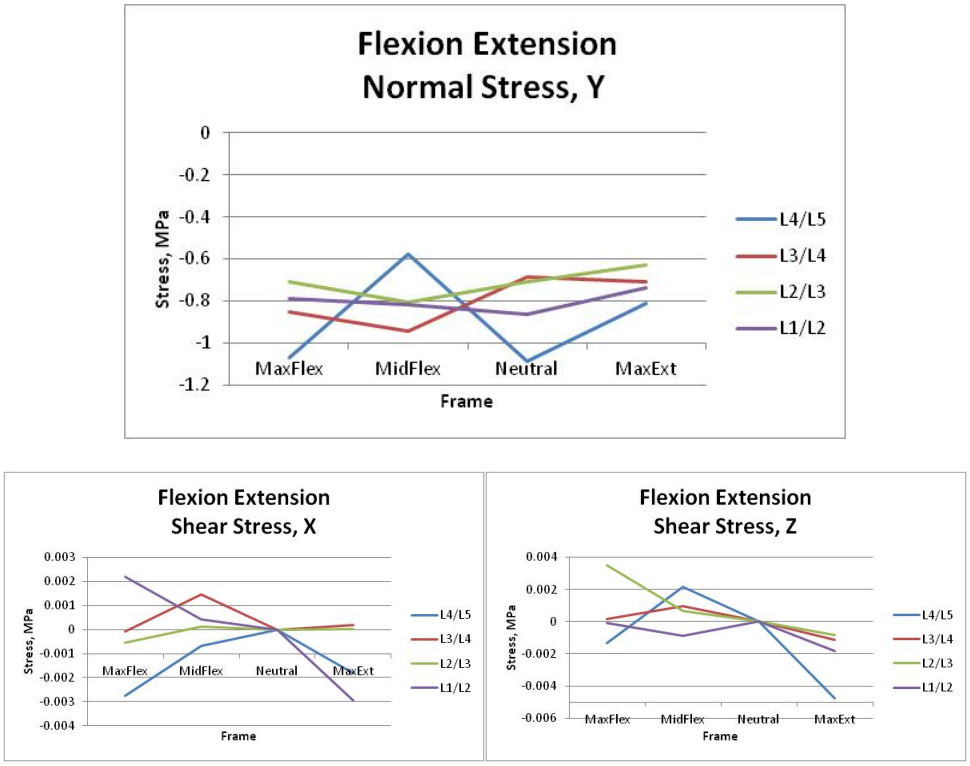

Figure 47. The average stress in the three principal directions for the preoperative fusion subjects during flexion-extension.

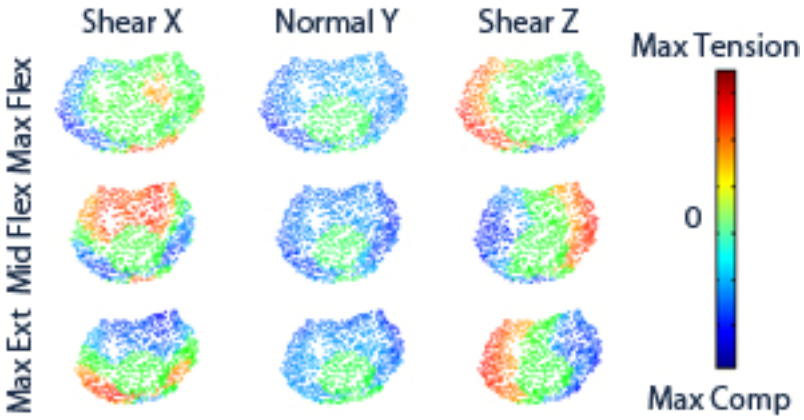

Figure 48. Stress profile for a preoperative fusion subject at a single level during the flexion-extension activity.

The postoperative fusion group interestingly had two spinal units L4/L5 and L3/L4 had average normal stress paths that had decreasing stress as the subjects moved from maximum flexion to maximum extension. The stress at L4/L5 and L3/L4 respectively was -1.06 ± 0.09 MPa and -0.84 ± 0.28 MPa at maximum flexion, -0.86 ± 0.28 MPa and -0.65 ± 0.40 MPa at mid flexion, -0.75 ± 0.19 MPa and -0.6 ± 0.2 MPa at neutral, and -0.64 ± 0.13 MPa and -0.41 ± 0.37 MPa at maximum extension. L1/L2 and L2/L3 spinal units had increasing stress from maximum flexion, -0.67 ± 0.23MPa and -0.58 ± 0.28 MPa, to mid flexion, -0.76 ± 0.17 MPa and -0.63 ± 0.32 MPa. The stress at L1/L2 and L2/L3 decreased from mid flexion, -0.76 ± 0.17 MPa and -0.63 ± 0.32 MPa, to neutral, -0.71 ± 0.11 MPa and -0.58 ± 0.30 MPa, and finally to maximum extension, -0.52 ± 0.19 MPa and -0.48 ± 0.26 MPa (Fig. 49). The sample subject in Figure 50 had small change from preoperative (Fig. 50). Appendix A.4 has all the subjects and it can be seen that the postoperative group has signs of major abnormal disc loading with areas of the disc under greater stress than in the normal subjects and less portions of the disc unloaded during the motion. Although the average stress path seemed to return to a more normal path, the subject's disc stress profiles still had abnormal stress loads from the increased out-of-plane motions.

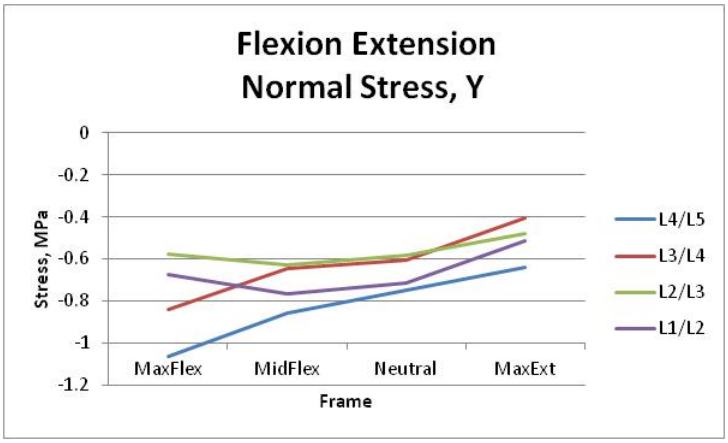

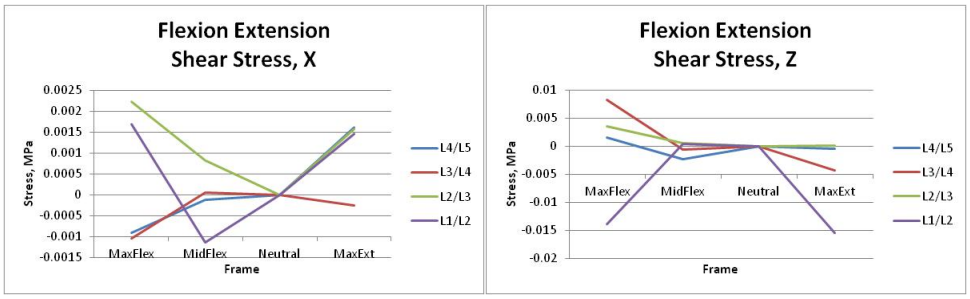

Figure 49. The average stress in the three principal directions for the postoperative fusion subjects during flexion-extension.

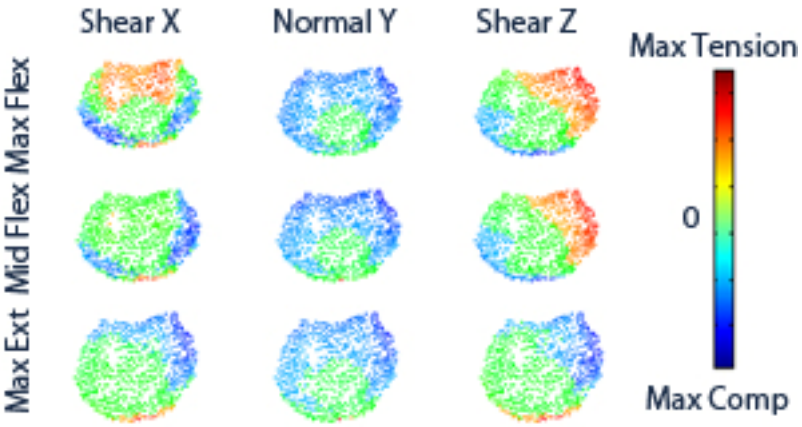

Figure 50. Stress profile for a preoperative fusion subject at a single level during the flexion-extension activity.

The preoperative facet group, although only containing two subjects, was the only group to have a tensile normal stress which occurred at the maximum extension frame for L4/L5 spinal unit. The stresses at L4/L5 were found to be -0.19 ± 0.64 MPa, -0.19 ± 0.53 MPa, -0.54 ± 0.02 MPa, and 0.16 ± 1.04 MPa at maximum flexion, mid flexion, neutral, and maximum extension respectively. The stresses at L1/L2 were found to be -0.63 ± 0.12 MPa, -0.29 ± 0.41 MPa, -0.56 ± 0.04 MPa, and -0.63 ± 0.24 MPa at maximum flexion, mid flexion, neutral, and maximum extension respectively. The stresses at L2/L3 were found to be -0.26 ± 0.37 MPa, -0.67 ± 0.63 MPa, -0.53 ± 0.01 MPa, and -0.28 ± 0.4 MPa at maximum flexion, mid flexion, neutral, and maximum extension respectively. The stresses at L3/L4 were found to be -0.37 ± 0.52 MPa, -0.53 ± 0.11 MPa, -0.54 ± 0.01 MPa, and -0.27 ± 0.39 MPa at maximum flexion, mid flexion, neutral, and maximum extension respectively. The rest of the spinal units had less relative change over the entire motion (Fig. 51). The disc stress profiles showed similar abnormal stress locations as in the preoperative fusion group with areas of the disc typically found under stress no longer carrying the load (Fig. 52).

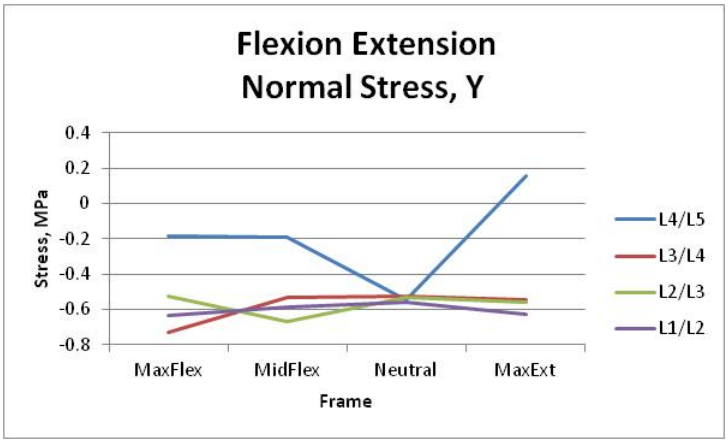

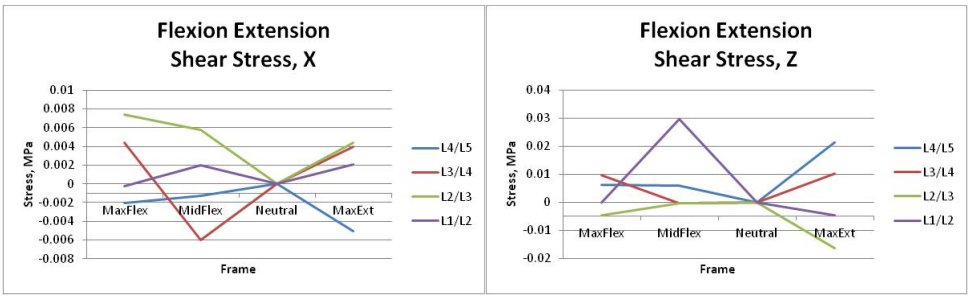

Figure 51. The average stress in the three principal directions for the preoperative facet subjects during flexion-extension.

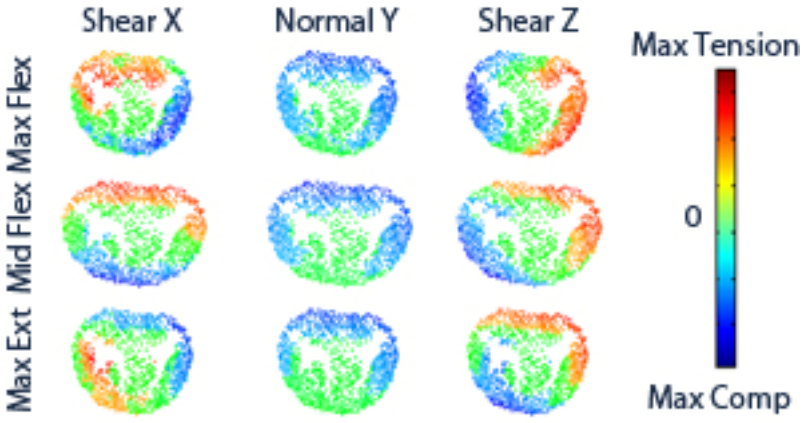

Figure 52. Stress profile for a preoperative facet subject at a single level during the flexion-extension activity.

The postoperative facet group had no spinal unit which returned to a more normal stress path. The L1/L2 and L2/L3 units both showed decreasing stress from neutral, -0.29 ± 0.41 MPa and -0.53 ± 0.05 MPa respectively, to maximum extensions, -0.23 ± 0.32 MPa and -0.25 ± 0.15 MPa respectively, and maximum flexion, -0.27 ± 0.39 MPa and -0.26 ± 0.13 MPa respectively. While L3/L4 level had increasing stress from maximum flexion, -0.32 ± 0.46 MPa, to mid flexion, -0.37 ± 0.52 MPa, as well as from neutral, -0.26 ± 0.37 MPa, to maximum extension, -0.32 ± 0.46 MPa (Fig. 53). The L4/L5 spinal unit does not show up on the graphs because the surgery required that disc be removed and replaced with instrumentation. The disc stress profiles showed similar abnormal stress locations as they did preoperatively and the two subjects did not seem to have any return to a more normal loading pattern (Fig. 54).

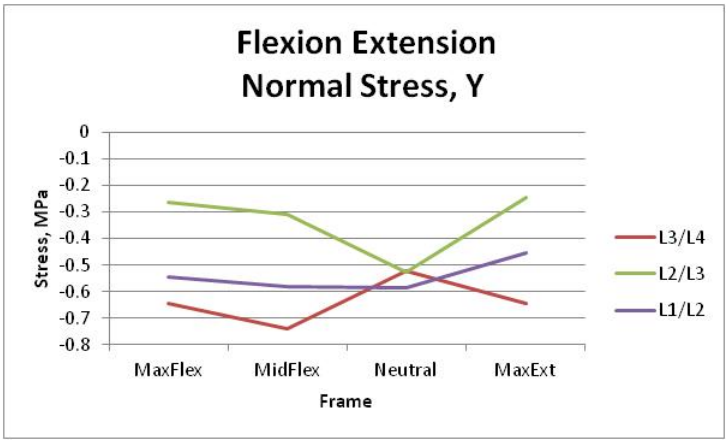

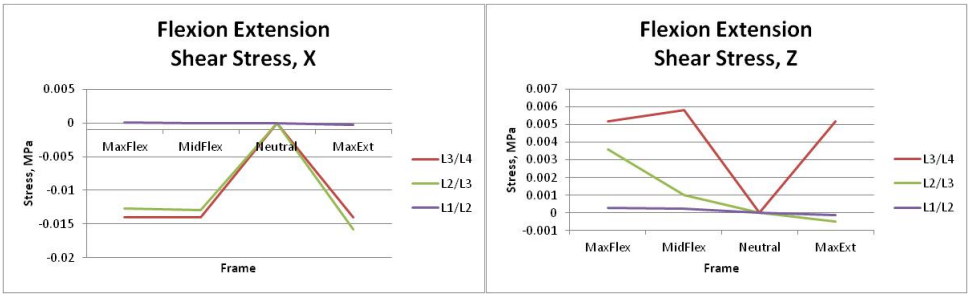

Figure 53. The average stress in the three principal directions for the postoperative facet subjects during flexion-extension.

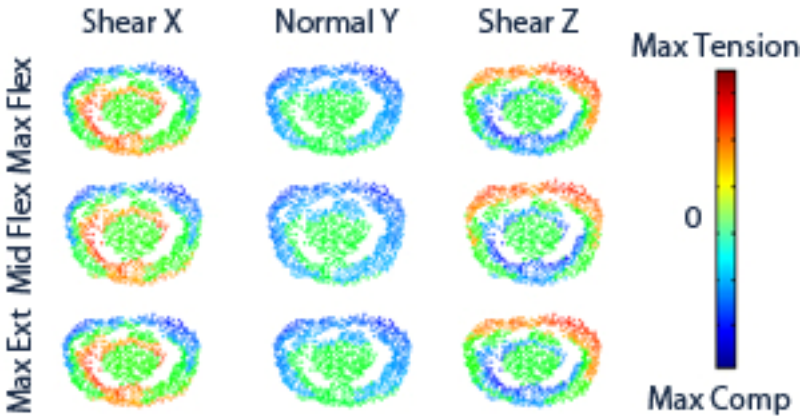

Figure 54. Stress profile for a postoperative facet subject at a single level during the flexion-extension activity.

The final group was the postoperative disc replacement subjects which again was a rather small group. Nonetheless looking at the normal stress the subjects had some levels return to a somewhat normal stress path from maximum flexion to maximum extension. The normal stresses were -0.65 ± 0.92 MPa at maximum flexion, -0.55 ± 0.78 MPa at mid flexion, -0.29 ± 0.41 MPa at neutral, and -0.39 ± 0.55 MPa at maximum extension at L1/L2. The normal stresses were -0.43 ± 0.6 MPa at maximum flexion, -0.46 ± 0.65 MPa at mid flexion, -0.31 ± 0.44 MPa at neutral, and -0.29 ± 0.40 MPa at maximum extension at L2/L3. The normal stresses were -0.49 ± 0.69 MPa at maximum flexion, -0.37 ± 0.53 MPa at mid flexion, -0.27 ± 0.39 MPa at neutral, and -0.24 ± 0.35 MPa at maximum extension at L3/L4. Finally at L4/L5 the stresses were -0.24 ± 0.33 MPa at maximum flexion, -0.33 ± 0.46 MPa at mid flexion, -0.24 ± 0.34 MPa at neutral, and -0.12 ± 0.17 MPa at maximum extension (Fig. 55). The disc stress profiles showed similar abnormal stress locations as in the other surgical subjects with no signs of return to a more normal pattern following the surgical intervention (Fig. 56).

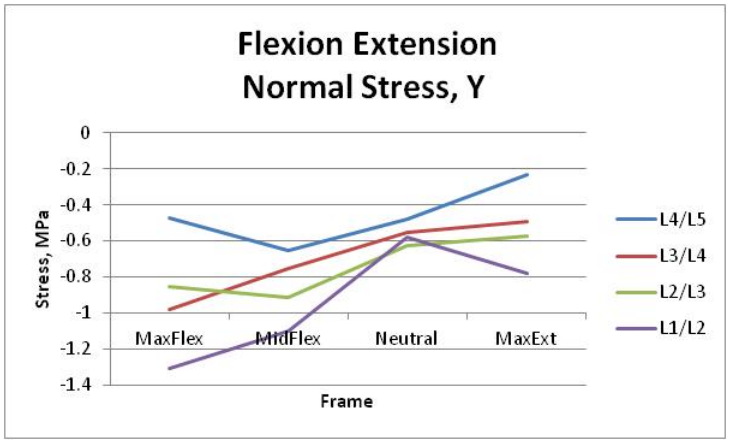

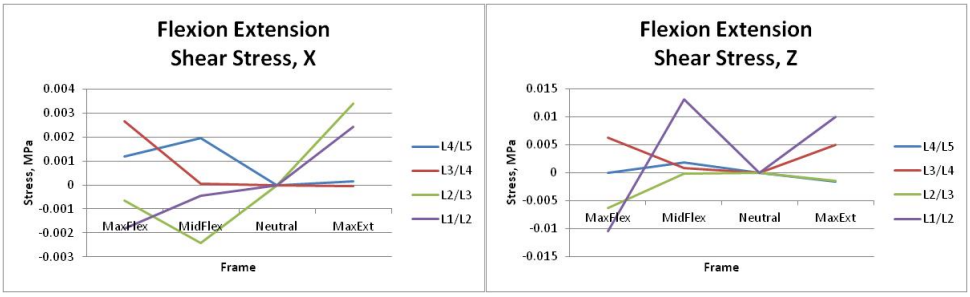

Figure 55. The average stress in the three principal directions for the postoperative disc subjects during flexion-extension.

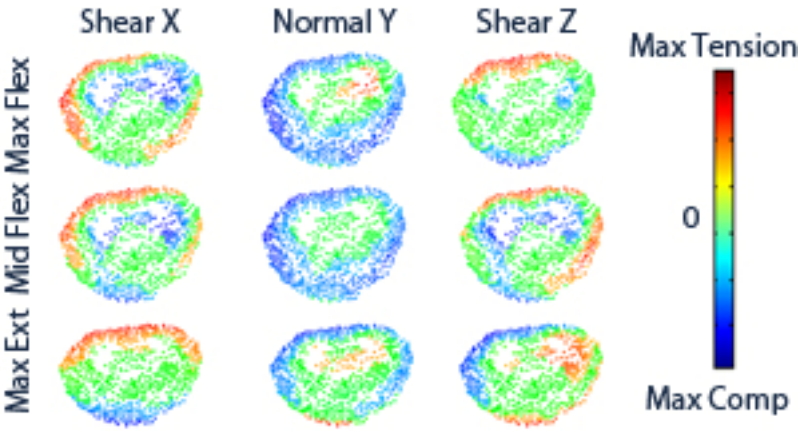

Figure 56. Stress profile for a preoperative fusion subject at a single level during the flexion-extension activity.

3.2.2.2 *Axial Rotation*

In the normal group the normal stress tends to get less compressive as the subject travels from neutral to maximum left or right. The L4/L5 spinal unit is the only spinal unit which increases stress when moving from neutral. The stress at maximum left was -0.33 ± 0.25 MPa at L1/L2, -0.43 ± 0.15 MPa at L2/L3, -0.32 ± 0.28 MPa at L3/L4, and -0.62 ± 0.18 MPa at L4/L5. The stress at neutral was -0.44 ± 0.25 MPa at L1/L2, -0.62 ± 0.16 MPa at L2/L3, -0.52 ± 0.32 MPa at L3/L4, and -0.58 ± 0.2 MPa at L4/L5. The stress at maximum right was -0.29 ± 0.26 MPa at L1/L2, -0.41 ± 0.19 MPa at L2/L3, -0.31 ± 0.28 MPa at L3/L4, and -0.66 ± 0.18 MPa at L4/L5 (Fig. 57). The decrease from neutral to maximum left and right is believed to the stress offloaded to the facets while the increase seemed to be a posterior compression at L4/L5. From the visualized normal magnitude stress profiles it can be seen that the healthy subjects stress profile stays relatively equal during the motion for this subject; however given the complex motion for some of the subjects, the normal stresses are not always equal. While the axial stresses in both the X and Z direction had mirrored stresses at the opposite maximums (Fig. 58).

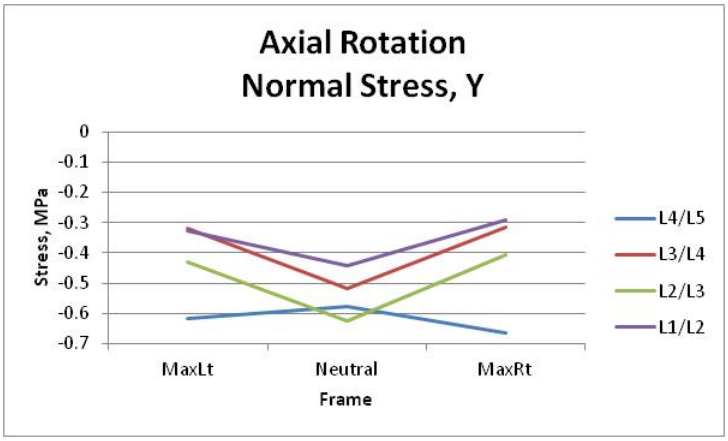

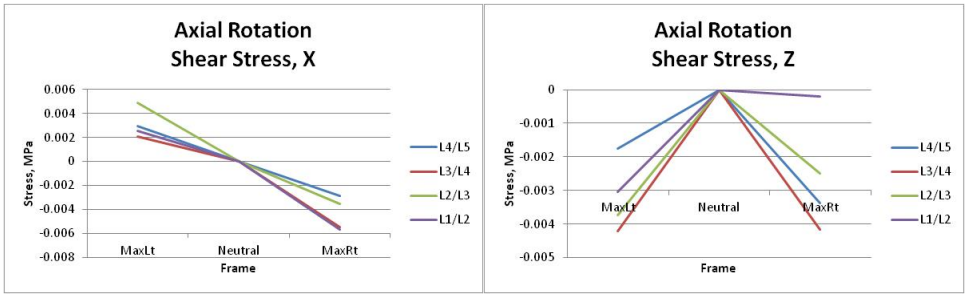

Figure 57. The average stress in the three principal directions for the healthy subjects during axial rotation.

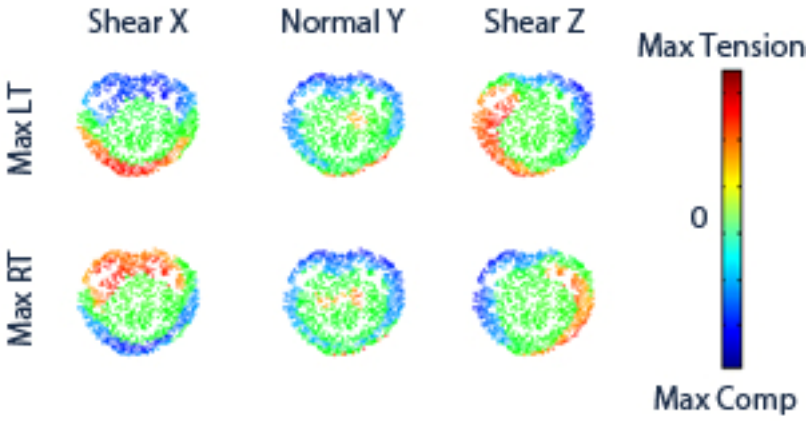

Figure 58. Stress profile for a healthy subject at a single level during the axial rotation activity.

The low back pain group for the axial rotation activity had all levels decrease in stress from neutral to maximum left and maximum right. The stress at maximum left was -0.44 ± 0.25 MPa at L1/L2, -0.52 ± 0.23 MPa at L2/L3, -0.41 ± 0.18 MPa at L3/L4, and -0.83 ± 0.28 MPa at L4/L5. The stress at neutral was -0.57 ± 0.26 MPa at L1/L2, -0.76 ± 0.36 MPa at L2/L3, -0.57 ± 0.13 MPa at L3/L4, and -1.01 ± 0.55 MPa at L4/L5. The stress at maximum right was -0.38 ± 0.23 MPa at L1/L2, -0.51 ± 0.24 MPa at L2/L3, -0.47 ± 0.2 MPa at L3/L4, and -0.87 ± 0.36 MPa at L4/L5 (Fig. 59). This decreasing stress at the maximum left and right seems to be the result that in some subjects the outer portions of the disc went into tension lowering the overall average stress in the disc as well as offloading the stress to the facets. The sample subject in Figure 60 had some mirroring of axial stresses between the maximums. The normal stress at maximum left showed the signs of lateral motion and maximum right showed the tension that occurs in some of the anterior portions of the discs.

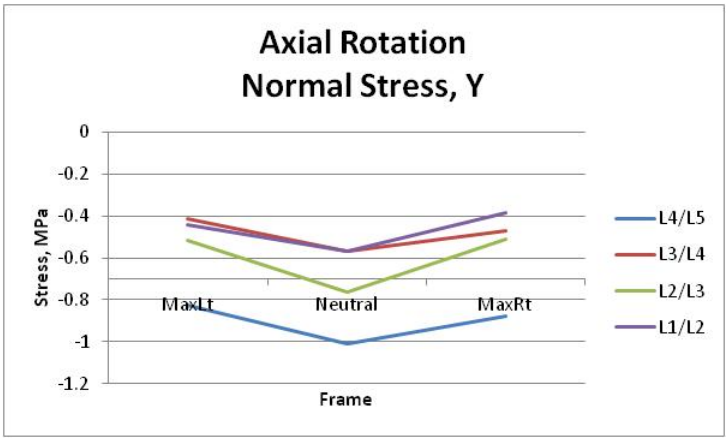

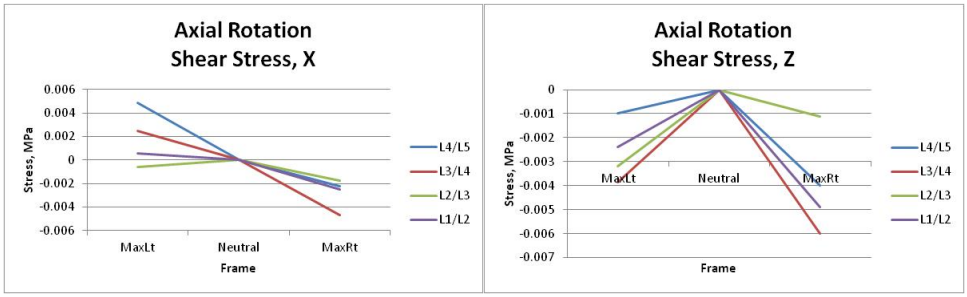

Figure 59. The average stress in the three principal directions for the low back pain subjects during axial rotation.

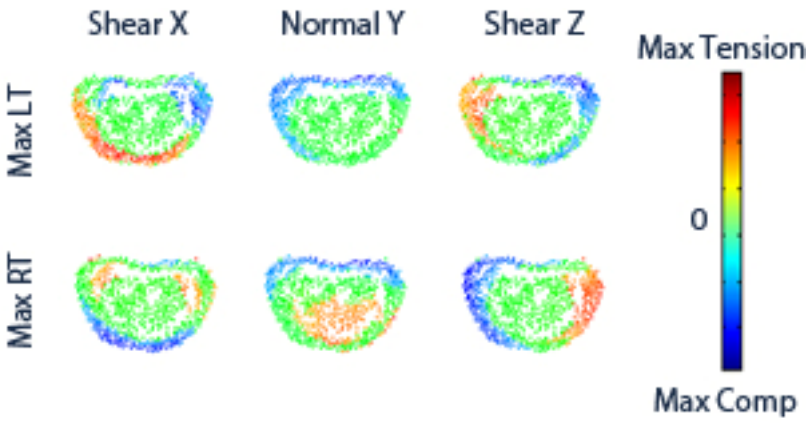

Figure 60. Stress profile for a low back pain subject at a single level during the axial rotation activity.

The degenerative groups' normal stresses also follow a similar average stress path as the low pain back group with decreasing stress from neutral to the two maximums. The rate of change from neutral at L1/L2, L3/L4, and L4/L5 to maximum is not as much as the low back pain group though. The stress at L1/L2 was -0.64 ± 0.35 MPa at maximum left, -0.68 ± 0.39 MPa at neutral, and -0.58 ± 0.31 MPa at maximum right. The stress at L2/L3 was -0.67 ± 0.12 MPa at maximum left, -0.95 ± 0.38 MPa at neutral, and -0.69 ± 0.33 MPa at maximum right. The stress at L3/L4 was -0.52 ± 0.19 MPa at maximum left, -0.57 ± 0.39 MPa at neutral, and -0.43 ± 0.28 MPa at maximum right. The stress at L4/L5 was -0.7 ± 0.31 MPa at maximum left, -0.77 ± 0.2 MPa at neutral, and -0.66 ± 0.26 MPa at maximum right (Fig. 61). The sample subject in Figure 60 is shows that the axial stresses no longer mirror between the maximums. The normal stresses show similar results to the low back pain subjects (Fig. 62).

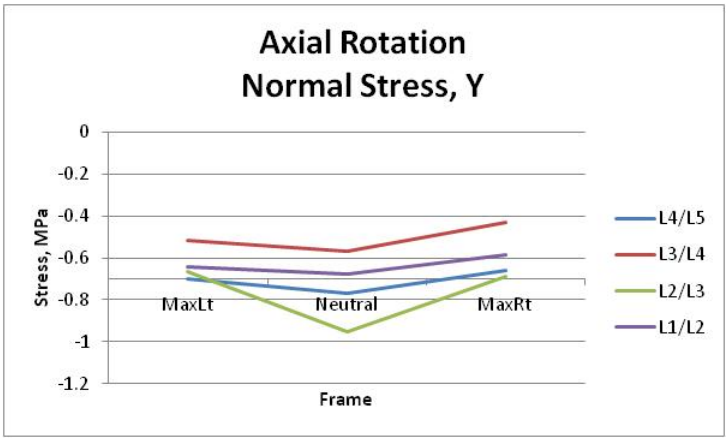

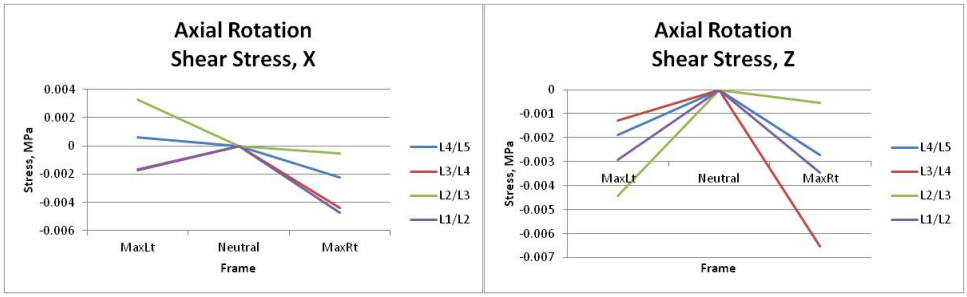

Figure 61. The average stress in the three principal directions for the degenerative subjects during axial rotation.

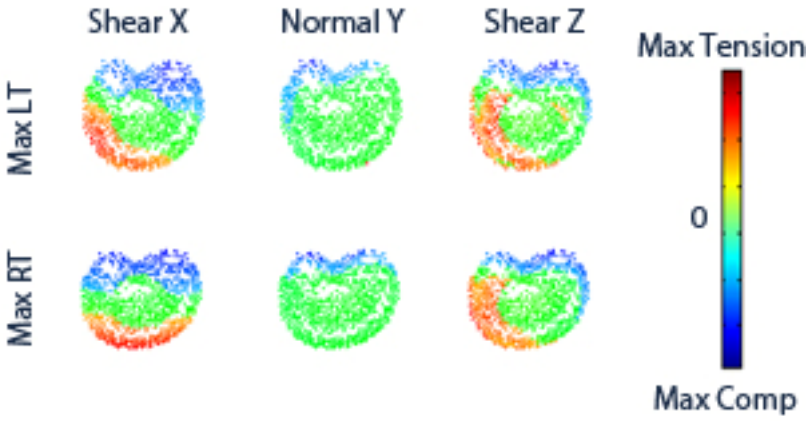

Figure 62. Stress profile for a degenerative subject at a single level during the axial rotation activity.

The preoperative fusion subjects had increased stress at all levels from neutral to maximum left and right except the L3/L4 spinal unit which followed with the more normal path of decreasing stress. The stress at maximum left was -1.09 ± 0.6 MPa at L1/L2, -0.94 ± 0.73 MPa at L2/L3, -0.66 ± 0.43 MPa at L3/L4, and -1.52 ± 0.57 MPa at L4/L5. The stress at neutral was -0.71 ± 0.45 MPa at L1/L2, -0.82 ± 0.7 MPa at L2/L3, -0.81 ± 0.71 MPa at L3/L4, and -1.25 ± 1.5 MPa at L4/L5. The stress at maximum right was -1.89 ± 0.62 MPa at L1/L2, -0.86 ± 0.56 MPa at L2/L3, -0.51 ± 0.41 MPa at L3/L4, and -1.37 ± 0.58 MPa at L4/L5 (Fig. 63). The individual subject discs show that the increase in stress follows with the increase in the out-of-plane motion of the compressive motions. Subjects show both compressive stresses from lateral bending and flexion during the axial rotation activity. The preoperative group was also the first group to have subjects under a more constant stress at the maximums causing the disc to not have a chance to rest (Fig. 64).

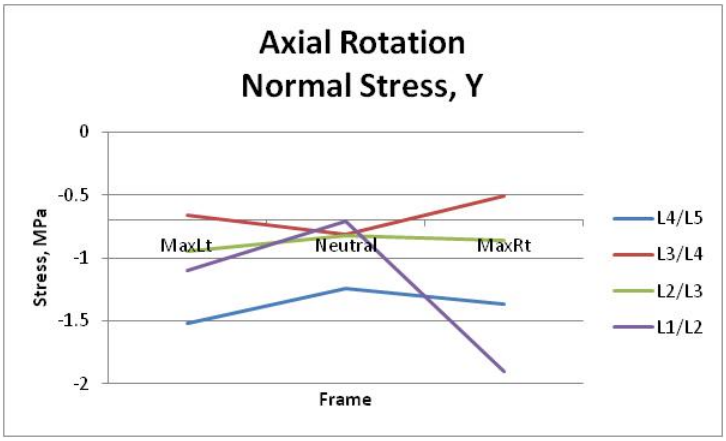

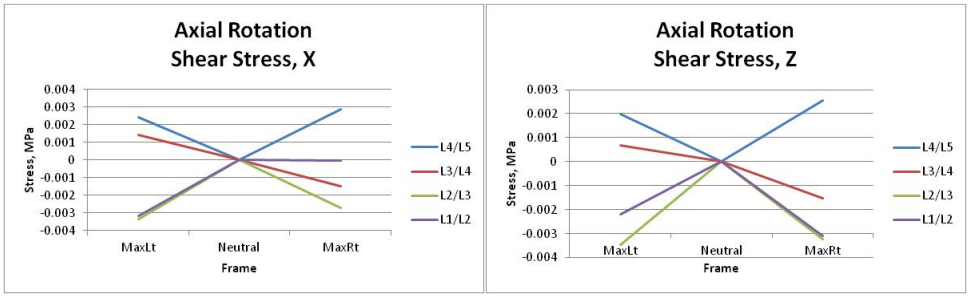

Figure 63. The average stress in the three principal directions for the preoperative fusion subjects during axial rotation.

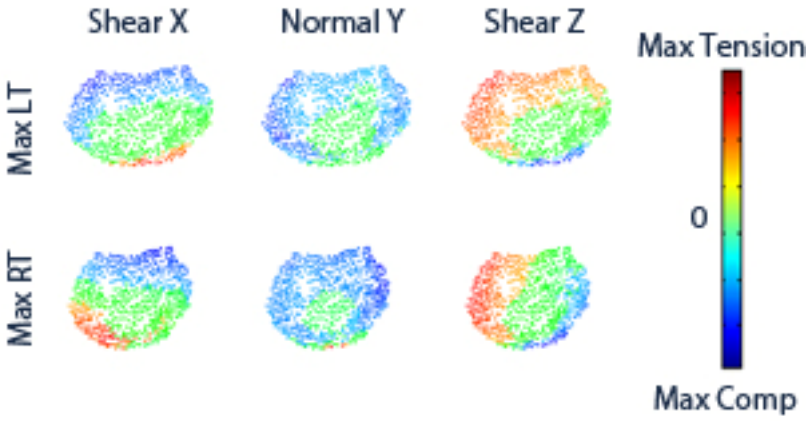

Figure 64. Stress profile for a preoperative fusion subject at a single level during the axial rotation activity.

Postoperatively the fusion group experiences relatively no change at L2/L3 and L3/L4 spinal unit for the normal average stress. The stresses at these levels were -0.65 ± 0.31 MPa and -0.72 ± 0.47 MPa at maximum left, -0.73 ± 0.33 MPa and -0.68 ± 0.34 MPa at neutral, and -0.71± 0.38 MPa and -0.7 ± 0.4 MPa at maximum right respectively. L4/L5 returned to a more normal pattern with normal stress decreasing toward the maximums. The stresses were -1.12 ± 0.02 MPa at maximum left, -1.23 ± 0.4 MPa at neutral, and -0.93 ± 0.16 MPa at maximum right. The L1/L2 level kept a similar normal stress path but decreased in magnitude from the preoperative average. The stresses were -0.48 ± 0.31 MPa at maximum left, -0.44 ± 0.38 MPa at neutral, and -0.57 ± 0.35 MPa at maximum right (Fig. 65). In Figure 66 it can be seen that the sample subject does not return to a more loading pattern following the fusion. Furthermore, the disc loading was still more constant over the disc. Subjects had both compressive stresses from lateral bending and flexion during the axial rotation activity.

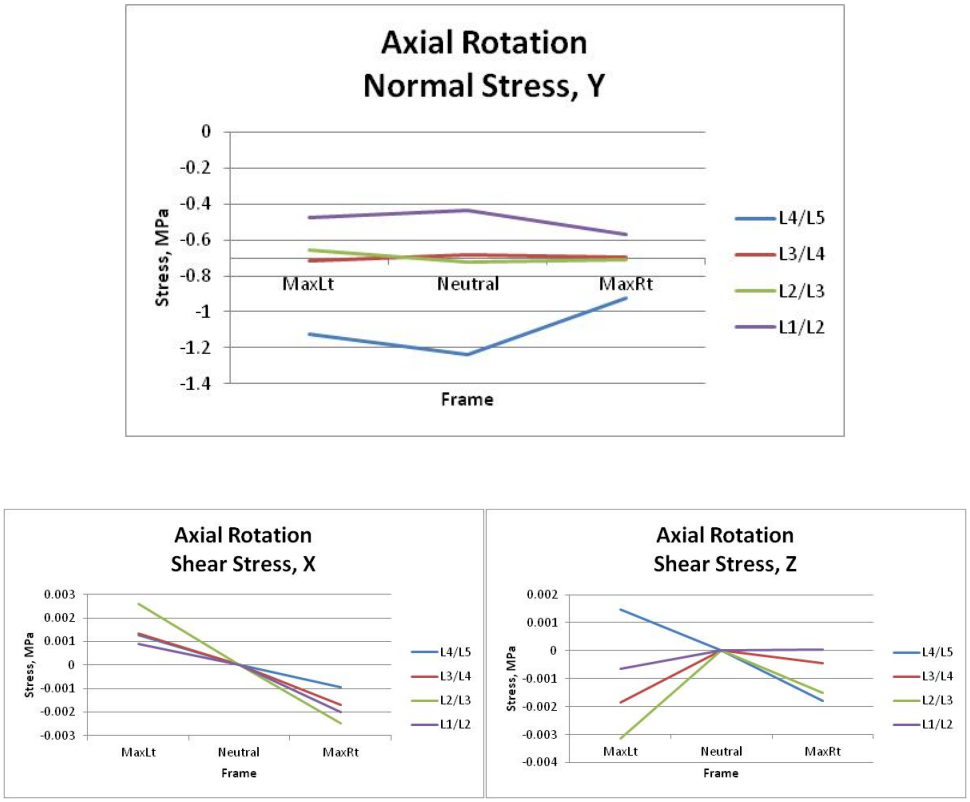

Figure 65. The average stress in the three principal directions for the postoperative fusion subjects during axial rotation.

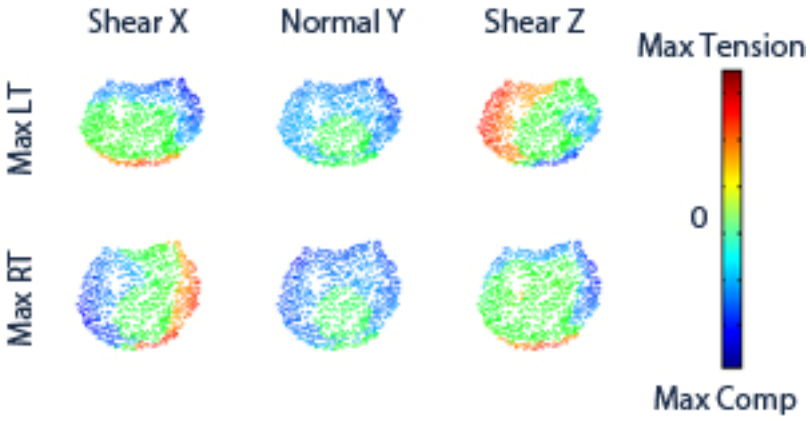

Figure 66. Stress profile for a postoperative fusion subject at a single level during the axial rotation activity.

The preoperative facet group was the first group to have spinal units, L3/L4 and L4/L5, which had decreasing stress from neutral to one side and increasing stress from neutral to the opposite side. The stresses at these levels were -0.22 ± 0.25 MPa and -0.46 ± 0.07 MPa at maximum left, -0.52 ± 0.01 MPa and -0.61 ± 0.12 MPa at neutral, and -0.75 ± 0.2 MPa and -0.88 ± 0.11 MPa at maximum right. The L2/L3 unit performed somewhat normal with decreasing stress from neutral to each side with stresses of -0.45 ± 0.3 MPa at maximum left, -0.57 ± 0.002 MPa at neutral, and -0.46 ± 0.11 MPa at maximum right. The L1/L2 level performed similar to the abnormal groups increasing stress as the subject moved from neutral to either side with stresses of -0.71 ± 0.07 MPa at maximum left, -0.6 ± 0.002 MPa at neutral, and -0.65 ± 0.46 MPa at maximum right (Fig. 67). The group's individual disc stress profiles show the stress created by the out-of-plane rotations with the sample subject in Figure 68 showing the slight amount of lateral bending at both maximums. The disc stresses are similar to the low back pain and degenerative groups.

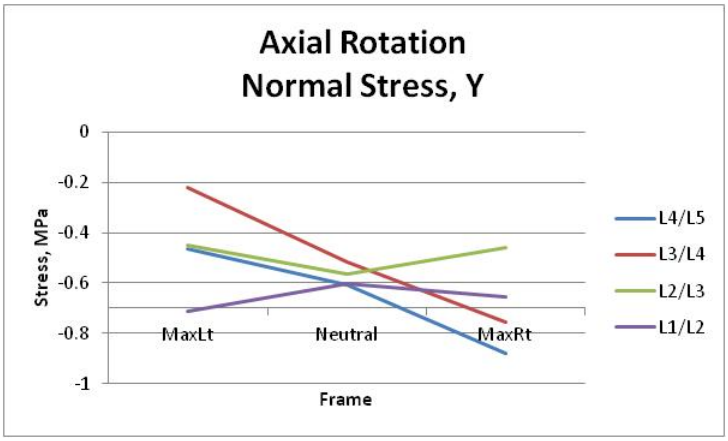

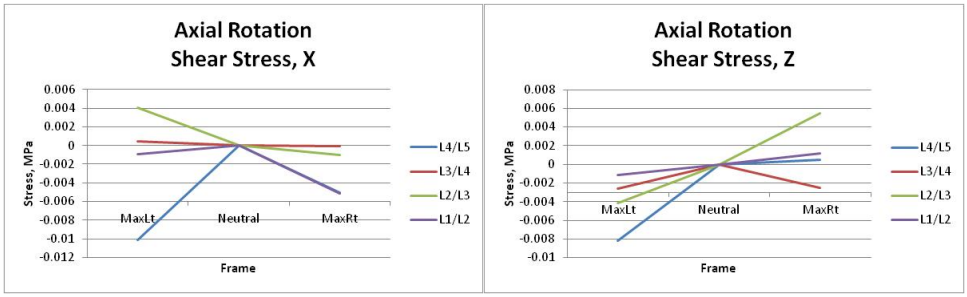

Figure 67. The average stress in the three principal directions for the preoperative facet subjects during axial rotation.

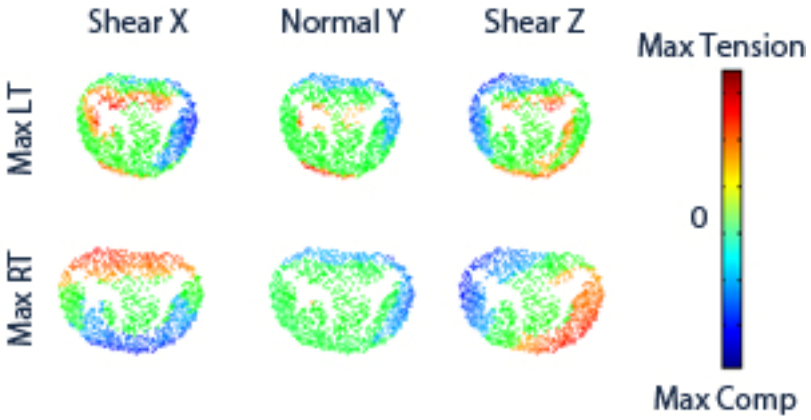

Figure 68. Stress profile for a preoperative facet subject at a single level during the axial rotation activity.

Postoperatively, the facet group has the L3/L4 spinal unit return to a normal path of decreasing normal stress. The stress was -0.28 ± 0.18 MPa at maximum left, -0.51 ± 0.01 MPa at neutral, and -0.41 ± 0.08 MPa at maximum right. The L1/L2 and L2/L3 spinal units perform similar to preoperative facet L3/L4 and L4/L5 spinal units. The stresses at the respective levels were -0.66 ± 0.14 MPa and -0.66 ± 0.53 MPa at maximum left, -0.63 ± 0.1 MPa and -0.56 ± 0.02 MPa at neutral, and -0.58 ± 0.17 MPa and -0.54 ± 0.04 MPa at maximum right (Fig. 69). The disc stress such as in Figure 70 found areas of larger tension which was previously under either smaller amount of tension or in some vertices under compression. The groups individual disc stress profiles appeared to resemble the similar patterns as the low back pain and degenerative groups.

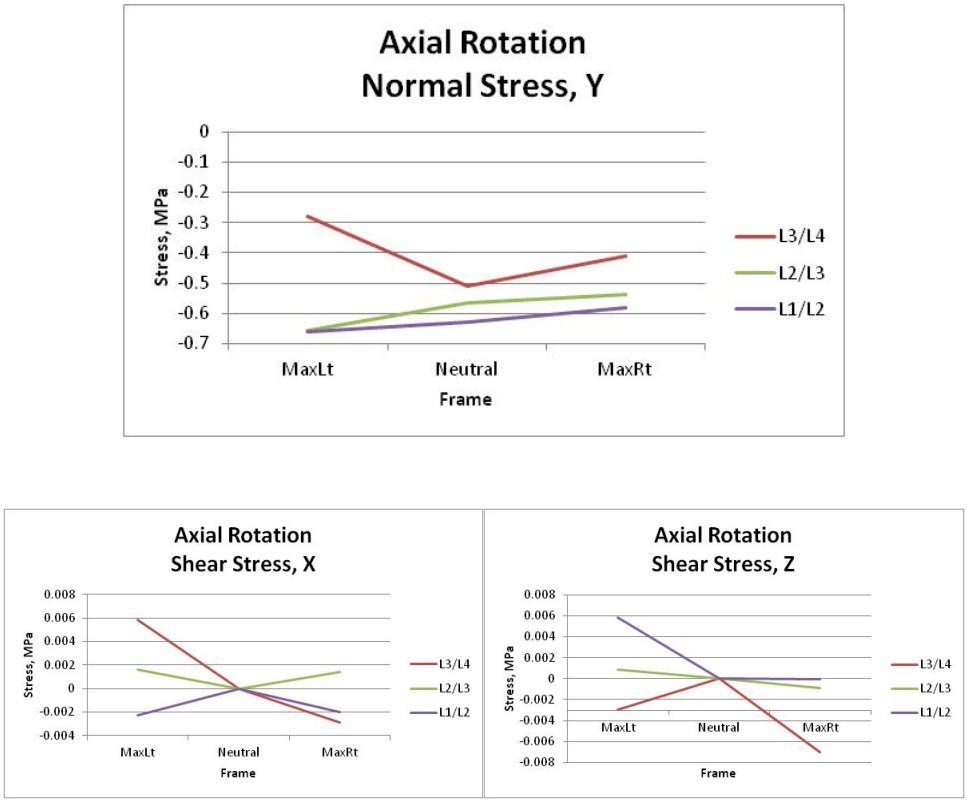

Figure 69. The average stress in the three principal directions for the postoperative facet subjects during axial rotation.

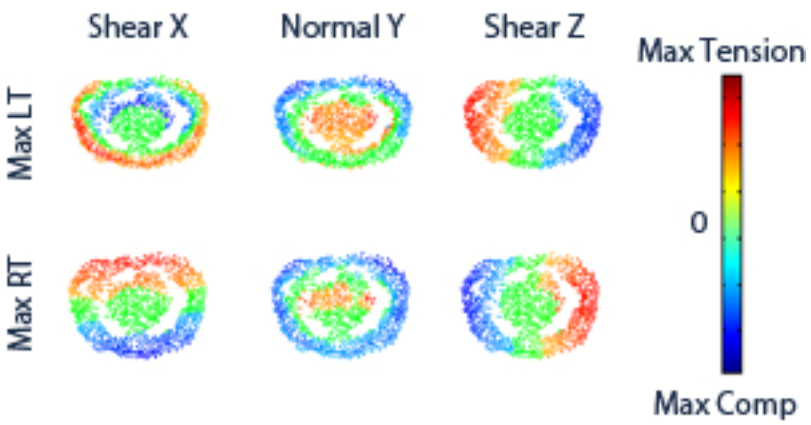

Figure 70. Stress profile for a postoperative facet subject at a single level during the axial rotation activity.

The postoperative disc subject's normal stress increased from neutral to the maximum left and right for all units except L1/L2. At the L2/L3, L3/L4, L4/L5 units the stresses were -0.76 ± 0.54 MPa, -0.82 ± 0.58 MPa, and -0.52 ± 0.36 MPa at maximum left. The stresses went to -0.55 ± 0.39 MPa, -0.54 ± 0.38 MPa, and -0.47 ± 0.33 MPa at neutral, and then to -0.81 ± 0.57 MPa, -0.80 ± 0.57 MPa, and -0.53 ± 0.38 MPa at neutral. The L1/L2 spinal unit followed the pattern similar to the facet group where the stress had increased from neutral to maximum right and decreasing from neutral to maximum left. The stress for this level was -0.45 ± 0.32 MPa at maximum left, -0.57 ± 0.4 MPa at neutral, and -0.66 ± 0.47 MPa at maximum right (Fig. 71). The group's individual disc stress profiles appeared to resemble the similar patterns as the preoperative fusion groups. The subjects were under a more constant stress at the maximums causing the disc to not have a chance to rest (Fig. 72).

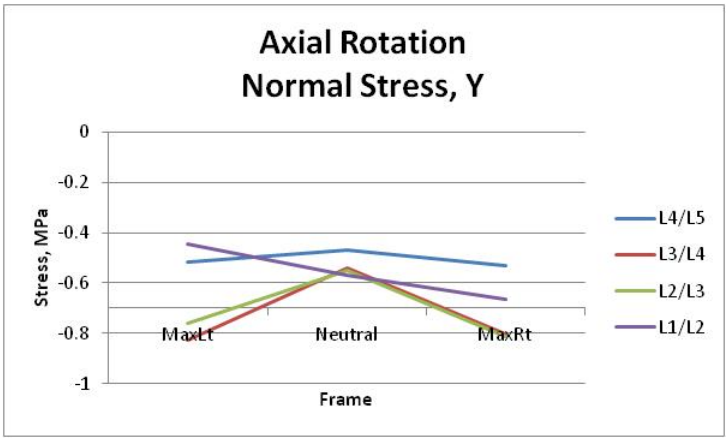

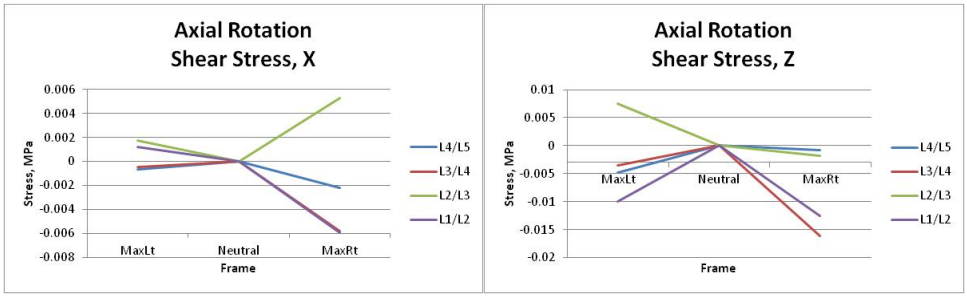

Figure 71. The average stress in the three principal directions for the postoperative disc subjects during axial rotation.

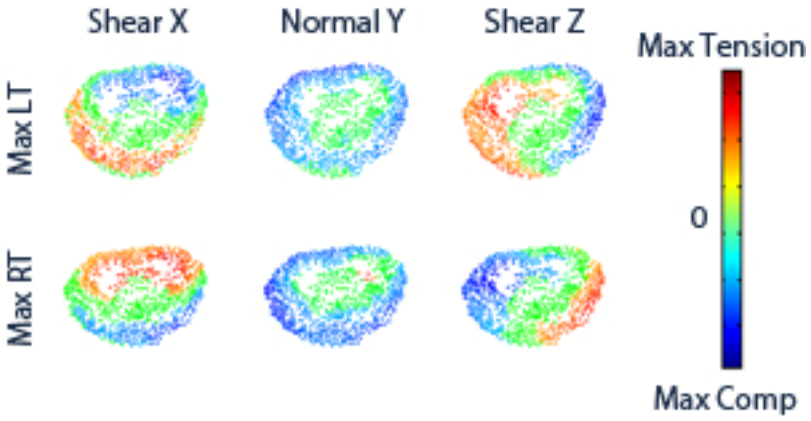

Figure 72. Stress profile for a postoperative disc subject at a single level during the axial rotation activity.

3.2.2.3 *Lateral Bending*

In the healthy group the normal stress tends to get less compressive as the subject travels from neutral to maximum left or right. The stresses at L1/L2, L2/L3, and L4/L5 were -0.31 ± 0.37 MPa, -0.47 ± 0.19 MPa, and -0.59 ± 0.26 MPa at maximum left, -0.4 ± 0.17 MPa, -0.53 ± 0.19 MPa, -0.59 ± 0.3 MPa at neutral, and -0.36 ± 0.34 MPa, -0.39 ± 0.2 MPa, and -0.59 ± 0.3 MPa at maximum right. The L3/L4 spinal unit is the only spinal unit which had a fairly small increase in stress when moving from neutral to maximum right. The stress at L3/L4 was -0.49 ± 0.21 MPa at maximum left, -0.49 ± 0.19 MPa at neutral, and -0.54 ± 0.36 MPa at maximum right (Fig. 73). Figure 74 shows the stress profile of a healthy subjects stress profile which followed well with the in-plane compressive motion. It also shows a slight amount of tensile stress on the side opposite to the motion although some subjects were found with an even larger area. The decrease from neutral to maximum left and right is believed to the stress offloaded to the facets as well as tensile stresses lowering the overall compressive stress.

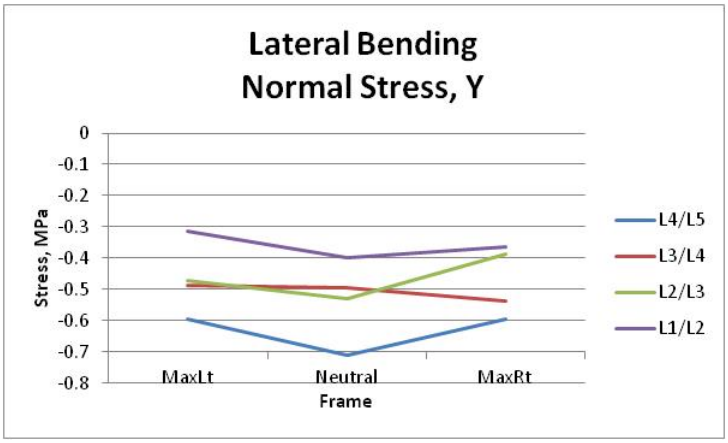

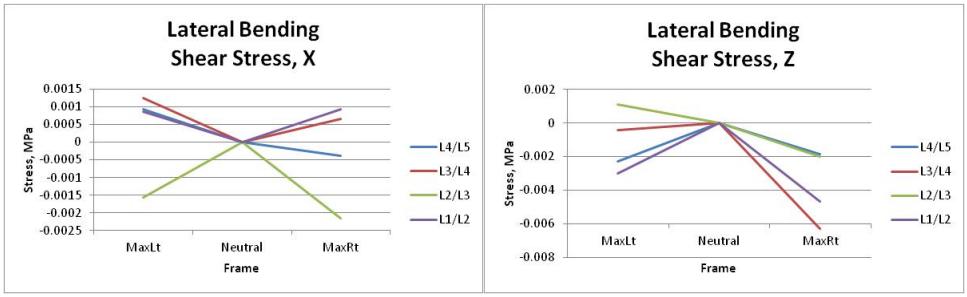

Figure 73. The average stress in the three principal directions for the healthy subjects during lateral bending.

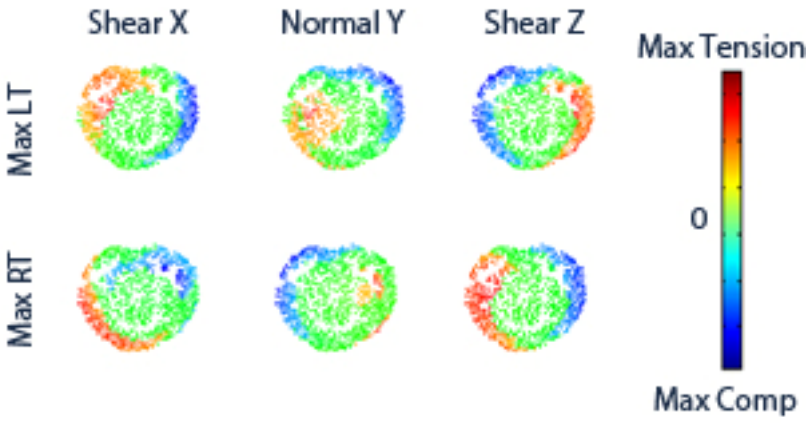

Figure 74. Stress profile for a healthy subject at a single level during the lateral bending activity.

The low back pain group experienced normal path motion at L4/L5 and L3/L4 spinal units with the stress decreasing from neutral to the maximums. The stress at L4/L5 was -0.87 ± 0.23 MPa at maximum left, -0.9 ± 0.19 MPa at neutral, and -0.76 ± 0.19 MPa at maximum right. The normal stress at L3/L4 was -0.51 ± 0.16 MPa at maximum left, -0.57 ± 0.14 MPa at neutral, and -0.55 ± 0.24 MPa at maximum right. The L2/L3 spinal unit had both on the average increasing and decreasing stress as the subjects moved to the opposite maximum. For this level the normal stress was -0.77 ± 0.34 MPa at maximum left, -0.61 ± 0.31 MPa at neutral, and -0.57 ± 0.22 MPa at maximum right. The L1/L2 spinal unit had increasing stress from neutral, -0.48 ± 0.17 MPa, to the maximums, -0.5 ± 0.22 MPa and -0.52 ± 0.18 MPa at left and right respectively (Fig. 75). From the individual disc stress, such as Figure 76, the low back pain group had abnormal loading patterns with areas of stresses in the anterior and posterior sections of the disc which followed in line with the increase in out-of-plane rotations during the motion.

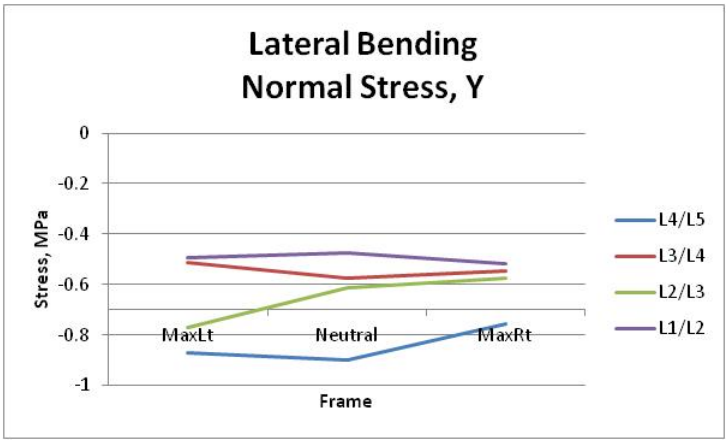

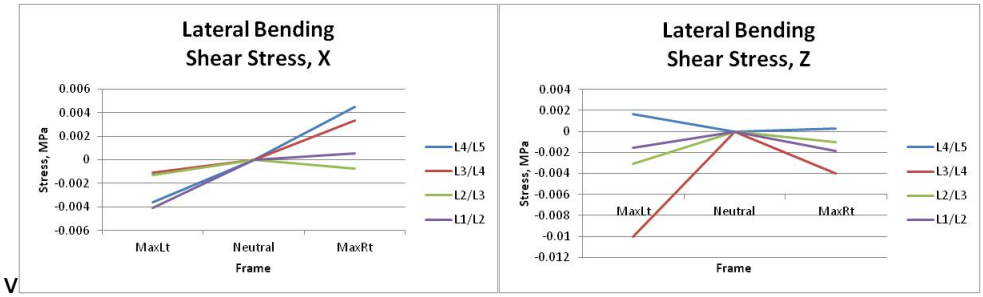

V

Figure 75. The average stress in the three principal directions for the low back pain subjects during lateral bending.

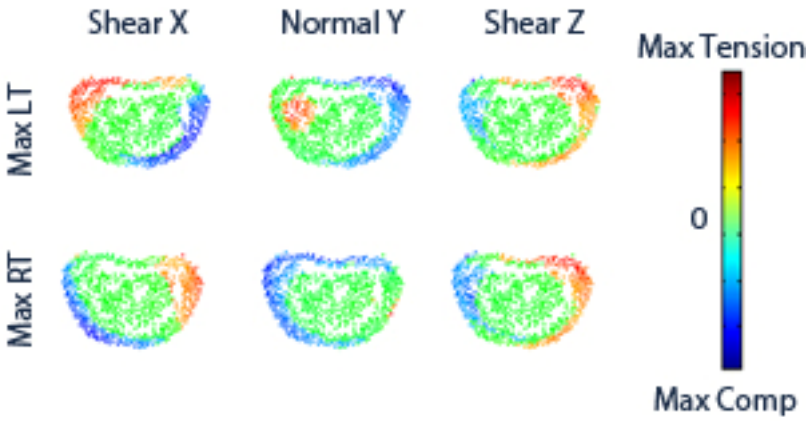

Figure 76. Stress profile for a low back pain subject at a single level during the lateral bending activity.

The degenerative group experienced normal path motion at L1/L2 spinal unit of decreasing normal stress as the subjects went from neutral, -0.65 ± 0.29 MPa, to the maximum left, -0.59 ± 0.4 MPa, and maximum right, -0.6 ± 0.35 MPa. The L2/L3 spinal unit had decreasing normal stress from neutral, -0.73 ± 0.5 MPa, to maximum right,-0.6 ± 0.33 MPa, and almost no change in average normal stress as the group moved to maximum left, -0.73 ± 0.5 MPa. The L3/L4 spinal unit had increasing normal stress from neutral,-0.54 ± 0.35 MPa, to the maximum left, -0.55 ± 0.26 MPa, and maximum right, -0.59 ± 0.43 MPa. The L4/L5 spinal unit had both on the average increasing and decreasing normal stress as the subjects moved to the opposite maximum. The stress at this level was -0.7 ± 0.21 MPa at maximum left, -0.68 ± 0.2 MPa at neutral, and -0.64 ± 0.23 MPa at maximum right (Fig. 77). From Figure 78 it can be seen that this degenerative subject had an offload of stress at the maximums and experienced small amounts of compression on the posterior of the disc. The degenerative group had a few subjects with abnormal loading patterns with high stresses in the anterior and posterior sections of the disc. This is in line with the increase in out-of-plane kinematic seen for the group.

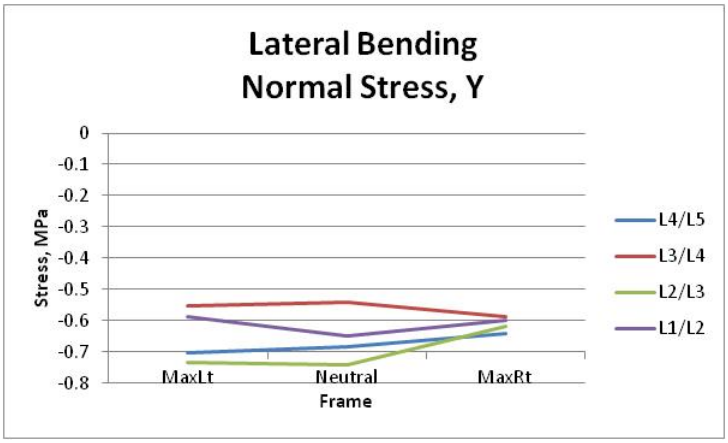

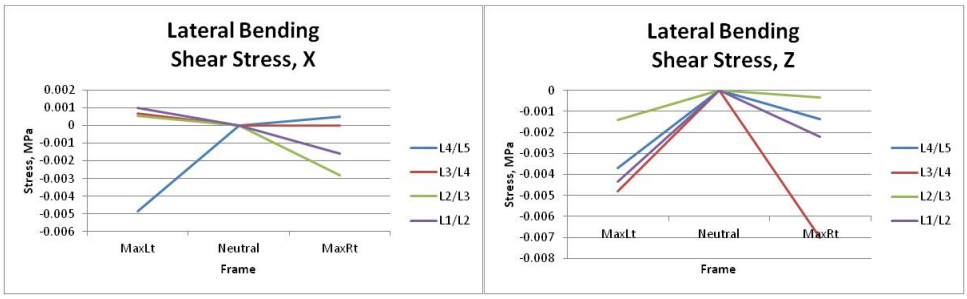

Figure 77. The average stress in the three principal directions for the degenerative subjects during lateral bending.

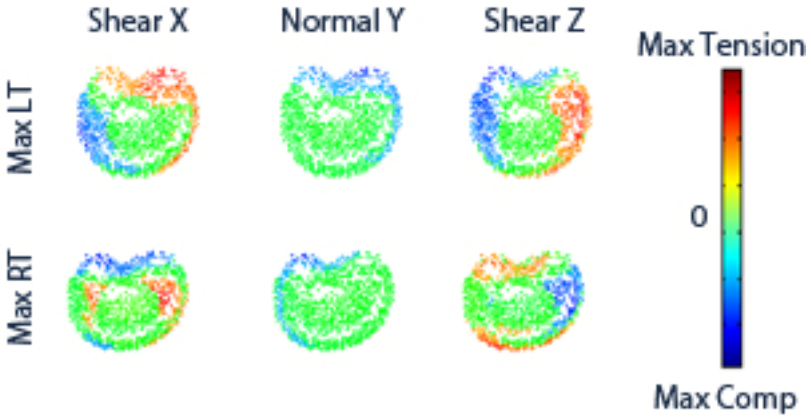

Figure 78. Stress profile for a degenerative subject at a single level during the lateral bending activity.

The preoperative fusion group had increasing normal stress from neutral to maximum right and decreasing normal stress from neutral to maximum left at the L1/L2 spinal unit. The stress at this level was -0.65 ± 0.62 MPa at maximum left, -0.81 ± 0.51 MPa at neutral, and -1.29 ± 0.32 MPa at maximum right. The L2/L3 spinal unit had decreasing stress from neutral, -0.76 ± 0.51 MPa, to maximum right, -0.68 ± 0.43 MPa, and almost no change in average stress moving towards maximum left, 0.76 ± 0.59 MPa. The L3/L4 spinal unit had increasing normal stress from neutral, -0.61 ± 0.47 MPa, to the maximum left, -0.68 ± 0.36 MPa, and to maximum right, -0.77 ± 0.69 MPa. The L4/L5 spinal unit had increasing normal stress to maximum right,-0.96 ± 1.24 MPa, and almost no change in normal stress as the group moved to maximum left, -0.85 ±0.94 MPa, from the neutral stress, -0.81 ± 0.77 MPa (Fig. 79). From the individual disc stresses, the preoperative fusion group had subjects with abnormal loading patterns with high stresses in different places over the entire disc. This coincides with the increase seen in the out-of-plane rotations of the group during the kinematic analysis. The sample disc in Figure 80 shows compressive stress over a large portion of the outer disc which is not allowing the disc to unload.

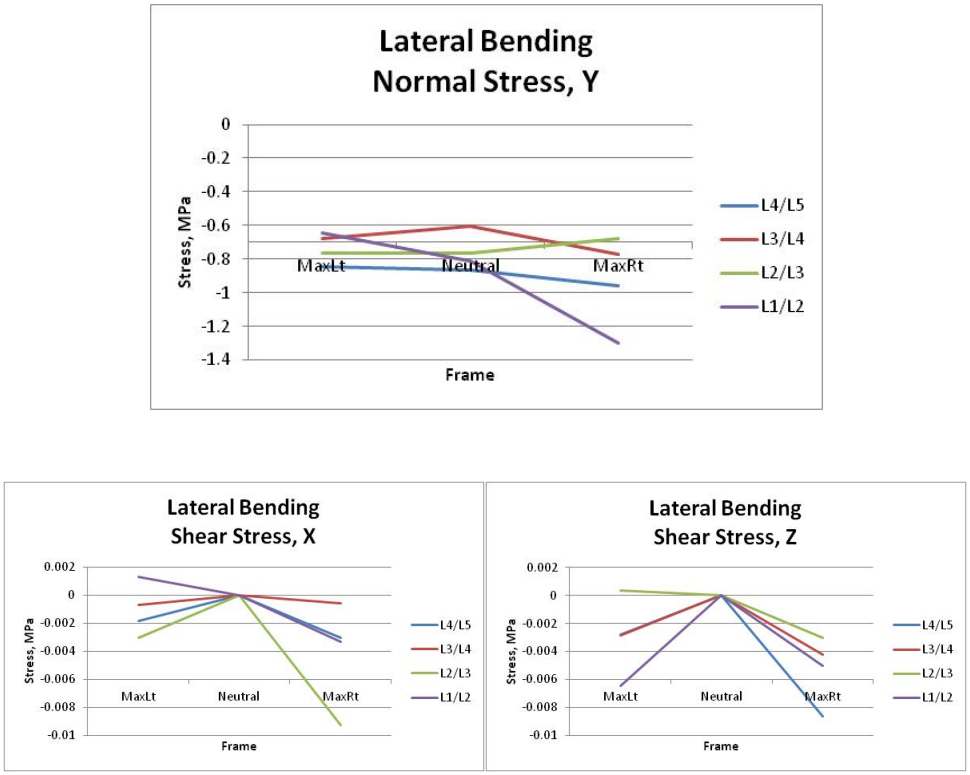

Figure 79. The average stress in the three principal directions for the preoperative fusion subjects during lateral bending.

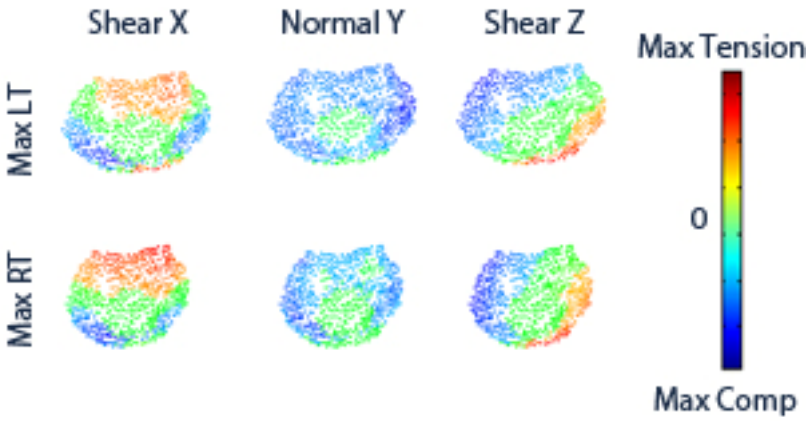

Figure 80. Stress profile for a preoperative fusion subject at a single level during the lateral bending activity.

Postoperatively, the fusion group had L1/L2 and L2/L3 return to a more normal path of decreasing average stress as the group moved to the maximums. The stress at these levels were -0.53 ± 0.42 MPa and -0.63 ± 0.33 MPa at maximum left, -0.62 ± 0.37 MPa and -0.69 ± 0.3 MPa at neutral, and -0.47 ± 0.37 MPa and -0.66 ± 0.37 MPa at maximum right respectively. The L3/L4 spinal unit had increasing stress as the group moved to the maximums which showed no change from the preoperative group. The normal stress at L3/L4 was -0.76 ± 0.46 MPa at maximum left, -0.71 ± 0.43 MPa at neutral, and -0.73 ± 0.38 MPa at maximum right. The L4/L5 spinal unit had increasing normal stress from neutral, -0.86 ± 0.28 MPa, to maximum left,-0.91 ± 0.29 MPa, and decreasing normal stress to maximum right, -0.81 ± 0.42 MPa (Fig. 81). Figure 82 shows that there was little change postoperatively to the individual disc stress of the group. The group still encountered increased disc stress throughout the motion and did not return to a normal loading pattern at all levels.

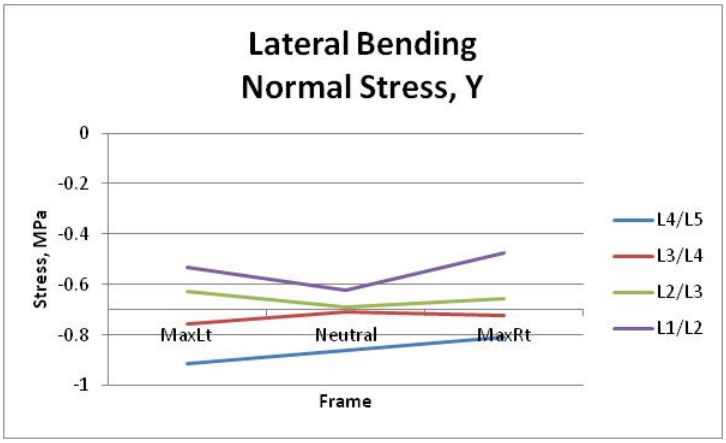

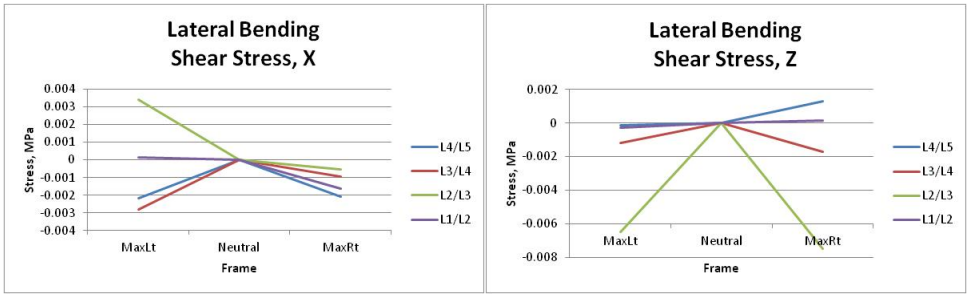

Figure 81. The average stress in the three principal directions for the postoperative fusion subjects during lateral bending.

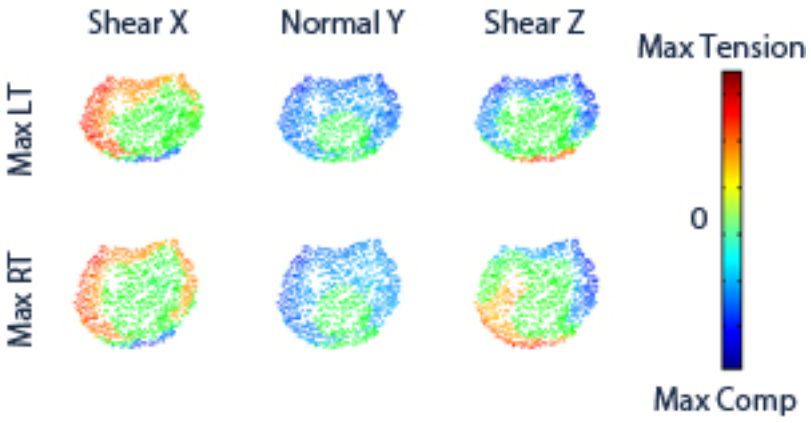

Figure 82. Stress profile for a postoperative fusion subject at a single level during the lateral bending activity.

The preoperative facet group had normal decreasing normal stress from neutral to the maximums for L1/L2 and L3/L4 spinal unit. The stress at these levels were -0.48 ± 0.16 MPa and -0.37 ± 0.32 MPa at maximum left, -0.6 ± 0.5 MPa and -0.5 ± 0.001 MPa at neutral, and -0.49 ± 0.17 MPa and -0.38 ± 0.17 MPa at maximum right respectively. The L2/L3 unit experienced increasing normal stress to the maximum right, -0.64 ± 0.18 MPa, and decreasing stress to the maximum left, -0.48 ± 0.07 MPa from a neutral stress of -0.56 ± 0.001 MPa. The L4/L5 spinal unit had little change in normal stress to maximum left, -0.5 ± 0.59 MPa, and decreasing normal stress to the maximum right, -0.43 ± 0.21 MPa, from the neutral, -0.52 ± 0.03 MPa (Fig. 83). Figure 84 shows a sample preoperative facet subject which had a rather normal loading pattern with a slight shift towards the anterior of the disc due to the increase in out-of-plane flexion-extension rotation. This disc was also unloaded on the opposite side of motion but did not reach a tensile stress as in the normal group. This group also showed similar results to the low back pain group, degenerative group, and the preoperative fusion at some of the levels.

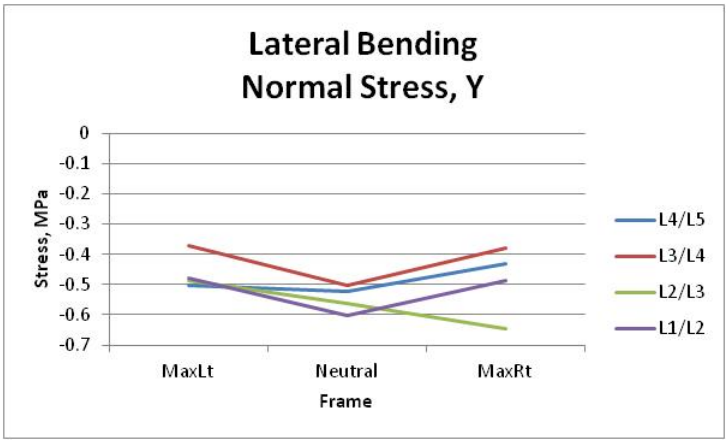

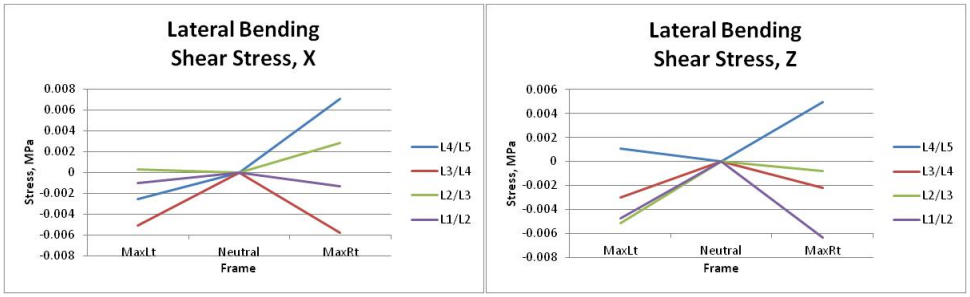

Figure 83. The average stress in the three principal directions for the preoperative facet subjects during lateral bending.

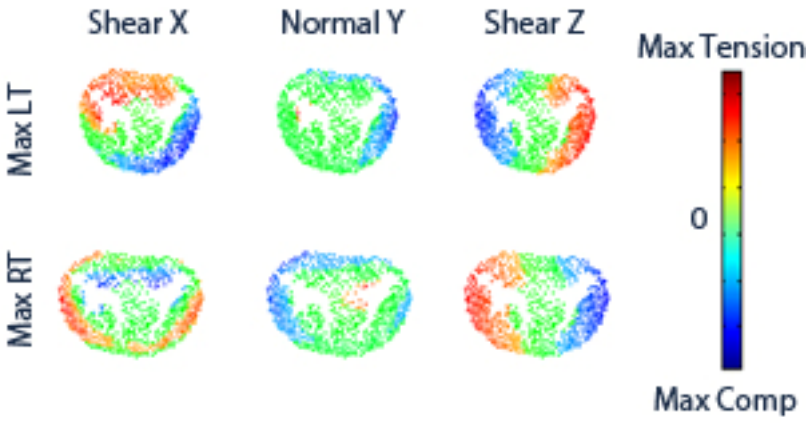

Figure 84. Stress profile for a preoperative facet subject at a single level during the lateral bending activity.

Postoperatively the facet group had increasing normal stress from neutral to maximums at L1/L2 with stress of -0.66 ± 0.19 MPa at maximum left, -0.6 ± 0.06 MPa at neutral, and -0.7 ± 0.05 MPa at maximum right. From a neutral stress of -0.55 ± 0.04 MPa the L2/L3 spinal unit had a decreasing stress to the maximum left, -0.34 ± 0.36 MPa, and maximum right, -0.38 ± 0.26 MPa. The L3/L4 unit experienced increasing normal stress to the maximum right and decreasing stress to the maximum left. The stress was -0.41 ± 0.01 MPa at maximum left, -0.51 ± 0.01 MPa at neutral, and -0.63 ± 0.15 MPa for this level (Fig. 85). The disc shown in Figure 86 shows that following surgery the disc is unloading the stress at the maximums but is not experiencing a compressive load similar to normal or even one seen preoperatively. From this subject it would appear that the surgery actually negatively impacted the loading patterns by negatively affecting the kinematics. Overall this group had loading patterns more similar to the low back pain and degenerative groups.

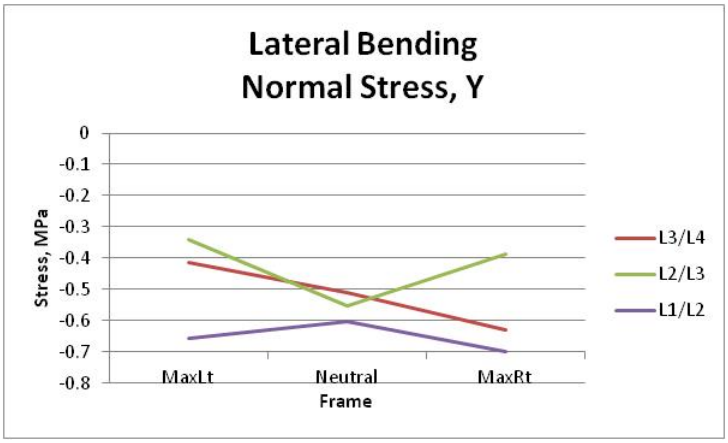

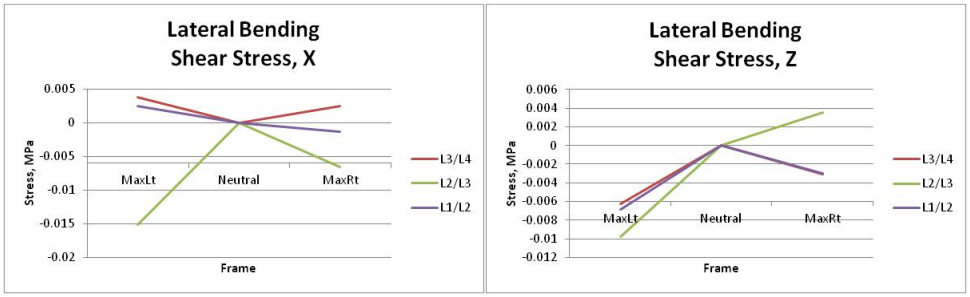

Figure 85. The average stress in the three principal directions for the postoperative facet subjects during lateral bending.

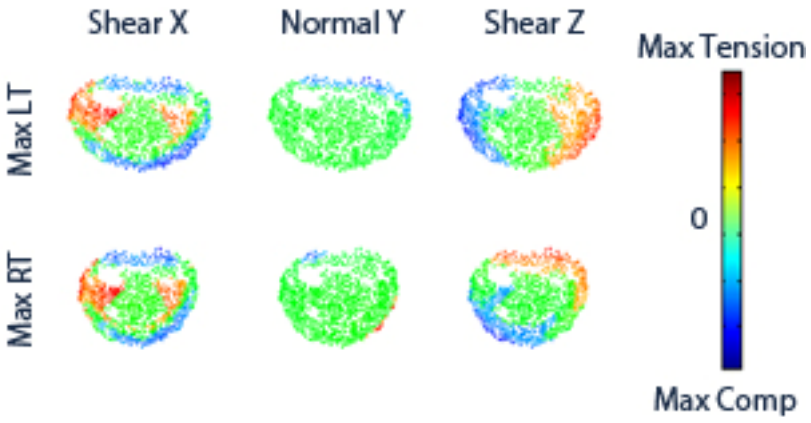

Figure 86. Stress profile for a postoperative facet subject at a single level during the lateral bending activity.

The final group postoperative disc had experienced increased normal stress from neutral to the maximums for L1/L2 unit. The normal stress at L1/L2 was -1.04 ± 0.74 MPa at maximum left, -0.57 ± 0.4 MPa at neutral, and -0.74 ± 0.52 MPa at maximum right. The L2/L3 and L4/L5 unit had a more normal path of decreasing stress from neutral to the maximums. For these respective levels the normal stresses were -0.53 ± 0.38 MPa and -0.25 ± 0.18 MPa at maximum left, -0.55 ± 0.39 MPa and -0.47 ± 0.33 MPa at neutral, and -0.36 ± 0.25 MPa and -0.34 ± 0.24 MPa at maximum right. The L3/L4 spinal unit had both increasing normal stress from neutral to maximum left and decreasing stress from neutral to maximum left. The normal stress at L3/L4 was -0.65 ± 0.46 MPa at maximum left, -0.54 ± 0.38 MPa at neutral, and -0.41 ± 0.29 MPa at maximum right (Fig. 87). Figure 88 shows that for the sample subject the loading at maximum left showed signs of compression on the posterior of the disc in an abnormal location. Maximum right has a more normal loading pattern with a slight shift of the compressive normal stress to anterior of the disc. The rest of the subject discs showed similar loading patterns to the degenerative and low back pain subjects. The surgery did not seem to fully return to the subjects to the normal loading patterns.

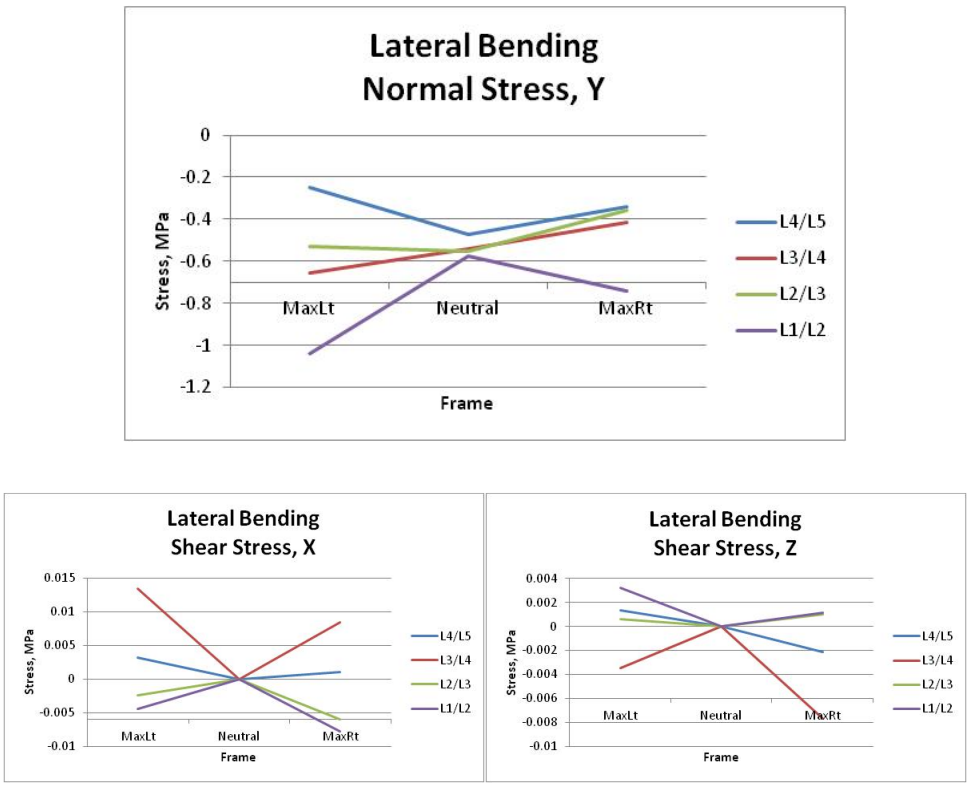

Figure 87. The average stress in the three principal directions for the postoperative disc subjects during lateral bending.

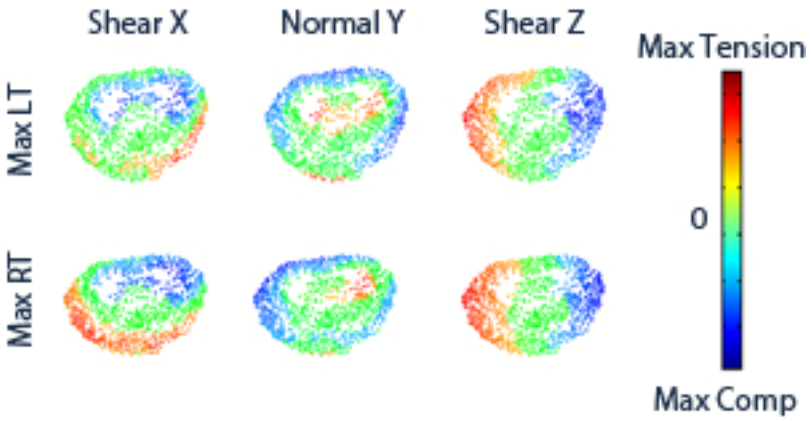

Figure 88. Stress profile for a postoperative disc subject at a single level during the lateral bending activity.

3.1.2.4. Sectioned Disc Stress

Although the average stress from the different groups did not find any significant differences, there did appear to be visual differences in the discs. In order to assess this stress change, the disc was partitioned into nine different areas (Fig. 89). The average rate of change of stress from the neutral stress within the nine sections was also determined. There were also no significant differences in either results, but utilizing both analyses the visual trends did become clearer from the previous section. For the following results all data can be found in the attached file under the appropriate sheet for the type and activity.

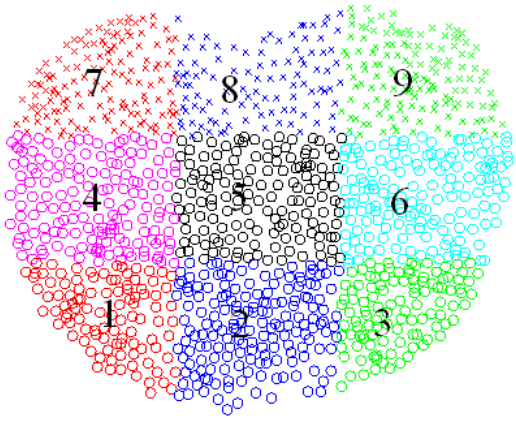

Figure 89. Stress profile for a postoperative disc subject at a single level during the lateral bending activity.

During the flexion extension activity, the healthy group had decreasing average stress from maximum flexion to maximum extension in sections 1-6. The sections 1-3 had the greatest change in stress from neutral to maximum flexion. In some cases at maximum extension the stress decreased from the neutral stress in the posterior sections 7-9 which is most likely the result of the stress offloading to the facets. The posterior stress did decrease from neutral to maximum flexion; however the stress magnitude at these three sections were only slightly lower in magnitude than the stress in the anterior sections. At levels L1/L2, L2/L3, and L3/L4 the posterior stresses in sections 7-9 were nearly equal to the anterior stresses in section 1-3 at maximum flexion. The low back pain and degenerative groups had similar results to the healthy group and did not show any differences in the aforementioned rates of stress change from neutral. The low back pain group did though have increased posterior stresses at L4/L5 such that all levels had nearly equal stresses in section 1-3 and sections 7-9 at maximum flexion. This change was taken one step further in the degenerative group as all sections besides section 5 were nearly equal in the stress average at maximum flexion. Moving onto the fusion group, the preoperative discs had some of the highest overall average stresses in all sections of the disc. At maximum flexion the posterior stress was actually higher than the anterior stress at all levels. The changes from neutral were completely different from the previous groups and had abnormal patterns. Postoperatively, the stresses had decreased from the preoperative amounts; however they were still relatively high when compared to the previous three groups. The posterior stresses had lowered though to the point that they were no longer greater than the anterior stresses at maximum flexion for levels L4/L3, L3/L2, and L1/L2. The changes from neutral had returned to a healthier pattern for the anterior of the discs; however the posterior stresses were found to increase from neutral to maximum flexion for L4/L5 and L3/L4. The facet group did not fare any better with

the preoperative group having some of the lowest overall stresses. At maximum flexion once again the posterior stresses were found to be greater than the anterior stresses for all levels. The change in stress from neutral was abnormal for all levels with L4/L5 having increased posterior stresses from neutral to maximum flexion, L3/L4 and L2/L3 having decreasing anterior stresses from neutral to maximum flexion, and L1/L2 having decreasing anterior stresses from mid flexion to maximum flexion. Postoperatively the group had an increase in overall stress with the posterior stresses still greater than the anterior stresses at maximum flexion. The abnormal changes from neutral were still found in L3/L4, L2/L3, and L1/L2. Finally the postoperative discs subjects appeared to have average stresses at all locations similar to the healthy group, but abnormalities were found in the change in stress from neutral. L1/L2, L2/L3, and L3/L4 had increasing posterior stress from neutral to maximum flexion, L4/L5 had a higher change at mid flexion than maximum flexion, and L1/L2 had increased anterior stresses from neutral to maximum extension.

During the lateral bending activity, for most groups at the maximum locations the three sections in the direction of motion had higher stress than the opposite side. The only group to break that pattern was the postoperative disc subjects which at maximum left had higher stress in section 7 instead of section 9 at L2/L3. Maximum right had two levels, L4/L5 and L1/L2, also break the pattern with section 3 experiencing more stress than section 1. It should be noted that at L4/L5 and L2/L3 the neutral values were also higher in the sections and the stress did decrease. The decrease in stress during the motion for all groups came in the posterior sections. For the healthy group at L4/L5 the change in stress from maximum left to maximum right was balanced over opposite sections. For example, at maximum right section 7 had 0.67 MPa and section 9 had 1.19 MPa. Now at maximum left section 7 had 1.29 MPa and section 9 had 0.65 MPa. No other group had this occur during the

activity. From neutral the healthy group saw the greatest increase in stress in section 6 at levels L4/L5 and section 9 for all other levels at the maximum left frame. At maximum right, the greatest increase came in section 4 for L4/L5, section 7 for L3/L4 and L1/L2, and section 1 for L2/L3. The low back pain group had maximum changes from neutral at section 3 for L3/L4 and L1/L2 and section 9 for L4/L5 and L2/L3 for maximum left frame. At maximum right the L4/L5 level experienced an increase from the neutral stress at section 4 but it was a very small change. The L3/L4 level had an increase at section 1, and the L1/L2 and L2/L3 had increases in section 7. The degenerative group experienced increased stress in the posterior section 7 at maximum left and section 9 at maximum right. The fusion group had increased overall stress throughout the disc. The healthy group had a range of stresses from 0.13 to 1.19 MPa while the preoperative fusion group had increased to 0.24 to 2.16 MPa during the activity. At the maximum left the L4/L5 level for the group was the only group that had an average change from neutral which was negative over the entire disc. Furthermore at maximum left all posterior section 7-9 had negative change from neutral which showed that the group was either flexing forward or the vertebral bodies were vertically separated. At the other levels section 6 was the maximum for L3/L4 and L1/L2, and section 9 was the maximum for L2/L3. At maximum right section 1 was the area of highest change from neutral for L4/L5 and L1/L2, and section 4 was the highest change from neutral for L3/L4 and L2/L3. Postoperatively the range of stresses were still higher but had decreased slightly to 0.23 to 1.88 MPa. At maximum left the greatest stress change from neutral was in section 9 for all levels. This posterior loading carried over to maximum right to section 7 for all levels besides L4/L5 which had the highest change in section 4. The preoperative facet group had the greatest changes from neutral in the posterior, section 9 and 7, for both maximums at all levels. Postoperatively at maximum left for L3/L4 and L1/L2 the greatest

change had moved to section 6 while at L2/L3 it was now in anterior section 1. Finally the postoperative disc subjects had minor change from neutral in section 9 for L4/L5 level and section 3 for L2/L3 level. Section 9 was the area of largest change for L1/L2, and section 3 was the largest change for L3/L4 both were larger changes. At maximum right the disc subjects had section 7 as area of greatest change from neutral for L4/L5, and section 1 for level L1/L2 and L2/L3. Interestingly the postoperative disc subjects had section 9 as the highest change of stress from neutral at L3/L4 showing the posterior motion of the group during the motion.

During axial rotation the while the fusion group still has the highest overall stresses, there are no real patterns of high stress or areas of similar stress change within the groups. That being said the changes from neutral for the groups if taken as a range of differences did show that as the disc degenerate the range gets larger. When comparing preoperative to postoperative the range does decrease but still remains greater than the healthy range. The stress ranges were 0.442 MPa for healthy group, 0.721 MPa for low back pain group, 1.053 MPa for degenerative group, 1.574 MPa for preoperative fusion group, 0.777 MPa for the postoperative fusion group, 1.059 MPa for the preoperative facet group, 0.749 MPa for the postoperative facet group, and 0.72 MPa for the postoperative disc group (Table 5). The changes in the stress range would appear to be a sign of the increase in out-of-plane compressive motion for the groups as the subjects' discs degenerate.

Table 5. Stress changes from neutral during the axial rotation activity for all groups.

Identifier	Maximum Decrease in Stress (MPa)	Maximum Increase in Stress (MPa)	Stress Range (MPa)
Healthy	0.32	0.122	0.442
Low Back Pain	0.64	0.081	0.721
Degenerative	0.93	0.123	1.053
Preoperative Fusion	0.69	0.884	1.574
Postoperative Fusion	0.449	0.328	0.777
Preoperative Facet	0.422	0.637	1.059
Postoperative Facet	0.242	0.507	0.749
Postoperative Disc	0.223	0.497	0.72

3.1.2.5. Adjacent Segment Comparison

From the kinematic study done on the fusion subjects it was found that there was no evidence of increased motion throughout the subjects (Appendix A.3). For this reason it is our belief while fusion does alleviate the pain at the specific spinal unit the overall problem is not addressed. At the first superior level the average change was a loss of rotation for each of the three rotations during the three activities. This loss in motion created an average stress change of -0.29 MPa at maximum flexion, -0.59 MPa at mid flexion, -0.29 MPa at neutral, and -0.23 MPa at maximum extension when comparing the nine subjects postoperatively to preoperatively during flexion-extension. During axial

rotation the change was -0.43 MPa at maximum left, -0.43 MPa at neutral, and -0.21 MPa at maximum right. Finally, the lateral bending changed -0.32 MPa at maximum left, -0.31 MPa at neutral, and -0.08 MPa at maximum right. While there are some subjects who have increased stress at some of the frames, the overall average shows that the stress decreased postoperatively after having a fusion surgery. Using the sectioned discs from the previous section, there was no trend as to where the decrease in stress was located. Some subjects had decreased stress over the entire disc while others had decreased stress in only some of the nine sections. What was found is that with less motion, the stress required to displace the disc was lower. Therefore given that our subjects had decreased kinematic motion, there was no evidence in the stress analysis to suggest that the adjacent segment degeneration would occur in the adjacent discs due to an increase in the average stress.

3.2. Ligament Stress

3.2.1. Flexion-Extension

The ligaments analyzed during this motion showed that as the subject moved from maximum flexion to maximum extension the stress in the ligament decreased. This is to be expected as the rigid motion dictated that the transverse processes and spinal process get closer. Interestingly though when examining the left and right intertransverse ligament (ITL) stress it can be noted that the healthy subjects had a more even stress between the two. As the disc degenerates and the subject groups started to have increased out-of-plane motions, and the stress in the ligaments was no longer balanced. For example preoperative fusion subjects experienced 0.59 MPa of stress on the left ITL while the right carried only 0.97 MPa at mid flexion. Now once the subjects reached maximum flexion the numbers jumped to 1.33 MPa on the left ITL and 1.65 MPa on the right ITL. At maximum extension it is expected that the stress on the right and left ITL would be zero; however most of the

groups had at least one subject with stress at that frame. Moreover as the groups had increased disc degeneration and more out-of-plane motion more subjects would appear with stress in the two ITLs at maximum extension. The stress on the interspinous ligament (ISL) and supraspinous ligament (SSL) as expected decreased from maximum flexion to maximum extension. Surprisingly, the healthy group at L3/L4 had an average stress of 11.41 MPa which is quite close to the 12.6 ± 7.1 MPa failure stress reported[43]. The ISL also came close to the failure stress of 1.8 ± 0.3 MPa at an average stress of 1.48 MPa. One group that went over the failure stress was the preoperative facet group which had an average stress of 13.15 MPa at maximum flexion for L2/L3 spinal unit. The failure stress at that level is 9.9 ± 5.8 MPa. The other groups had individuals come close to and in some cases carry stress over the failure rates, but none of the average stresses were over the reported failure numbers. All the average values are in Table 6.

Table 6. Stress in the ligaments during flexion-extension activity in MPa.

Identifier	Frame	L1/L2				L2/L3				L3/L4				L4/L5			
		Left ITL	Right ITL	SSL	ISL	Left ITL	Right ITL	SSL	ISL	Left ITL	Right ITL	SSL	ISL	Left ITL	Right ITL	SSL	ISL
Healthy	MaxFlex	1.10	1.10	3.55	0.77	1.44	1.39	4.95	0.96	1.58	1.71	11.41	1.48	1.46	1.36	5.77	1.39
	MidFlex	0.74	0.79	2.37	0.51	0.86	0.73	2.79	0.54	0.77	0.83	5.91	0.77	0.70	0.56	3.24	0.78
	MaxExt	0.05	0.05	0.06	0.01	0.14	0.06	0.20	0.04	0.01	0.10	0.00	0.00	0.16	0.05	0.03	0.01
LBP	MaxFlex	1.39	1.22	4.38	0.95	3.61	3.16	8.15	1.58	1.70	1.58	10.98	1.43	1.49	0.87	4.03	0.97
	MidFlex	1.06	0.94	3.20	0.70	0.54	0.62	2.64	0.51	0.90	0.82	6.12	0.80	0.59	0.65	1.78	0.43
	MaxExt	0.02	0.04	0.00	0.00	0.12	0.07	0.21	0.04	0.14	0.54	1.12	0.15	0.08	0.00	0.00	0.00
Degen	MaxFlex	1.96	1.32	5.66	1.23	1.57	1.76	6.06	1.17	1.42	1.74	10.31	1.34	1.42	1.39	5.16	1.25
	MidFlex	1.35	1.11	3.98	0.86	1.31	1.16	4.36	0.84	0.74	1.35	6.70	0.87	0.84	0.66	2.90	0.70
	MaxExt	0.31	0.03	0.05	0.01	0.11	0.29	0.00	0.00	0.11	0.27	0.26	0.03	0.09	0.06	0.01	0.00
PreOp Fusion	MaxFlex	1.33	1.65	6.02	1.31	1.42	1.60	5.40	1.05	1.05	0.69	5.13	0.67	0.69	1.09	3.00	0.72
	MidFlex	0.59	0.97	2.96	0.64	0.77	0.58	2.45	0.47	0.32	0.06	1.07	0.14	0.63	0.50	1.77	0.43
	MaxExt	0.21	0.19	0.00	0.00	0.61	0.38	0.81	0.16	0.48	0.18	0.44	0.06	0.57	0.04	0.08	0.02
PostOp Fusion	MaxFlex	1.19	1.01	4.66	1.01	3.34	3.40	7.52	1.45	4.93	3.66	10.17	1.32	0.61	0.55	2.45	0.59
	MidFlex	0.62	0.53	2.59	0.56	0.50	0.53	1.97	0.38	0.66	0.33	2.12	0.28	0.31	0.26	0.83	0.20
	MaxExt	0.39	0.08	0.19	0.04	0.39	0.20	0.24	0.05	0.28	0.45	0.99	0.13	0.24	0.16	0.27	0.07
PreOp Facet	MaxFlex	0.44	0.32	1.45	0.31	7.25	7.61	13.15	2.55	3.84	3.01	0.00	0.00	1.22	0.91	1.81	0.44
	MidFlex	0.34	0.29	1.51	0.33	0.84	0.32	2.07	0.40	0.24	0.32	4.98	0.65	1.12	0.12	1.21	0.29
	MaxExt	0.00	0.07	0.00	0.00	0.68	1.01	0.00	0.00	8.43	7.52	0.00	0.00	1.36	1.21	1.34	0.32
PostOp Facet	MaxFlex					1.12	1.65	8.14	1.57	0.00	0.00	0.31	0.04				
	MidFlex					0.94	1.29	6.73	1.30	0.00	0.00	1.33	0.17				
	MaxExt					0.24	0.71	3.04	0.59	0.00	0.00	0.31	0.04				
PostOp Disc	MaxFlex	0.00	0.00	0.00	0.00	0.24	0.00	0.07	0.01	0.18	0.00	1.67	0.22	0.99	0.38	3.35	0.81
	MidFlex	0.00	0.00	0.00	0.00	0.00	0.00	0.04	0.01	0.00	0.00	0.05	0.01	0.19	0.00	1.72	0.42
	MaxExt	0.00	0.00	0.00	0.00	0.21	0.00	0.00	0.00	0.00	0.00	0.00	0.00	0.00	0.19	0.00	0.00

3.2.2. Axial Rotation

During this activity none of the ligaments came close to the failure rates and no major trends can be found. It would be expected that in a controlled axial rotation the right and left ITL would be under similar stresses; however that does not happen in any of groups. From the kinematic results it can be seen that none of the group had a smooth in-plane rotation which is evident in the loading conditions of the ligaments. Table 7 shows the measured stresses in the ligaments. The instability of the vertebras during the complex motion which the ligaments were trying to control was apparent in the range of stresses and lack of clear stress trends.

Table 7. Stress in the ligaments during axial rotation activity in MPa.

Identifier	Frame	L1/L2				L2/L3				L3/L4				L4/L5			
		Left ITL	Right ITL	SSL	ISL	Left ITL	Right ITL	SSL	ISL	Left ITL	Right ITL	SSL	ISL	Left ITL	Right ITL	SSL	ISL
Healthy	**Max Rt**	0.44	0.62	1.04	0.23	0.21	0.20	0.33	0.07	0.06	0.74	0.15	0.04	0.31	0.34	0.88	0.22
	Max Lt	0.54	0.34	1.00	0.22	0.29	0.38	0.66	0.13	0.28	0.20	0.43	0.11	0.39	0.24	0.96	0.24
LBP	**Max Rt**	0.30	0.76	1.38	0.30	0.19	0.70	0.92	0.18	0.19	0.69	1.32	0.35	0.39	0.75	1.88	0.46
	Max Lt	0.59	0.25	1.00	0.22	0.53	0.62	1.11	0.22	0.33	0.56	1.92	0.50	0.59	0.45	1.65	0.40
Degen	**Max Rt**	0.32	0.62	1.07	0.24	0.76	0.67	1.95	0.38	0.51	0.67	3.07	1.60	0.35	1.10	1.79	0.43
	Max Lt	0.44	0.53	1.31	0.29	1.28	0.28	2.01	0.39	0.34	0.14	1.33	0.69	0.35	0.82	1.56	0.38
PreOp Fusion	**Max Rt**	0.67	0.74	2.40	0.52	0.64	0.96	2.40	0.47	0.22	0.99	2.72	0.71	0.58	0.38	1.46	0.35
	Max Lt	1.05	0.38	2.41	0.53	1.56	0.90	3.90	0.75	0.47	0.24	1.03	0.27	0.84	0.53	2.29	0.55
PostOp Fusion	**Max Rt**	0.21	0.53	1.01	0.22	0.39	1.03	2.01	0.39	0.18	0.62	1.34	0.35	0.26	0.11	0.15	0.04
	Max Lt	0.62	0.33	1.26	0.28	0.84	0.47	2.08	0.40	0.47	0.06	0.63	0.17	0.12	0.34	0.32	0.08
PreOp Facet	**Max Rt**	0.00	0.63	0.02	0.00	0.02	0.56	1.26	0.25	0.07	1.03	4.17	1.08	0.00	0.29	0.39	0.10
	Max Lt	0.00	0.00	0.00	0.00	1.11	0.09	3.07	0.60	1.56	0.57	5.89	1.53	0.25	0.16	0.30	0.08
PostOp Facet	**Max Rt**	0.54	0.00	0.77	0.17	0.06	0.34	0.53	0.10	0.12	0.47	2.33	0.61				
	Max Lt	1.00	0.00	0.18	0.04	0.00	0.78	0.04	0.01	0.38	0.16	0.26	0.07				
PostOp Disc	**Max Rt**	0.00	0.00	0.00	0.00	0.00	0.12	0.00	0.00	0.00	0.38	0.74	0.20	1.22	0.02	3.04	0.74
	Max Lt	0.00	0.49	0.00	0.00	0.00	0.07	0.50	0.08	0.00	0.12	1.01	0.26	0.00	0.00	0.00	0.00

3.2.3. Lateral Bending

During the lateral bending activity, the ligaments did not reach failure amounts, but there are some trends in the data. During a pure in-plane motion it is expected that the ITL on the opposite side of the motion will be under stress while the other would not. In most of the healthy subjects this was seen, but in groups with large out-of-plane motions the ITL on the side of motion was under stress. A good example is L3/L4 for the healthy subjects which had a left ITL stress of 1.27 MPa and a right ITL stress of 0 MPa at maximum right. At the same level the degenerative group had an average stress of 2.34 MPa in the left ITL and 0.25 MPa in the right ITL. While this did not always show in the data it can be useful in determining joint stability. One of the other trends is that in all levels besides L2/L3 the stress in the SSL and ISL were lowest for the healthy group. This corresponded with the healthy group having lower amounts of out-of-plane rotations which would increase the distance between the spiny processes for two corresponding vertebral bodies. The final trend found was that in the healthy group the higher ITL stress resulted in a higher stress in SSL and ISL. Such as level L4/L5 where at maximum right the left ITL was 1.24 MPa, the SSL was 0.55 MPa, and the ISL was 0.12 MPa. Moving to the maximum left the stress in the right ITL became 1.29 MPa at maximum left which also increased the SSL stress to 0.60 MPa and the ISL stress to 0.13 MPa. Taking the same case for low back pain group the left ITL was 1.52 MPa with a stress of 2.26 MPa on the SSL and 0.49 MPa on the ISL. Moving to the maximum left the stress of 1.41 MPa was lower on the right ITL but a higher stress of 2.9 MPa on the SSL and 0.63 MPa on the ISL. It is hypothesized that this is a result of the out-of-plane motions experienced by subjects during the motion creating increased distance between the transverse processes during the motion. All average values can be found in Table 8 for the groups.

Table 8. Stress in the ligaments during lateral bending activity.

Identifier	Frame	L1/L2				L2/L3				L3/L4				L4/L5			
		Left ITL	Right ITL	SSL	ISL	Left ITL	Right ITL	SSL	ISL	Left ITL	Right ITL	SSL	ISL	Left ITL	Right ITL	SSL	ISL
Healthy	Max Rt	1.24	0.00	0.55	0.12	1.80	0.00	1.81	0.35	1.27	0.00	1.44	0.38	1.78	0.00	1.07	0.26
	Max Lt	0.05	1.29	0.60	0.13	0.04	1.53	1.87	0.36	0.00	1.22	0.92	0.24	0.00	1.97	1.55	0.38
LBP	Max Rt	1.52	0.09	2.26	0.49	1.25	0.01	0.91	0.18	2.29	0.10	4.89	1.27	1.26	0.06	1.08	0.26
	Max Lt	0.12	1.41	2.90	0.63	0.00	1.45	1.23	0.24	0.11	1.94	4.50	1.17	0.00	1.34	0.70	0.17
Degen	Max Rt	1.73	0.01	1.86	0.41	1.85	0.00	0.93	0.18	2.34	0.25	4.62	1.20	0.75	0.24	0.89	0.22
	Max Lt	0.06	1.60	2.07	0.45	0.02	1.74	2.08	0.41	0.05	1.66	1.86	0.49	0.15	1.20	0.86	0.21
PreOp Fusion	Max Rt	1.46	0.08	0.72	0.16	1.24	0.01	0.34	0.07	1.09	0.00	1.18	0.31	0.70	0.10	0.35	0.09
	Max Lt	0.39	1.31	2.52	0.55	0.07	1.28	1.43	0.28	0.29	1.58	4.93	1.29	0.39	0.98	2.50	0.61
PostOp Fusion	Max Rt	1.35	0.58	2.34	0.51	1.71	0.11	2.19	0.43	1.08	0.39	5.16	1.34	0.69	0.56	1.63	0.40
	Max Lt	0.07	1.33	0.84	0.19	0.21	1.52	0.61	0.12	0.11	1.24	2.09	0.55	0.15	0.41	0.48	0.12
PreOp Facet	Max Rt	1.04	0.00	0.00	0.00	0.77	0.00	2.35	0.46	0.60	0.00	0.23	0.06	1.03	0.00	0.18	0.05
	Max Lt	0.00	0.63	0.00	0.00	0.00	1.20	0.47	0.09	0.00	0.64	0.96	0.25	0.02	0.98	0.54	0.13
PostOp Facet	Max Rt	1.11	0.00	1.17	0.26	1.43	0.00	0.00	0.00	1.20	0.00	2.89	0.75				
	Max Lt	0.00	2.24	0.54	0.12	0.00	1.90	0.16	0.03	0.00	1.59	5.71	1.49				
PostOp Disc	Max Rt	0.71	0.00	0.75	0.17	1.80	0.00	0.78	0.15	0.13	0.00	0.00	0.00	0.79	0.00	0.00	0.00
	Max Lt	0.00	0.00	0.00	0.00	0.23	0.18	0.60	0.12	0.00	0.10	0.00	0.00	0.00	0.35	0.00	0.00

3.3. Validation

The first validation step was done to determine if the disc's coordinate frame code was working as well as test the performance of the un-deformed length code. With the plate rotated throughout the 3D space the coordinate frames were accurately able to reorient the plates so the compression was within the Y direction and the X and Z remained along the correct edges. Next the plate which was at a distance of 10mm was assumed to have an average stress of -1/3 MPa on it. Running the un-deformed length code it was determined that the length would be 15mm which is the correct length given the linear elastic material properties used. Finally the plate was compressed to 5mm and the simulation was able to correctly determine the stress was -2/3 MPa in the Y direction (Fig. 90). This simulation was run multiple times with the plates in multiple locations and all tests came back with the same results.

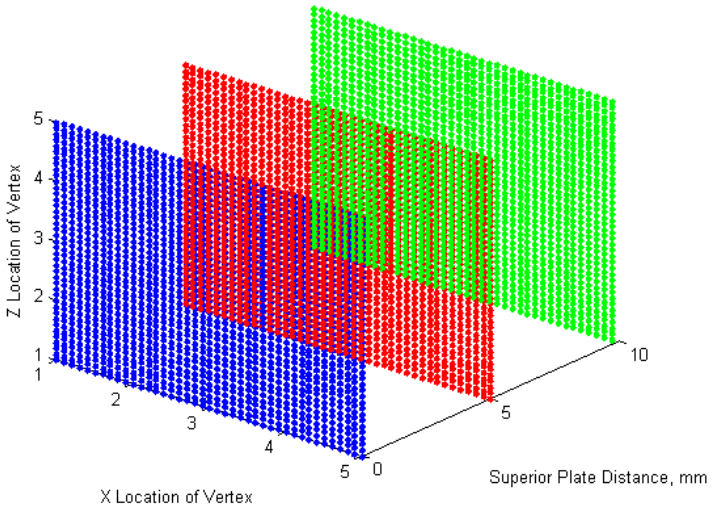

Figure 90. Simulation run to validate that the disc coordinate frame and un-deformed length codes were running as intended...

The validation of the intervertebral disc stress was done within finite element testing simulation for a generic 2 material disc model. Figure 91 shows the results from a compression on a two material disc. It can be seen that the annulus is at -0.1276 MPa after the compression. Running the discrete code with a compressive over a similar set of points the discrete code determined that the stress between the plate and the ground was -0.1275 MPa for the annulus. Similarly, the finite code found a stress of -0.08696 MPa for the nucleus, and the discrete found a stress of -0.083 MPa (Fig. 91). The shear stress model run in the finite element simulator found an annulus stress of between -0.04123 - 0.04268 MPa in the annulus and 0.02523 MPa in the nucleus (Fig. 92). For a 5mm translation the shear stress at the points was found to have a calculated stress of -0.0435 MPa for the annulus and -0.0278 MPa for the nucleus. The final test done was a combined motion of compression and shearing with the goal to determine the error of the combined motion for the sample disc. In this test a 5mm compression and translation were applied. The finite element code found a stress of 0.167 MPa in the annulus and 0.1122 MPa in the nucleus (Fig 93). The discrete code found that given the same displacements the stress in the annulus was 0.15 MPa and 0.1 MPa in the nucleus. The difference between the two models is around 10% with the difference being from the missing stress of the disc bulging as well as the errors found in the other two tests. The discrete code does not calculate the normal stress in the X and Z directions currently; however the finite model shows stresses of -0.0058 MPa in the nucleus and -0.0089 MPa in the annulus due to material interactions.

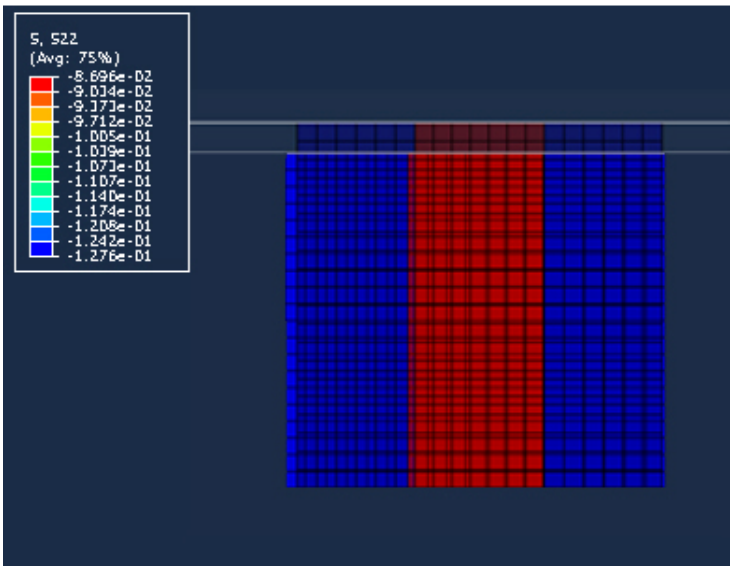

Figure 91. Compression test to validate the normal stress calculations from the discrete code.

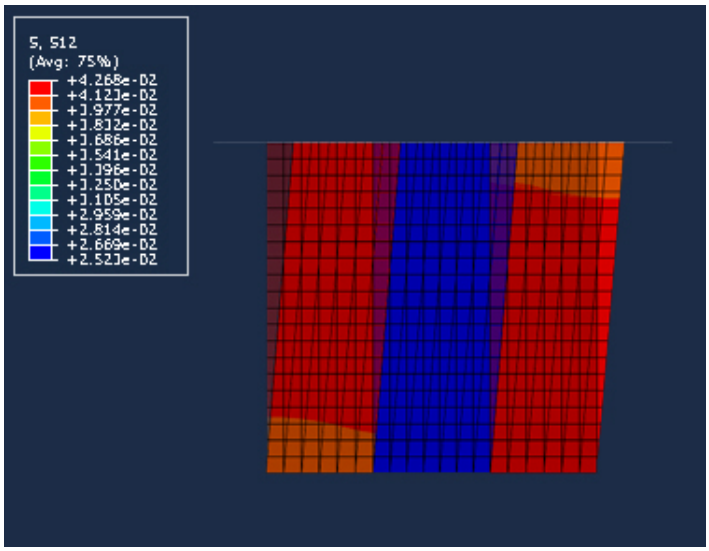

Figure 92. Shear test to validate the shear stress calculations from the discrete code.

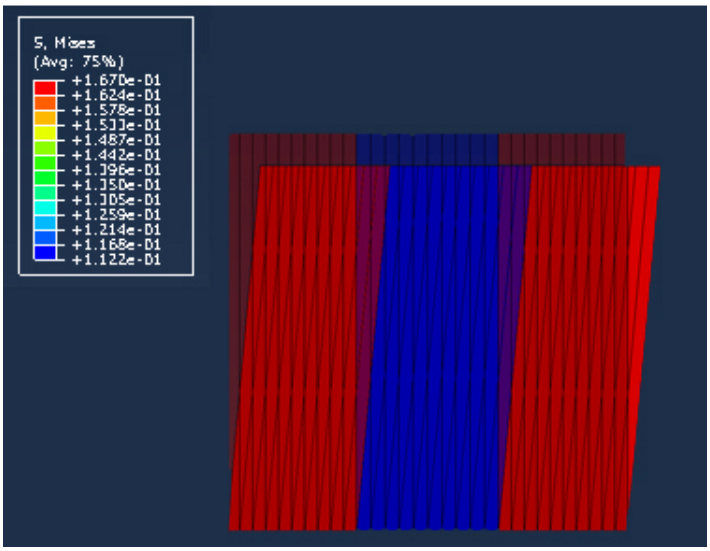

Figure 93. Shear test to validate the shear stress calculations from the discrete code.

The in vivo comparison was done between our model based on motion acquired from fluoroscopy where the rigid motion of the vertebral bodies is known and previously validated[76], and the in vivo data from Wilke et al.[37, 38] which was obtained from a pressure transducer from one volunteer over the course of 24 hours implanted at L4/L5. Wilke found that the pressure for lying prone was 0.1 MPa, standing was 0.5 MPa, flexed forward was 1.1 MPa, flexed backwards was 0.6 MPa, maximum during lateral bending was 0.6 MPa, and maximum during axial rotation was 0.7 MPa. From our healthy subjects the average stress at standing was 0.65 MPa at L4/L5, 0.50 MPa at L3/L4, 0.50 MPa at L2/L3, and 0.56 MPa at L1/L2. At maximum flexion our model seemed to have a slightly lower average at 0.84 MPa at L4/L5, 0.52 MPa at L3/L4, 0.47 MPa at L2/L3, and 0.69 MPa at L1/L2. At maximum extension the measured average stress was -0.55 MPa at L4/L5, -0.42 MPa at L3/L4, -0.43 MPa at L2/L3, and -0.56 MPa at L1/L2. During lateral bending the highest average stress was found to be -0.66 MPA at L4/L5, -0.32 MPa at L3/L4, -0.43 MPa at L2/L3, and -0.33 MPa at L1/L2. Finally, the

highest stress at maximum axial rotation was -0.6 MPa at L4/L5, -0.54 MPa at L3/L4, -0.47 MPa at L2/L3, and -0.36 MPa at L1/L2. The slight differences between the two models was assumed to be due to the collagen fibers in our model are not completely subject specific and some people may have more motion allowed before the fibers start to resist motion. This will change the overall stress in the disc as the can add tensile stress lowering the overall average compressive stress. Furthermore, the test done by Wilke was an invasion procedure which may have caused slight limitations in motion. That being said the discrete code average stresses at L4/L5 seem to compare very well to the in vivo data collected by Wilke.

Direct comparison with current finite elastic models will not be complete in the validation of using discrete modeling. This is because all current finite models assume that an ideal force is inputted in the spine. This causes much more ideal conditions with most simulations happening with complete in-plane motion. In such model as one created by Renner et al.[69] which was done with hyperelastic material properties. In this study the authors applied a flexion-extension moment as well as two different compressive preloads to cadaveric lumbar spinal column which may not be representative of real human motion. A closer model came from Natarajan et al.[71] which utilized an EMG-assisted model designed by Granata and Marras [77, 78] to input muscular force and trunk kinematics from in vivo testing. While this model has better inputted data, the trunk motion is acquired from an apparatus attached to the outside of the skin[79]. For their tests the subjects were asked to perform eight different tasks while carrying a 30 lb box. In the standing position the maximum stress was around 1.7 MPa. From flexion to upright standing the maximum stress in the disc was found to be 4.5 MPa. Finally during lateral bending the maximum stress was 6 MPa. Although our subjects are not carrying any extra weight it was found that in the upright position the

maximum stress on average was 2.2 MPa. During the flexion extension activity the maximum stress got as high as 4.76 MPa. Lateral bending had a maximum stress as high as 4.19 MPa. While the two models are slightly different the location and magnitudes of the stresses compare well between the two models.

Recently Shaobai Wang[80] from Massachusetts Institute of Technology developed a similar discrete model. In his model, the points were collected at the superior and inferior points tracking the surfaces of a single level, L3/L4, during a flexion-extension activity while carrying a weight. From the superior and inferior planes a 3D mesh was generated at each frame. Using finite element software, the change in the mesh from one frame to a reference frame was calculated to find the stress in the disc. In this model the reference frame was the supine position for the three patients. The resulting stresses were 1.3 MPa at standing, 0.2 MPa at maximum flexion, and 0.6 MPa at maximum extension. One of the patients in this study was also found to have a fiber stress of 20.5 MPa in a section of the posterior disc. While this model has some good aspects, the major flaw is in the determination of the reference frame being supine. My first attempt at the discrete code showed that using the MRI supine position creates tension in the disc at standing. This tension is in the posterior section of the disc where the fibers are the stiffest. Without fibers, my preliminary linear elastic model showed using MRI supine as the reference can create 2 MPa or more of posterior tension. This value would severely increase with the addition of fibers as well as having the patient flex. It was determined that the tension in the disc could not correct being that the body is under a compressive load at standing. This led to the creation of the un-deformed disc height calculation.

3.4. Sensitivity Analysis

Sensitivity analysis was first run to determine the effects of the number of points on the contact area and the resulting length measurement. This was done by utilizing the contact area from a healthy subject with the mesh size changed to determine the effect on the measured un-deformed length. The mesh size refers to the distance between points on the surface. The different size used for the sensitivity testing were: 2 mm, 1.75 mm, 1.5 mm, 1.25 mm, 1 mm, 0.75 mm, 0.5 mm, and 0.25 mm. While there is a definite change as more points are added this will not significantly change the results as long as the number of points can accurately define the surface (Fig 94). The length only changed about 3.6% from longest length at a mesh of 1.75mm to the shortest length at a mesh of 0.25mm while the number of points increased from about 500 to 17,000. While the stress at neutral will remain the same no matter the mesh size, the sensitivity of the stress at the other frames must be known. To determine the greatest difference the maximum flexion frame was chosen given that this will be the occurrence of the maximum displacements. At the largest length the average stress at maximum flexion was 0.93MPa. The shortest length created an average stress of 0.88 MPa which is about a 5.7% difference. For the groups in this study it was decided that a mesh size of 0.25mm would be chosen as it will give the best possible representation of the contact surfaces.

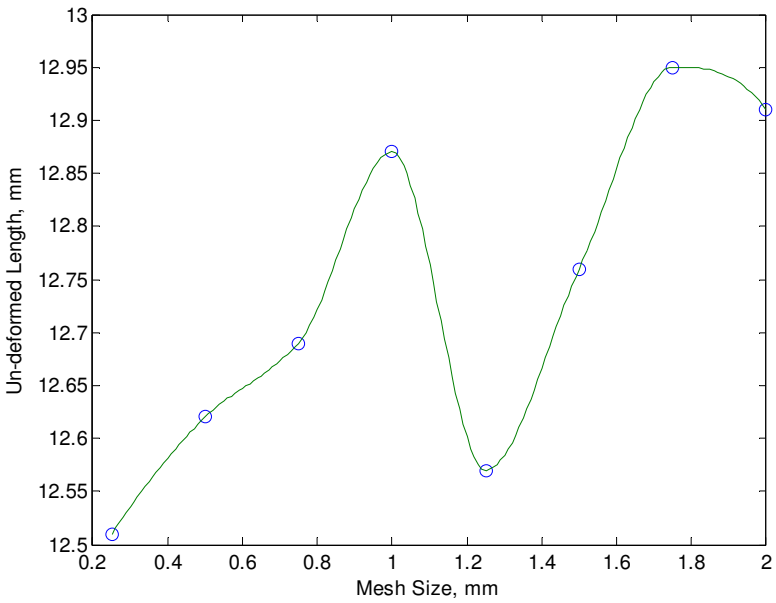

Figure 94. Sensitivity analysis to determine the influence the mesh size on the surface area has on the measured un-deformed length.

Chapter 4. Discussion

This dissertation resulted in the first soft tissue stress computational model that works directly with in vivo kinematics and subject specific models without the use of finite element modeling. The current discrete model is much faster taking mere minutes to run all three activities over the entire lumbar spinal column while only suffering around 10% loss in overall stress. With the inclusion of disc bulging in the future, it is thought that this error will greatly decrease. One of the more novel ideas was the determination of an un-deformed disc height. While disc heights are used as classification tool for degeneration by doctors, they are normally measured in the supine position under loading conditions which are not carrying the body's complete compressive load. When modeled, the disc is assumed to have a uniform preload. It is never discussed that the load would be applied non-uniformly across the surface due to the contact area on the vertebral bodies. In this case our method of removing the preload to determine an un-deformed length allows for a more natural distribution of the assumed preload. Interestingly from the subjects examined after the preload is removed the un-deformed lengths are rather consistent throughout the levels.

When comparing our normal subjects kinematics to that of literature our patients had 11.8°, 9.6°, 12.2°, 13.1° of flexion at L1/L2, L2/L3, L3/L4, L4/L5 respectively. White and Punjabi[68] noted 12°, 14°, 15°, and 17°, Pearcy et al.[81] noted 13°, 14°, 13°, and 16°, and Dvorak[82,83] noted 11.9°, 14.5°, 15.3°, and 18.2° respectively. With our fusion subjects a study was performed using implanted bead and at the adjacent level to the fusion (L3/L4) the researchers found approximately 5.5° of flexion extension which the same amount we found at the spinal unit post-operatively for our patients[84]. Chen et al.[72]

finite element model found that with a single fusion at L4/L5 the overall motion was decreased by 36.3% which is slightly more than the 29.6% our patients are experiencing.

The overall reasons for why the subjects have increased amount of out-of-plane motion and a decrease of in-plane motions are unclear several factors could be at the root of the problem. One problem discussed in the literature is the impact of the adjacent disc on the outcome of adjacent segments need for further surgery. They found that clinical outcome were worse for patients with normal discs at the adjacent level, but there was no significant differences between the groups need for additional surgery[57]. Our group has been discussed the problem may be muscular, caused by pain management. Ongoing research is being conducted with the muscles of the volunteers; however, at this moment no results have been reached. Lifting exercise research has shown that in volunteers with low back pain activate their erector spinae for longer periods of time than normal volunteers[47]. A study done on cyclists had subjects with pain showed a loss of co-contraction of the lower lumbar multifidus[48]. With pain management, it has been shown in the knee that there is an interrelationship between pain and gait motion[85, 86], but no studies were found in the spine. It is our belief though that if the out-of-plane motion was addressed the rate of degeneration could be lessened at the early signs of back pain. A possible solution for low back pain patients may come in the form of retraining the muscles so the kinematics of the spine reflects more of the average motion. This may also prevent adjacent segment disease in surgery patients. While physical therapy is aimed at helping the patients regain motion after surgery, our finding show that the patients are not significantly different after weeks of therapy. Perhaps the people need to spend more time in therapy relearning their trunk kinematics in an effort to reduce adjacent segment degeneration in patients.

To the best of our knowledge, this study is the first to describe the in-vivo out-of-plane motions and their effect on the stress of the intervertebral disc. Taking the rigid bone movements from fluoroscopy the stress location at the different loading conditions closely followed the determined kinematic pattern. During the flexion-extension exercise, examining the normal tress in Figure 95 it can be seen that the average stress for the healthy, low back pain, and degenerative group together while the surgical groups both preoperative and postoperative have much different stress paths and magnitudes. The fusion subjects also were found to have a lower overall average postoperatively. During axial rotation, the healthy tended to have the lowest overall stresses with the stress increasing with increase of the group type for example preoperative fusion is higher than low back pain. Furthermore, postoperative stresses tended to be lower for the averages as well (Fig. 96). Finally with lateral bending activity, healthy was on the lowest stress at all levels between the four major groups (healthy, low back pain, degenerative, and fusion) at all levels besides L4/L5 (Fig. 97). While there were trends, no significant differences in the stress averages could be found; however, the individual discs showed that stress in discs with more out-of-plane motion causes the stress to drift. Furthermore, the fusion subjects tended to have a less concentrated stress meaning that the maximum stress on the disc acted over a larger area. It is believed that this drifting stress as well as the less concentrated stress will cause the disc to be under a more constant load as we move around in our daily lives. Adding in the examination of the stresses in the ligaments, the instability of motion is evident in the loading patterns with in some cases the ligaments being forced into failure causing damage. This damage will create less constraint in the motion further allowing the subject to have out-of-plane motions.

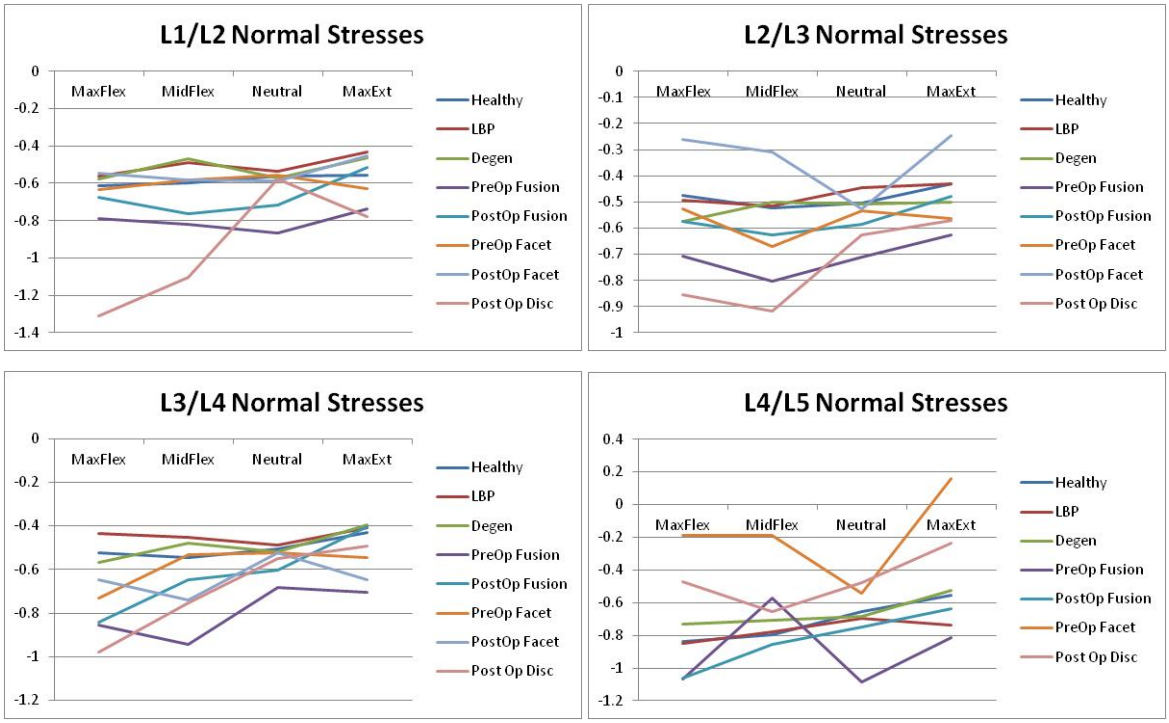

Figure 95. The average stress in the normal directions for each of the different groups at the four different levels during flexion-extension.

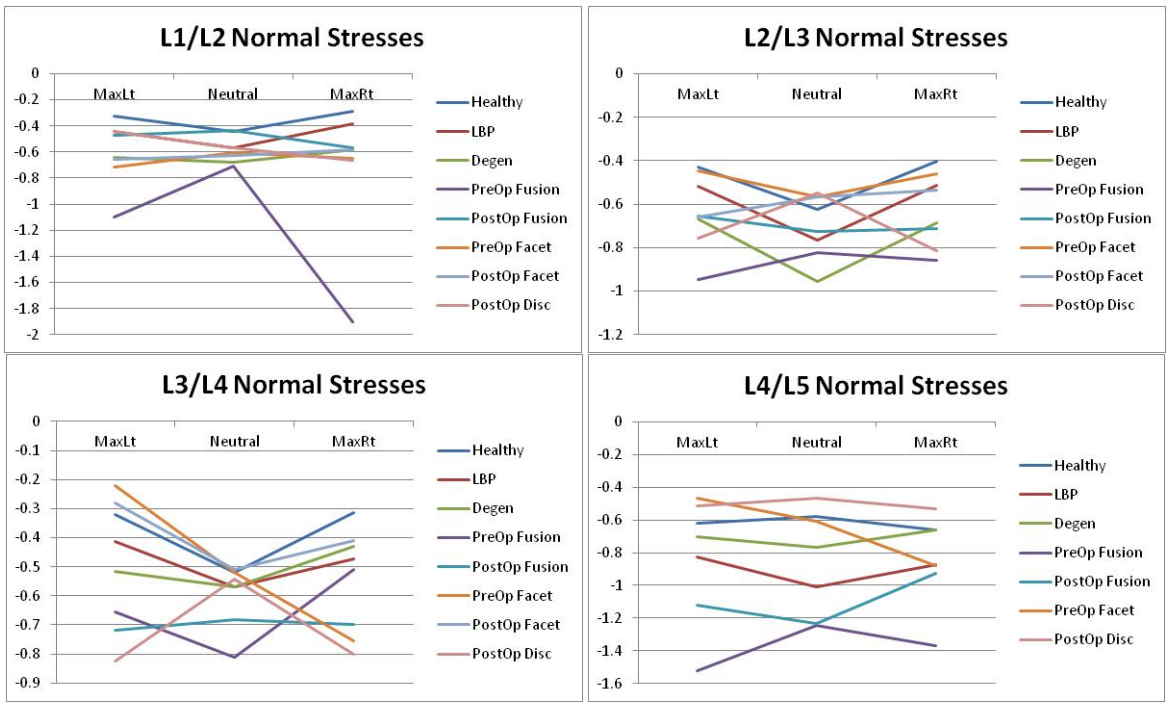

Figure 96. The average stress in the normal directions for each of the different groups at the four different levels during axial rotation.

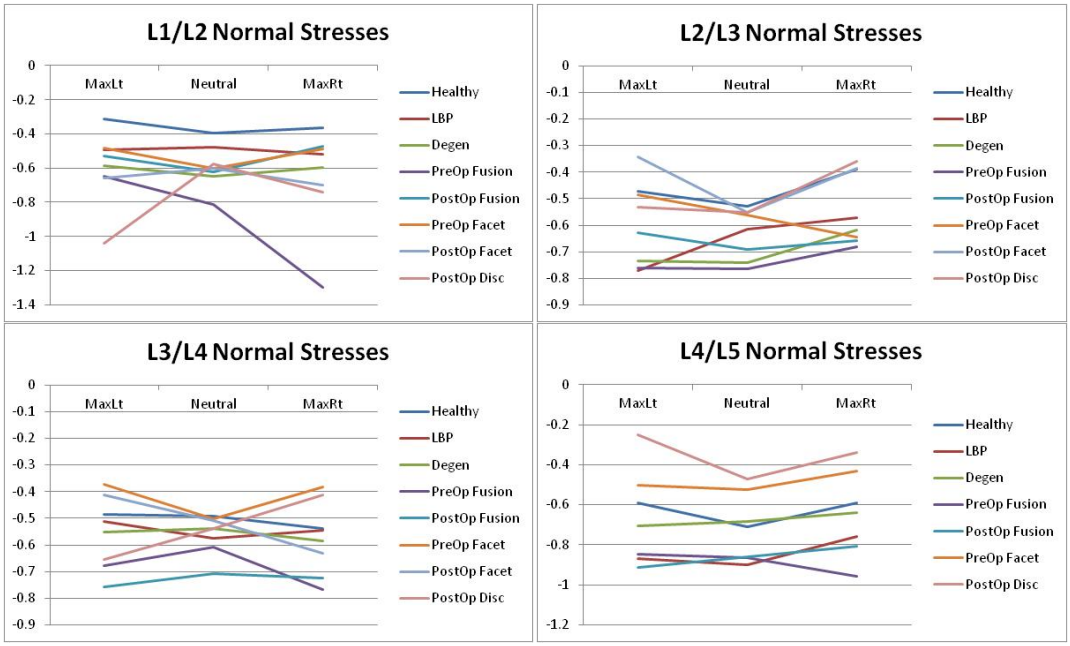

Figure 97. The average stress in the normal directions for each of the different groups at the four different levels during lateral bending.

Once the disc was segmented in nine individual sections some of the visual differences seen could be quantified. For the flexion-extension activity it would appear that the posterior stress played a large role in how the groups differ with the more degenerative groups having higher posterior stress than anterior stress. Furthermore the change in stress from neutral showed how some of the subjects had their stress fields affected by out-of-plane motion. With lateral bending most of the changes in the groups were found to be within the posterior or outer most sections. Some of the groups had levels with increases in the anterior sections which would appear to signify the flexion occurring during the motion. Finally, while the axial rotation activity does not show stress patterns during the activity the range of overall changes from neutral did have increasing ranges as the groups became more degenerative. This is in line with the kinematics showing increased out-of-plane compressive rotations. Overall it would appear that the posterior of the disc is the largest area of

change over the different group types when the activity is compressive in nature, and the range of stress acting on the disc for non-compressive motions. Our results compare well with Schmidt et al.[87] who did finite element research into intradiscal pressures in the intervertebral disc under combined loading. Although the loading conditions were idealized moments, they concluded that combined moments lead to higher stresses in the posterolateral section of the disc. This would lead to having the region susceptible to disc failure.

Many long term clinical studies have been conducted to reveal that while patients acquire adjacent segment degeneration, there was no clinical correlation. Lehmann et al.[58] studied 32 patients over a 30 year period. Nearly half of the patients developed instability at the segment superiorly adjacent there was no clinical correlation between the patients. Penta et al.[60] conducted a 10 year study where two similar groups of patients were compared. One group received a fusion and the other group received a different treatment. They concluded that there was no significant difference in rates of adjacent segment disease with approximately one-third of patients developed degeneration at the adjacent levels. Interestingly of our 6 surgery patients a third of them showed an overall increase in overall motion at the adjacent segment; however making a correlation to adjacent segment degeneration would be pure speculation.

Chapter 5. Future Work

While the discrete model current configuration is a good start some improvements could be made. For the intervertebral disc using a higher resolution MRI to image and segment more discs could be used to optimize the disc classification and allow for a more subject specific disc model. Next overlaying more frames in order to track the surfaces over a more complete motion would allow for new material to be included. Currently, the strain rate of the collagen fibers cannot be found because with limited frames it is unclear when the fibers activate. As more frames are used the strain rate of the collagen fibers can be modeled allowing for viscoelastic material modeling of the fibers. One other improvement would be the inclusion of disc bulging to allow for measurement of volumetric changes which in turn will allow for poroelastic material modeling being an option. Finally with some code optimization the complete code could be integrated into existing systems to allow for near real-time stress analysis and be a useful clinical tool.

As for the other soft tissues in the lumbar region the code needs to be optimized in order to be useful in determining muscle stresses. The current model is missing the sacrum which is the location of the origin of the major muscles. Currently the stress calculated can only be linear between two points and does not account for any lateral motion caused by compression. Most muscle span multiple levels so a wrapping code must be designed to determine how the muscle fibers will wrap as well as volumetric changes as the muscle contracts and elongates. Furthermore, while the code performs well on passive materials such as the disc and ligaments; the muscles are an active material. Current modeling techniques have no way to determine whether the muscle is passive or active. The ligaments will improve with adding more frames as they may then be modeled with viscoelastic material properties.

References

1) National Center for Health Statistics http://www.cdc.gov/nchs/
2) Roberts MP. Complications of lumbar disc surgery. In: Hardy RW Jr, ed. *Lumbar Disc Disease*. 2nd Ed. New York: Raven, 161-169, 1993.
3) Weinstein PR. Lumbar stenosis. In: Hardy RW Jr., ed. *Lumbar Disc Disease*. 2nd Ed. New York: Raven, 241-255, 1993.
4) Taylor VM, Deyo RA, Cherkin DC, Kreuter W. Low back pain hospitalization: Recent United States trends and regional variations. *Spine* 1994;19(11):1207-1213.
5) Luo X, Pietroban R, Sun S, Liu G, Hey L. Estimates and Patterns of Direct Health Care Expenditures Among Individuals With Back Pain in the United States. Spine. 2004. 29(1). P. 79-86.
6) World Health Organization http://www.who.int
7) Kelsey JL, White AA. Epidemiology and Impact of Low-Back Pain. *Spine*, 1980. 5(2). P. 133-142.
8) North American Spine Society, 2000. http://www.spine.org/articles/spondylolisthesis.cfm
9) Niosi C, Oxland T. *Degenerative mechanics of the lumbar spine*. *The Spine Journal* 4 (2004). 202S-208S
10) Humzah M. D., Soames R. W. Human intervertebral disc: structure and function. *Anat Rec.* 1988 April; 220(4): 337–356.
11) van den Hooff, A. Histological age changes in the annulus fibrosus of the human intervertebral disc. *Gerontologia*. 1964; 9:136-149.
12) Markolf K, Morris J. The structural components of the intervertebral discs. *J Bone Joint Surg AM* 1974; 56:675-687.
13) Gray, H. *Anatomy of the human body.* Philadelphia: Lea & Febiger, 1918; Bartleby.com, 2000. www.bartleby.com/107/.
14) Keyes DC, Compere EL. The normal and pathological physiology of the nucleus pulposus and the intervertebral disc. An anatomical, clinical, and experimental study. *J Bone Joint Surg Am*, 1932 Oct 01;14(4):897-938
15) Lindahl, 0. Uber den Wassergehalt des Knorpels. Acta Orthopaedica Scandinavica, 1948:17, 134.
16) Cassidy, J. J., A. Hiltner, and E. Baer. Hierarchical Structure of the Intervertebral Disc, *Connective Tissue Research* 1989;23:75–88.
17) Marchand, F, Ahmed AM. Investigation of the Laminate Structure of Lumbar Disc Anulus Fibrosus, *Spine* 1990;15:402–410.

18) Taylor, JR. Growth of the human IVD and vertebral bodies. J Anat. 1975;120:149-161
19) Guerin HAL, Elliott DM. Structure and Properties of Soft Tissue in the Spine. *Spine Technology Handbook*. Elsevier. 2006.
20) Bogduk N, Pearcy MJ, Hadfield G. Anatomy and biomechanics of psoas major. *Clin Biomech* 1992; 7:109-119.
21) Farfan HF. Form and function of the musculoskeletal system revealed by mathematical analysis of the lumbar spine. An essay. *Spine* 1995; 20:1462-1474.
22) Andersson, E, Oddsson L, Grundstrom H, et al. The role of the psoas and iliacus muscles for stability and movement of the lumbar spine, pelvis, and hip. *Scand J Med Sci Sports* 1995; 1:10-16.
23) Gracovetsky S. An hypothesis for the role of the spine in human locomotion: A challenge to current thinking. *J Biomed Eng* 1985; 3:205-216.
24) Gracovetsky S, Farfan HF, Lamy C. The mechanism of the lumbar spine. *Spine* 1981; 6:249-262.
25) Penning L. Psoas muscle and lumbar spine stability: A concept uniting existing controversies. Critical review and hypothesis. *Eur Spine J* 2000; 6:577-585.
26) Macintosh JE, Bogduk N, Munro RR. The morphology of the human lumbar multifidus. *Clin Biomech* 1986; 1:196-204.
27) Macintosh JE, Bogduk N, Pearcy MJ. The effects of flexion on the geometry and actions of the lumbar erector spinae. *Spine* 1993. 18:884-893.
28) Panjabi MM, Krag M, Summers D, et al. Biomechanical time-tolerance of fresh cadaveric human spine specimens. *Jour of Ortho Res* 1985; 3:292-300.
29) Ganlante JO. Tensile properties of the human lumbar annulus fibrosus. *Acta Ortho Scand [Suppl]* 1967; 100:1-91.
30) Nachemson A. Lumbar Intradiscal Pressure. *Acta Orthop. Scand. Suppl*. 1960; 43.
31) Nachemson A. The Influence of Spinal Movements on the Lumbar Intradiscal Pressure and on the Tensile Stresses in the Annulus Fibrosus. *Acta Orthop. Scand.* 33,183.
32) Nachemson A, Elfstrom G. Intravital Dynamic Pressure Measurements in Lumbar Discs: A Study of Common Movements, Maneuvers and Exercises. Stockholm: Almqvist & Wiksell. 1970
33) Nachemson A, Morris J M. In vivo Measurements of Intradiscal Pressure: Discometry, A Method for the Determination of Pressure in the Lower Lumbar Discs. *Bone J. Surg* 1964; 46A, 1077.

34) Cunningham BW, Kotani Y, McNulty PS, et al. The Effect of Spinal Destabilization and Instrumentation on Lumbar Intradiscal Pressure: An In Vitro Biomechanical Analysis. *Spine* 1997; 22:2655–2663.

35) McNally DS, Adams MA. Internal Intervertebral Disc Mechanics as Revealed by Stress Profilometry. *Spine* 1992. 17:66–73.

36) McNally, DS, Adams MA, Goodship AE. Development and Validation of a New Transducer for Intradiscal Pressure Measurement. *J. Biomed. Eng.*1992; 14:495–498.

37) Wilke HJ, Neef P, Caimi M, et al. New In Vivo Measurements of Pressures in the Intervertebral Disc in Daily Life. *Spine* 1995; 24: 755-762

38) Wilke HJ, Neef P, Hinz B, et al. Intradiscal Pressure Together with Anthropometric Data - a data set for validation of models. *Clin Biomech* [Suppl] 2001; 1:111-126.

39) Green TP, Adams MA, Dolan P. Tensile Properties of the Annulus Fibrosus II Ultimate tensile strength and fatigue life. *Eur Spine J* 1993; 2:209-214.

40) Iatridis JC, Kumar S, and Foster RJ. Shear Mechanical Properties of Human Lumbar Annulus Fibrosus. *J. Orthop. Res.* 1999; 17:732–737.

41) Iatridis JC, Setton LA, Weidenbaum M. Alterations in the Mechanical Behavior of the Human Lumbar Nucleus Pulposus with Degeneration and Aging. *J. Orthop. Res.* 1997; 15:318–322.

42) Iatridis JC, Weidenbaum M, Setton LA. Is the Nucleus Pulposus a Solid or a Fluid? Mechanical Behaviors of the Nucleus Pulposus of the Human Inter- vertebral Disc. *Spine* 1996; 21:1174-1184.

43) Pintar FA, Yoganandan N, Myers T, et al. Biomechanical Properties of Human Lumbar Spine Ligaments. *J Biomech* 1992; 25:1351-1356.

44) Hukins DW. Kirby MC, Sikoryn TA, et al. Comparison of Structure, Mechanical Properties, and Functions of Lumbar Spinal Ligaments. Spine 1990; 15:787–795.

45) Weiss JA, GardinerJC, Ellis BJ, et al. Three-dimensional Finite Element Modeling of Ligaments: Technical Aspects. Med. Eng. Phys 2005; 27:895–861.

46) Belavý DL, Armbrecht G, Richardson, Carolyn A. Muscle Atrophy and Changes in Spinal Morphology: Is the Lumbar Spine Vulnerable After Prolonged Bed-Rest? *Spine* 2011; 36;137-145.

47) Ferguson SA , Marras WS, Burr DL, et al. Differences in motor recruitment and resulting kinematics between low back pain patients and asymptomatic participants during lifting exertions. *Clin Biomech* 2004;19:992-9.

48) Burnett AF, Cornelius MW, Dankaerts W, et al. Spinal kinematics and trunk muscle activity in cyclists: a comparison between healthy controls and non-specific chronic low back pain subjects—a pilot investigation. *Manual Therapy* 2004;4:211-219.

49) Hansen L, de Zee M, Rasmussen J, et al. Anatomy and Biomechanics of the Back Muscles in the Lumbar Spine With Reference to Biomechanical Modeling. *Spine* 2006; 31:1888-1899.

50) Videman T, Nurminen M.The Occurrence of Anular Tears and Their Relation to Lifetime Back Pain History: A Cadaveric Study Using Barium Sulfate Discography. *Spine* 2004; 29:2668-2676

51) de Scheppper EIT, Damen J, van Meurs JBJ, et al. The Association Between Lumbar Disc Degeneration and Low Back Pain. *Spine* 2010; 35:531-536.

52) Dunlop RB, Adams MA, Hutton WC. Disc Space Narrowing and the Lumbar Facet Joints. *J Bone and Joint Surg* 1984; 66:706-710.

53) Thompson JP, Pearce RH, Schechter MT, et al. Preliminary Evaluation of a Scheme for Grading the Gross Morphology of the Human Intervertebral Disc. *Spine* 1990; 15:411-415.

54) Dooris A, Goel V, Grosland N, et al. Load-sharing between anterior and posterior elements in a lumbar spine motion segment implanted with an artificial disc. *Spine* 2001; 26:E122-E129.

55) Stinton S. Determination and Comparison of In vivo Forces and Torques in Normal and Degenerative Lumbar Spines, Master's Thesis, University of Tennessee, 2005.

56) Etebar S, Cahill DW. Risk factors for adjacent-segment failure following lumbar fixation with rigid instrumentation for degenerative instability. *Journal of Neurosurgery (Spine 2)* 1999; 90: 163-169.

57) Throckmorton TW, Hilibrand AS, Mencio GA, et al. The impact of adjacent level disc degeneration on health status outcomes following lumbar fusion. *Spine* 2003;28:2546-50.

58) Lehmann TR, Spratt KF, Tozzi JE, et al. Long-term follow-up of lower lumbar fusion patients. *Spine* 1987; 12:97-104.

59) Luk KD, Lee FB, Leong JC, et al. The Effect on the Lumbosacral Spine of Long Spinal Fusion for Idiopathic Scoliosis: a minimum 10-year follow-up. *Spine* 1987; 12:996-1000.

60) Penta M, Sandhu A, Fraser RD. Magnetic resonance imaging assessment of disc degeneration 10 years after anterior lumbar interbody fusion. *Spine* 1995;20:743-7.

61) Weinhoffer SL, Guyer RD, Herbert M, et al. Intradiscal pressure measurements above an instrumented fusion. *Spine* 1995;20:526-31.

62) Huang RC, Lim MR, Girardi FP, et al. The Prevalence of Contraindications to Total Disc Replacement in a Cohort of Lumbar Surgical Patients. Spine 2004; 29:2538–2541.

63) Mirza SK. Point of View: Commentary on the Research Reports That Led to Food and Drug Administration Approval of an Artificial Disc. *Spine* 2005; 30: 1561–1564.

64) Medicare Program; Changes to the Hospital Inpatient Prospective Payment Systems and Fiscal Year 2006 Rates: Final Rule. Department of Health and Human Services, Centers for Medicare & Medicaid Services. <https://www.cms.hhs.gov/providers/hipps/cms-1500f.pdf>

65) Perrin G, Cristini A. Prevention of Adjacent Level Degeneration Above a Fused Vertebral Segment: Long Term Effect, After a Mean Follow-up of 8.27 years, of the Semi-Rigid Intervertebral Fixation as a Protective Technique for Pathological Adjacent Disc. <http://www.scientx.com/Downloads/ClinicalStudies/WhitePapers/IsobarTTL/SemiRigid11.pdf>

66) Castellvi AE, Huang H, Vestgaarden T. Stress Reduction in Adjacent Level Discs via Dynamic Instrumentation: A Finite Element Analysis. *SAS Jour* 2007; 1:74-81.

67) Tsouknidas A, Michailidia N, Savvakis, et al. A High Accuracy CT Bades FEM Model of the Lumbar Spine to Determine its Biomechanical Response. *Prep of Camera-Ready Contr to INSTICC Proceedings* 2010.

68) White AA, Punjabi MM. *Clinical Biomechanics of the Spine*, 2nd ed. Philadelphia: Lipincott, 1990.

69) Renner SM, Natarajan RN, Patwardhan AG, et al. Novel Model to Analyze the Effect a Large Compressive Follower Pre-load on Range of Motions in a Lumbar Spine. *Jour of Biomech* 2007; 40:1326-1332.

70) Lu YM, Hutton WC, Gharpuray. Do Bending, Twisting, and Diurnal Fluid Changes in the Disc Affect the Propensity to Prolapse? A Viscoelastic Finite Element Model. *Spine* 1996; 21: 2570-2579;

71) Natarajan RN, Williams JR, Lavender SA, et al. Relationship Between Disc Injury and Manual Lifting: A Poroelastic Finite Element Model Study. *Proc of Inst of Mech Engr, Part H: Jour of Engr in Med* 2008; 222:195.

72) Chen C, Cheng C, Liu C, et al. Stress analysis of the disc adjacent to interbody fusion in lumbar spine. *Med Eng and Phys* 2001.23:483-91.

73) Abdel Fatah EE, Shirley NR, Jantz R, Mahfouz MR. Improving Sex Estimation from Crania Using a Novel Three-dimensional Quantitative Method. Accepted awaiting publication *Journal of Forensic Science*.

74) Abdel Fatah EE, Shirley NR, Mahfouz MR, Auerbach BM. A three-dimensional analysis of bilateral directional asymmetry in the human clavicle. *American Journal of Physical Anthropology* 2012. 149(4) 547–559.

75) Mahfouz MR, Hoff WA, Komistek RD, Dennis DA. A robust method for registration of three-dimensional knee implant models to two-dimensional fluoroscopy images. *IEEE Transactions of Medical Imaging* 2003. 22(12): 1561-1574.

76) Liu F. Theoretical modeling and experimental validation of in vivo mechanics for subjects having variable cervical spine conditions. PhD. thesis, University of Tennessee, Knoxville, 1997.

77) Granata KP, Marras WS. An EMG-assisted model of trunk loading during free-dynamic lifting. *Journal of Biomechanics* 1995. 28(11): 1309-1317.

78) Marras WS, Granata KP. The Development of an EMG-Assisted Model to Assess Spine Loading During Whole-Body Free Dynamic Lifting. *Journal of Electromyography and Kinesiology* 1997. 7(4): 259-268.

79) Marras WS, Fathallah FA, Miller RJ, et al. Accuracy of a three-dimensional lumbar motion monitor for recording dynamic trunk motion characteristics. *International Journal of Industrial Ergonomics* 1992. 9(1): 75-87.

80) Wang S. In vivo Lumbar Spine Biomechanics: Vertebral Kinematics, Intervertebral Disc Deformation, and Disc Loads. PhD. thesis, Massachusetts Institute of Technology, Cambridge, 2012.

81) Pearcy M, Portek I, Shepherd J. Three-dimensional x-ray analysis of normal movement in the lumbar spine. Spine 1984.9:294-297

82) Dvorak J, Panjabi MM. Functional radiographic diagnosis of the lumbar spine. Spine 1991.16:562-71.

83) Dvorak J, Panjabi MM, Novotny JE, et al. Clinical validation of functional flexion-extension roentgenograms of the lumbar spine. Spine 1991.16:943-50.

84) Anderst WJ, Vaidya R, Tashman S. A technique to measure three-dimensional in vivo rotation of fused and adjacent lumbar vertebrae. The Spinal Journal 2008.8:991-7.

85) Hurwitz DE, Hulet CH, Andriacchi TP, et al. Gait compensations in patients with osteoarthritis of the hip and their relationship to pain and passive hip motion. Journal of Orthopedic Research 2005. 4:629-35.

86) Shrader MW, Draganich LF, Pottenger LA, et al. Effects of Knee Pain Relief in Osteoarthritis on Gait and Stair-Stepping. Clinical Orthopedics and Related Research 2004. 188-93.
87) Schmidt H, Kettler A, Heuer F, et al. Intradiscal Pressure, Shear Strain, and Fiber Strain in the Intervertebral Disc Under Combined Loading. Spine 2007. 32(7):748-755.

Appendix

A.1. Gram-Schmidt Process

The Gram–Schmidt process is a method for orthonormalising a set of vectors in an inner product space. The Gram–Schmidt process takes a finite, linearly independent set $S = \{v_1, \ldots, v_k\}$ for $k \leq n$ and generates an orthogonal set $S' = \{u_1, \ldots, u_k\}$ that spans the same k-dimensional subspace of R^n as S.

Start with the definition of the projection operator which is

$$\operatorname{proj}_{\mathbf{u}}(\mathbf{v}) = \frac{\langle \mathbf{v}, \mathbf{u} \rangle}{\langle \mathbf{u}, \mathbf{u} \rangle} \mathbf{u},$$

where <v,u> is the inner product of vector u and v. For two vectors the process works like

$$\mathbf{u}_1 = \mathbf{v}_1,$$

$$\mathbf{u}_2 = \mathbf{v}_2 - \operatorname{proj}_{\mathbf{u}_1}(\mathbf{v}_2),$$

where u_2 is the new vector orthogonal to u_1. This technique is known to produce some errors when implemented in a computer setting due to rounding errors so there is a modified version

$$\begin{aligned}
\mathbf{u}_k^{(1)} &= \mathbf{v}_k - \operatorname{proj}_{\mathbf{u}_1}(\mathbf{v}_k), \\
\mathbf{u}_k^{(2)} &= \mathbf{u}_k^{(1)} - \operatorname{proj}_{\mathbf{u}_2}(\mathbf{u}_k^{(1)}), \\
&\vdots \\
\mathbf{u}_k^{(k-2)} &= \mathbf{u}_k^{(k-3)} - \operatorname{proj}_{\mathbf{u}_{k-2}}(\mathbf{u}_k^{(k-3)}), \\
\mathbf{u}_k^{(k-1)} &= \mathbf{u}_k^{(k-2)} - \operatorname{proj}_{\mathbf{u}_{k-1}}(\mathbf{u}_k^{(k-2)}).
\end{aligned}$$

A.2. Adjacent Disc

Isolating the superior adjacent level from the fusion site, there was found to be no significant differences preoperative versus postoperative. This analysis was done on the flexion extension activity. Figure 98 shows the difference of the rotations from post-operative to pre-operative. From these graphs it is shown that the overall trend is a loss in motion. Thus, it is concluded the fusion was not causing any hyper mobility in our patients as previously reported in other articles.

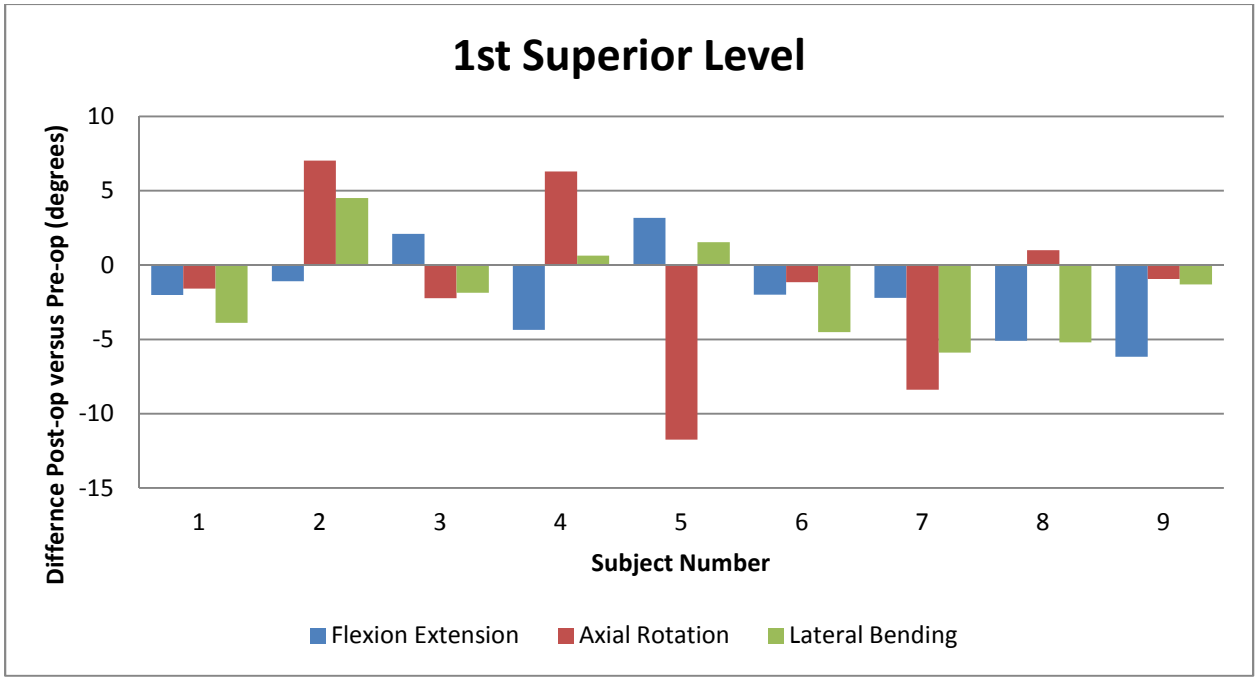

Figure 98. Change in total rotation after fusion for patient's completing a flexion extension activity.

A.3. Subject Initial Length Data

Table 9. Un-deformed Disc Lengths for All Subjects in millimeters.

Identifier	L4/L5	L3/L4	L2/L3	L1/L2	Identifier	L4/L5	L3/L4	L2/L3	L1/L2
Healthy 1	10.69	9.9	11.19	9.99	Pre op Fusion 1	14.66	13.35	14.58	10.32
Healthy 2	12.5	11.52	9.89	8.4	Pre op Fusion 2	18.18	13.15	10.17	12.64
Healthy 3	14.32	10.69	10.89	10.61	Pre op Fusion 3	17.16	15.43	15.04	12.75
Healthy 4	15.62	12.12	12.48	12.62	Pre op Fusion 4	5.9	7.46	7.12	7.07
Healthy 5	16.11	9.94	11.64	13.85	Pre op Fusion 5	13.15	17.1	13.86	13.53
Healthy 6	16.98	11.6	14.36	10.56	Pre op Fusion 6	15.49	11.26	15.05	14.72
Healthy 7					Pre op Fusion 7	10.39	10.16	11.47	10.55
Healthy 8	13.35	12.62	11.2	12.83	Pre op Fusion 8	13.53	14.29	13.84	12.61
Healthy 9	9.65	8.18	7.33	7.68	Pre op Fusion 9	12.12	13.11	7	8.7
Healthy 10	14.96	12.98	11.55	11.94	Pre op Fusion 10	20.58	15.53	15.54	14.78
Low Back Pain 1	17.3	15.31	14.77	15.44	Post op Fusion 1	N/A	13.24	14.46	10.24
Low Back Pain 2	19	11.92	12.33	14.66	Post op Fusion 2	17.81	12.9	9.99	12.35
Low Back Pain 3	13.79	13.17	16.09	15.28	Post op Fusion 3	17.13	15.4	15.01	12.73
Low Back Pain 4	12.73	9.4	9.87	8.4	Post op Fusion 4	N/A	7.5	7.15	7.11
Low Back Pain 5	13.75	13.15	10.13	11.24	Post op Fusion 5	N/A	17.77	14.4	14.1
Low Back Pain 6	13.73	11.57	11.54	10.93	Post op Fusion 6	16.16	11.67	15.64	15.31
Low Back Pain 7					Post op Fusion 7	N/A	10.4	11.76	10.82
Low Back Pain 8	13.73	11.37	12.91	9.96	Post op Fusion 8	N/A	N/A	13.93	12.7
Low Back Pain 9	14.4	8.82	10.04	8.36	Post op Fusion 9	N/A	13.36	7	9
Low Back Pain 10	10.98	9.68	9.45	10.63	Pre op Facet 1	15.8	13.71	14.88	13.31
Degenerative 1	11.43	9.89	11.31	10.05	Pre op Facet 2	12.48	12.58	10.68	11.08
Degenerative 2	10.78	9.44	10.09	10.61	Post op Facet 1	N/A		12.14	13.76
Degenerative 3	15.44	13.91	12.65	11.69	Post op Facet 2	N/A	15.19	12.68	10.89
Degenerative 4	12	12.25	12.54	10.08	Post op Disc 1				
Degenerative 5	12.97	12.03	12.27	11.68	Post op Disc 2	8.63	9.86	7	8.39
Degenerative 6	9.74	5.65	9.66	9.64					
Degenerative 7	10.37	11	12.9	11.53					
Degenerative 8	11.29	12.45	10.23	9.59					
Degenerative 9	10.87	10.93	10.14	11.58					
Degenerative 10	14.31	12.44	10.02	9.35					

A.4. Subject Stress Data

A.4.1 Flexion-Extension

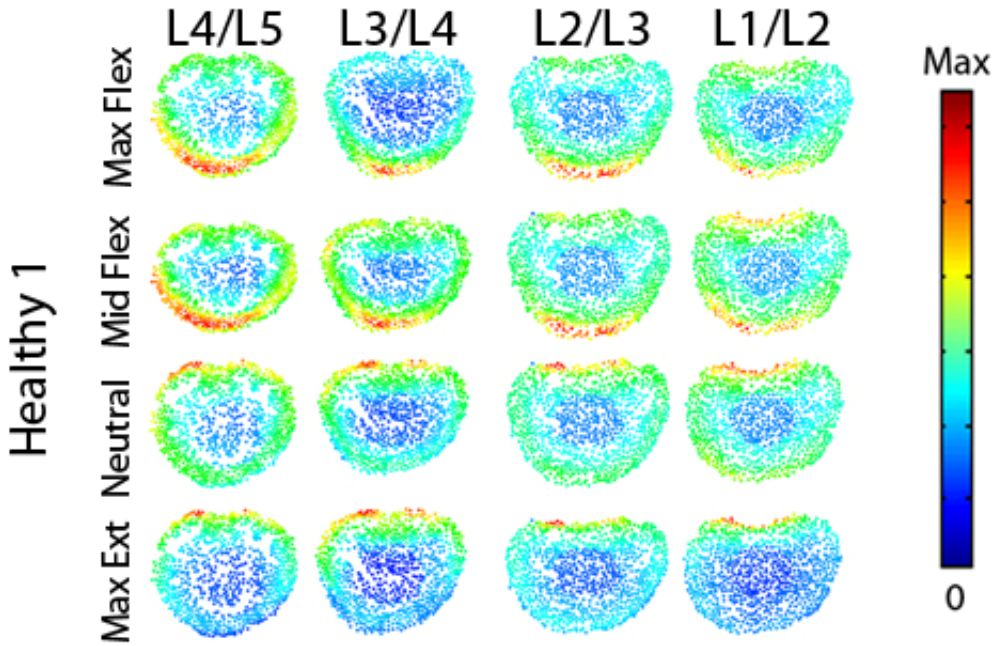

Figure 99. Magnitude stress at each atlas vertex for all levels at each major frame for Healthy 1.

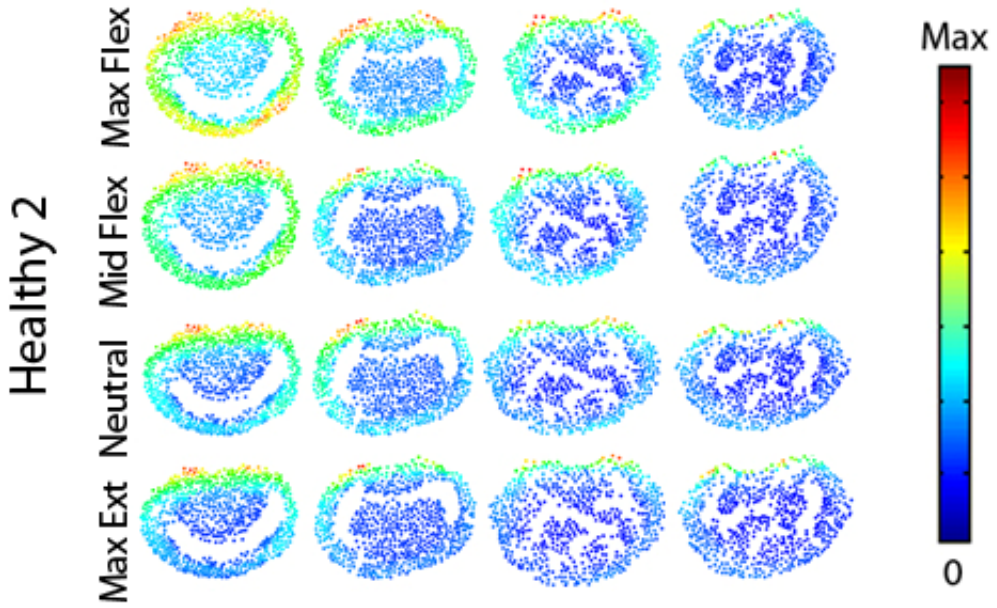

Figure 100. Magnitude stress at each atlas vertex for all levels at each major frame for Healthy 2.

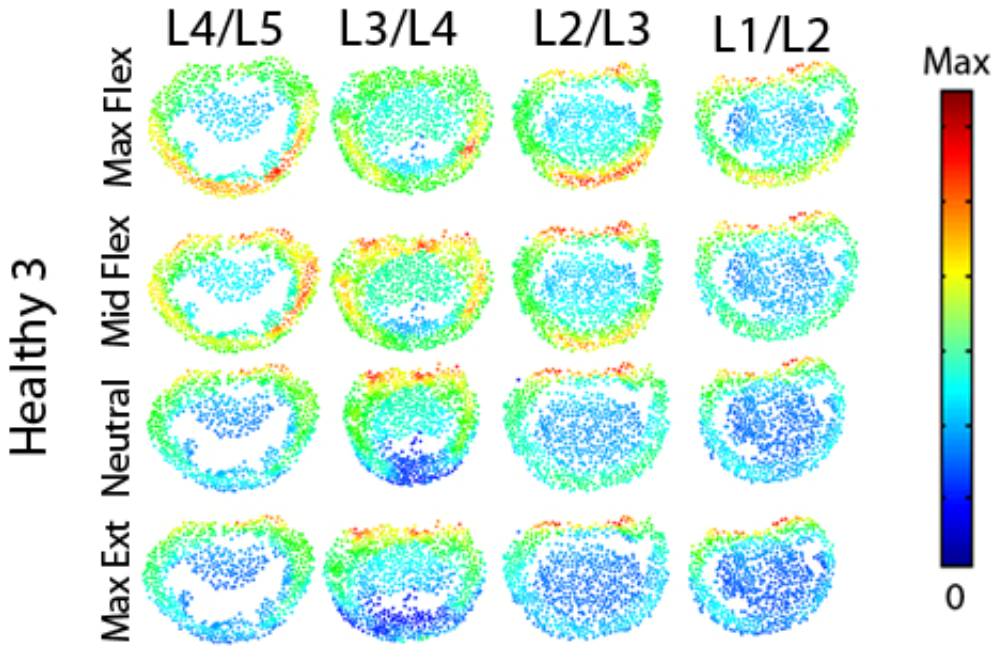

Figure 101. Magnitude stress at each atlas vertex for all levels at each major frame for Healthy 3.

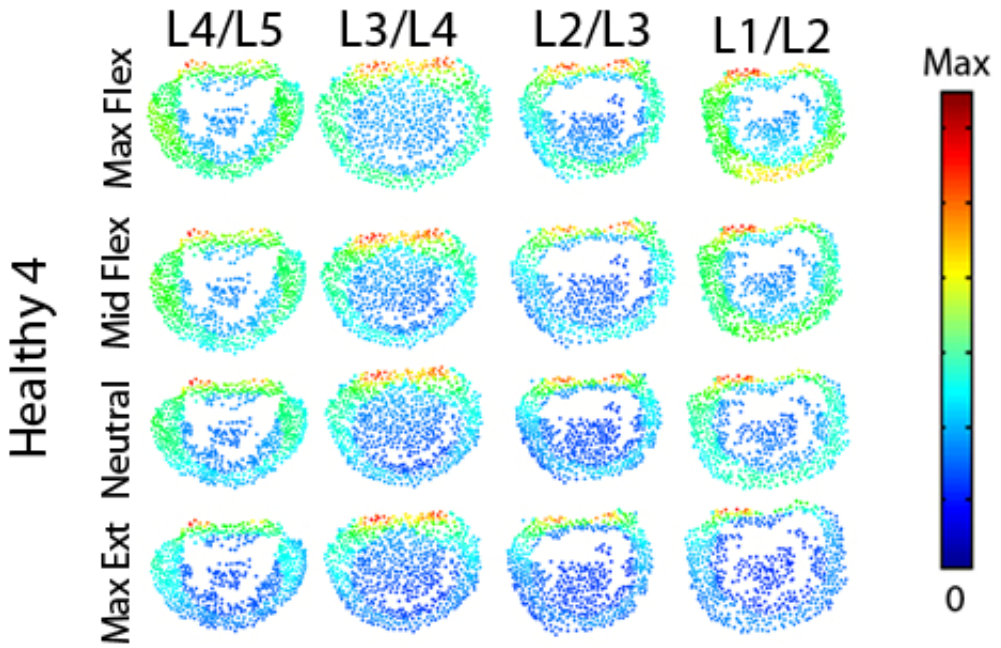

Figure 102. Magnitude stress at each atlas vertex for all levels at each major frame for Healthy 4.

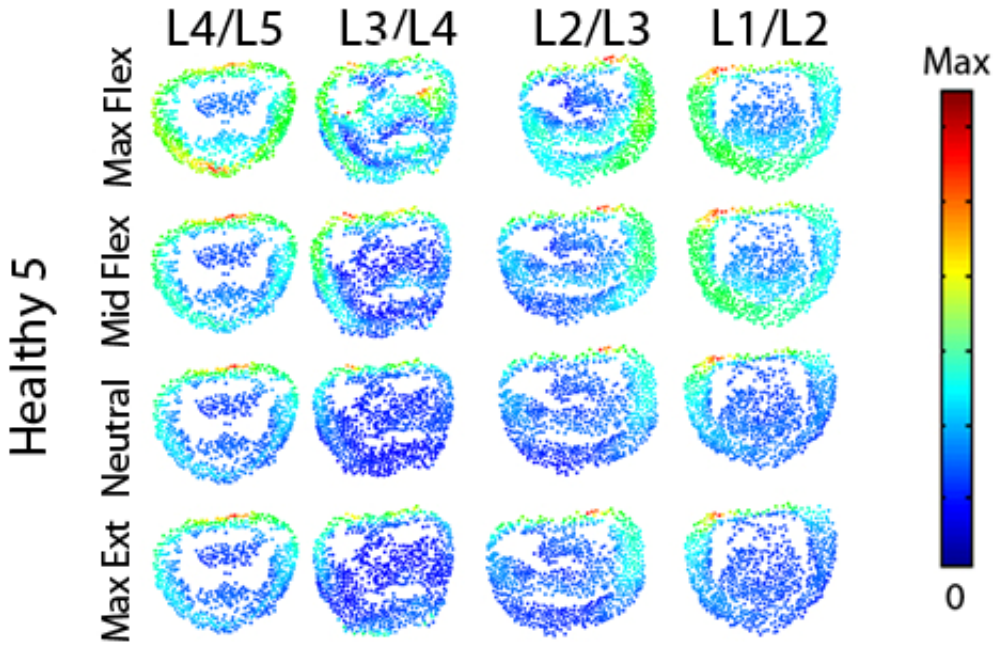

Figure 103. Magnitude stress at each atlas vertex for all levels at each major frame for Healthy 5.

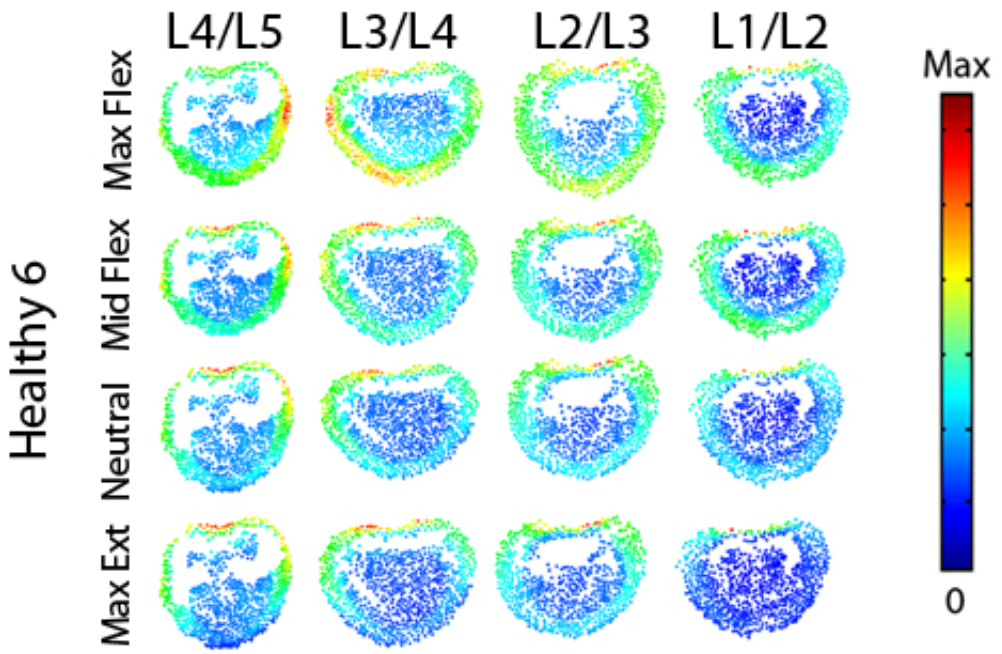

Figure 104. Magnitude stress at each atlas vertex for all levels at each major frame for Healthy 6.

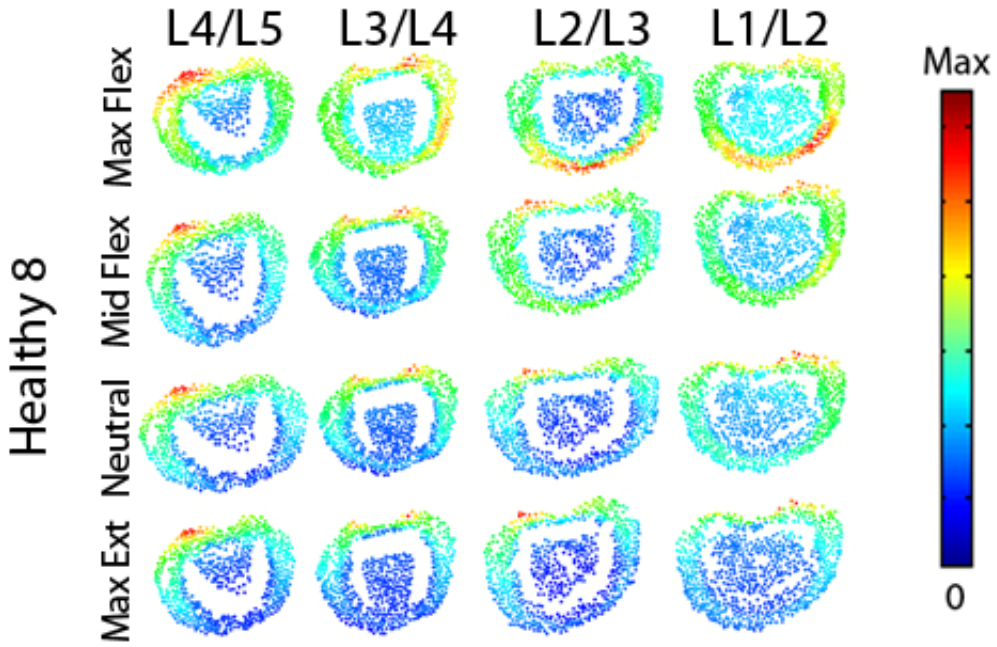

Figure 105. Magnitude stress at each atlas vertex for all levels at each major frame for Healthy 8.

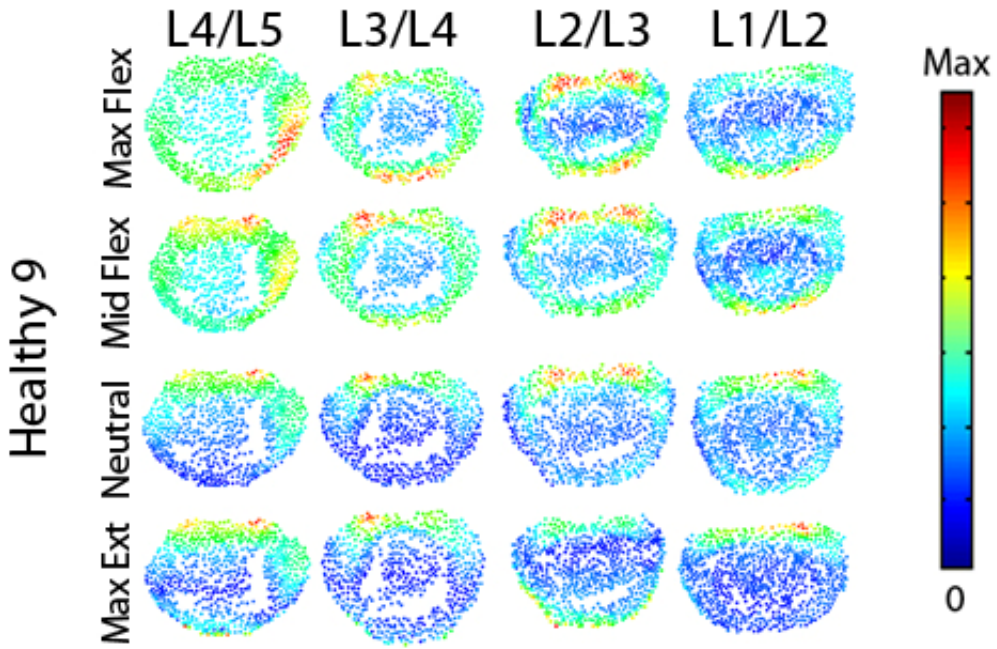

Figure 106. Magnitude stress at each atlas vertex for all levels at each major frame for Healthy 9.

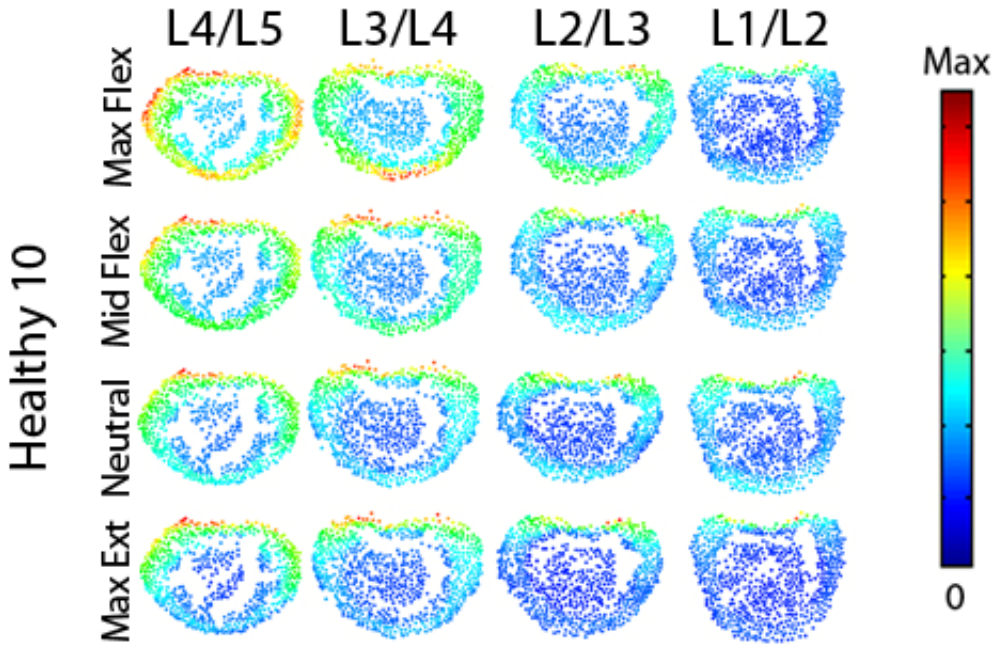

Figure 107. Magnitude stress at each atlas vertex for all levels at each major frame for Healthy 10.

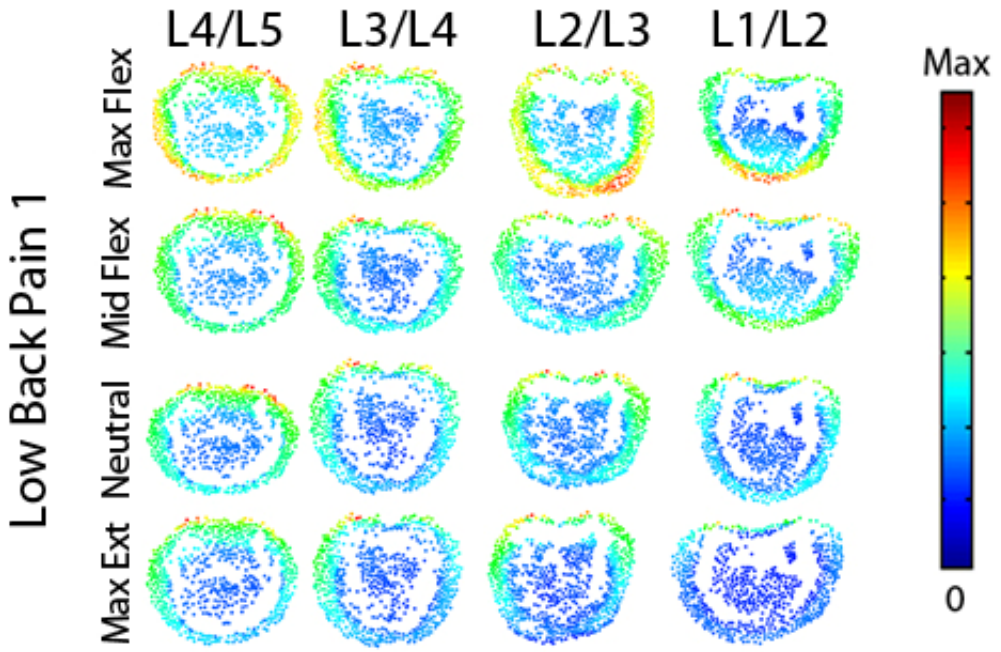

Figure 108. Magnitude stress at each atlas vertex for all levels at each major frame for Low Back Pain 1.

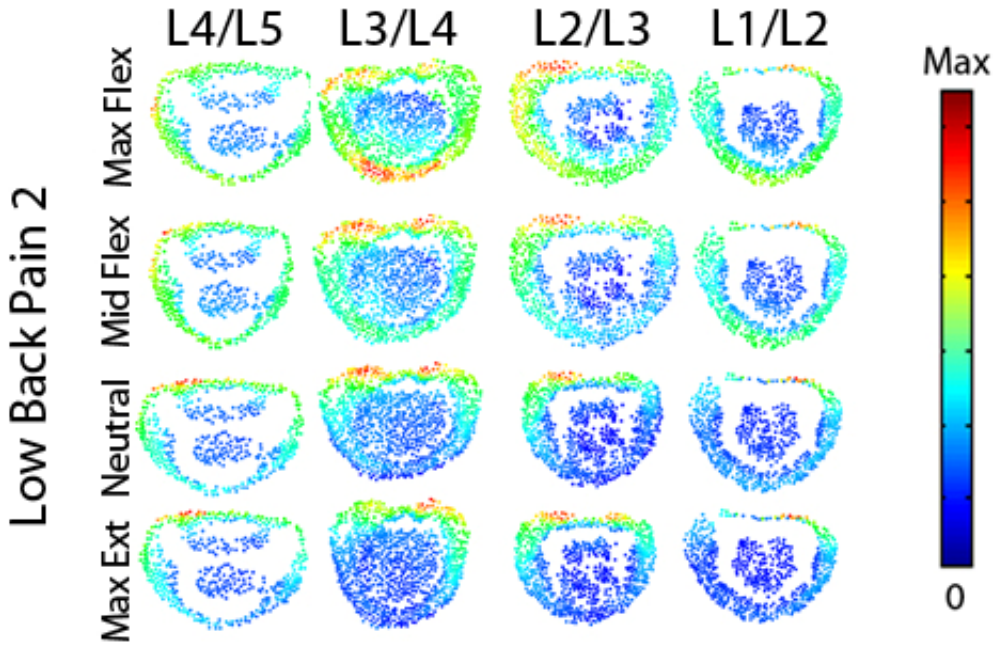

Figure 109. Magnitude stress at each atlas vertex for all levels at each major frame for Low Back Pain 2.

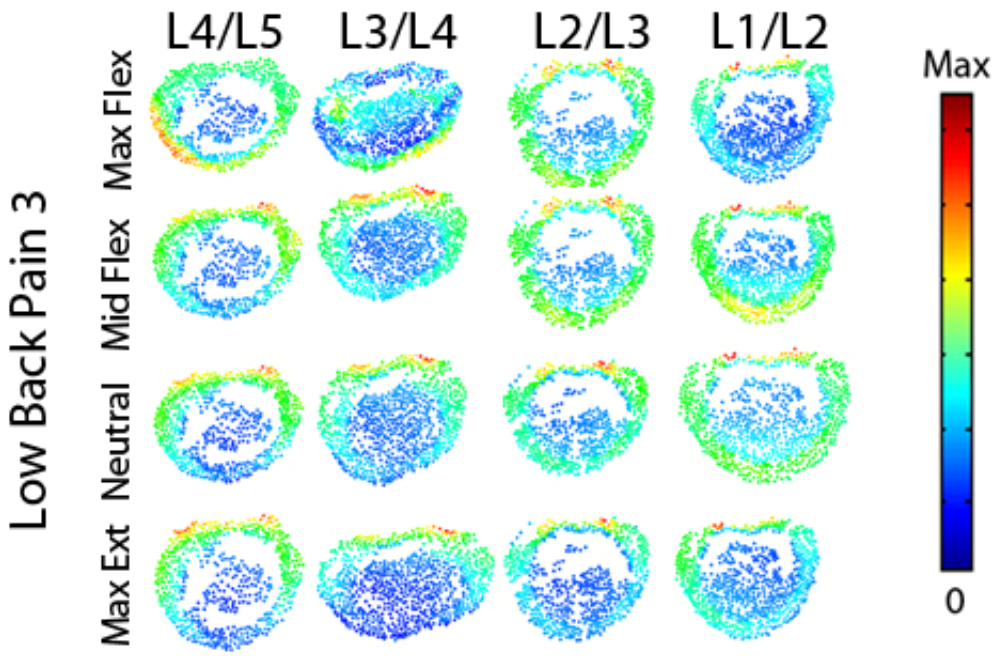

Figure 110. Magnitude stress at each atlas vertex for all levels at each major frame for Low Back Pain 3.

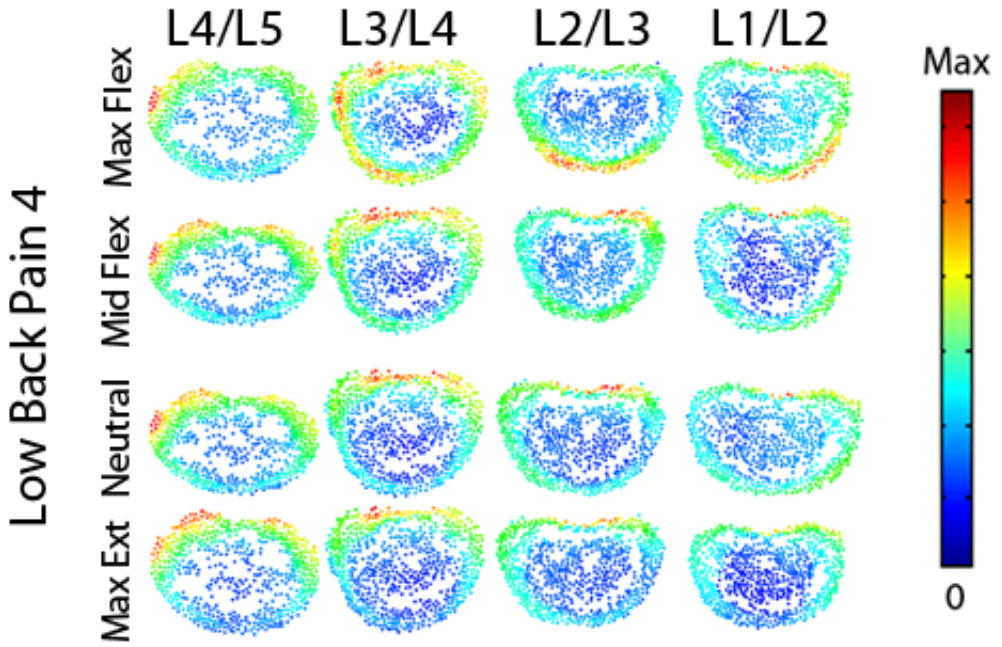

Figure 111. Magnitude stress at each atlas vertex for all levels at each major frame for Low Back Pain 3.

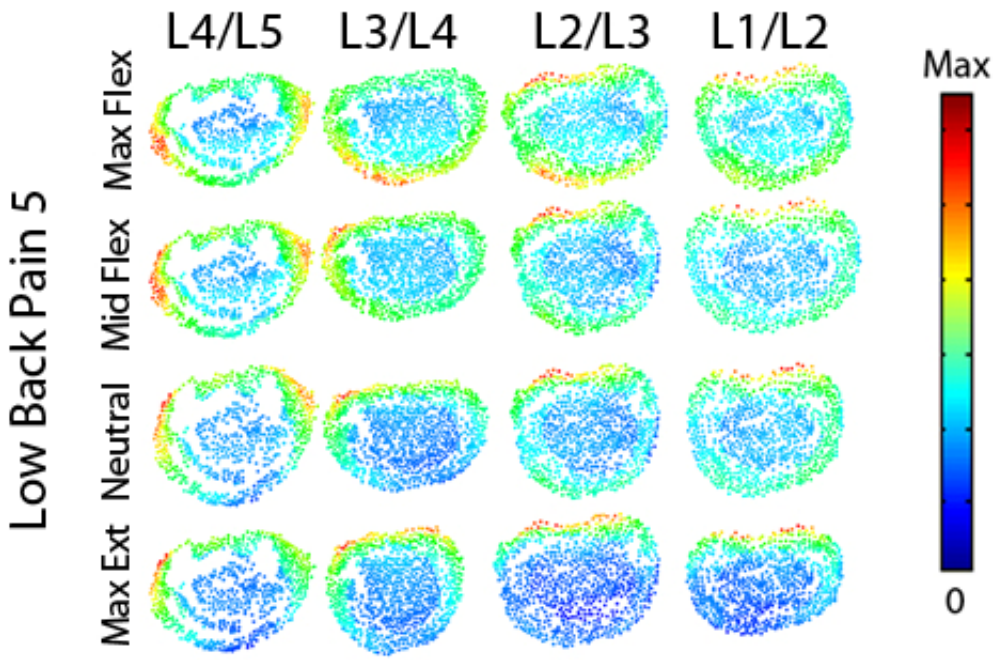

Figure 112. Magnitude stress at each atlas vertex for all levels at each major frame for Low Back Pain 4.

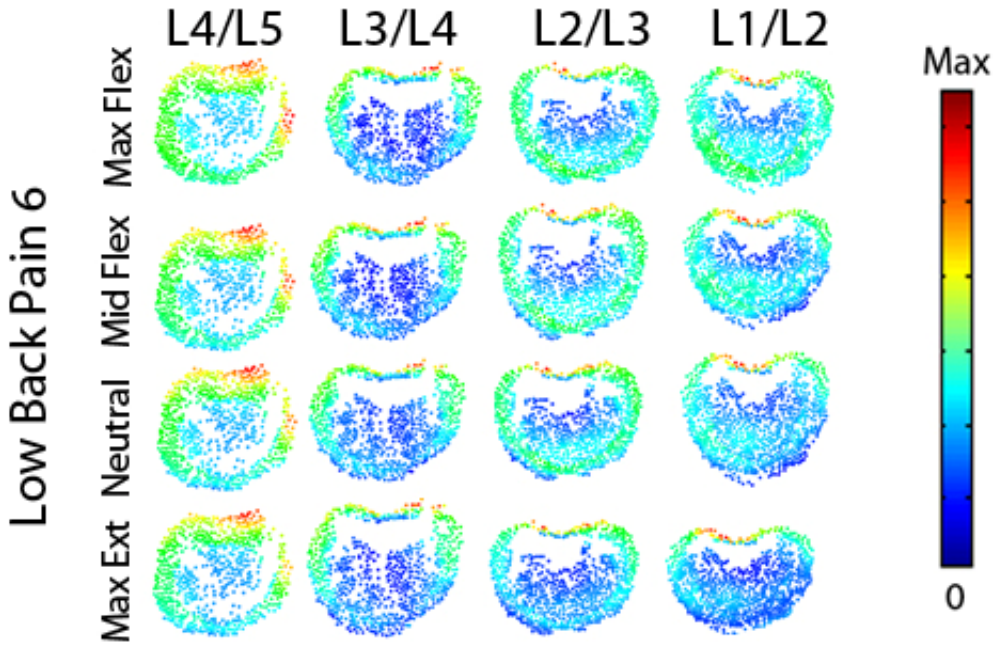

Figure 113. Magnitude stress at each atlas vertex for all levels at each major frame for Low Back Pain 6.

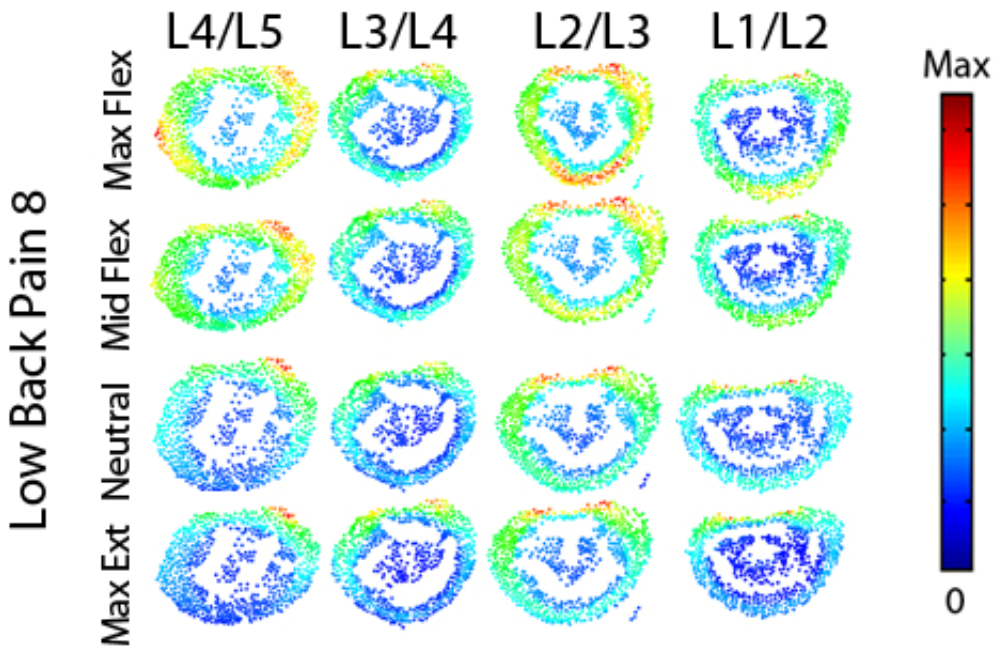

Figure 114. Magnitude stress at each atlas vertex for all levels at each major frame for Low Back Pain 8.

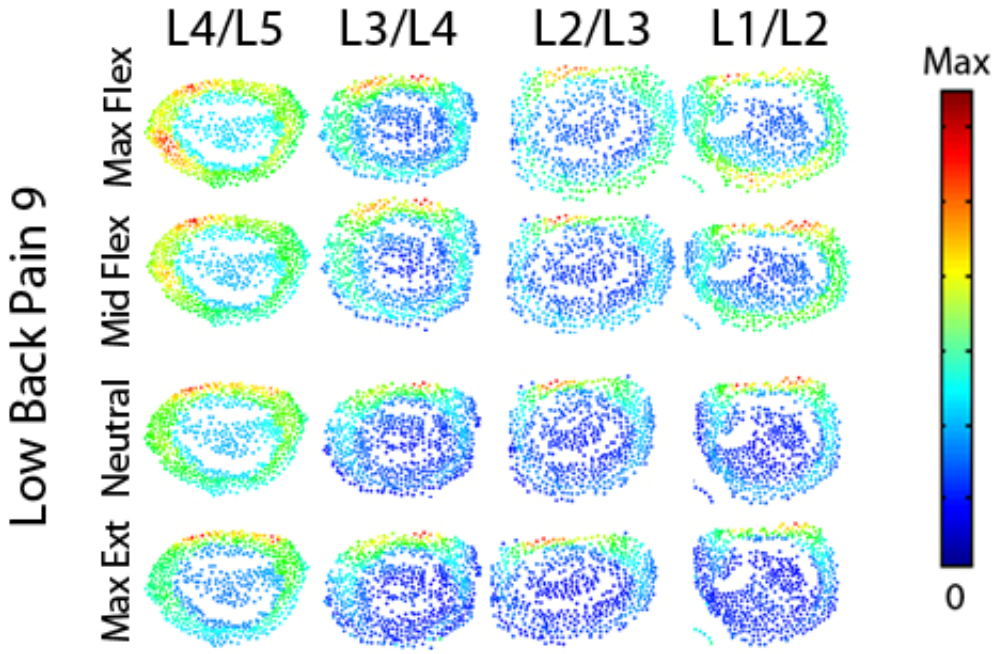

Figure 115. Magnitude stress at each atlas vertex for all levels at each major frame for Low Back Pain 9.

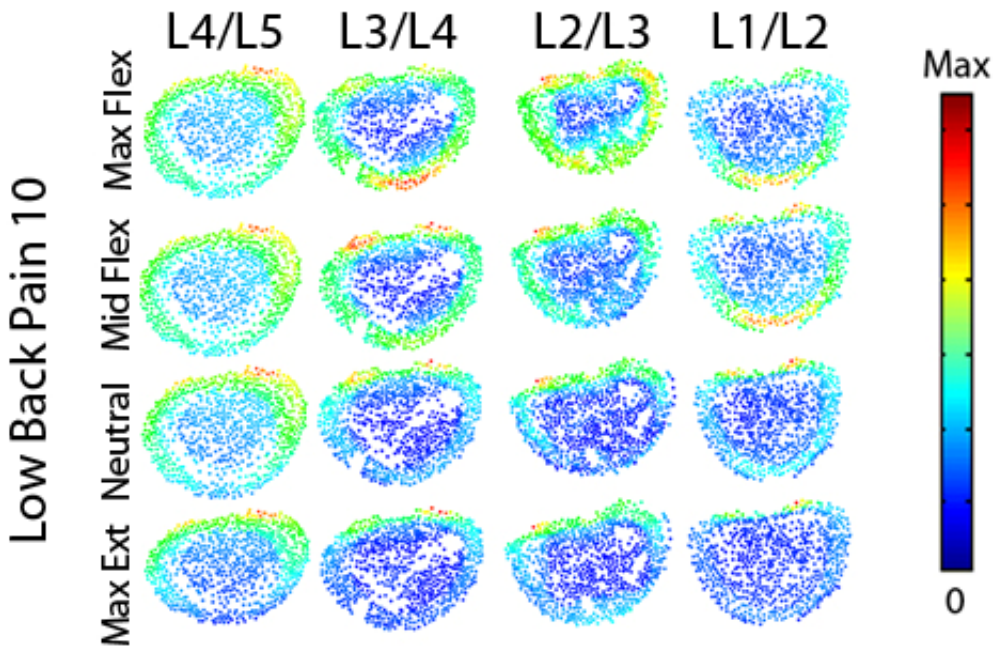

Figure 116. Magnitude stress at each atlas vertex for all levels at each major frame for Low Back Pain 10.

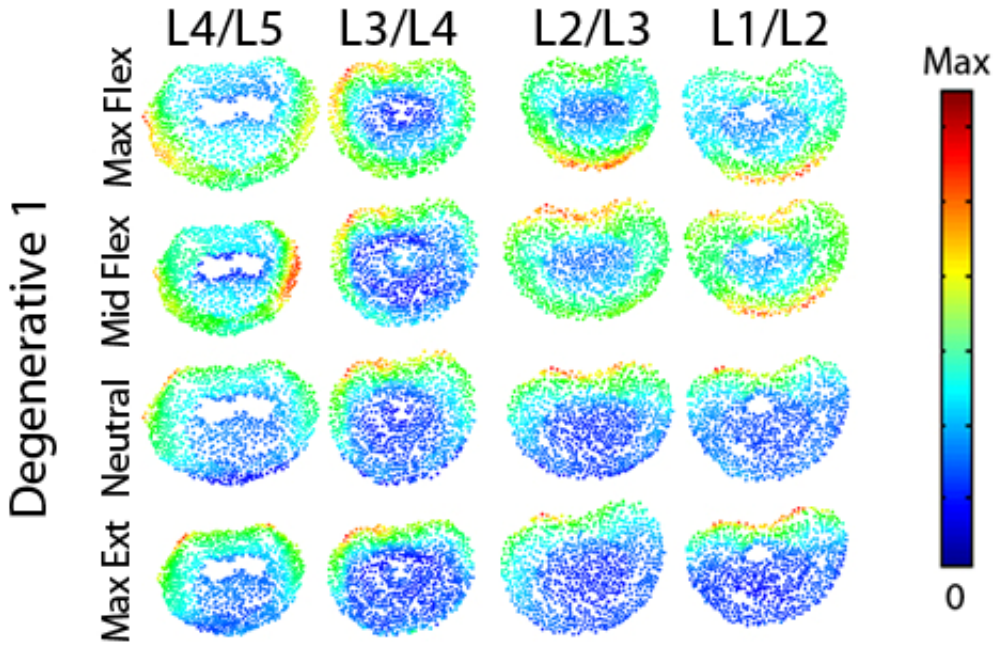

Figure 117. Magnitude stress at each atlas vertex for all levels at each major frame for Degenerative 1.

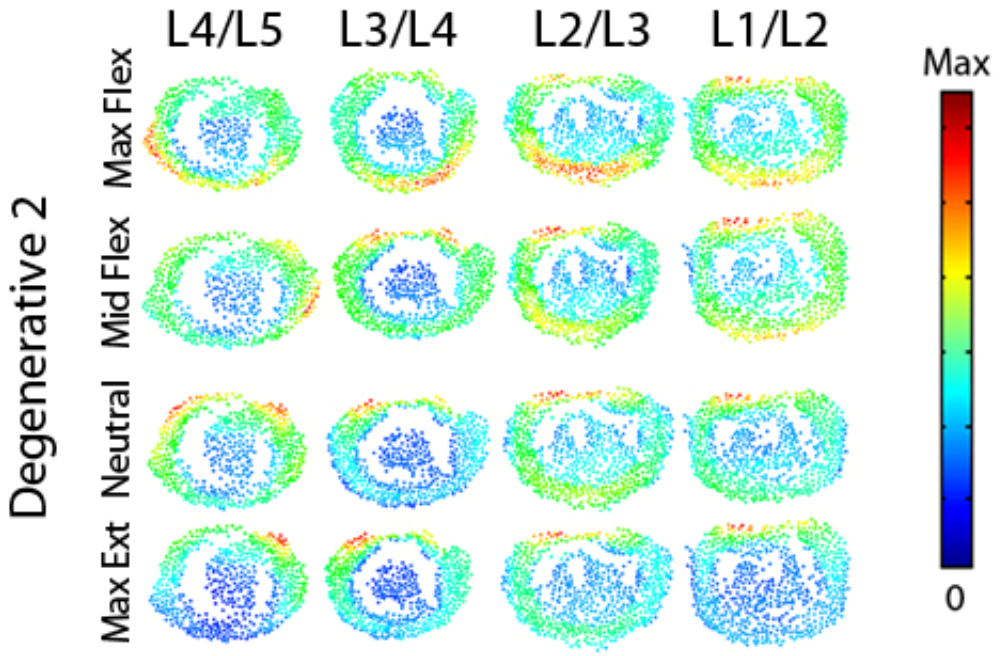

Figure 118. Magnitude stress at each atlas vertex for all levels at each major frame for Degenerative 2.

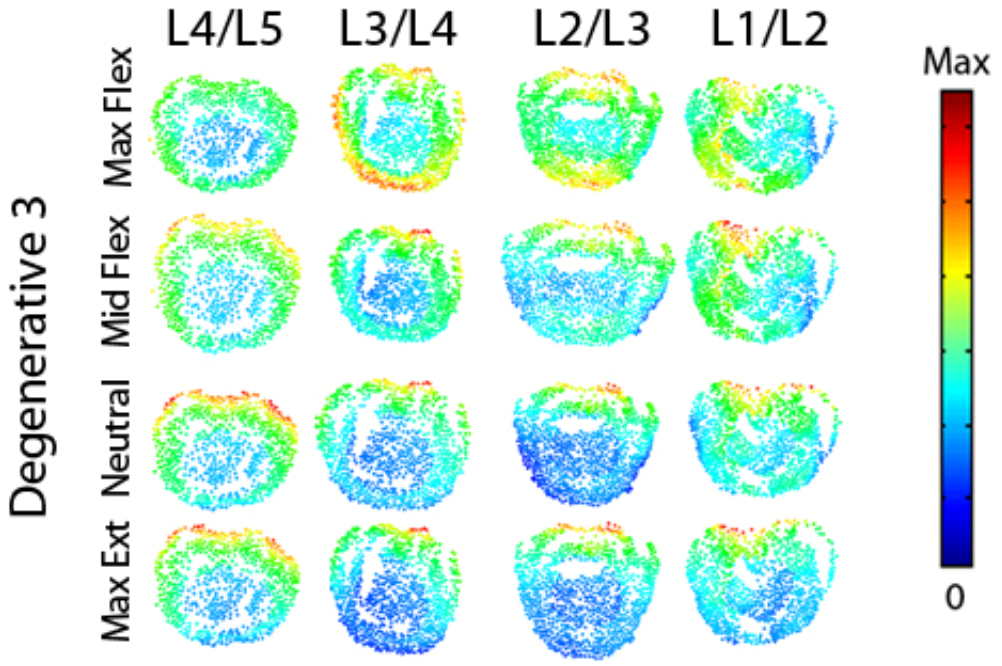

Figure 119. Magnitude stress at each atlas vertex for all levels at each major frame for Degenerative 3.

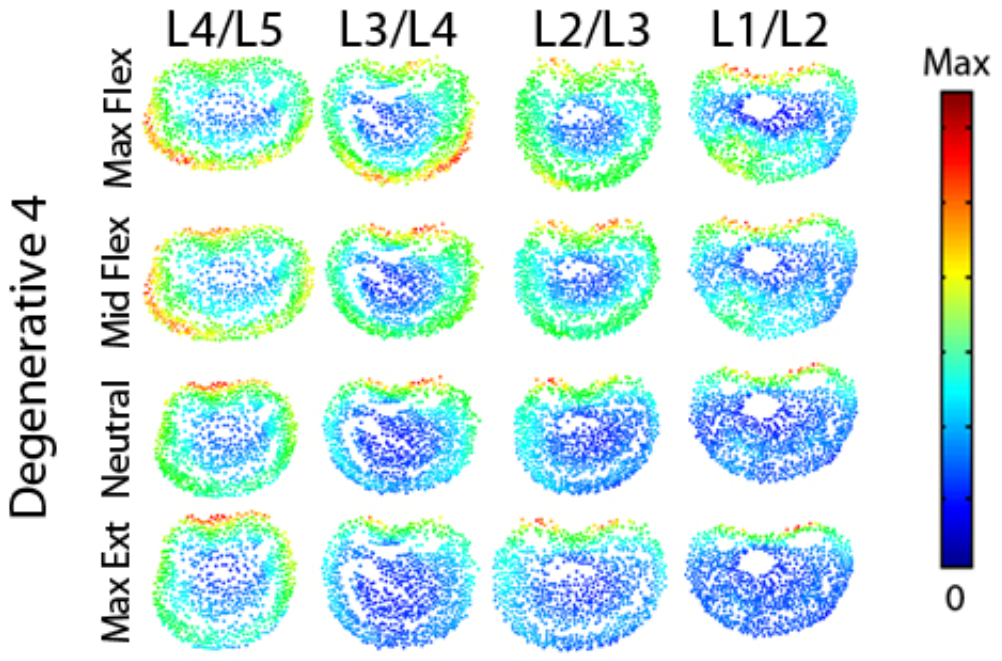

Figure 120. Magnitude stress at each atlas vertex for all levels at each major frame for Degenerative 4.

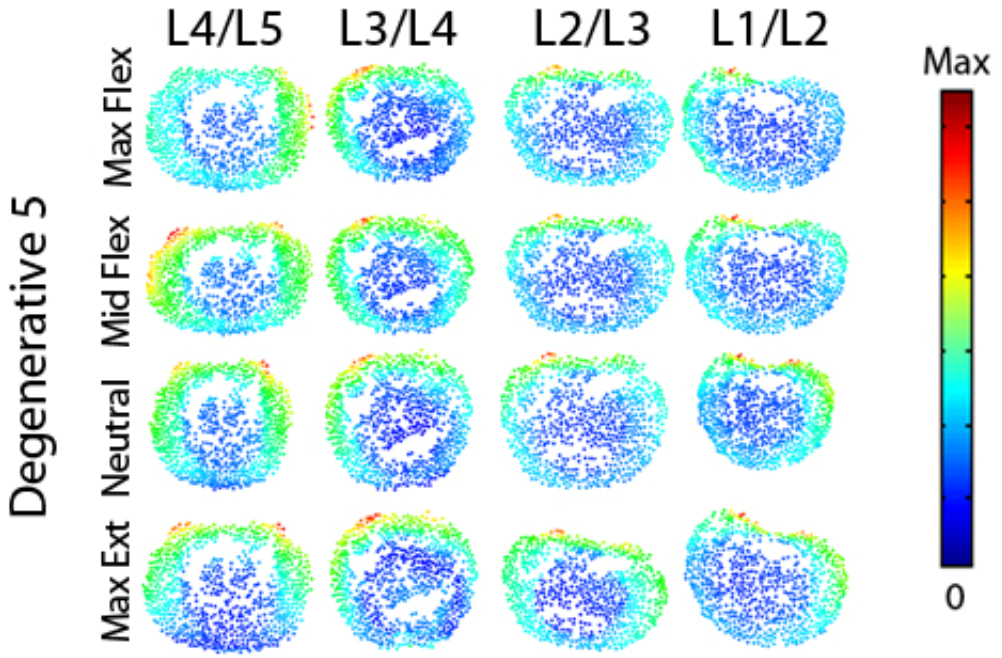

Figure 121. Magnitude stress at each atlas vertex for all levels at each major frame for Degenerative 5.

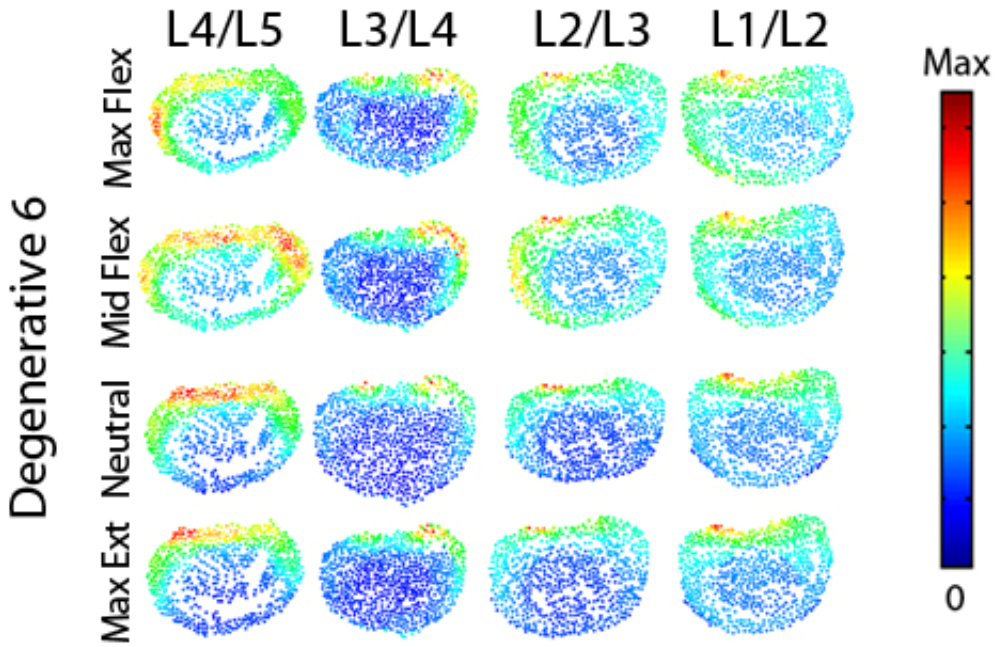

Figure 122. Magnitude stress at each atlas vertex for all levels at each major frame for Degenerative 6.

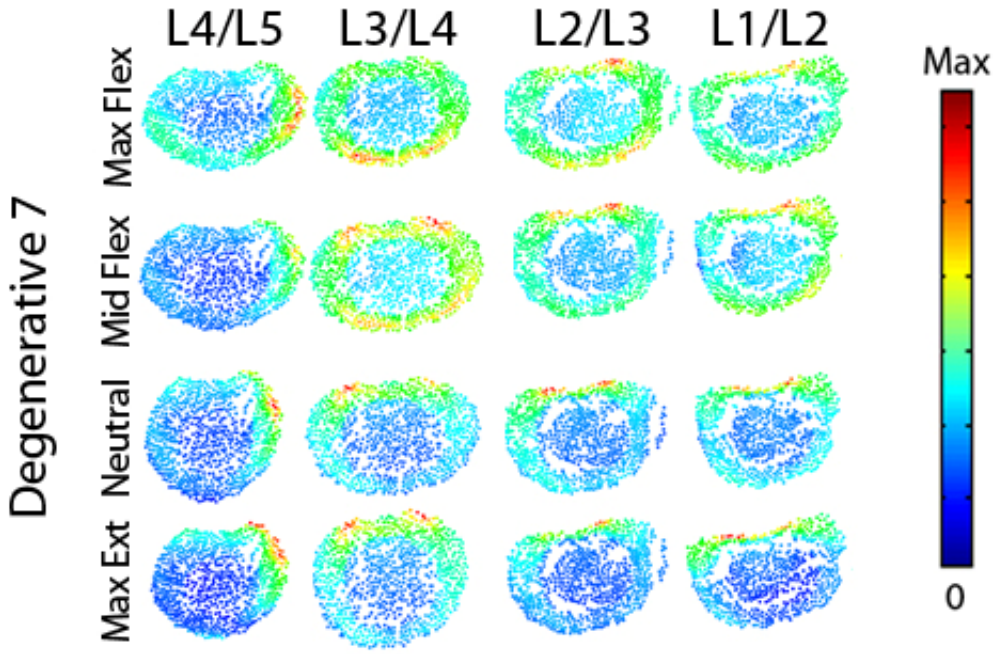

Figure 123. Magnitude stress at each atlas vertex for all levels at each major frame for Degenerative 7.

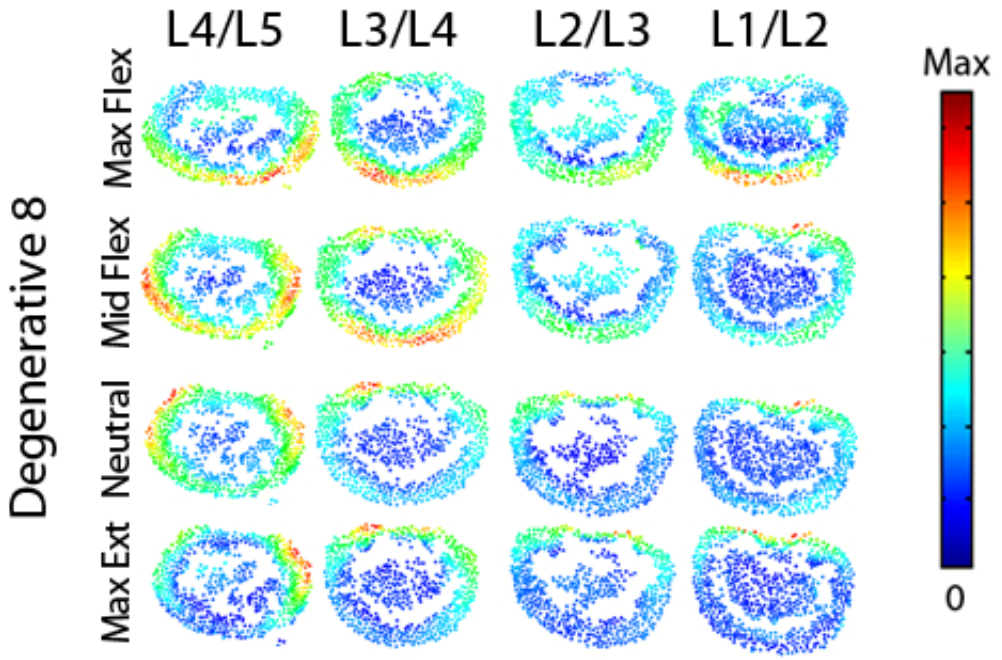

Figure 124. Magnitude stress at each atlas vertex for all levels at each major frame for Degenerative 8.

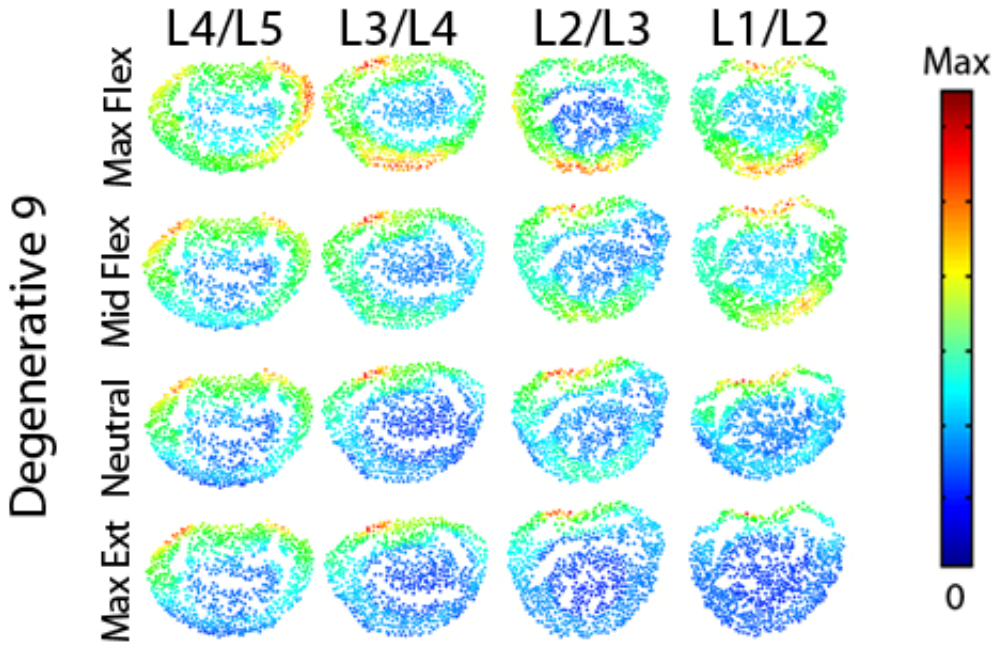

Figure 125. Magnitude stress at each atlas vertex for all levels at each major frame for Degenerative 9.

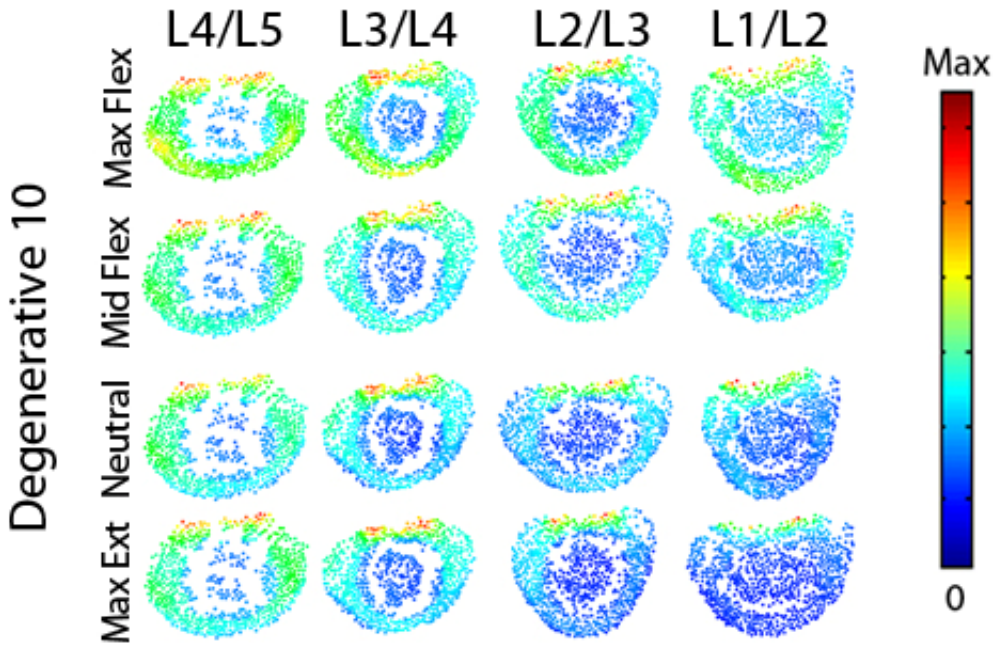

Figure 126. Magnitude stress at each atlas vertex for all levels at each major frame for Degenerative 10.

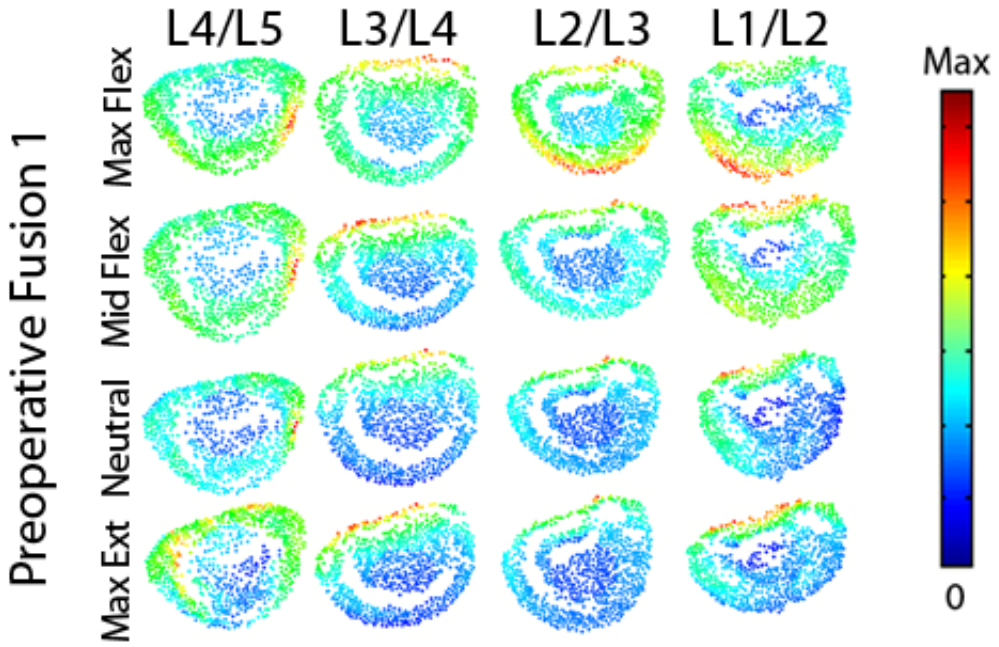

Figure 127. Magnitude stress at each atlas vertex for all levels at each major frame for Preoperative Fusion 1.

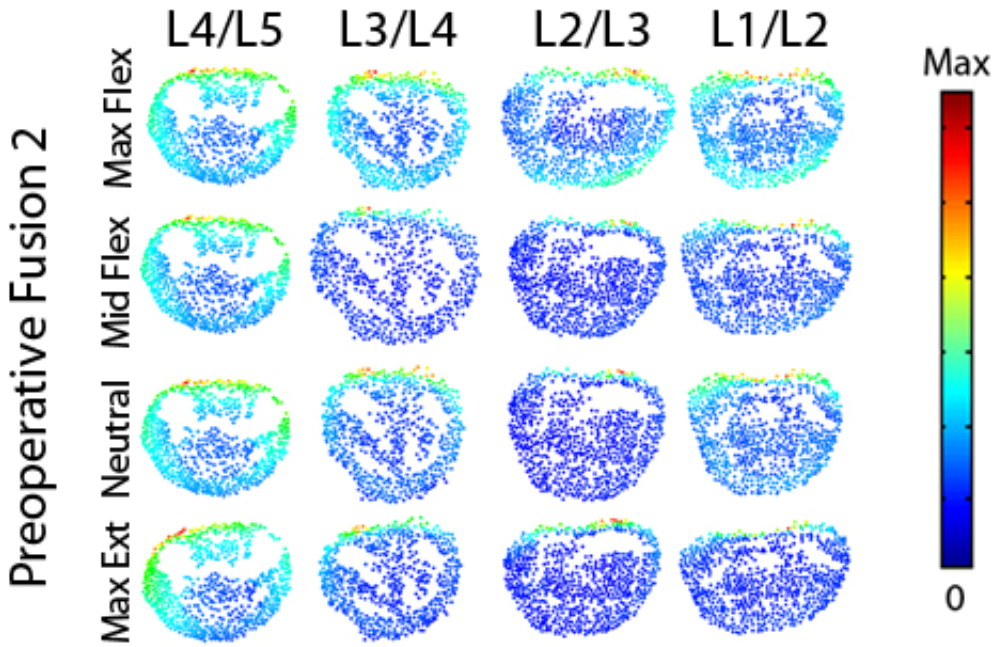

Figure 128. Magnitude stress at each atlas vertex for all levels at each major frame for Preoperative Fusion 2.

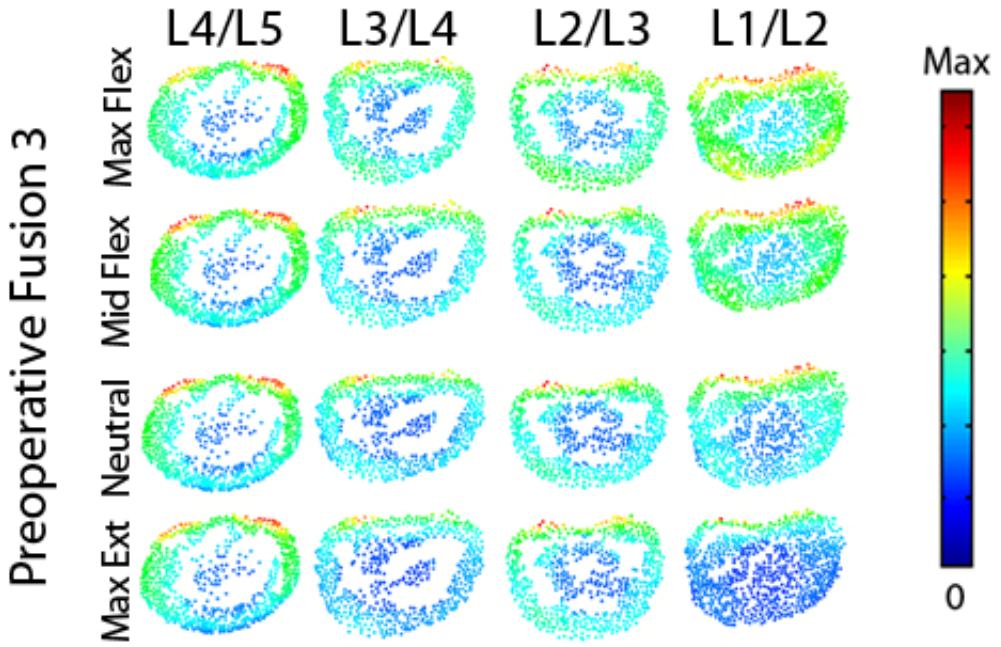

Figure 129. Magnitude stress at each atlas vertex for all levels at each major frame for Preoperative Fusion 3.

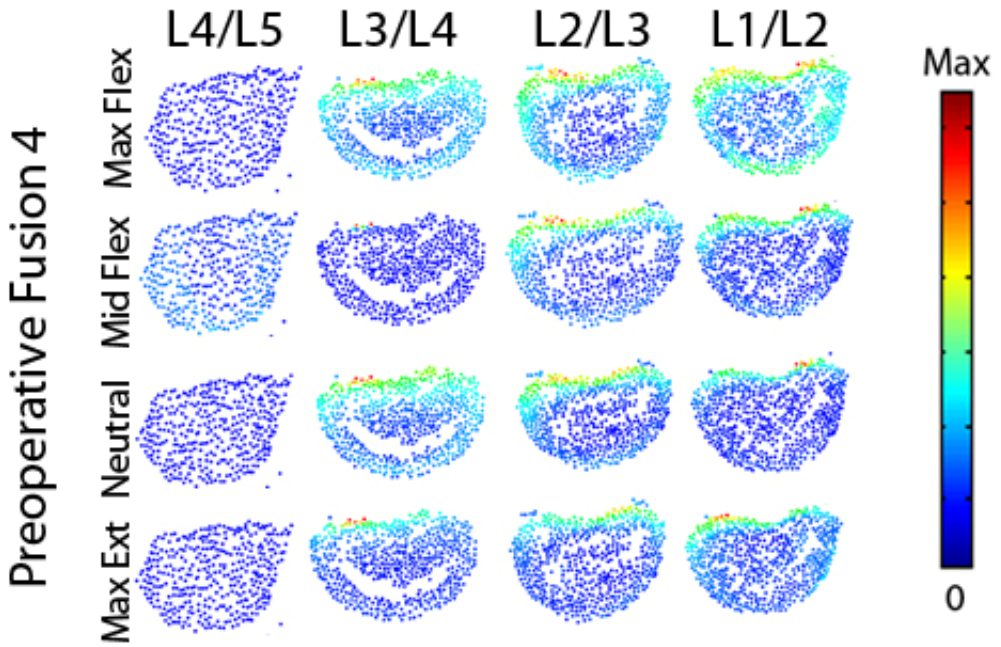

Figure 130. Magnitude stress at each atlas vertex for all levels at each major frame for Preoperative Fusion 4.

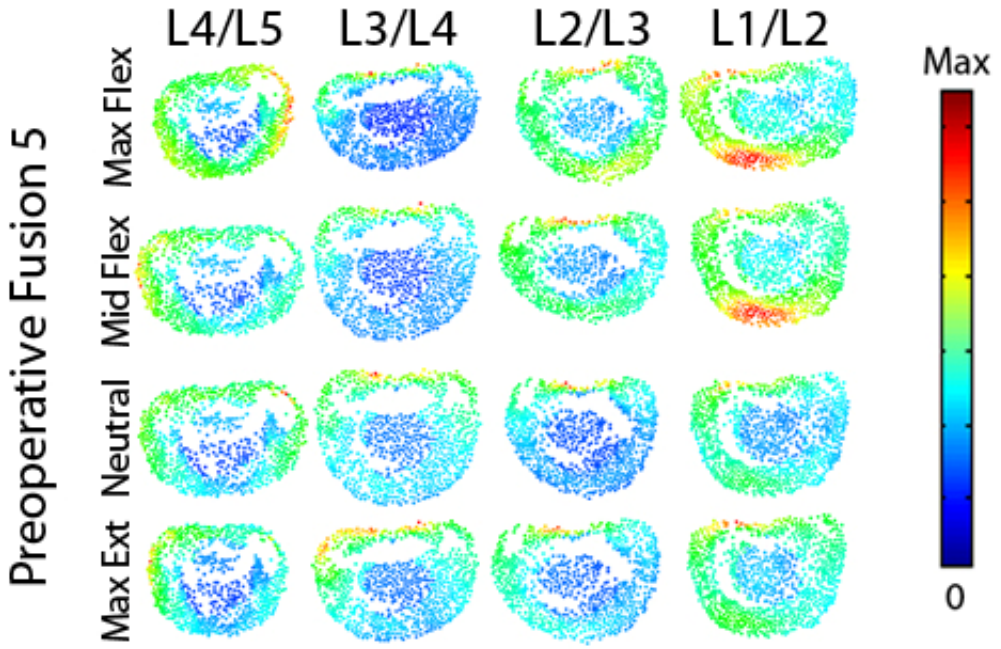

Figure 131. Magnitude stress at each atlas vertex for all levels at each major frame for Preoperative Fusion 5.

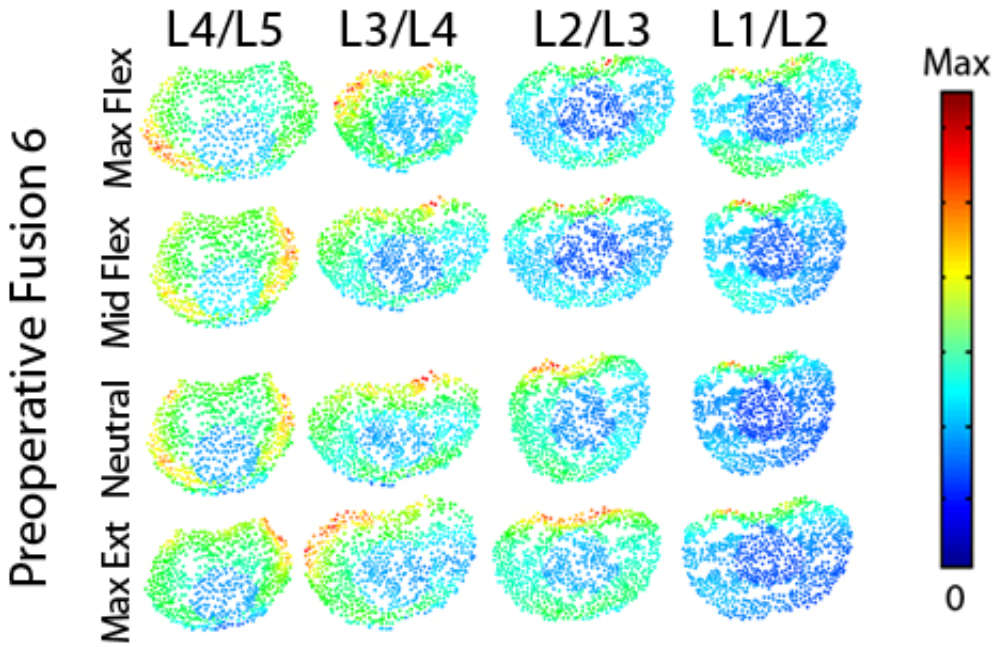

Figure 132. Magnitude stress at each atlas vertex for all levels at each major frame for Preoperative Fusion 6.

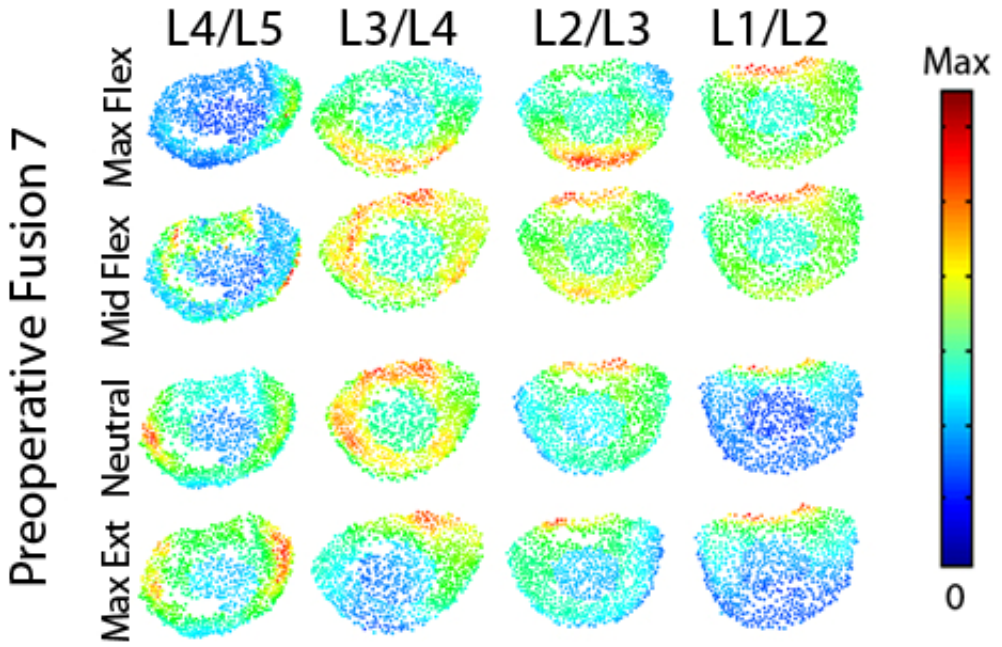

Figure 133. Magnitude stress at each atlas vertex for all levels at each major frame for Preoperative Fusion 7.

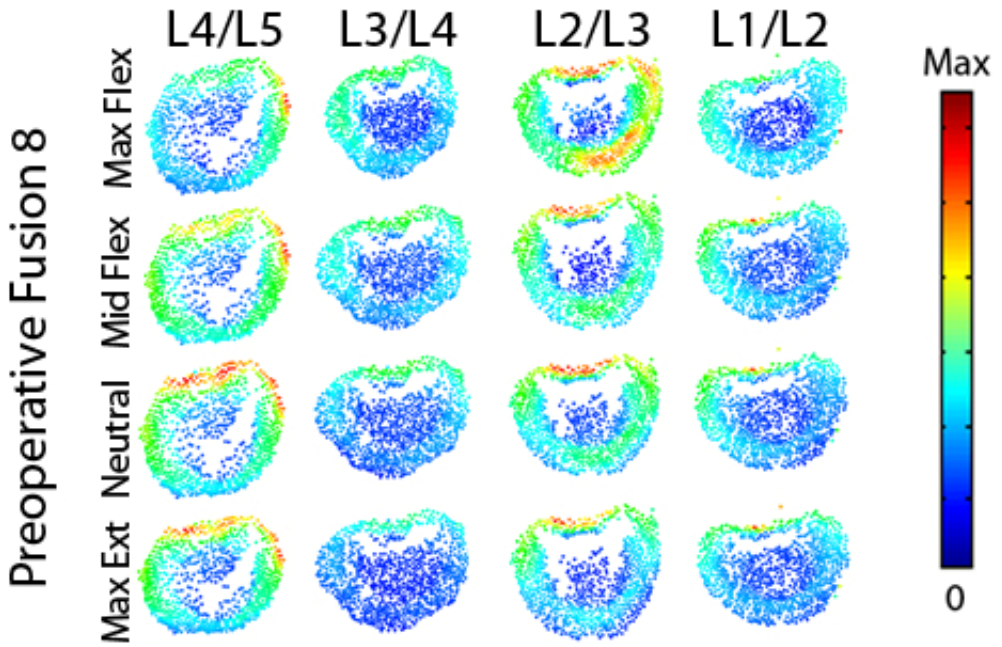

Figure 134. Magnitude stress at each atlas vertex for all levels at each major frame for Preoperative Fusion 8.

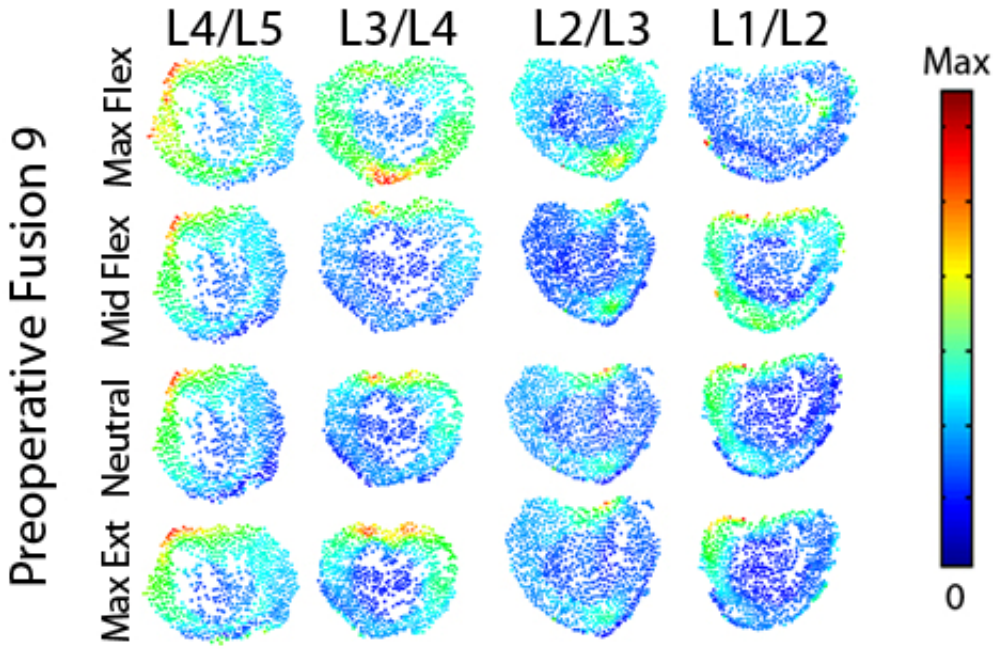

Figure 135. Magnitude stress at each atlas vertex for all levels at each major frame for Preoperative Fusion 9.

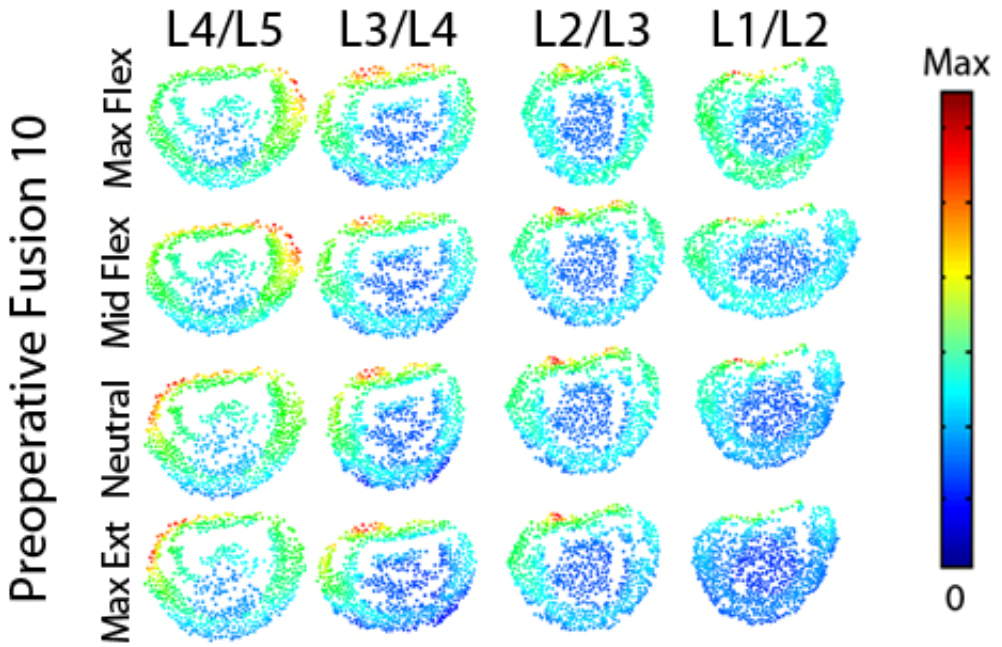

Figure 136. Magnitude stress at each atlas vertex for all levels at each major frame for Preoperative Fusion 10.

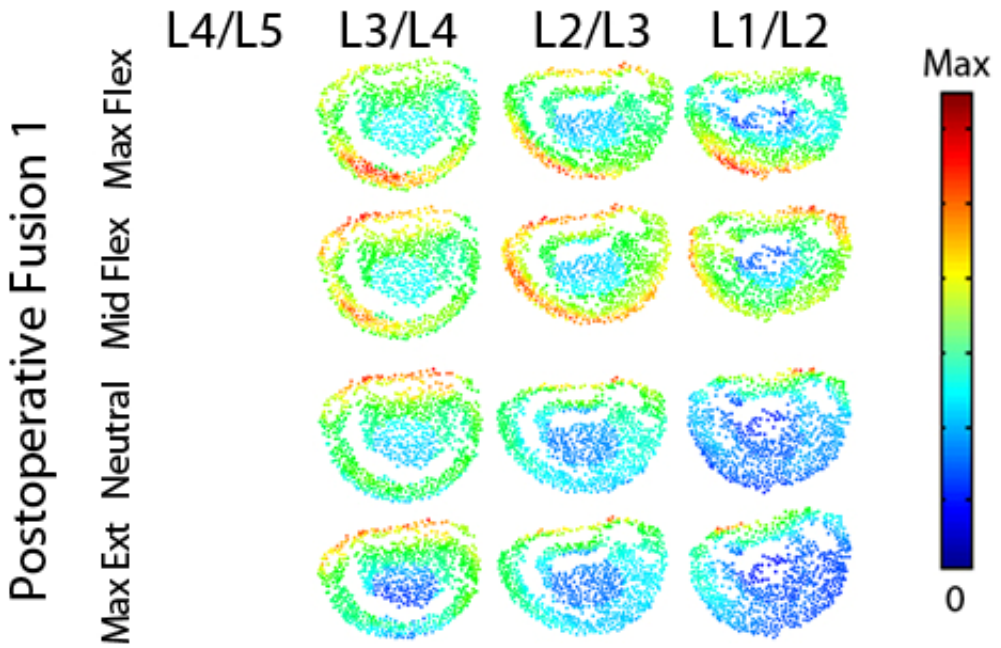

Figure 137. Magnitude stress at each atlas vertex for all levels at each major frame for Postoperative Fusion 1.

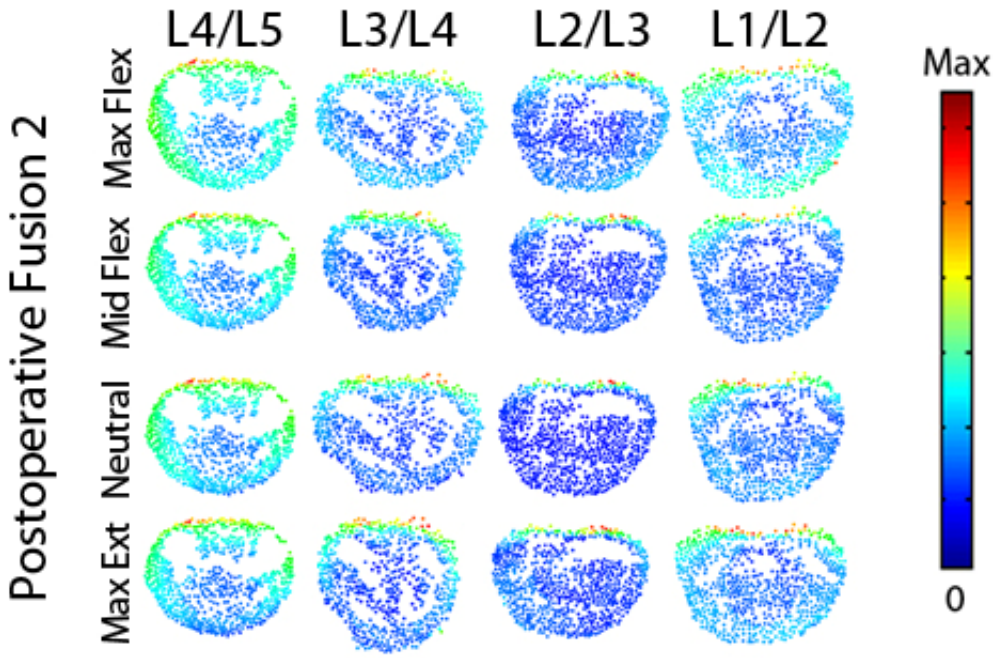

Figure 138. Magnitude stress at each atlas vertex for all levels at each major frame for Postoperative Fusion 2.

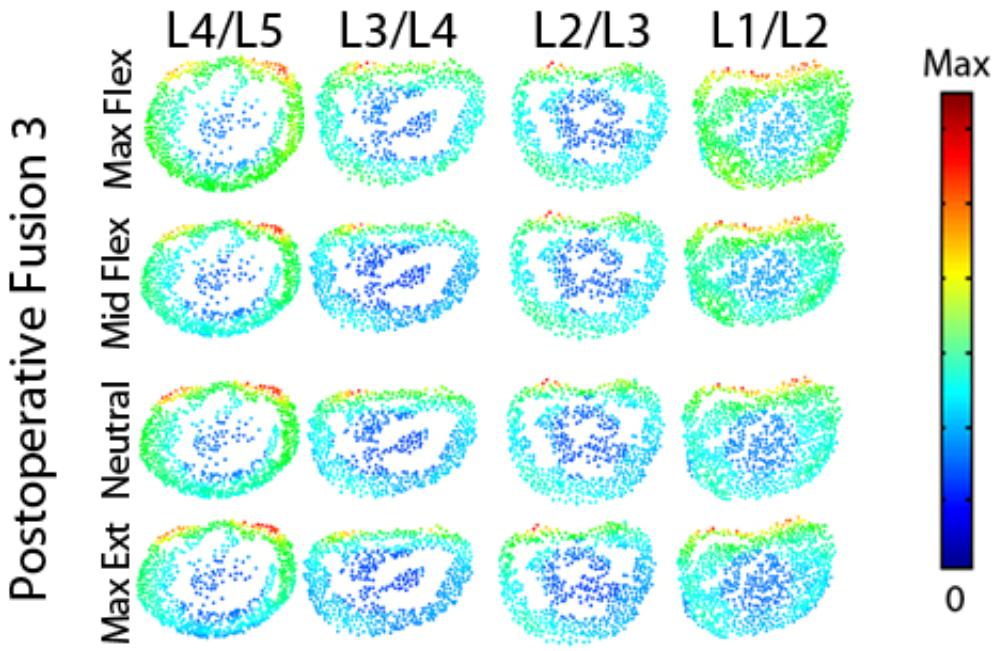

Figure 139. Magnitude stress at each atlas vertex for all levels at each major frame for Postoperative Fusion 3.

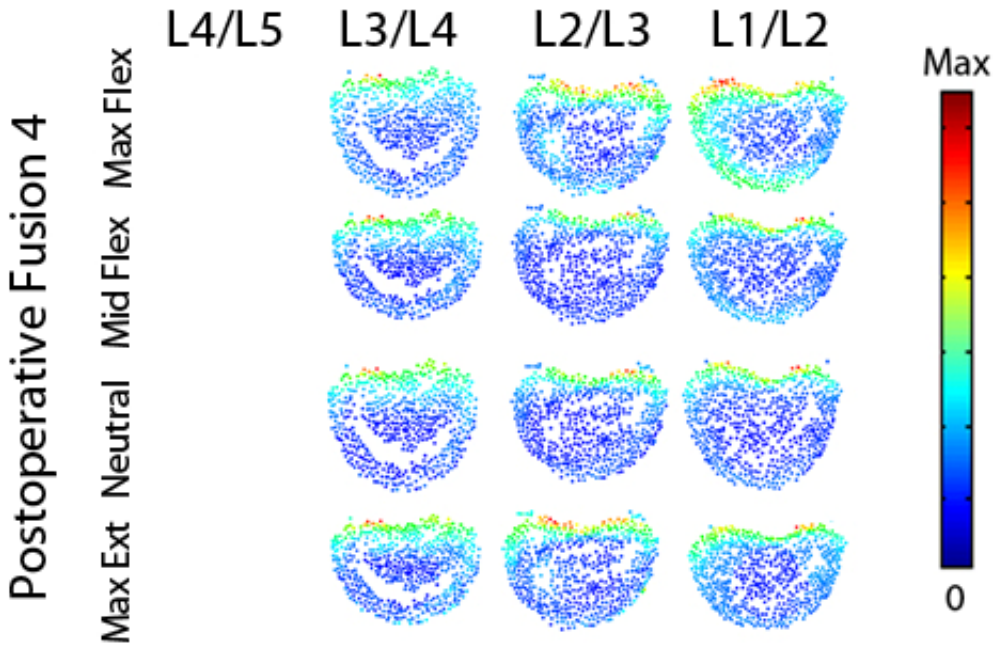

Figure 140. Magnitude stress at each atlas vertex for all levels at each major frame for Postoperative Fusion 4.

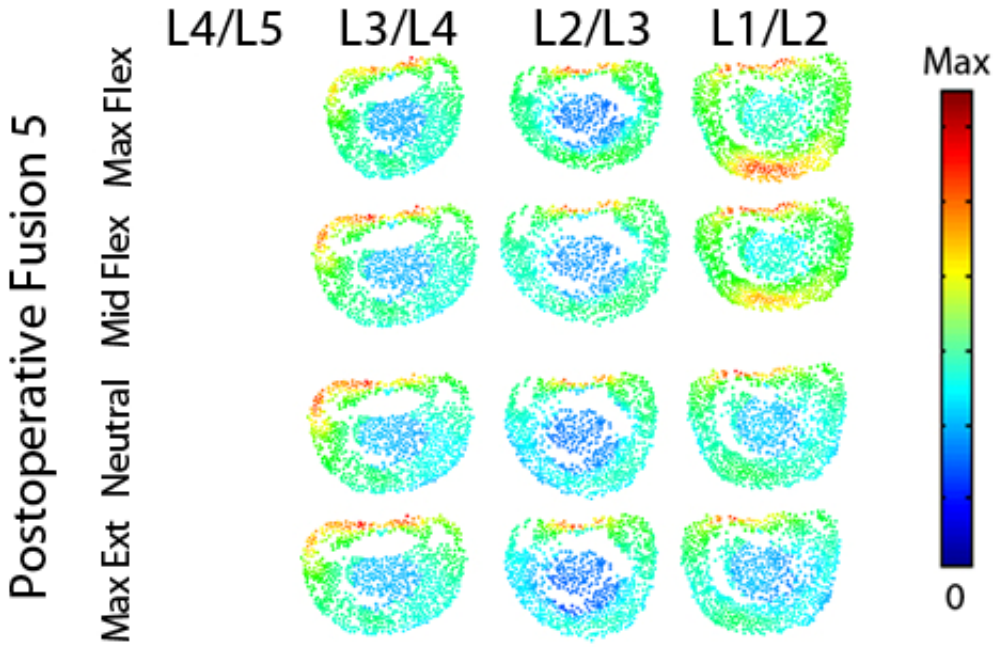

Figure 141. Magnitude stress at each atlas vertex for all levels at each major frame for Postoperative Fusion 5.

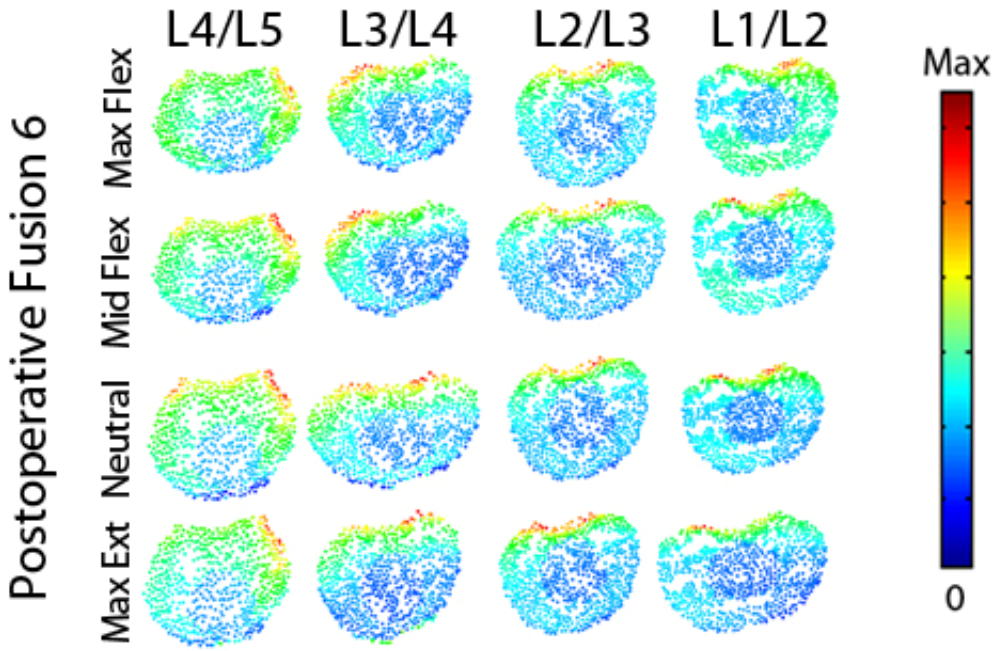

Figure 142. Magnitude stress at each atlas vertex for all levels at each major frame for Postoperative Fusion 6.

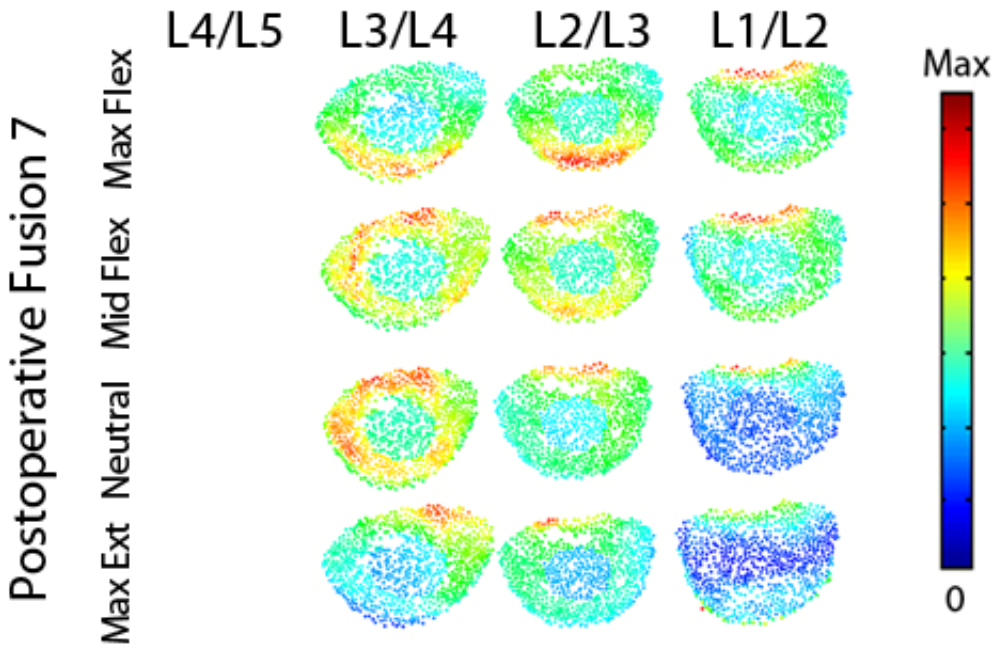

Figure 143. Magnitude stress at each atlas vertex for all levels at each major frame for Postoperative Fusion 7.

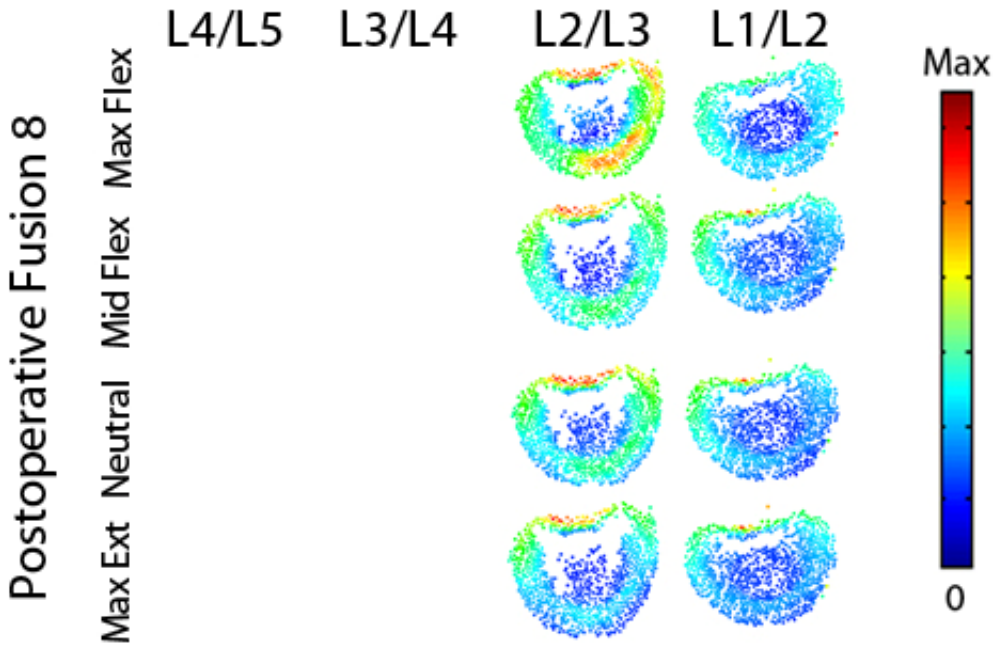

Figure 144. Magnitude stress at each atlas vertex for all levels at each major frame for Postoperative Fusion 8.

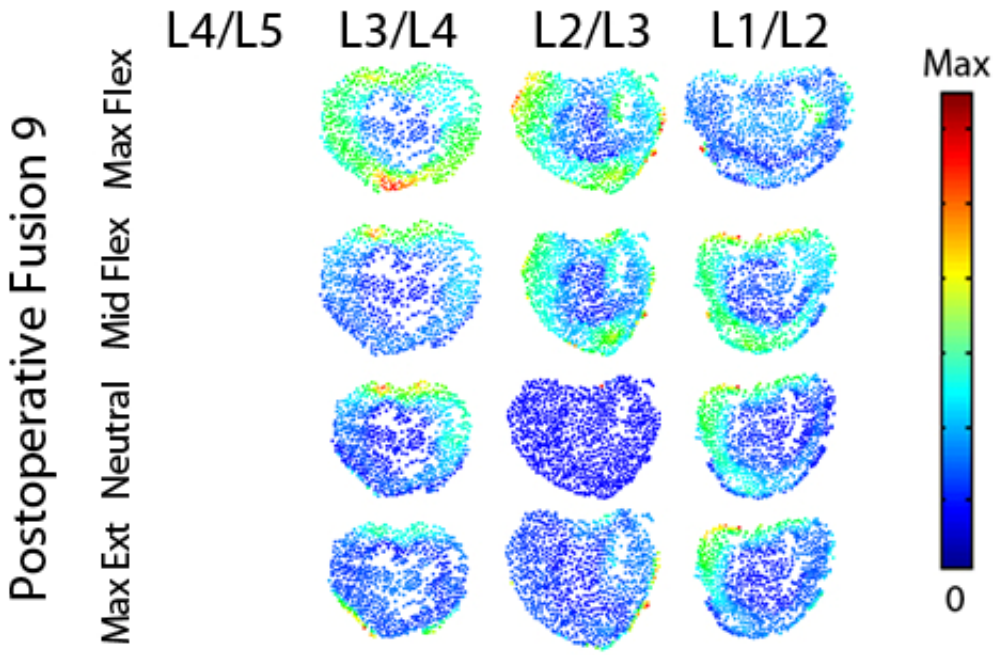

Figure 145. Magnitude stress at each atlas vertex for all levels at each major frame for Postoperative Fusion 9.

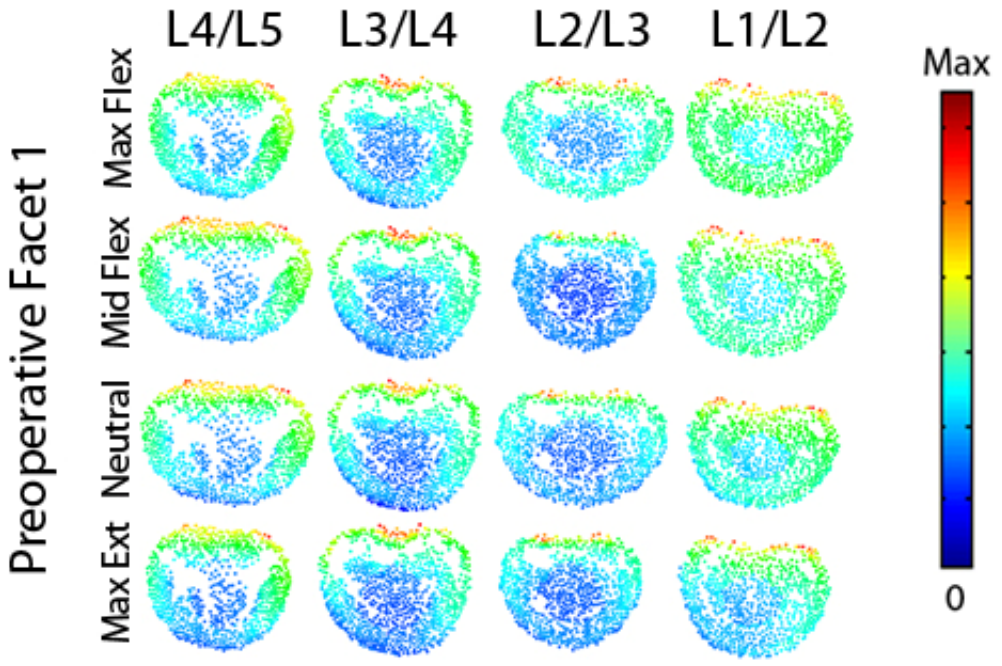

Figure 146. Magnitude stress at each atlas vertex for all levels at each major frame for Preoperative Facet 1.

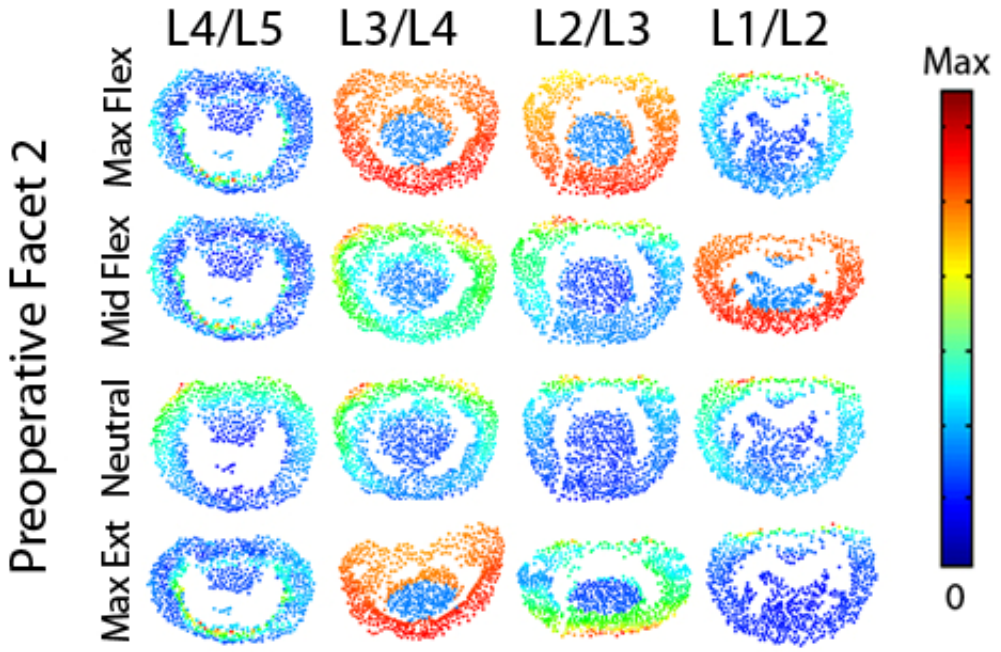

Figure 147. Magnitude stress at each atlas vertex for all levels at each major frame for Preoperative Facet 2.

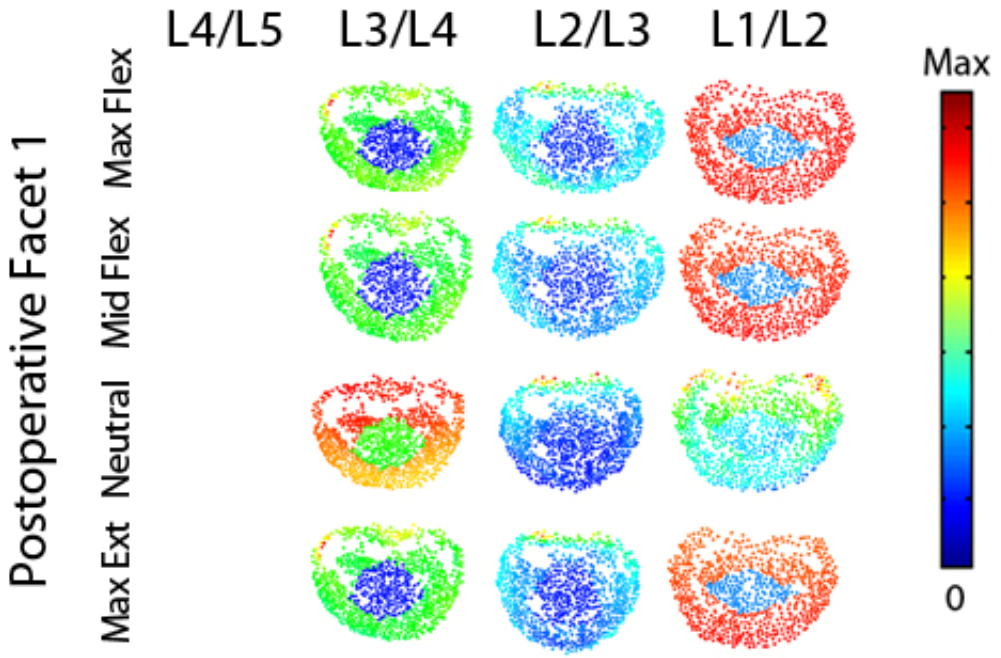

Figure 148. Magnitude stress at each atlas vertex for all levels at each major frame for Postoperative Facet 1.

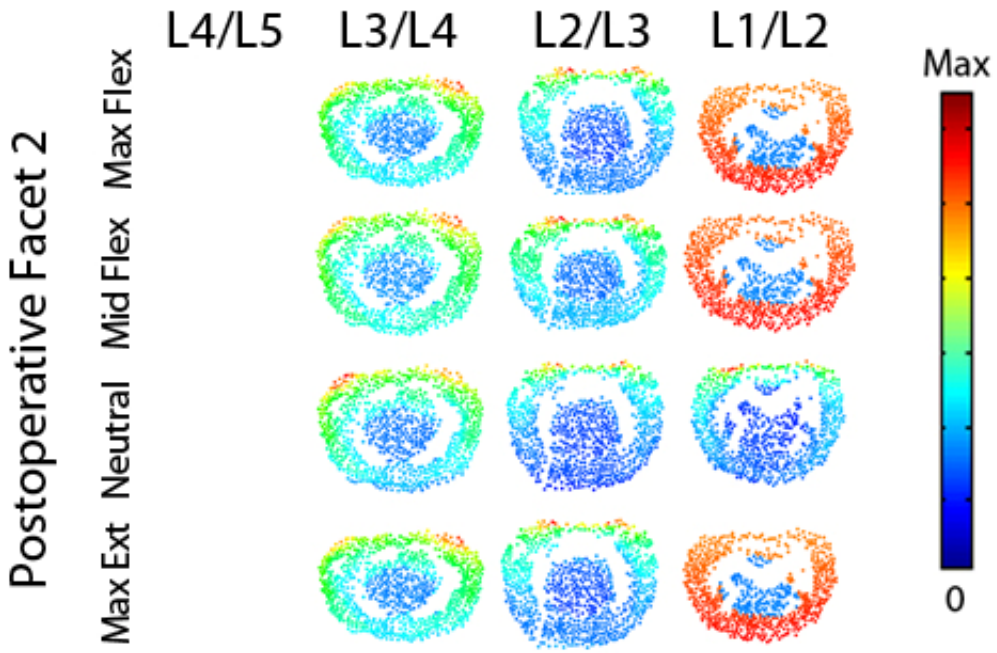

Figure 149. Magnitude stress at each atlas vertex for all levels at each major frame for Postoperative Facet 2.

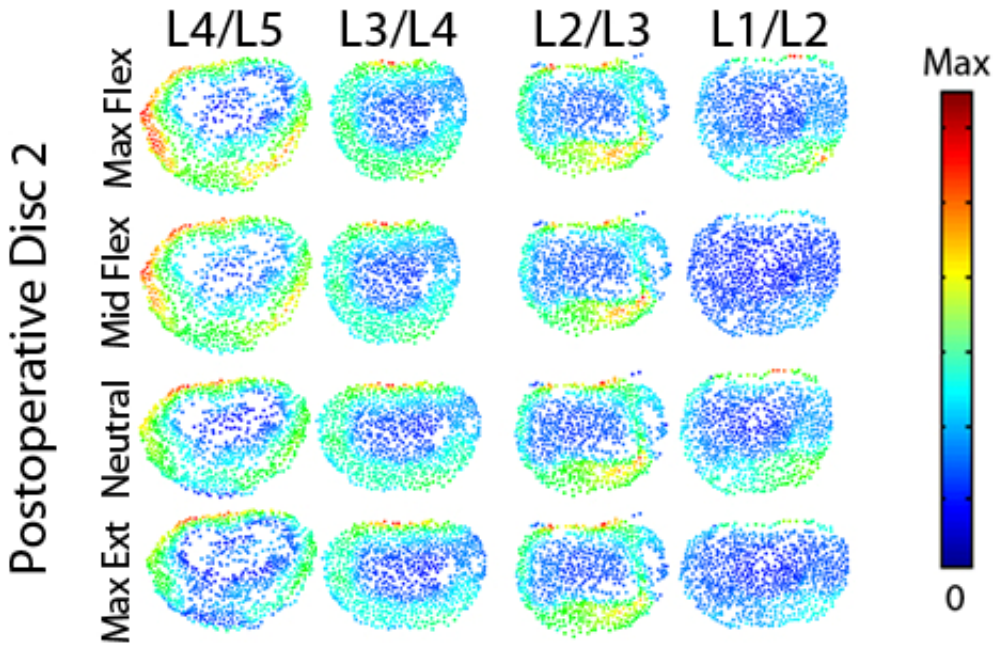

Figure 150. Magnitude stress at each atlas vertex for all levels at each major frame for Postoperative Disc 2.

A.4.2 Axial Rotation

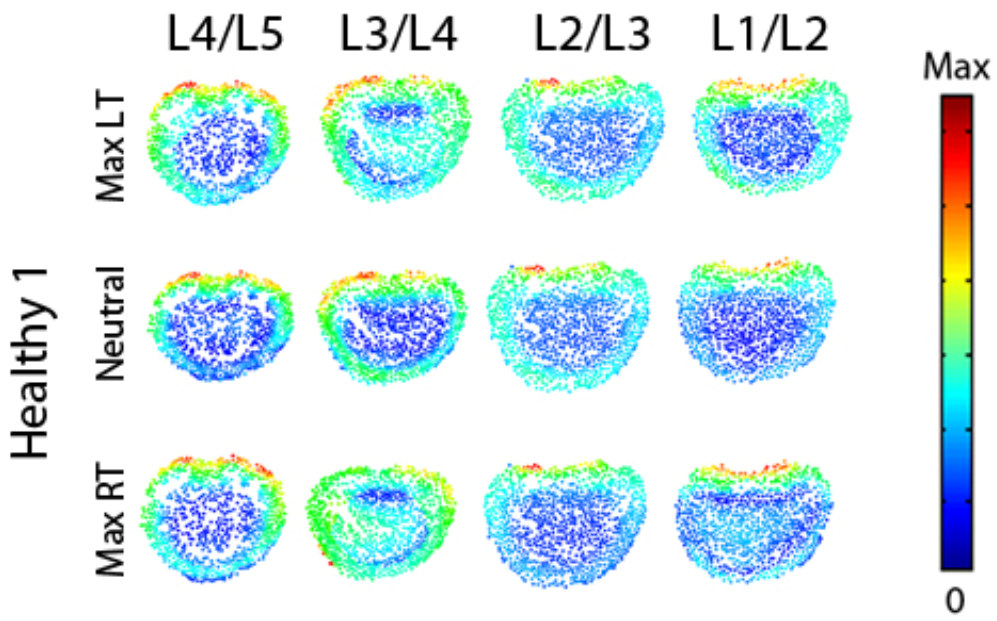

Figure 151. Magnitude stress at each atlas vertex for all levels at each major frame for Healthy 1.

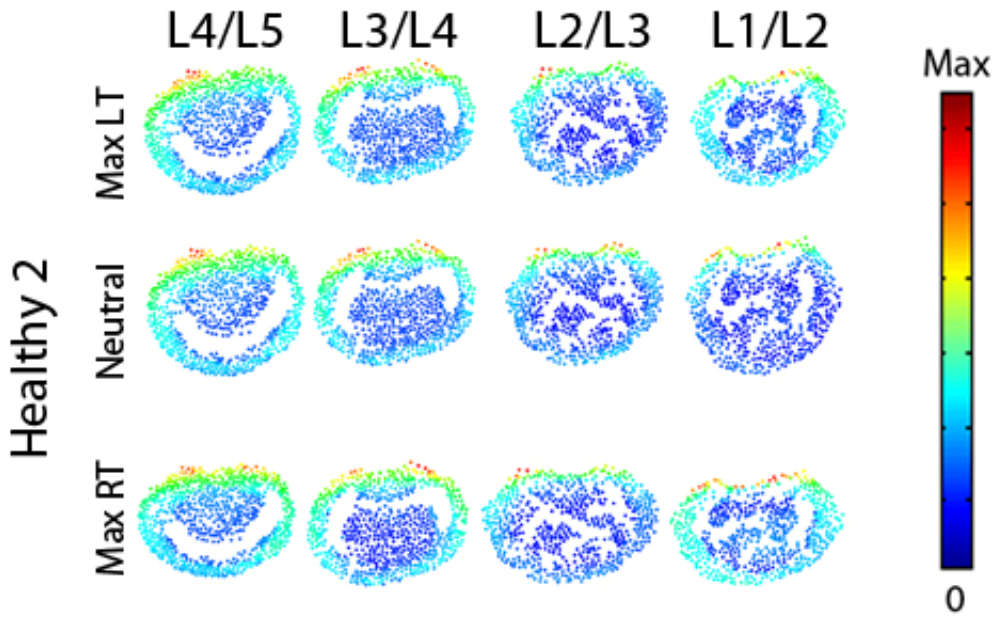

Figure 152. Magnitude stress at each atlas vertex for all levels at each major frame for Healthy 2.

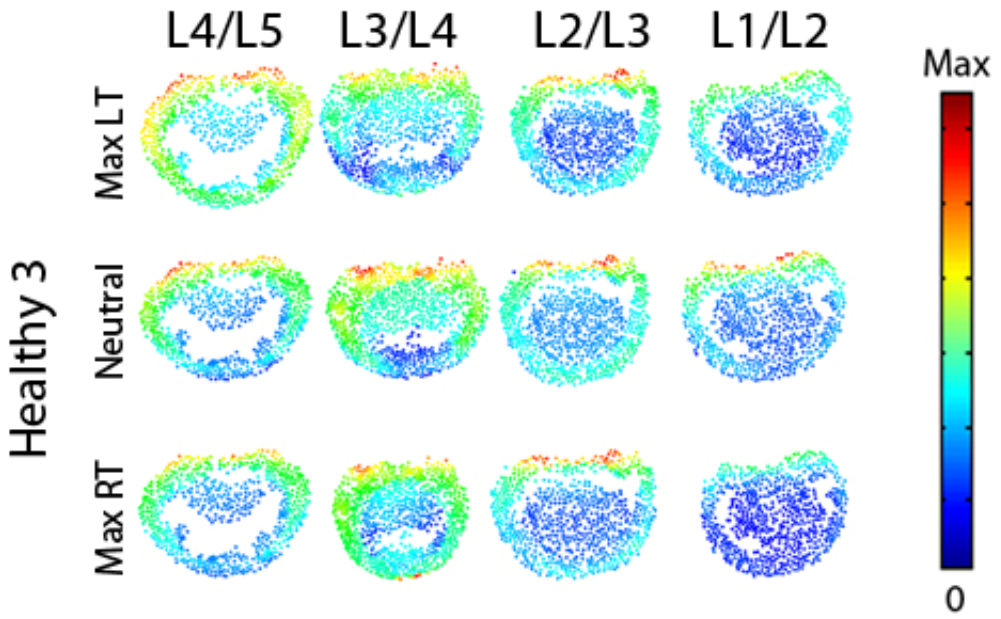

Figure 153. Magnitude stress at each atlas vertex for all levels at each major frame for Healthy 3.

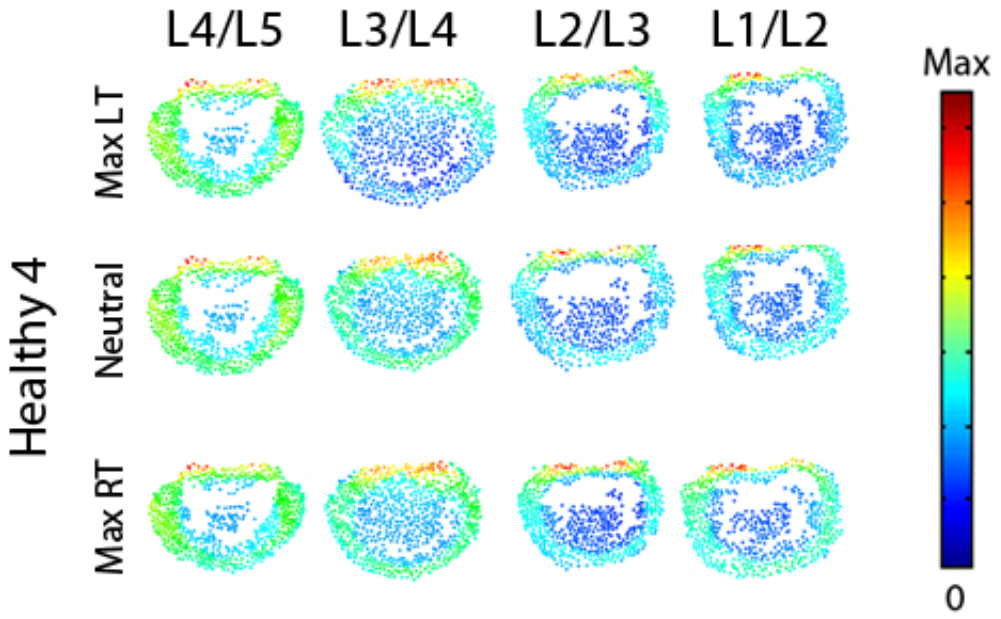

Figure 154. Magnitude stress at each atlas vertex for all levels at each major frame for Healthy 4.

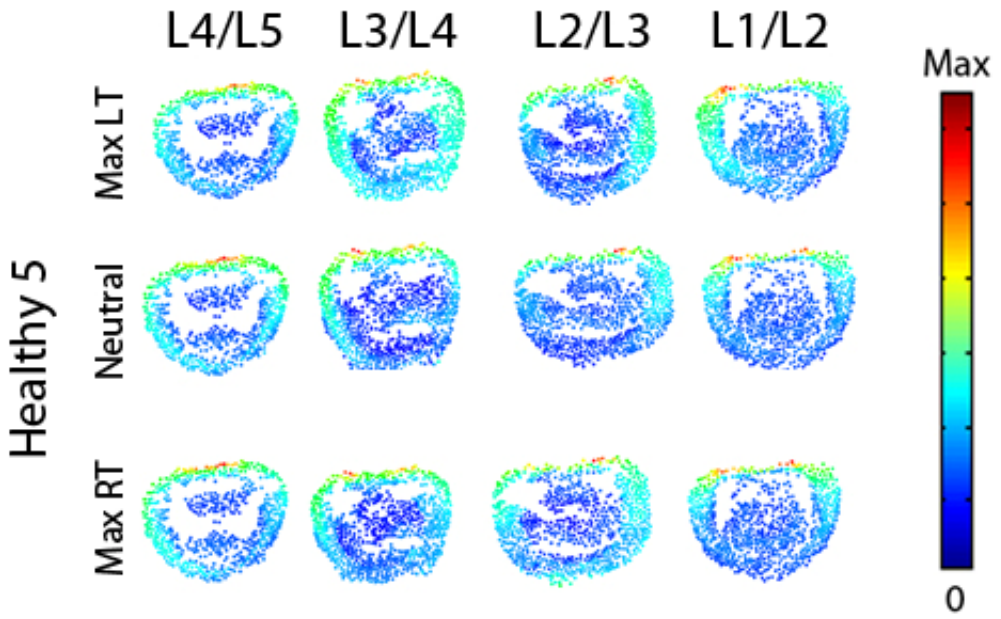

Figure 155. Magnitude stress at each atlas vertex for all levels at each major frame for Healthy 5.

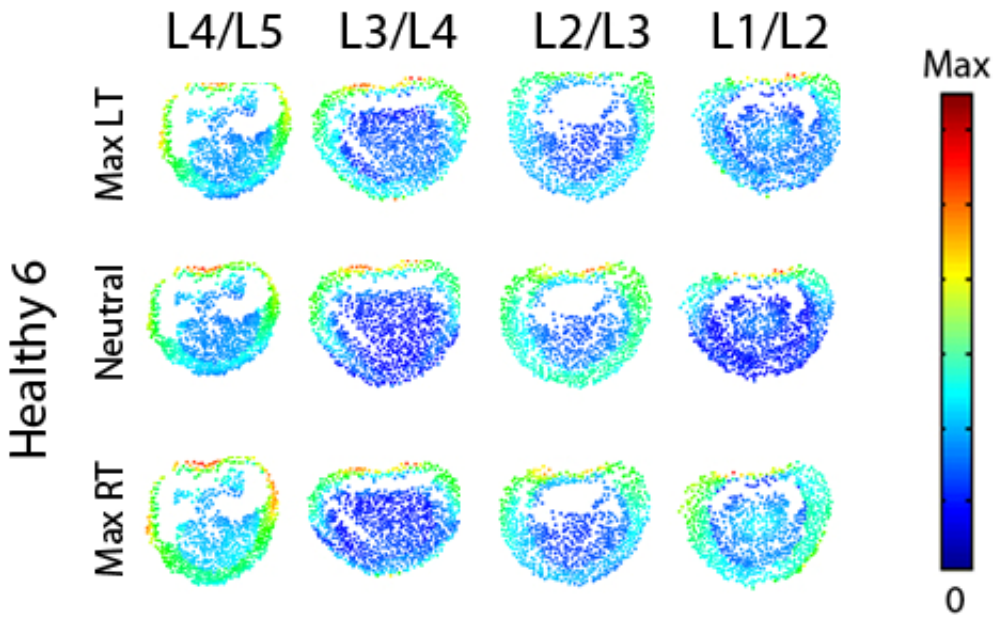

Figure 156. Magnitude stress at each atlas vertex for all levels at each major frame for Healthy 6.

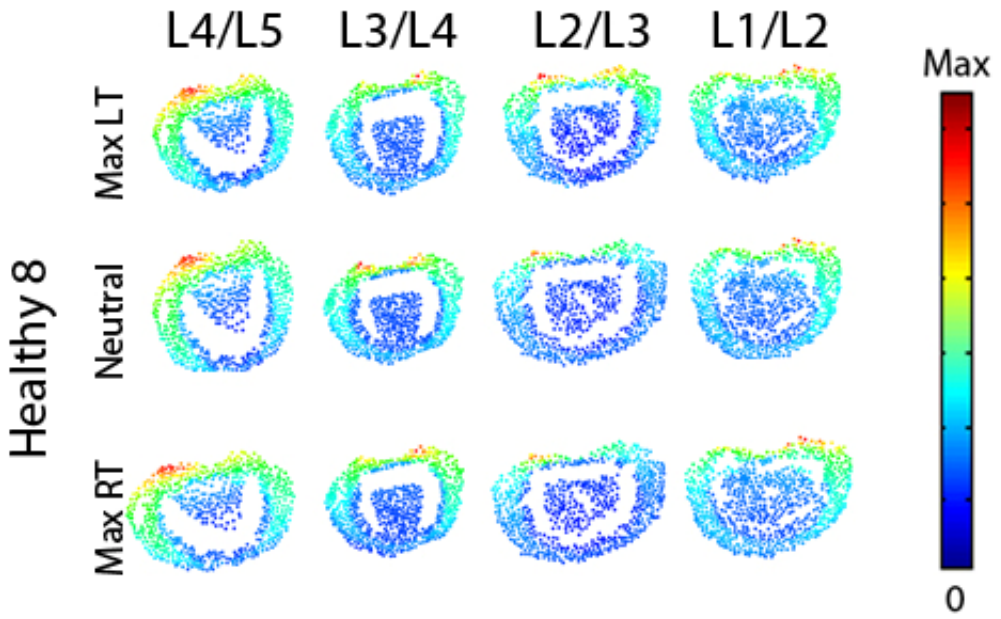

Figure 157. Magnitude stress at each atlas vertex for all levels at each major frame for Healthy 8.

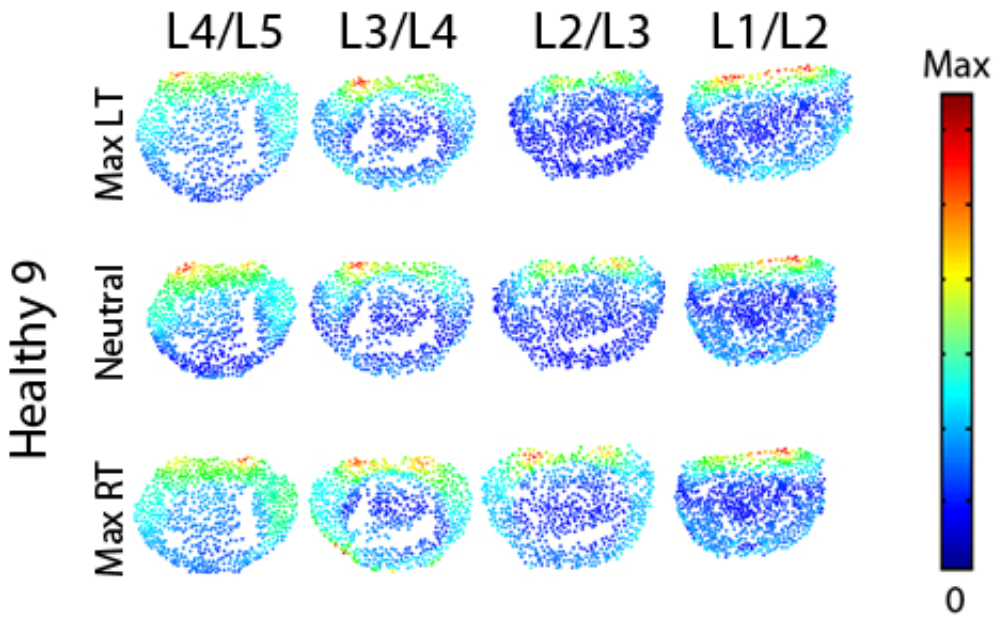

Figure 158. Magnitude stress at each atlas vertex for all levels at each major frame for Healthy 9.

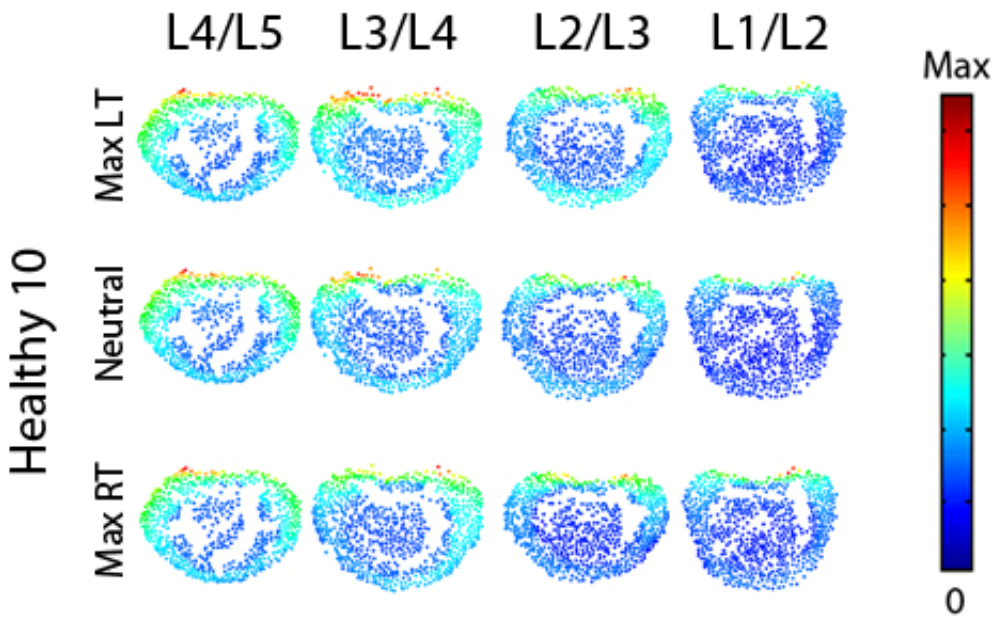

Figure 159. Magnitude stress at each atlas vertex for all levels at each major frame for Healthy 10.

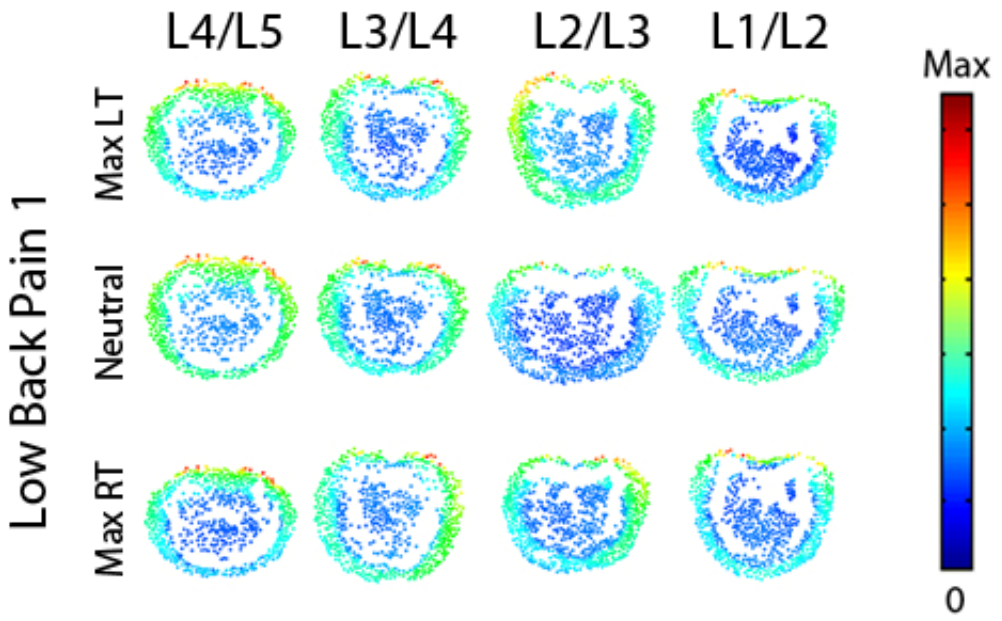

Figure 160. Magnitude stress at each atlas vertex for all levels at each major frame for Low Back Pain 1.

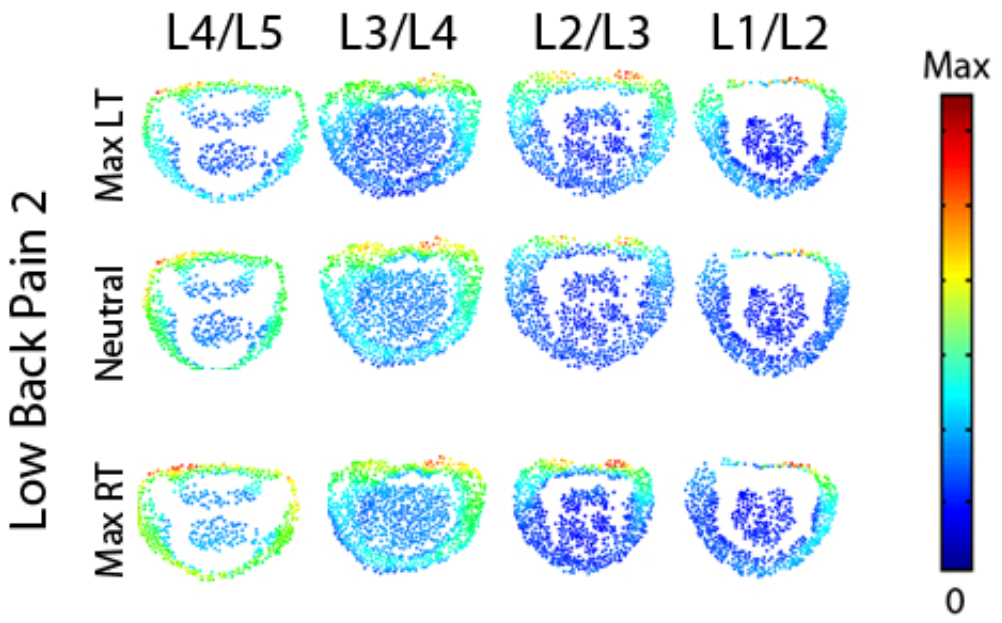

Figure 161. Magnitude stress at each atlas vertex for all levels at each major frame for Low Back Pain 2.

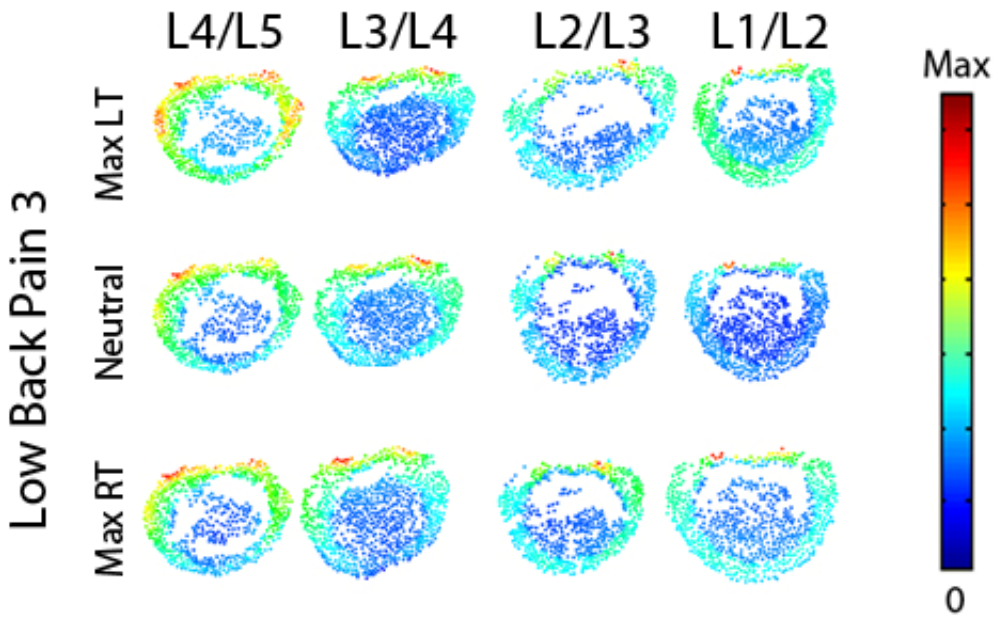

Figure 162. Magnitude stress at each atlas vertex for all levels at each major frame for Low Back Pain 3.

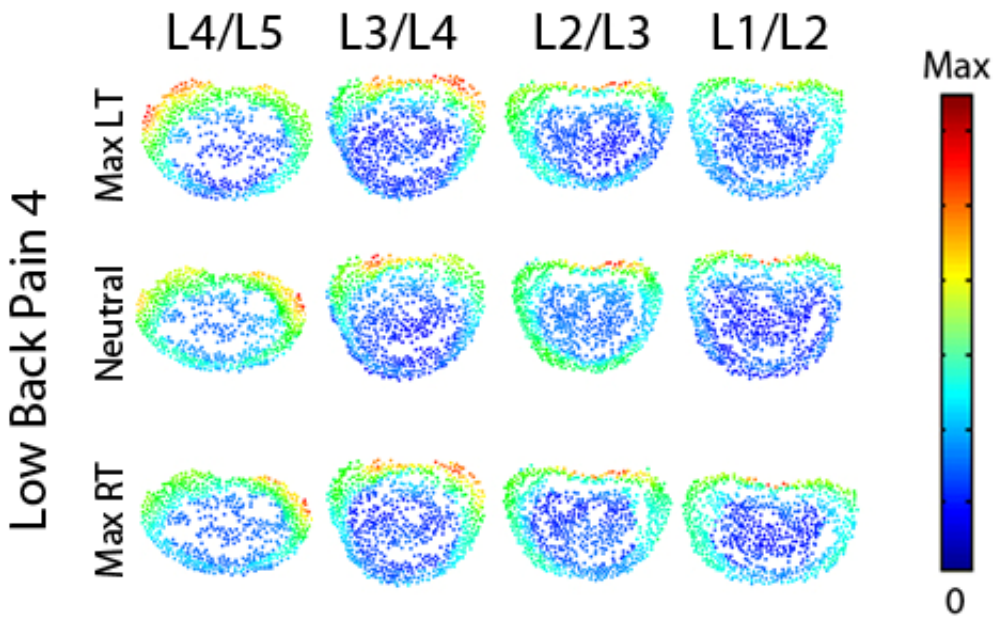

Figure 163. Magnitude stress at each atlas vertex for all levels at each major frame for Low Back Pain 4.

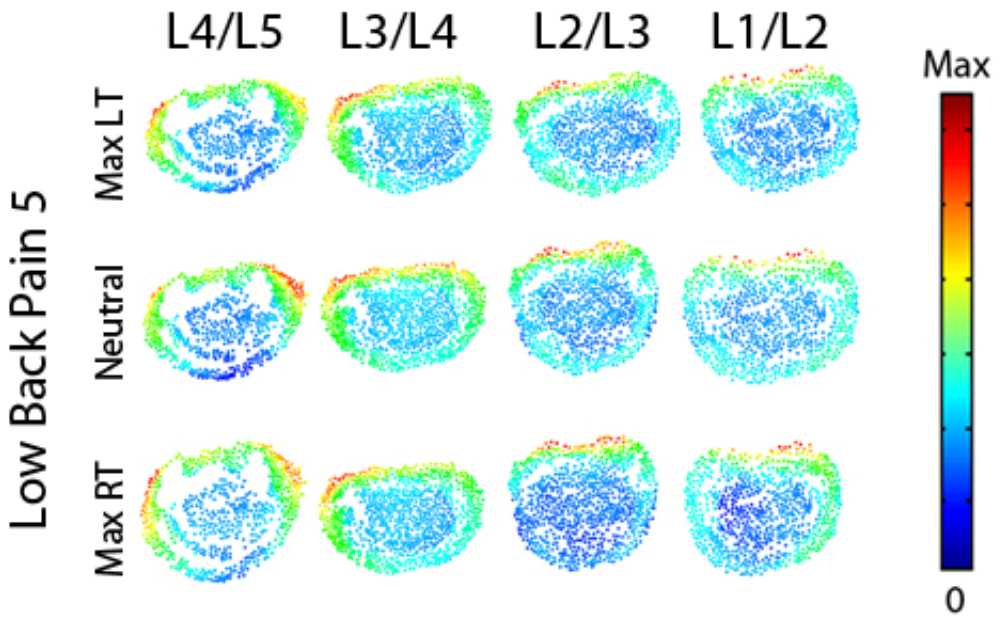

Figure 164. Magnitude stress at each atlas vertex for all levels at each major frame for Low Back Pain 5.

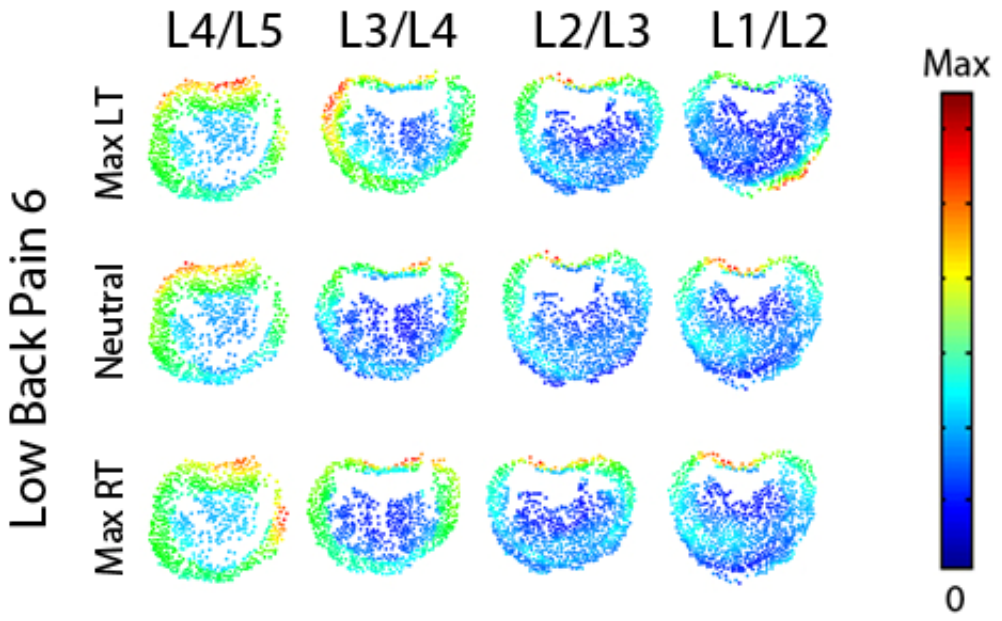

Figure 165. Magnitude stress at each atlas vertex for all levels at each major frame for Low Back Pain 6.

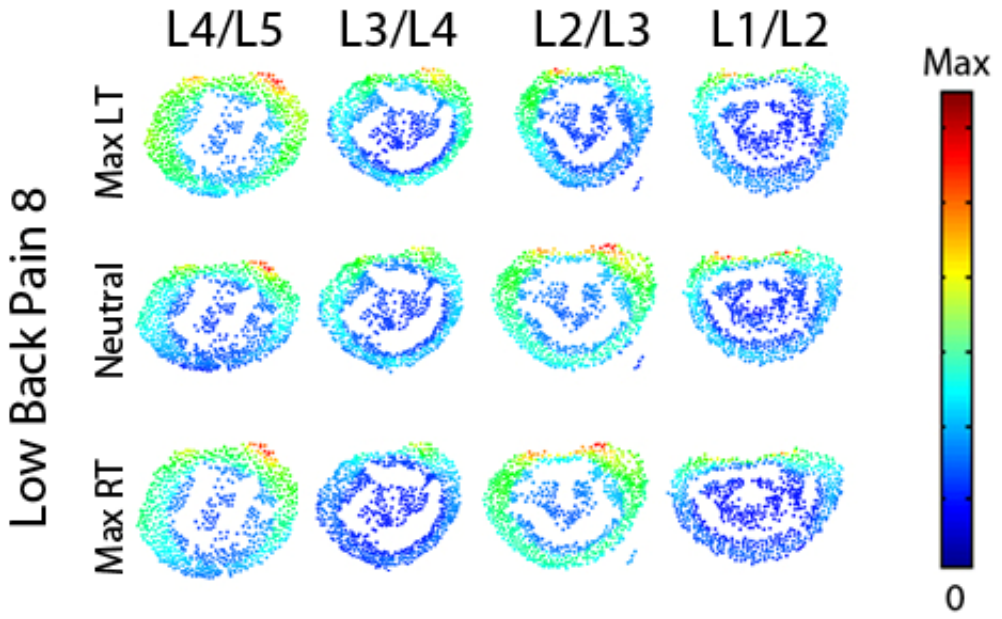

Figure 166. Magnitude stress at each atlas vertex for all levels at each major frame for Low Back Pain 8.

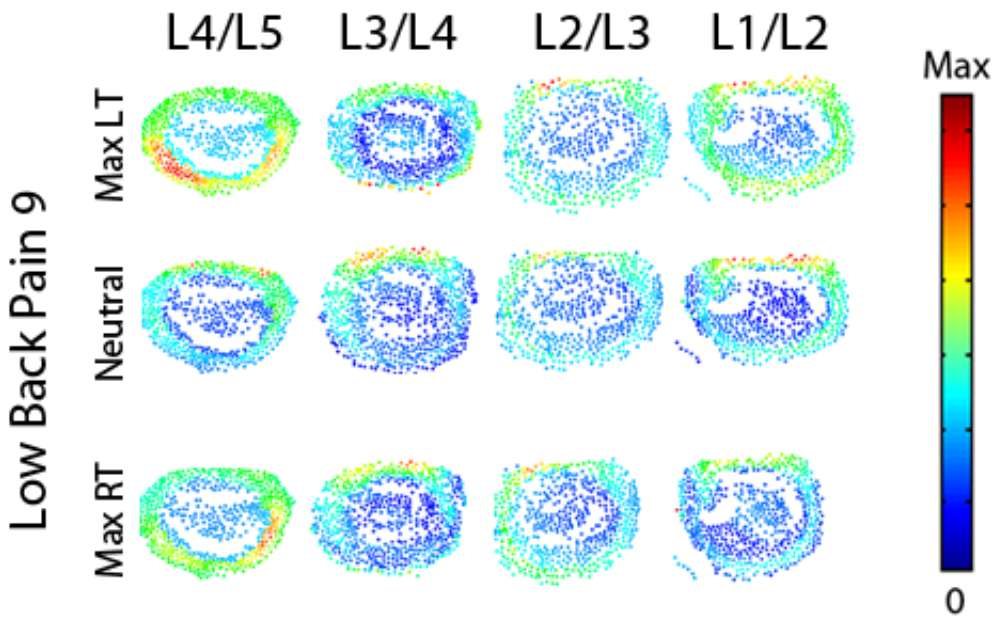

Figure 167. Magnitude stress at each atlas vertex for all levels at each major frame for Low Back Pain 9.

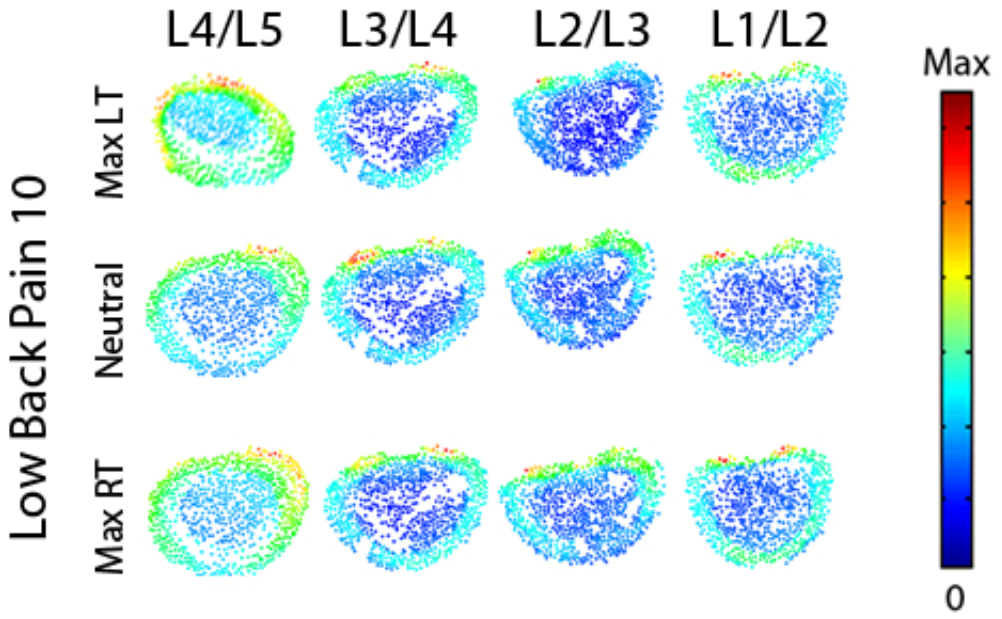

Figure 168. Magnitude stress at each atlas vertex for all levels at each major frame for Low Back Pain 10.

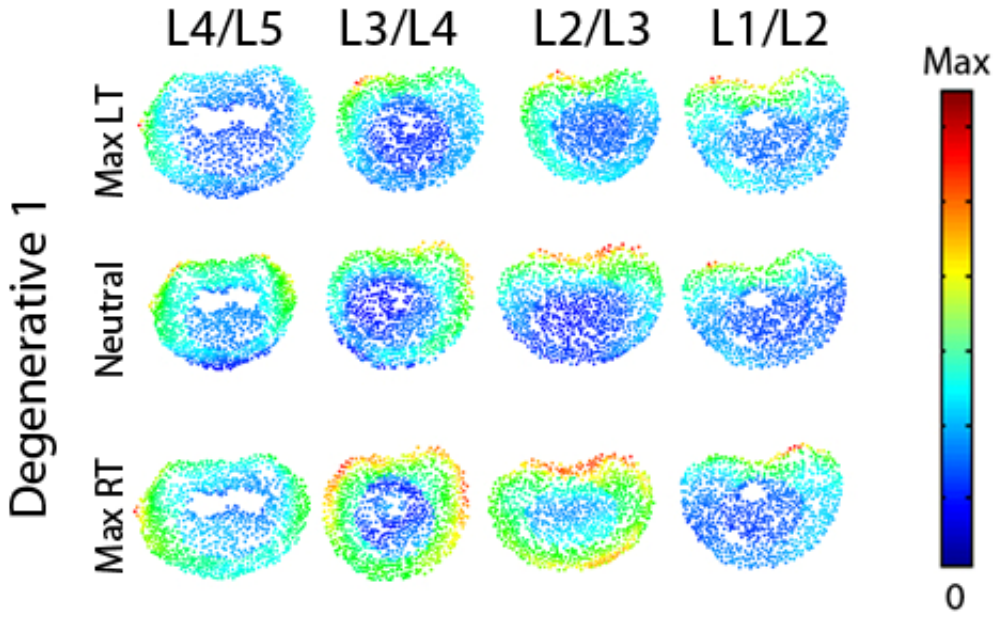

Figure 169. Magnitude stress at each atlas vertex for all levels at each major frame for Degenerative 1.

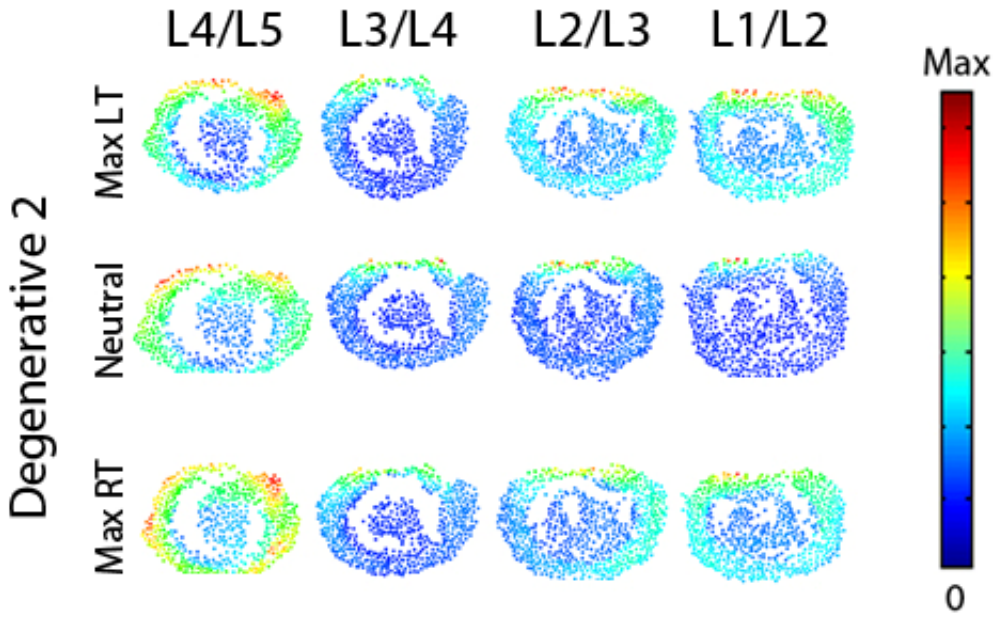

Figure 170. Magnitude stress at each atlas vertex for all levels at each major frame for Degenerative 2.

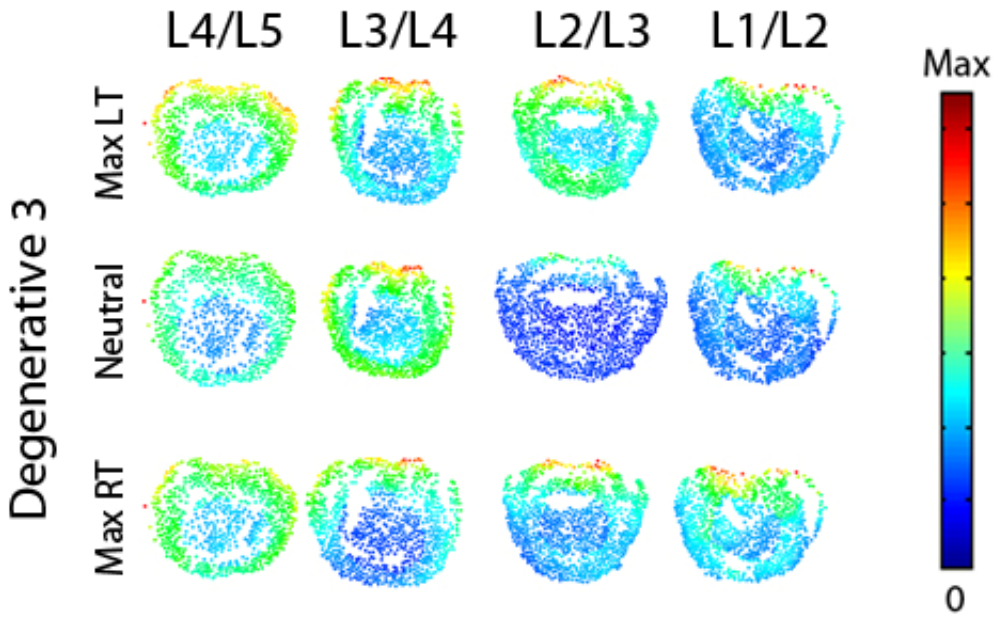

Figure 171. Magnitude stress at each atlas vertex for all levels at each major frame for Degenerative 3.

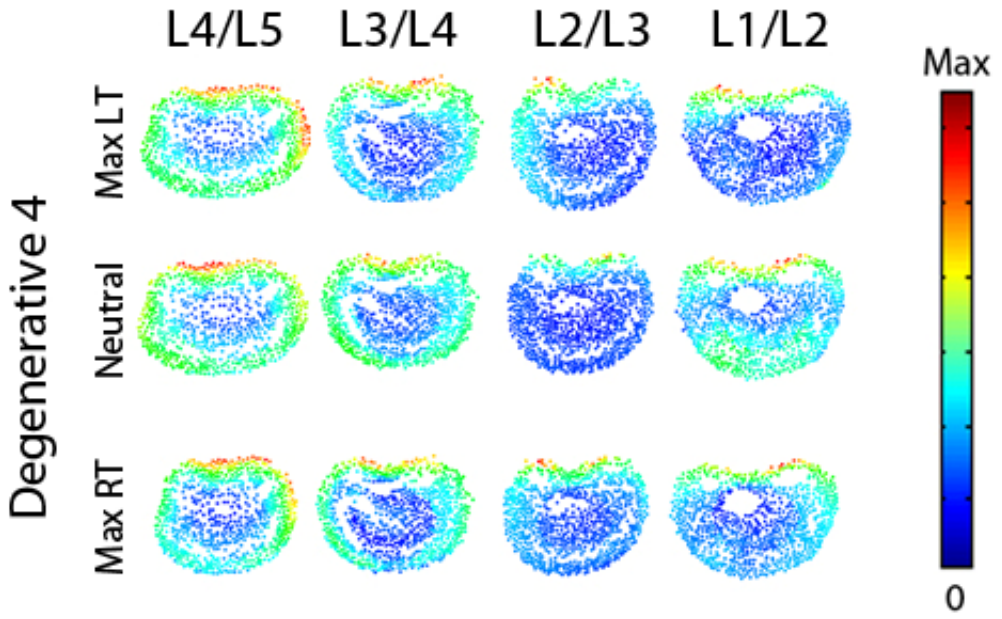

Figure 172. Magnitude stress at each atlas vertex for all levels at each major frame for Degenerative 4.

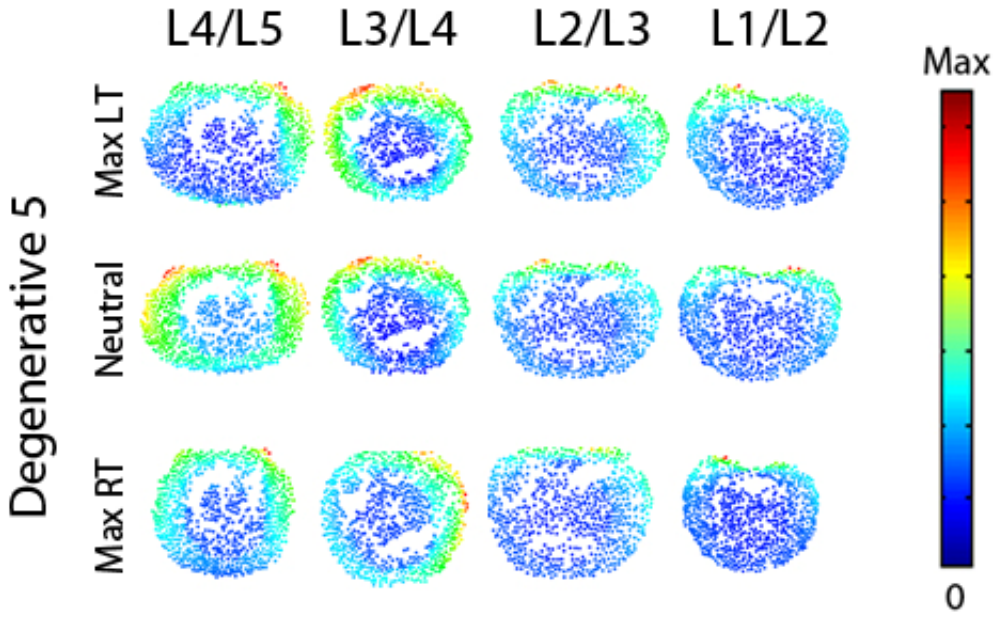

Figure 173. Magnitude stress at each atlas vertex for all levels at each major frame for Degenerative 5.

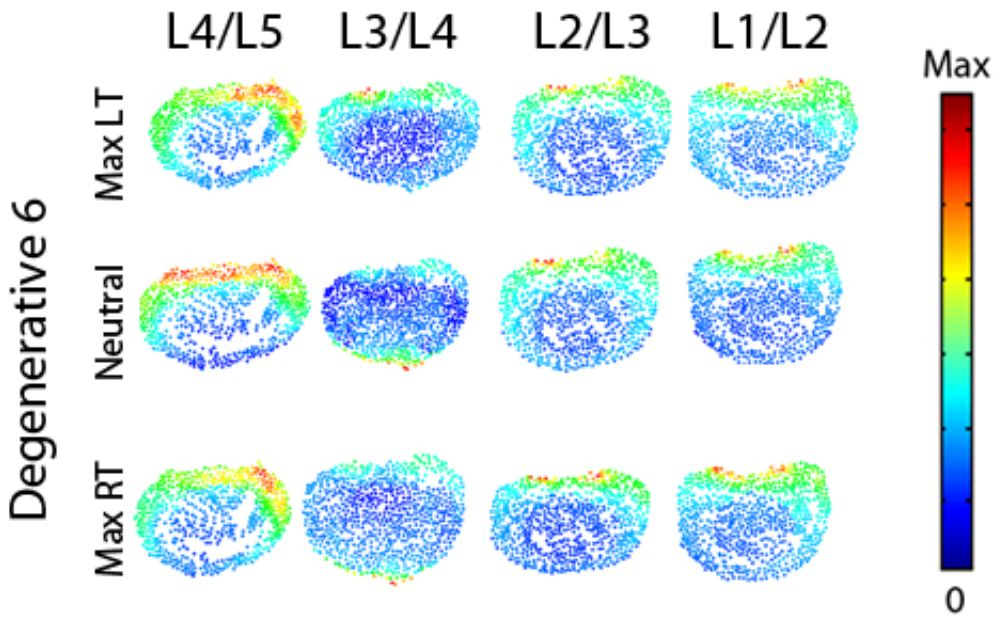

Figure 174. Magnitude stress at each atlas vertex for all levels at each major frame for Degenerative 6.

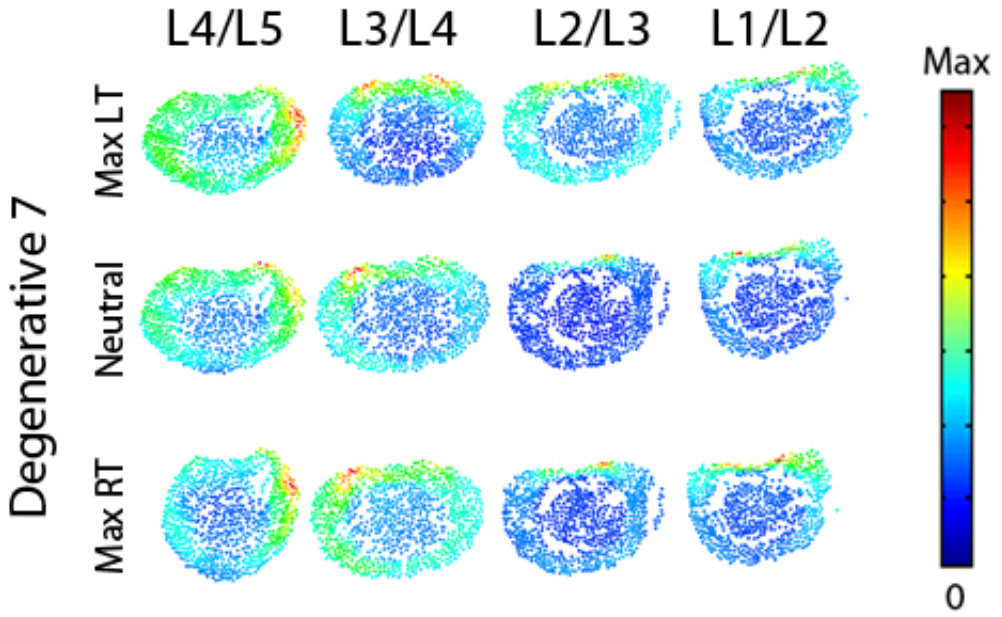

Figure 175. Magnitude stress at each atlas vertex for all levels at each major frame for Degenerative 7.

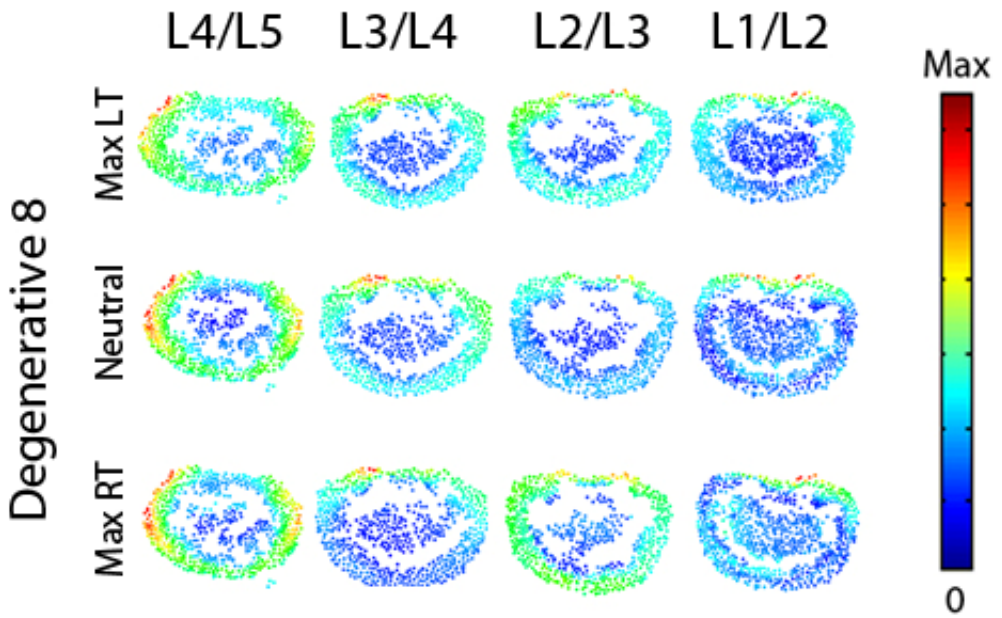

Figure 176. Magnitude stress at each atlas vertex for all levels at each major frame for Degenerative 8.

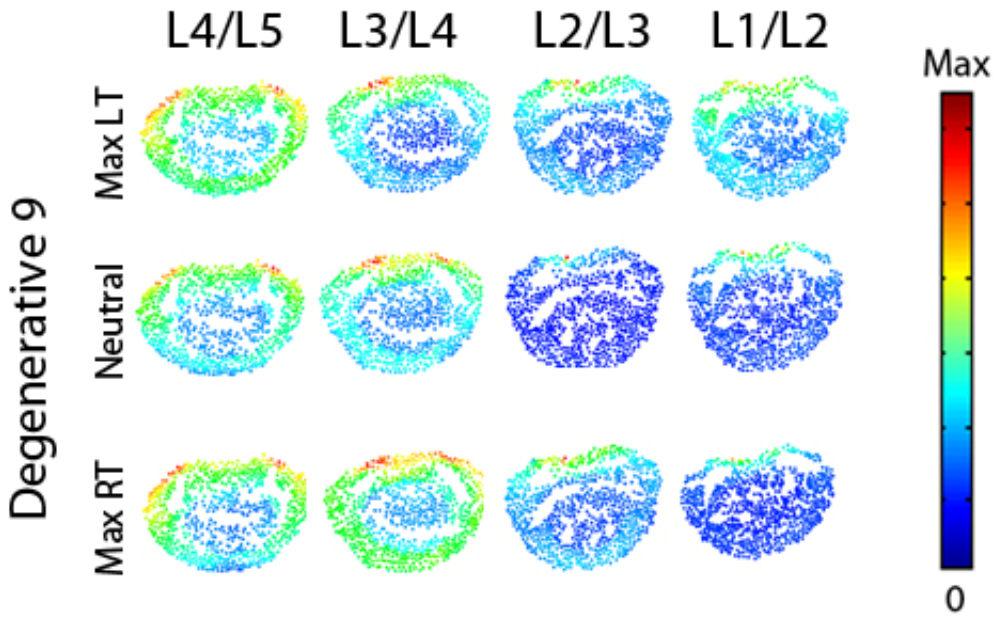

Figure 177. Magnitude stress at each atlas vertex for all levels at each major frame for Degenerative 9.

.

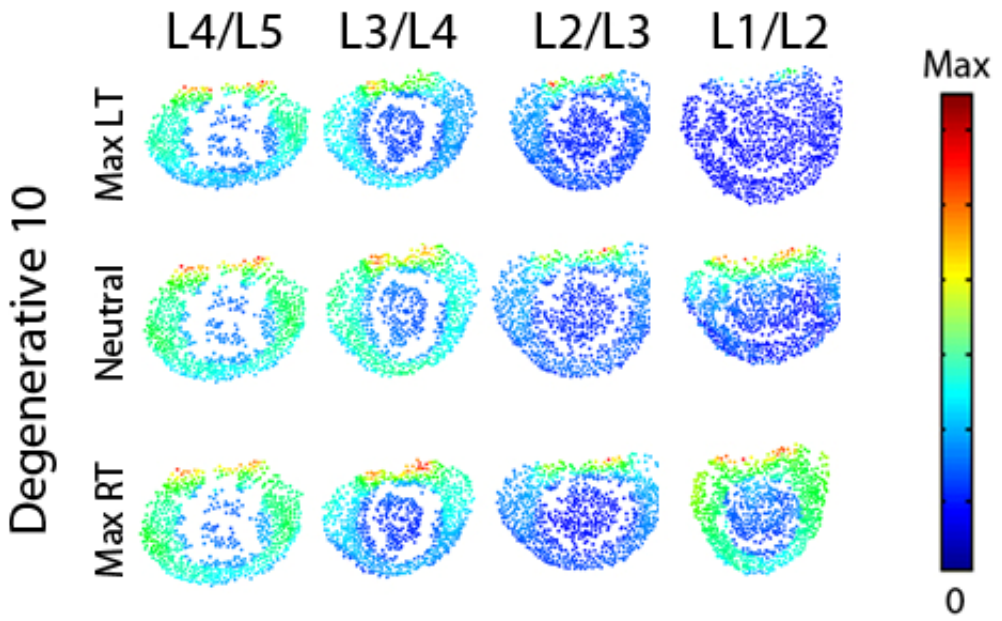

Figure 178. Magnitude stress at each atlas vertex for all levels at each major frame for Degenerative 10.

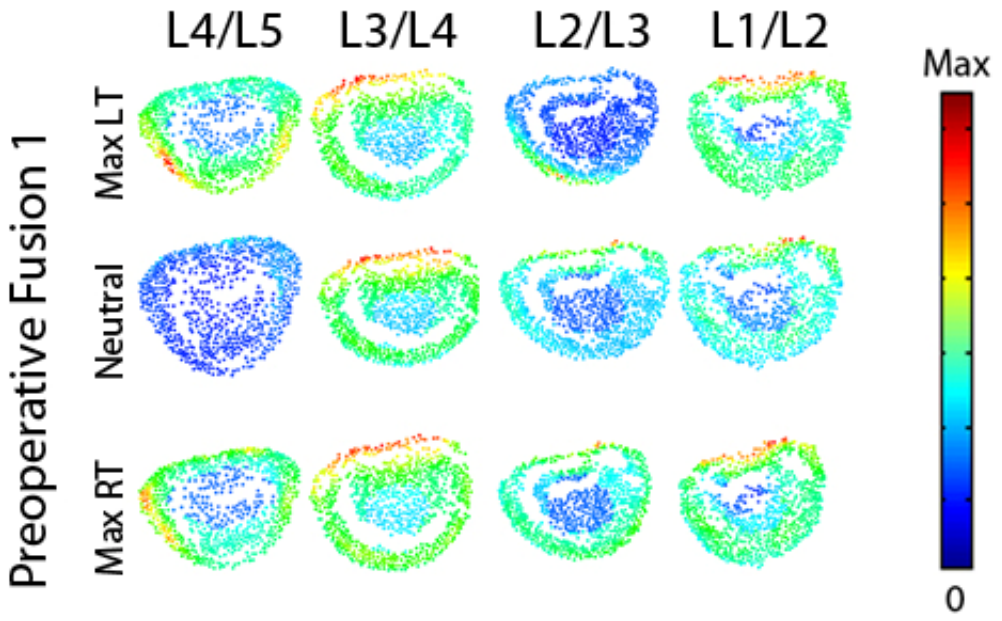

Figure 179. Magnitude stress at each atlas vertex for all levels at each major frame for Preoperative Fusion 1.

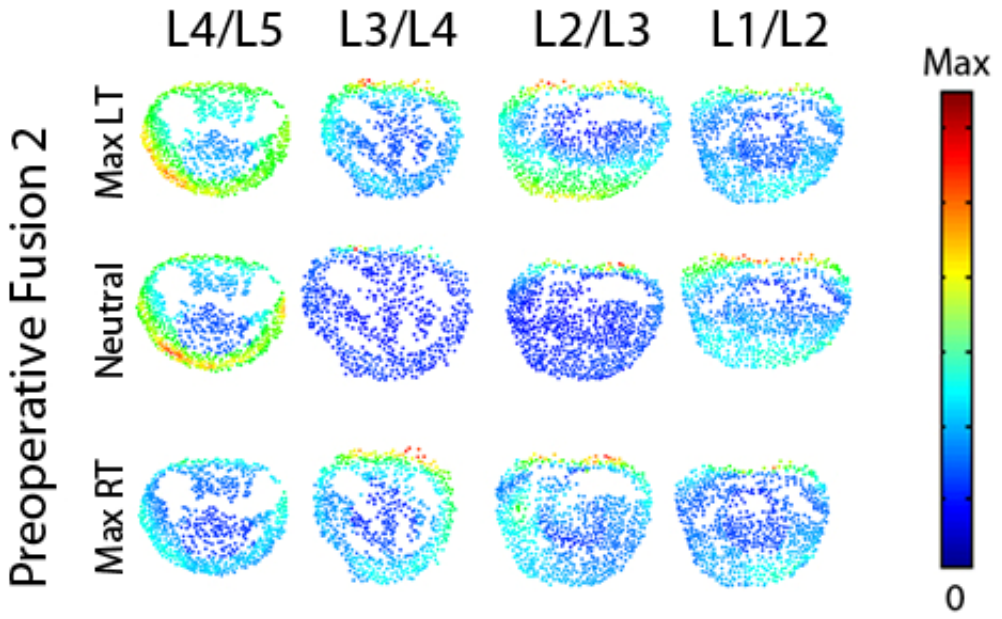

Figure 180. Magnitude stress at each atlas vertex for all levels at each major frame for Preoperative Fusion 2.

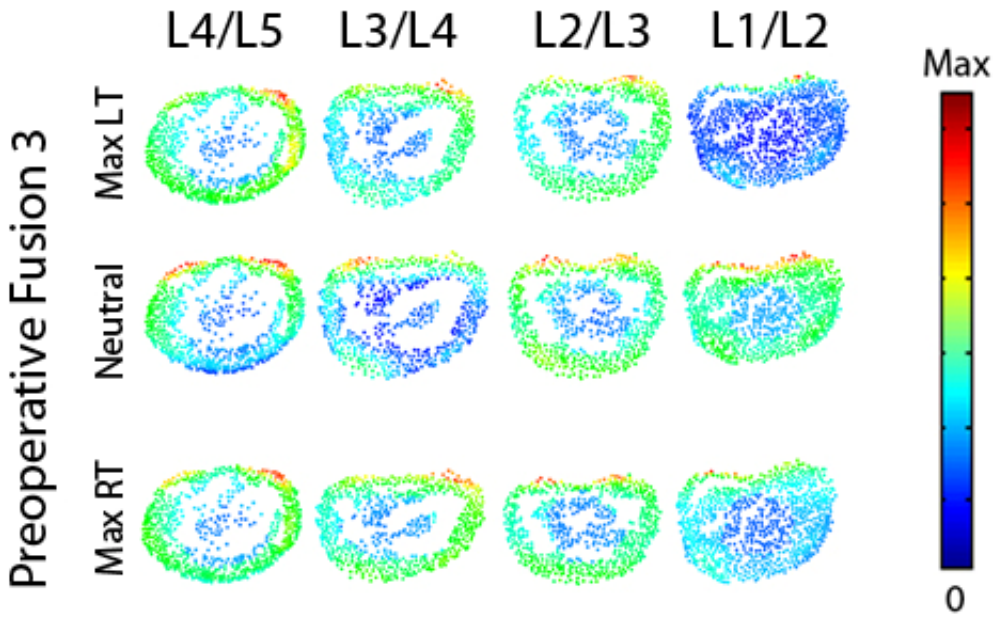

Figure 181. Magnitude stress at each atlas vertex for all levels at each major frame for Preoperative Fusion 3.

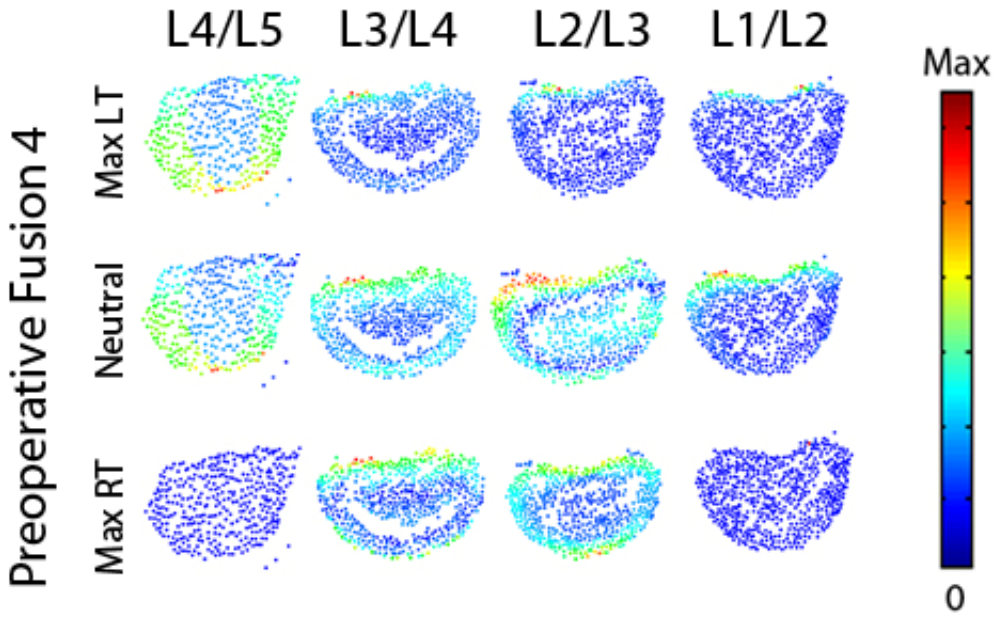

Figure 182. Magnitude stress at each atlas vertex for all levels at each major frame for Preoperative Fusion 4.

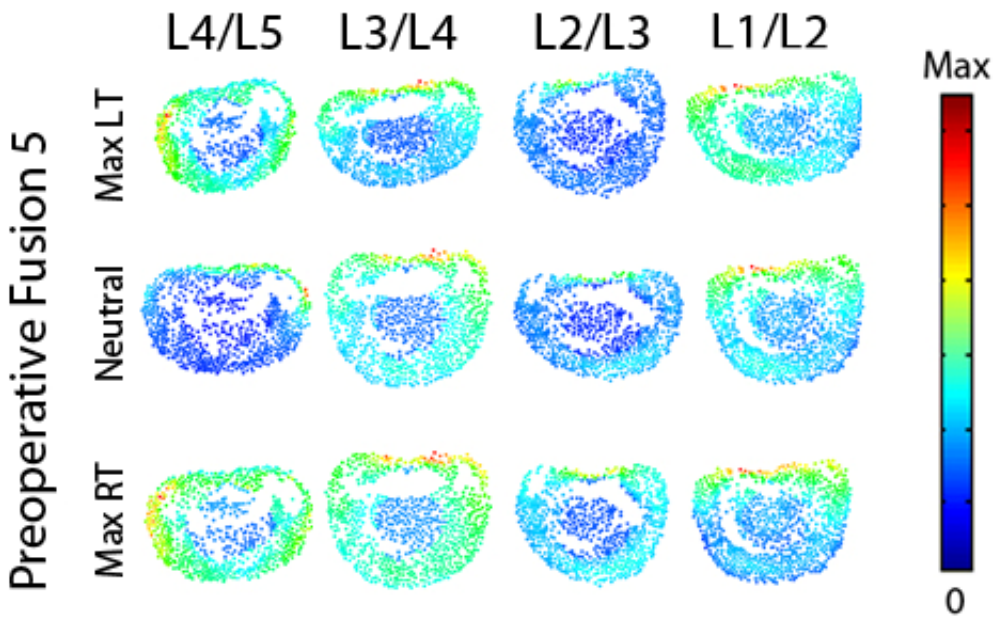

Figure 183. Magnitude stress at each atlas vertex for all levels at each major frame for Preoperative Fusion 5.

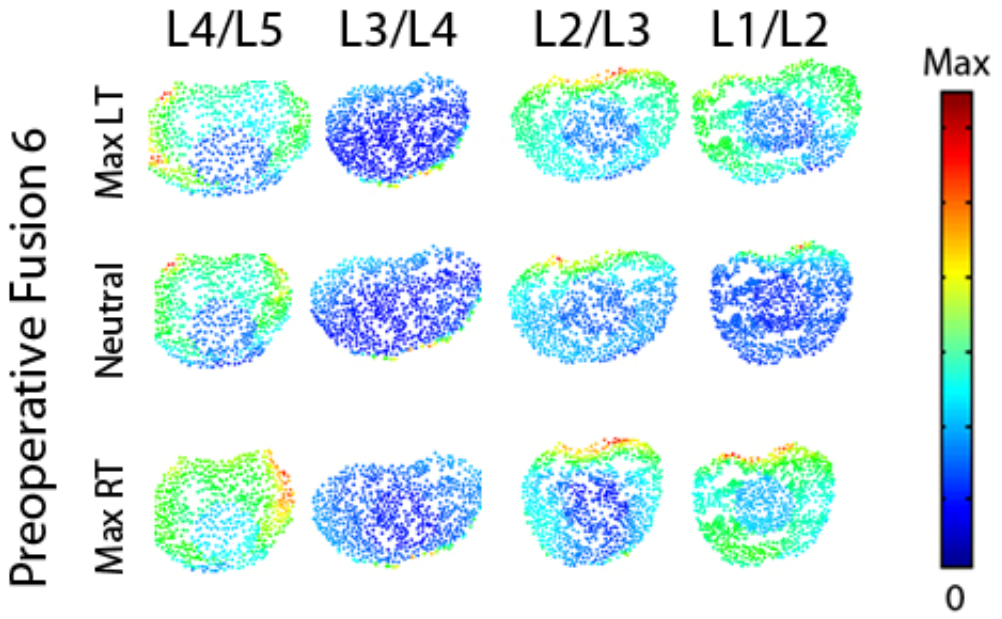

Figure 184. Magnitude stress at each atlas vertex for all levels at each major frame for Preoperative Fusion 6.

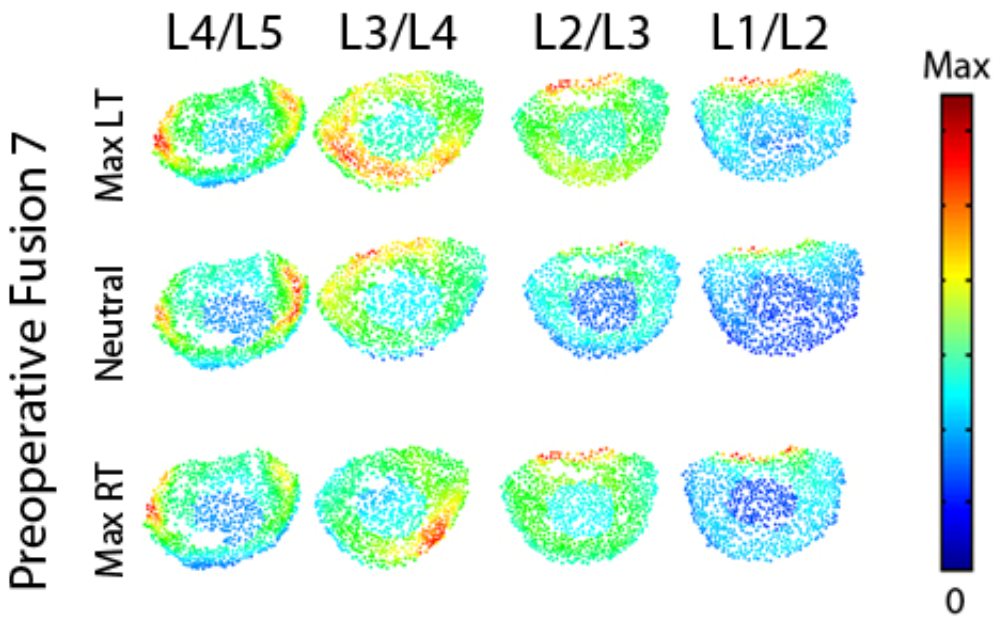

Figure 185. Magnitude stress at each atlas vertex for all levels at each major frame for Preoperative Fusion 7.

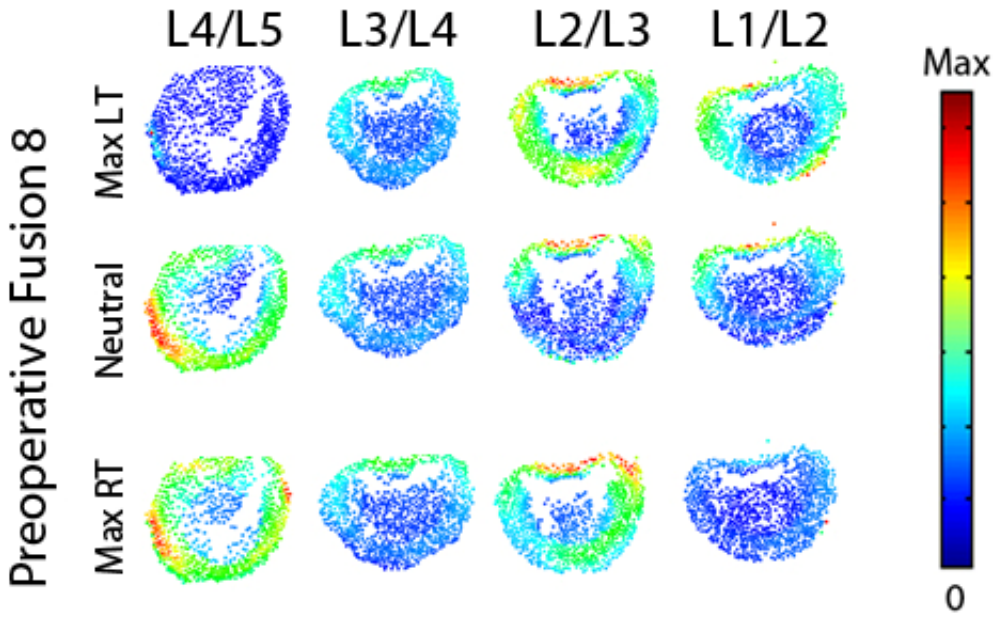

Figure 186. Magnitude stress at each atlas vertex for all levels at each major frame for Preoperative Fusion 8.

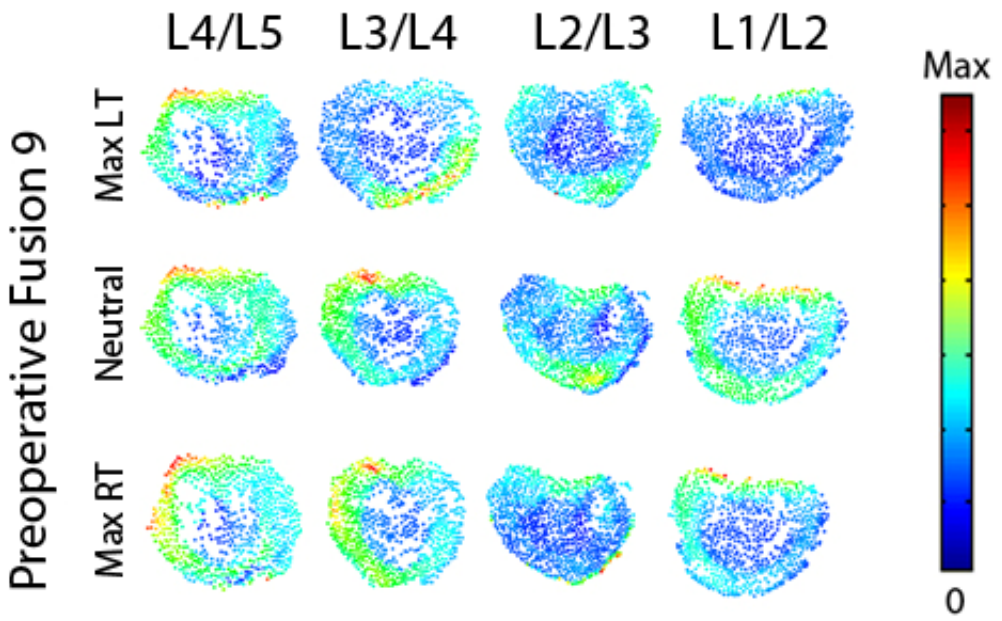

Figure 187. Magnitude stress at each atlas vertex for all levels at each major frame for Preoperative Fusion 9.

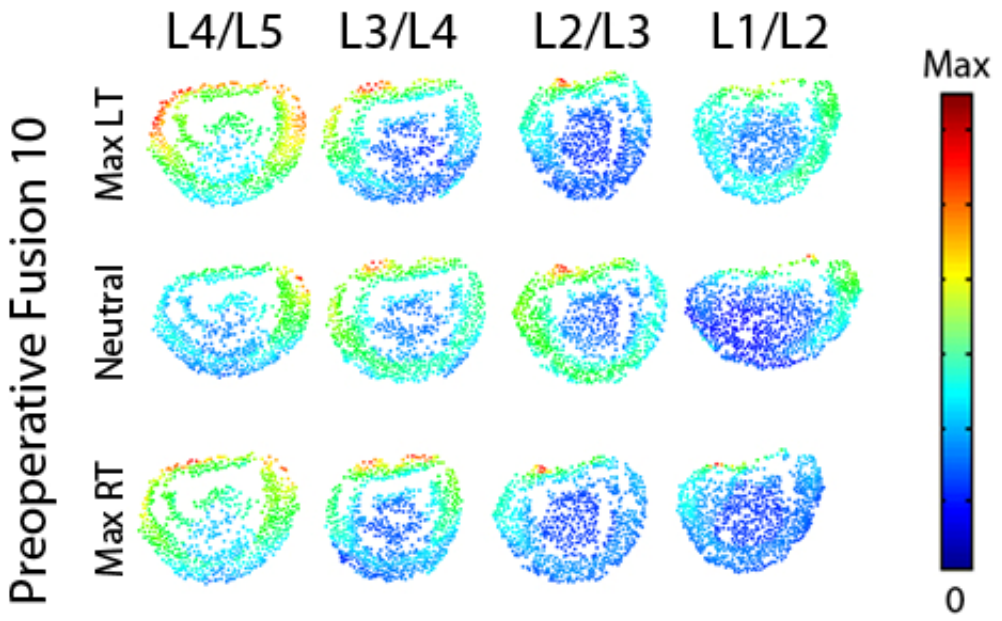

Figure 188. Magnitude stress at each atlas vertex for all levels at each major frame for Preoperative Fusion 10.

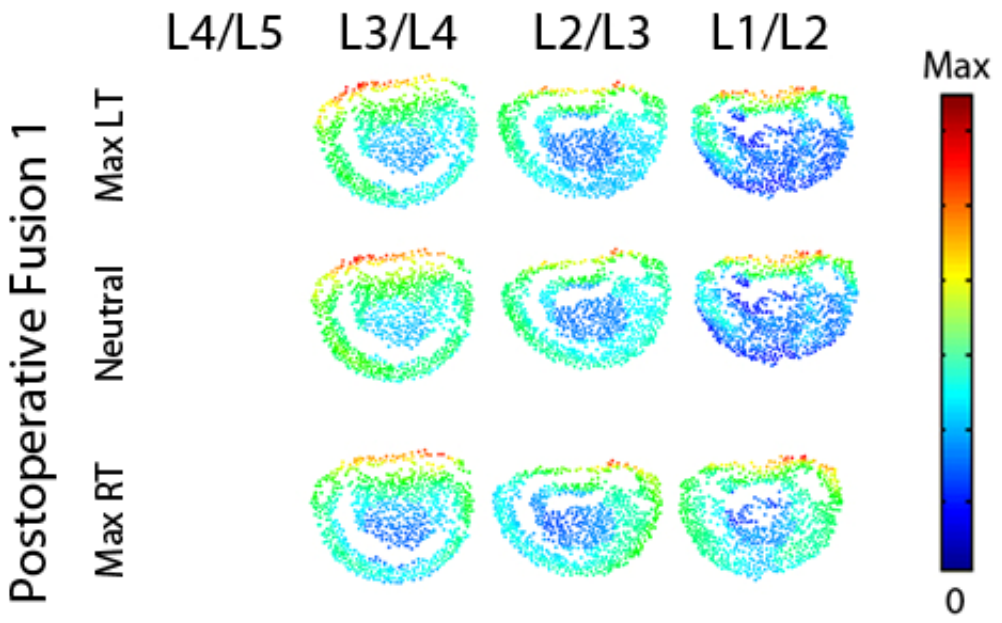

Figure 189. Magnitude stress at each atlas vertex for all levels at each major frame for Postoperative Fusion 1.

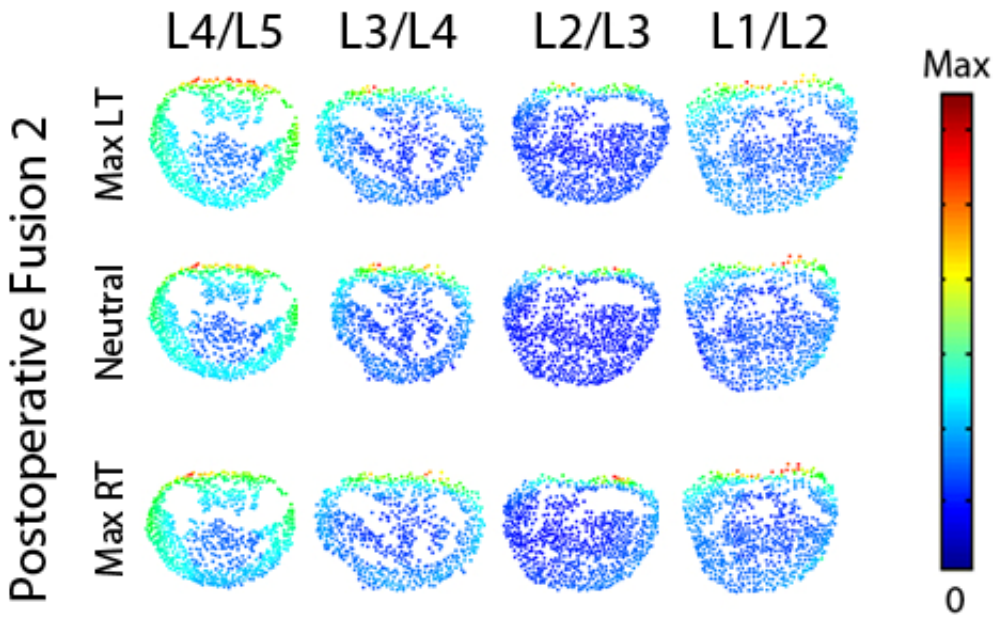

Figure 190. Magnitude stress at each atlas vertex for all levels at each major frame for Postoperative Fusion 2.

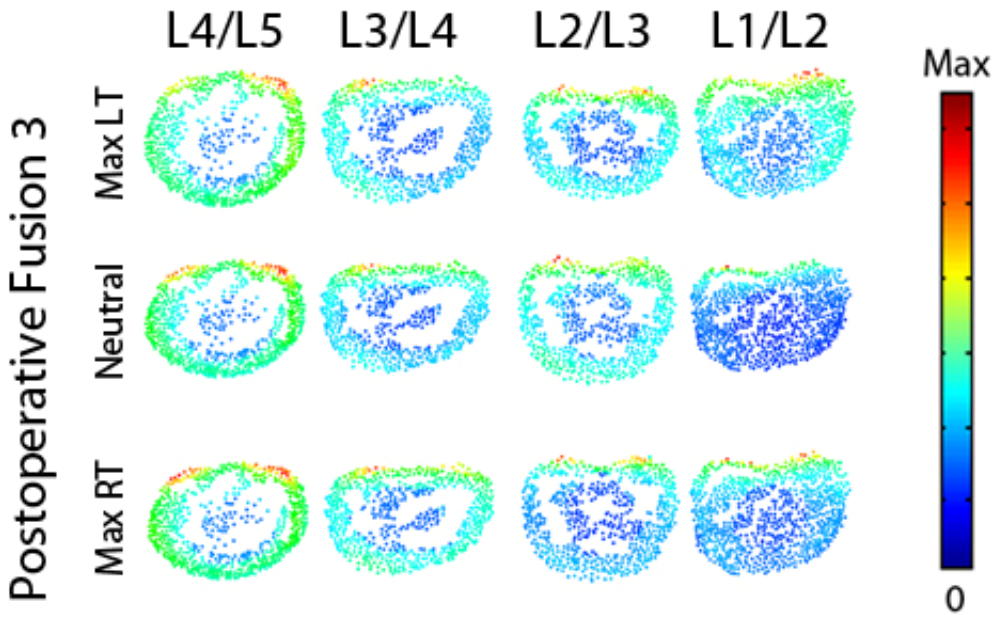

Figure 191. Magnitude stress at each atlas vertex for all levels at each major frame for Postoperative Fusion 3.

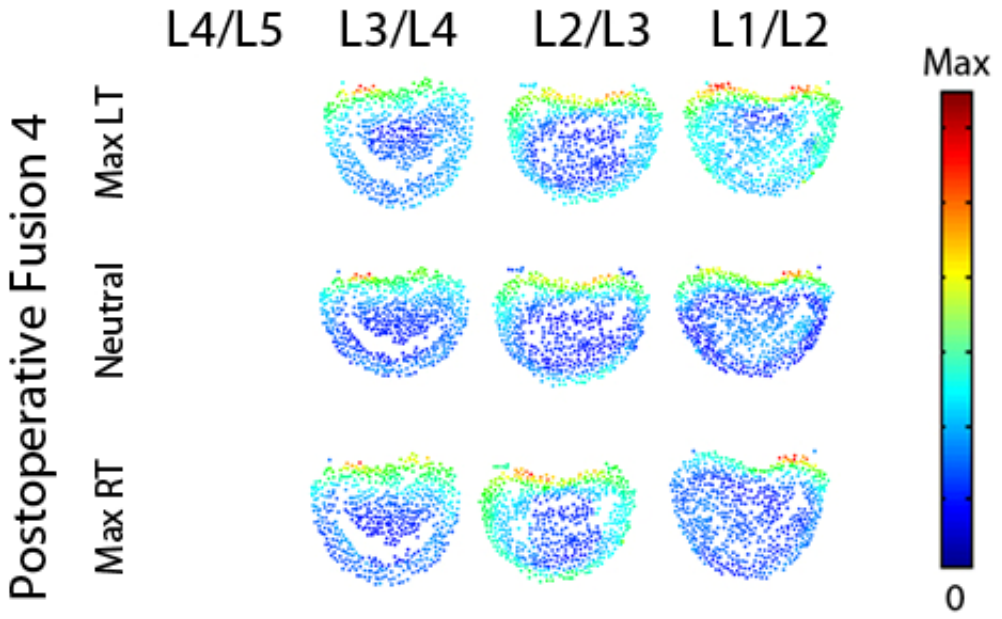

Figure 192. Magnitude stress at each atlas vertex for all levels at each major frame for Postoperative Fusion 4.

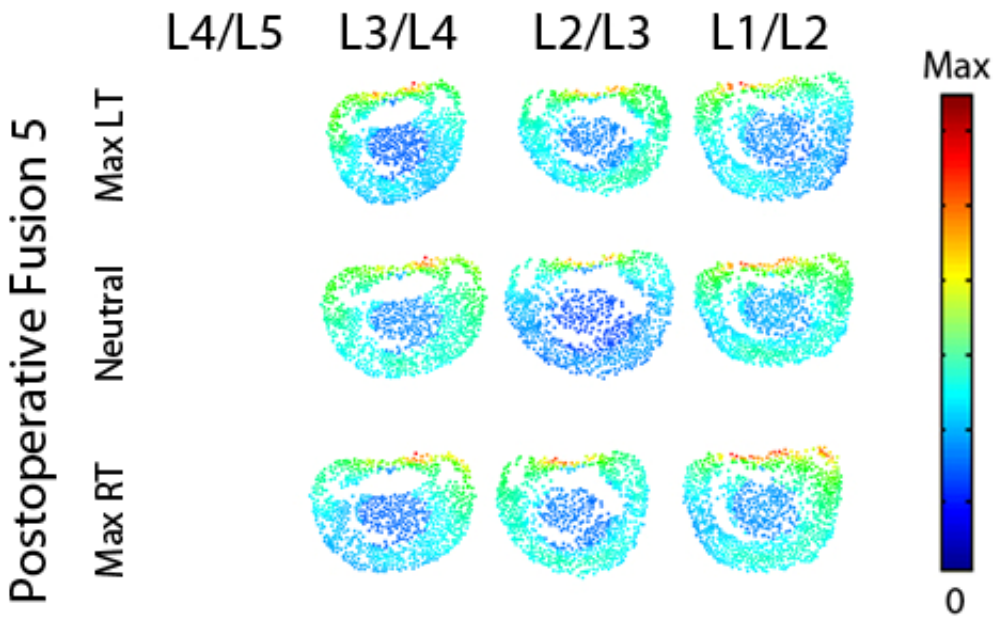

Figure 193. Magnitude stress at each atlas vertex for all levels at each major frame for Postoperative Fusion 5.

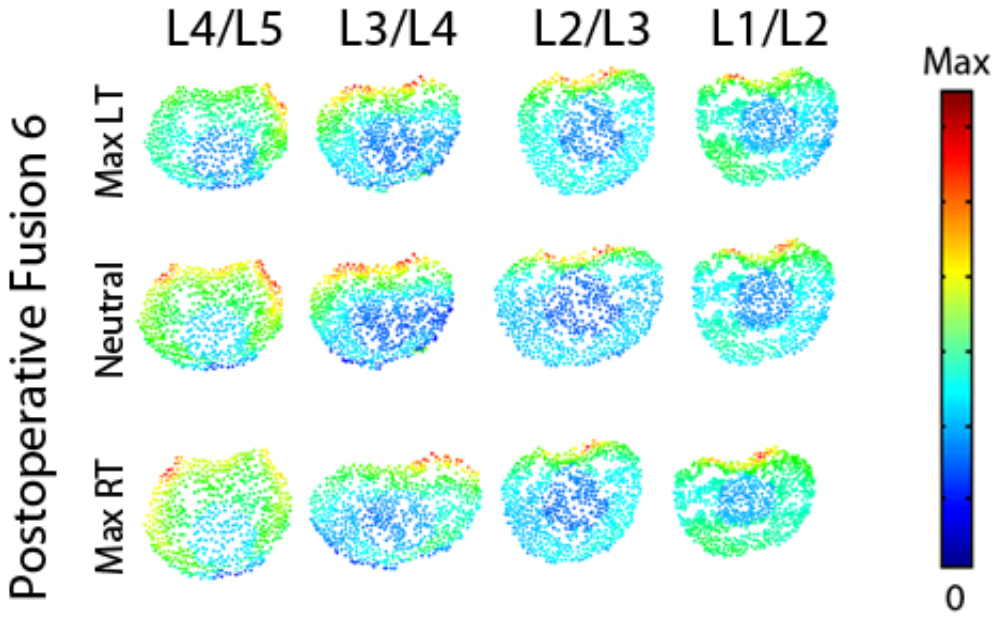

Figure 194. Magnitude stress at each atlas vertex for all levels at each major frame for Postoperative Fusion 6.

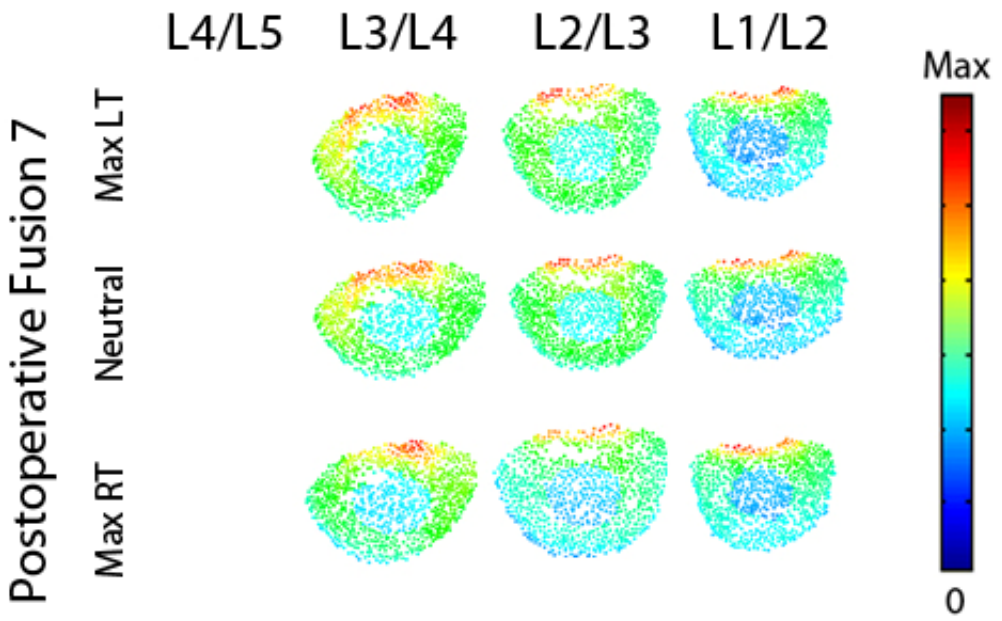

Figure 195. Magnitude stress at each atlas vertex for all levels at each major frame for Postoperative Fusion 7.

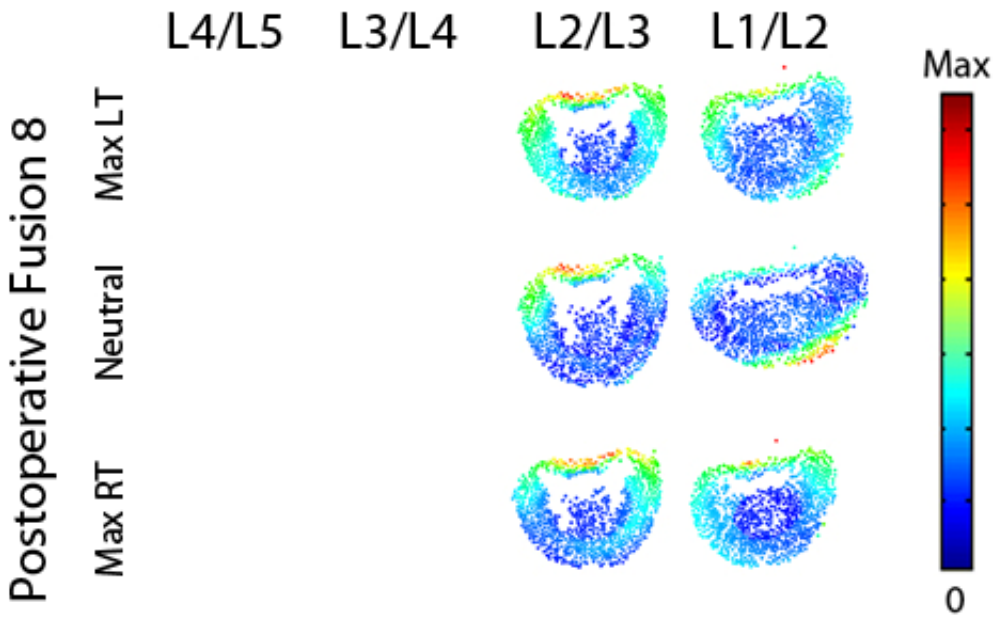

Figure 196. Magnitude stress at each atlas vertex for all levels at each major frame for Postoperative Fusion 8.

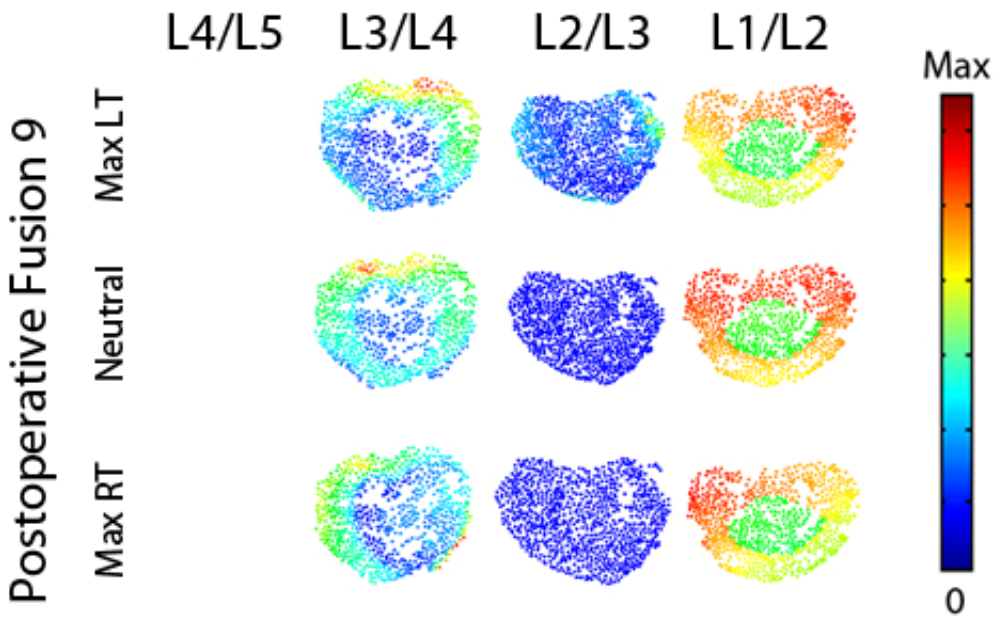

Figure 197. Magnitude stress at each atlas vertex for all levels at each major frame for Postoperative Fusion 9.

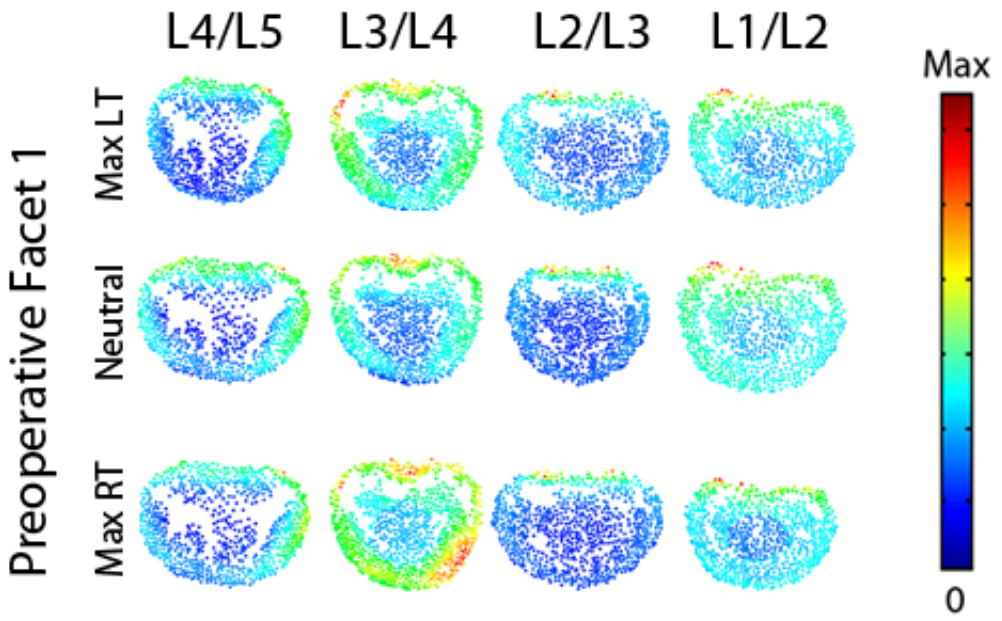

Figure 198. Magnitude stress at each atlas vertex for all levels at each major frame for Preoperative Facet 1.

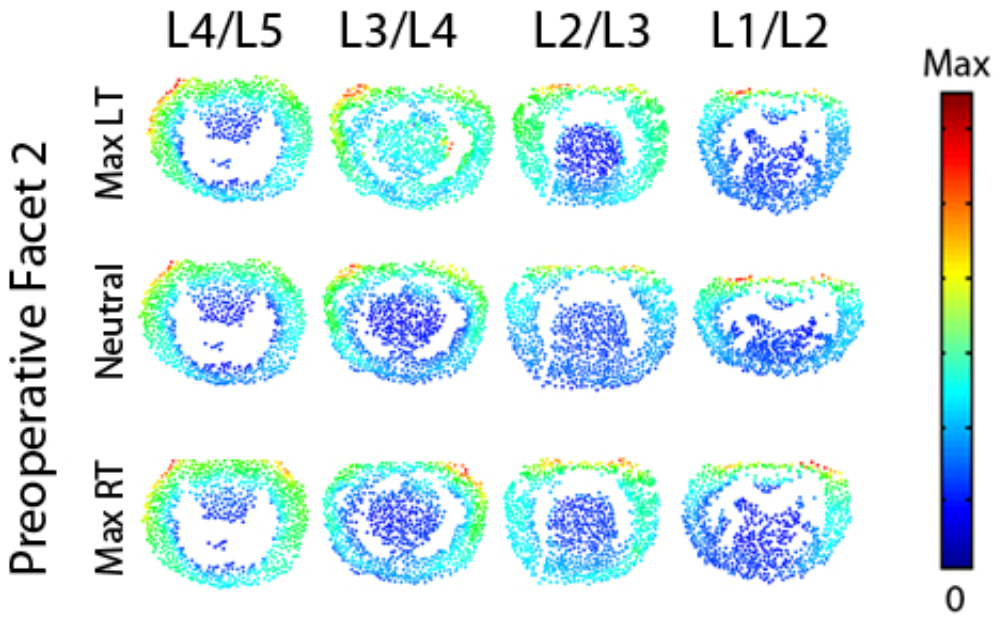

Figure 199. Magnitude stress at each atlas vertex for all levels at each major frame for Preoperative Facet 2.

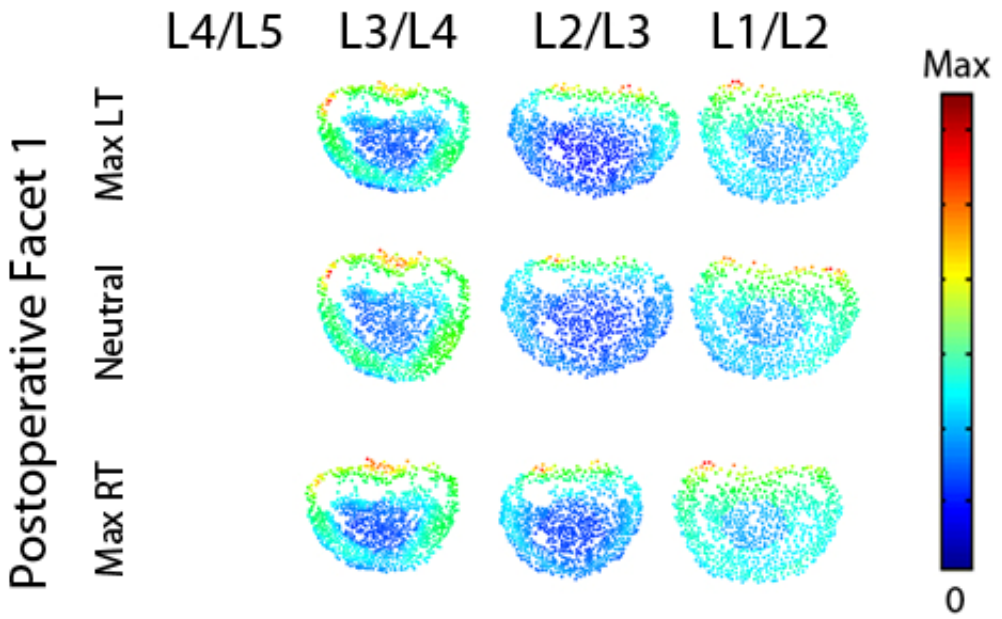

Figure 200. Magnitude stress at each atlas vertex for all levels at each major frame for Postoperative Facet 1.

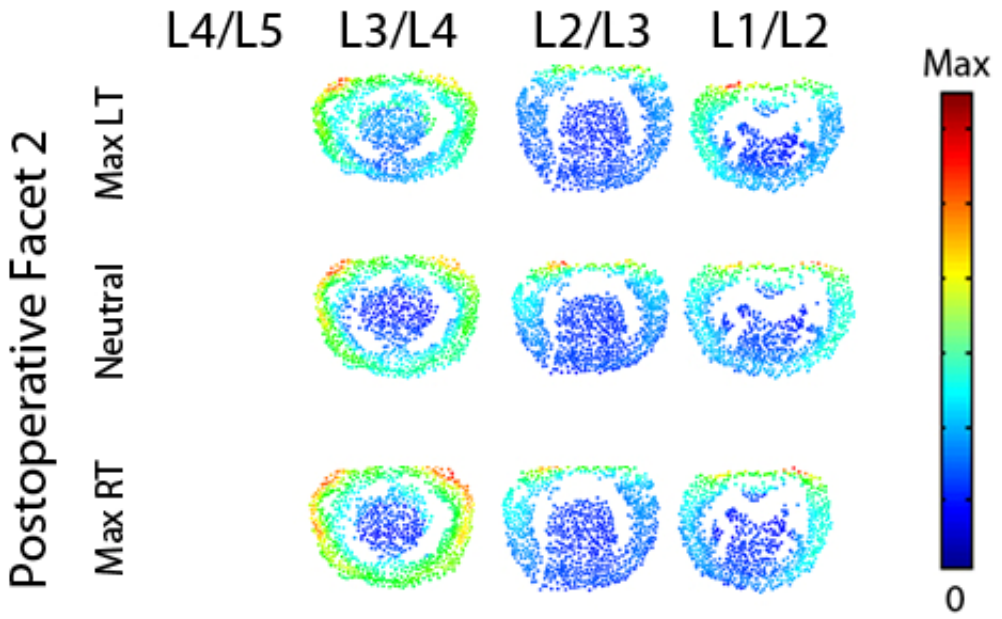

Figure 201. Magnitude stress at each atlas vertex for all levels at each major frame for Postoperative Facet 2.

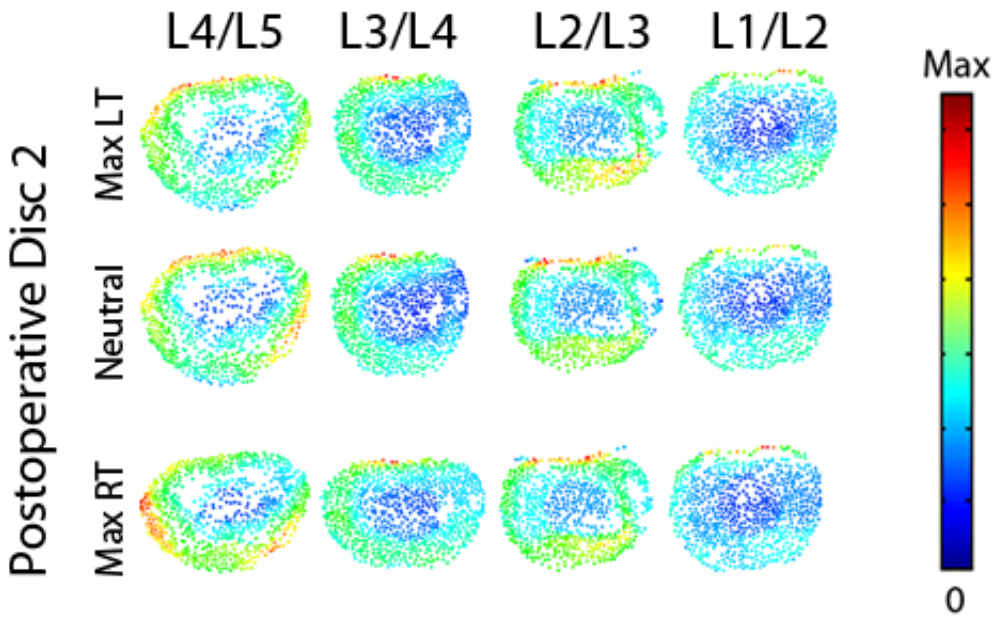

Figure 202. Magnitude stress at each atlas vertex for all levels at each major frame for Postoperative Disc 2.

A.4.3 Lateral Bending

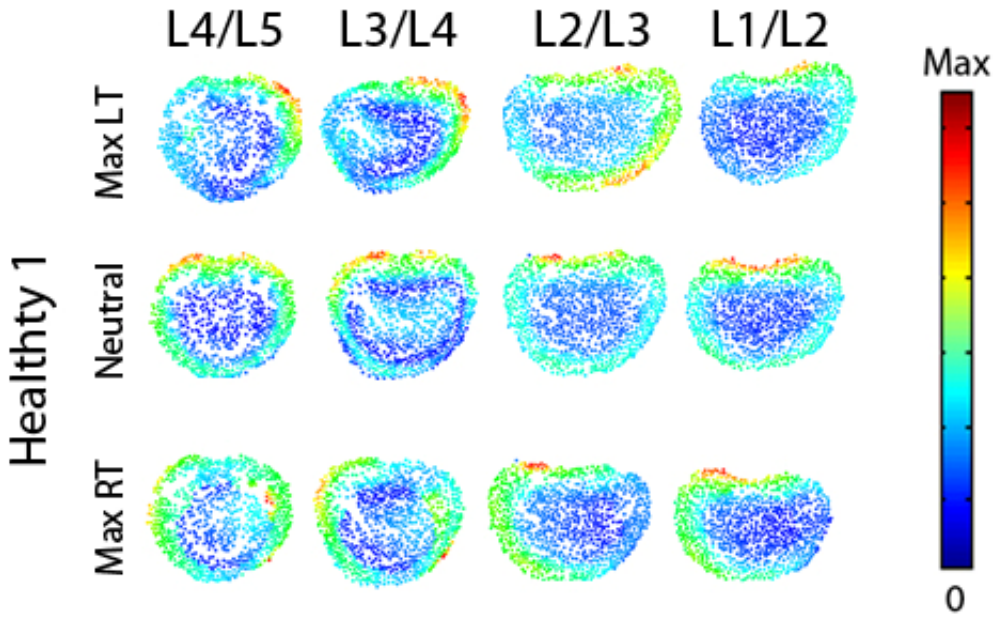

Figure 203. Magnitude stress at each atlas vertex for all levels at each major frame for Healthy 1.

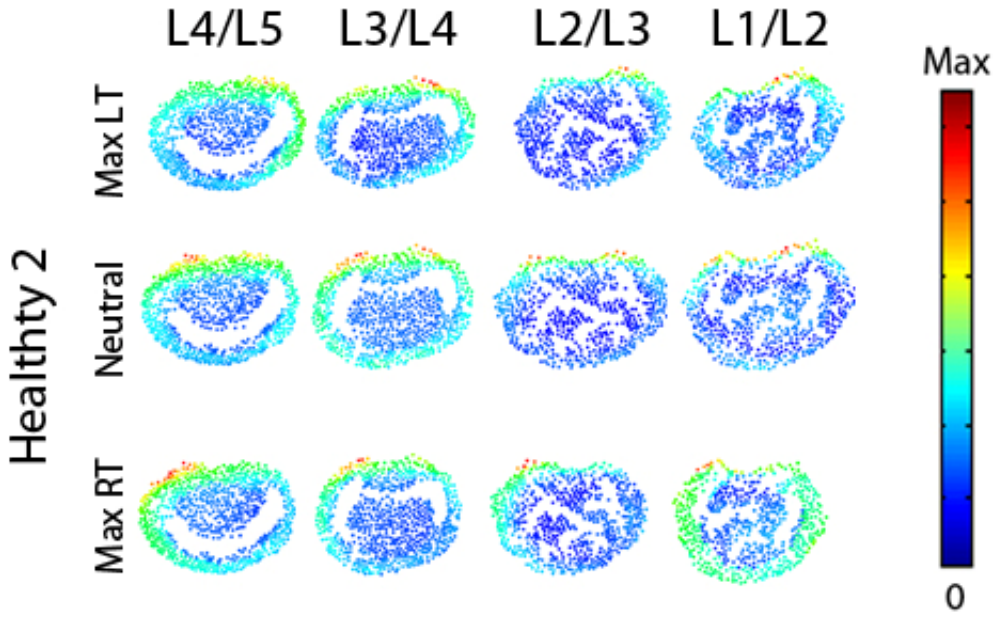

Figure 204. Magnitude stress at each atlas vertex for all levels at each major frame for Healthy 2.

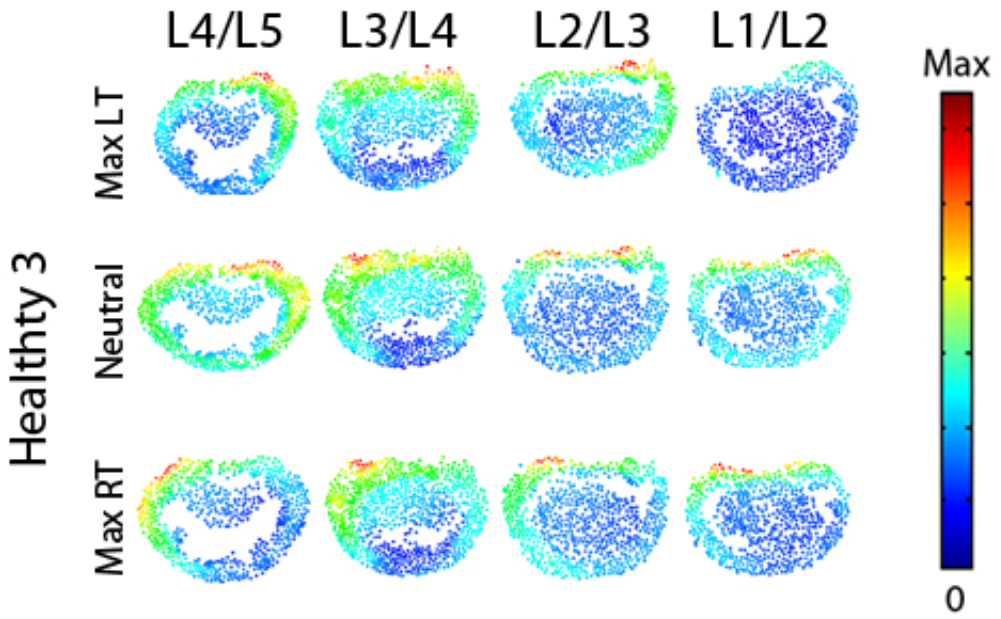

Figure 205. Magnitude stress at each atlas vertex for all levels at each major frame for Healthy 3.

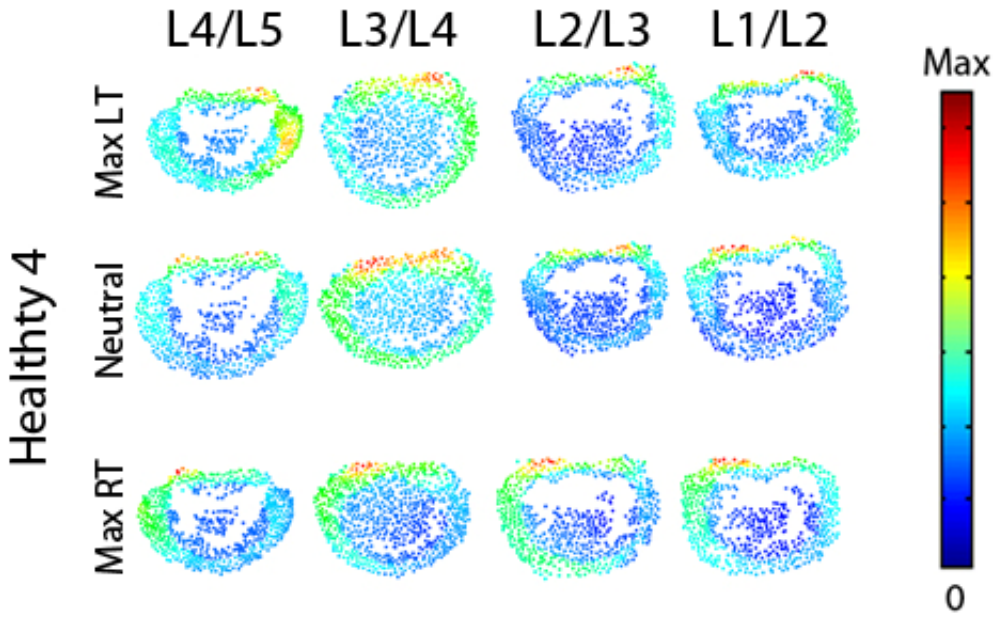

Figure 206. Magnitude stress at each atlas vertex for all levels at each major frame for Healthy 4.

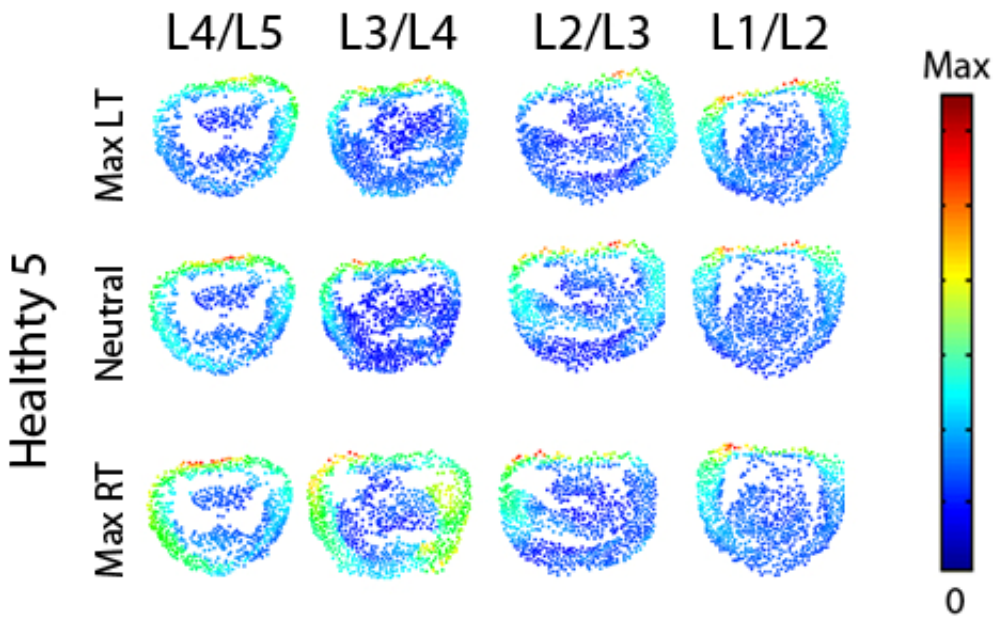

Figure 207. Magnitude stress at each atlas vertex for all levels at each major frame for Healthy 5.

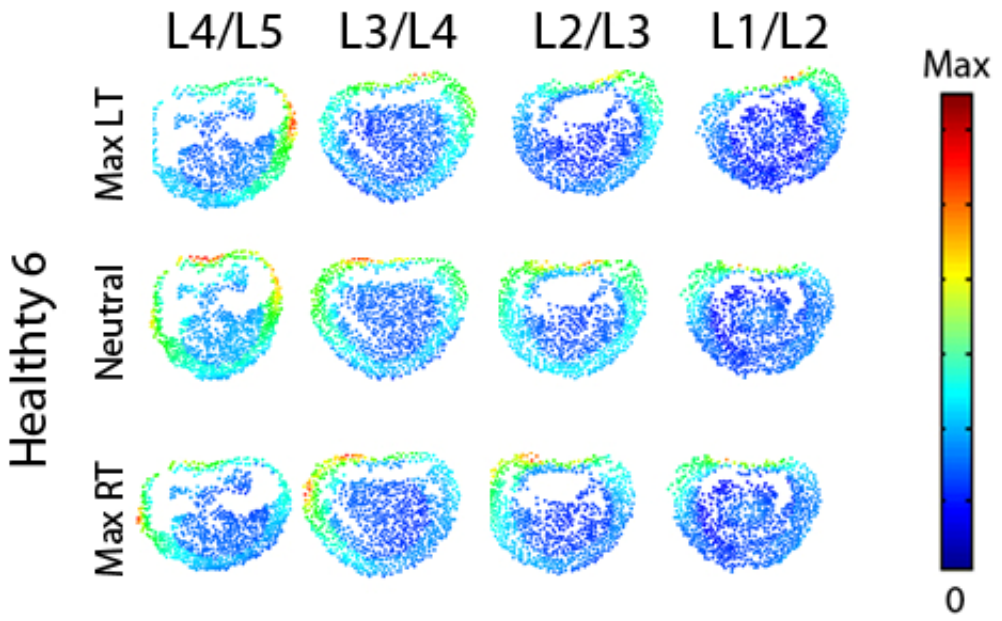

Figure 208. Magnitude stress at each atlas vertex for all levels at each major frame for Healthy 6.

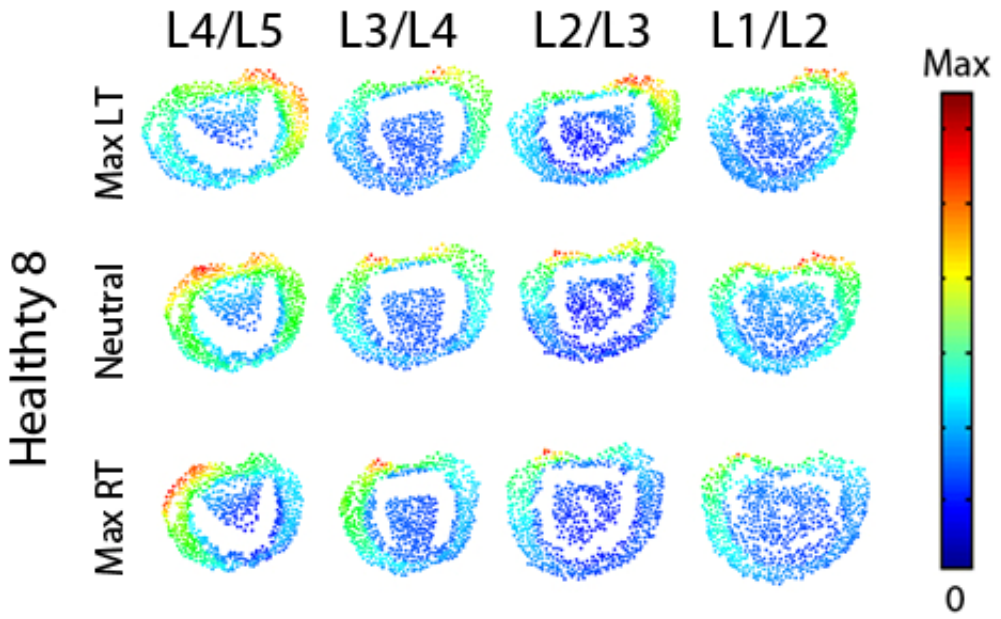

Figure 209. Magnitude stress at each atlas vertex for all levels at each major frame for Healthy 8.

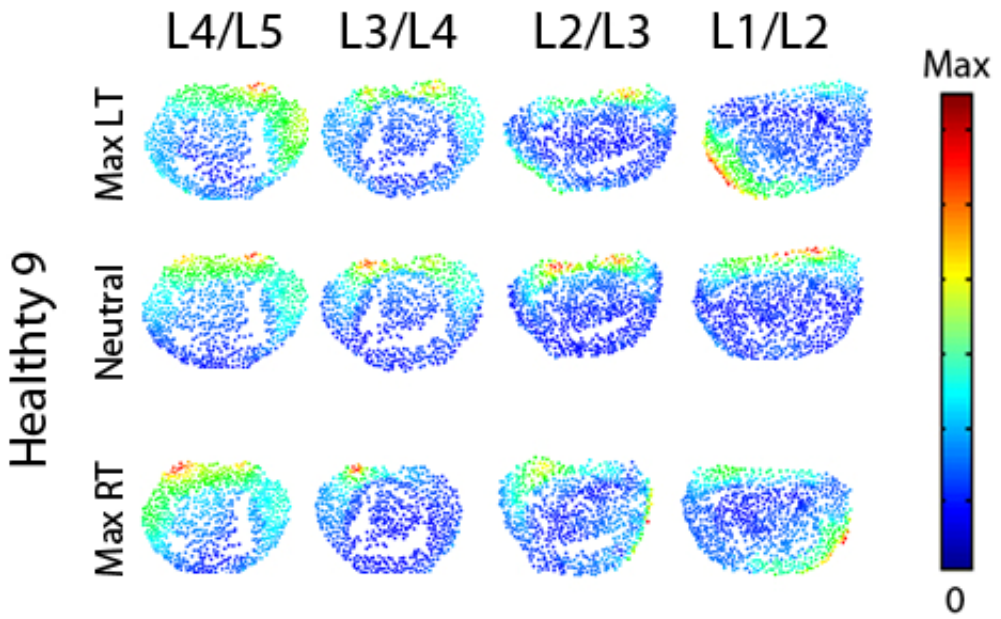

Figure 210. Magnitude stress at each atlas vertex for all levels at each major frame for Healthy 9.

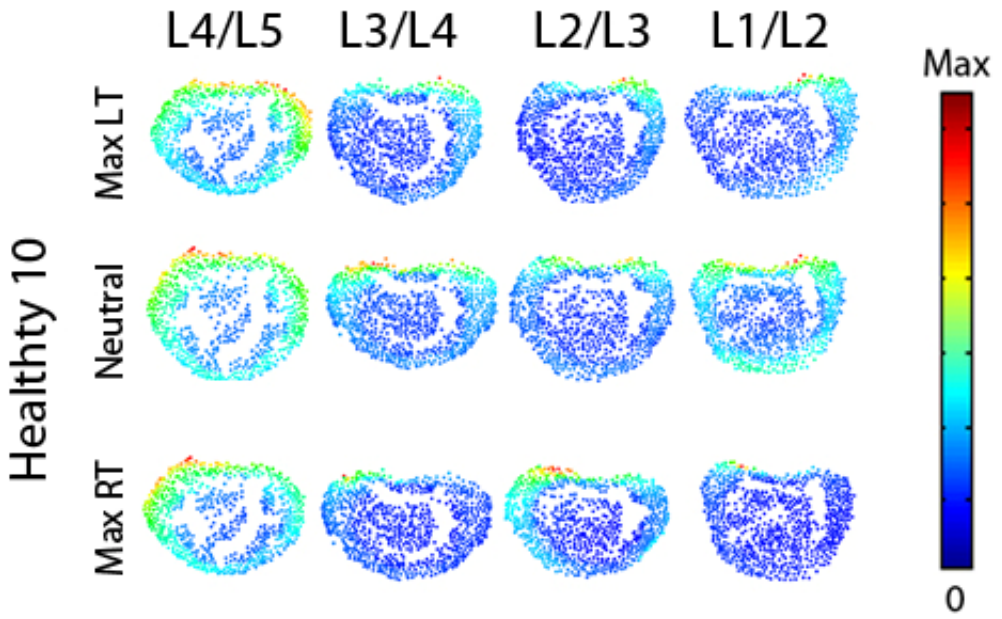

Figure 211. Magnitude stress at each atlas vertex for all levels at each major frame for Healthy 10.

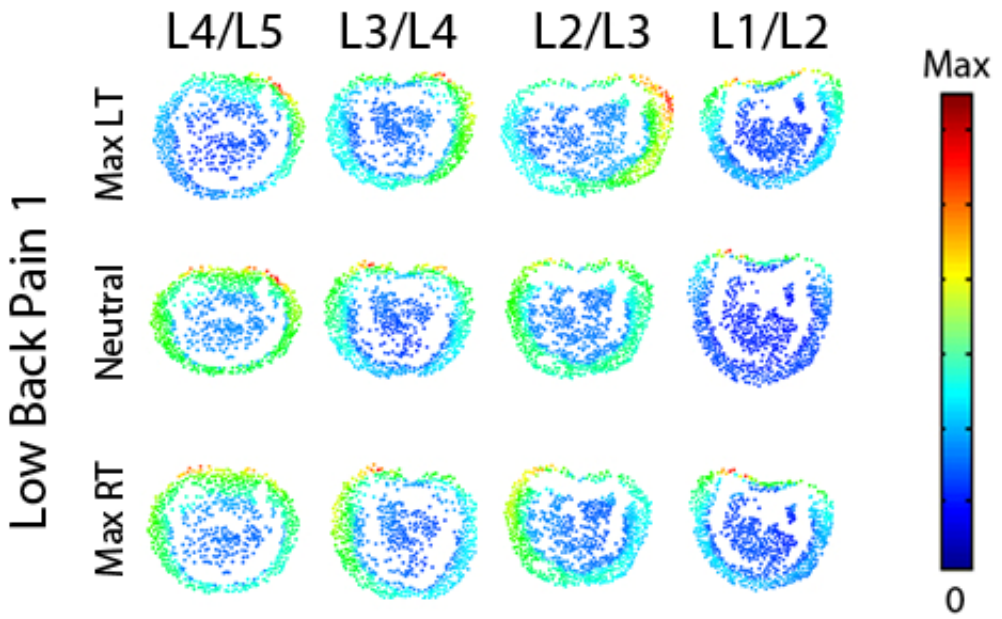

Figure 212. Magnitude stress at each atlas vertex for all levels at each major frame for Low Back Pain 1.

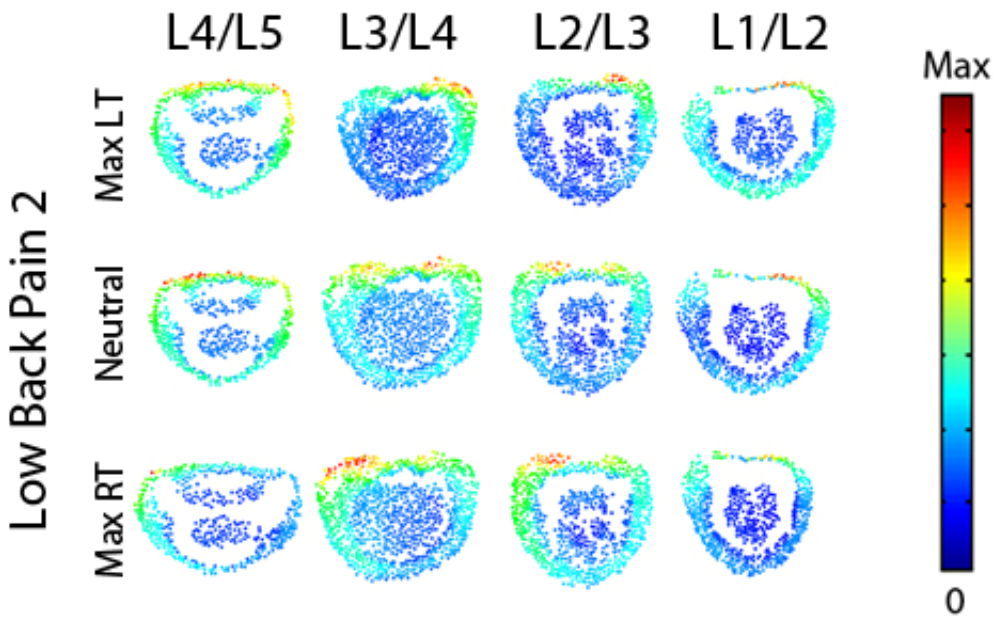

Figure 213. Magnitude stress at each atlas vertex for all levels at each major frame for Low Back Pain 2.

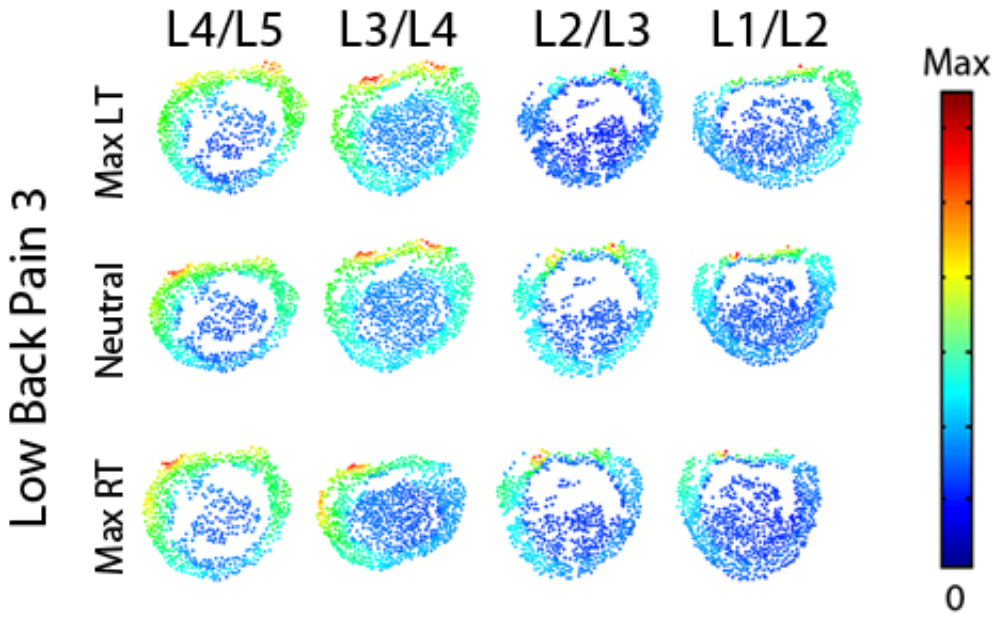

Figure 214. Magnitude stress at each atlas vertex for all levels at each major frame for Low Back Pain 3.

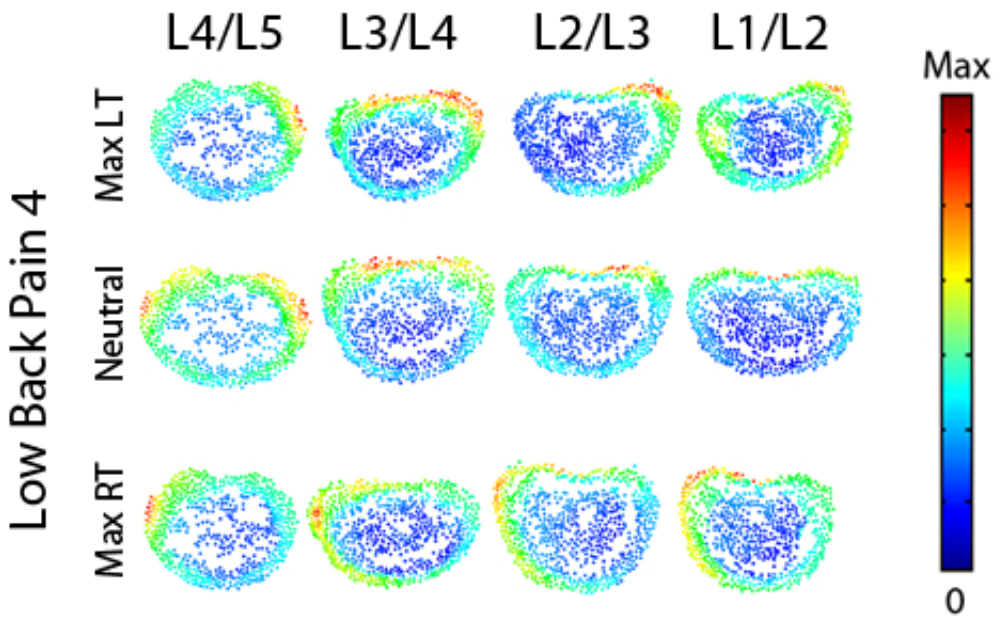

Figure 215. Magnitude stress at each atlas vertex for all levels at each major frame for Low Back Pain 4.

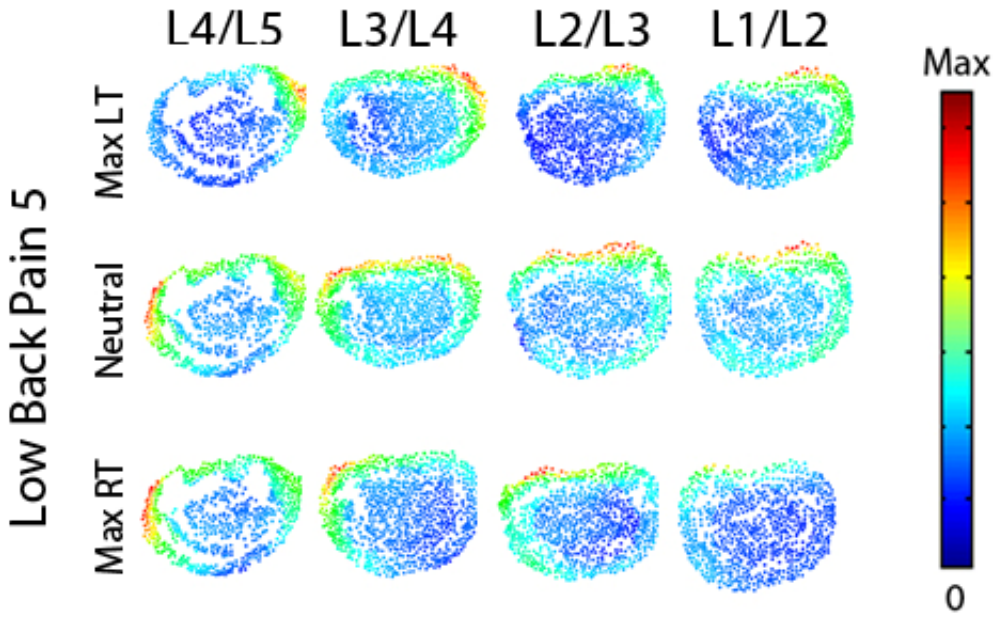

Figure 216. Magnitude stress at each atlas vertex for all levels at each major frame for Low Back Pain 5.

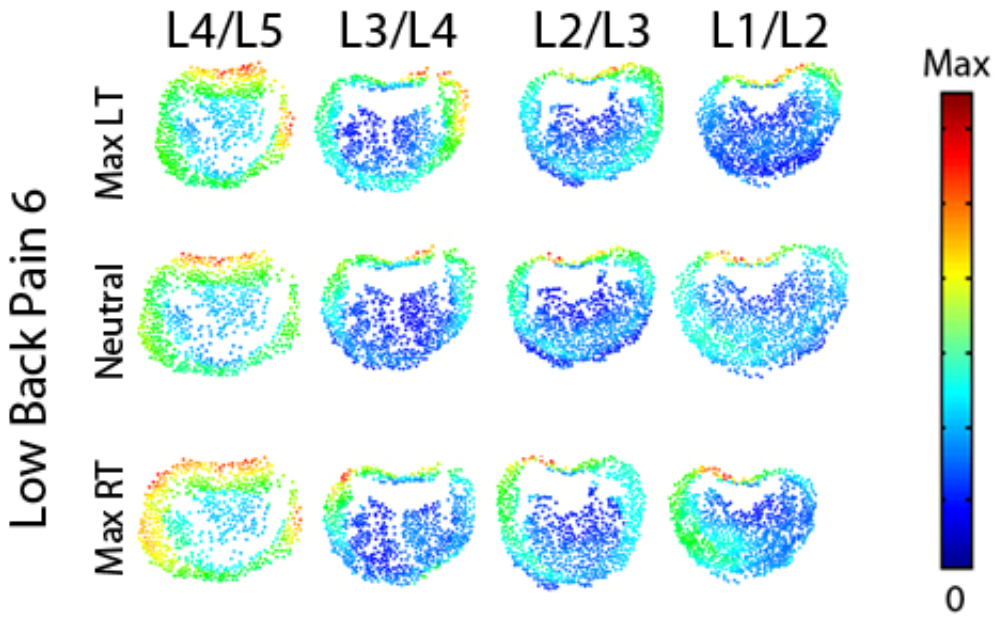

Figure 217. Magnitude stress at each atlas vertex for all levels at each major frame for Low Back Pain 6.

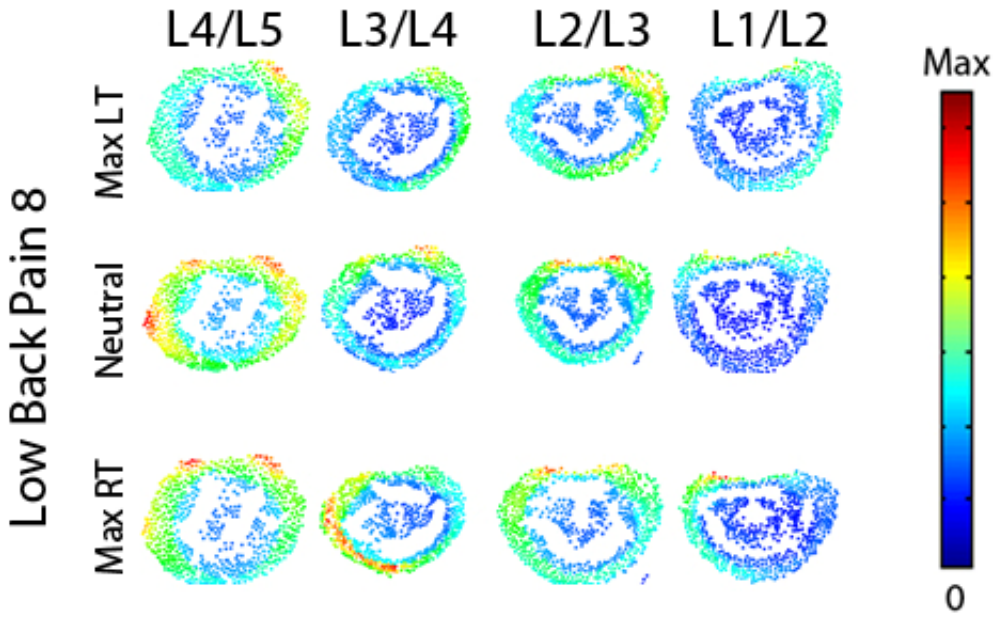

Figure 218. Magnitude stress at each atlas vertex for all levels at each major frame for Low Back Pain 8.

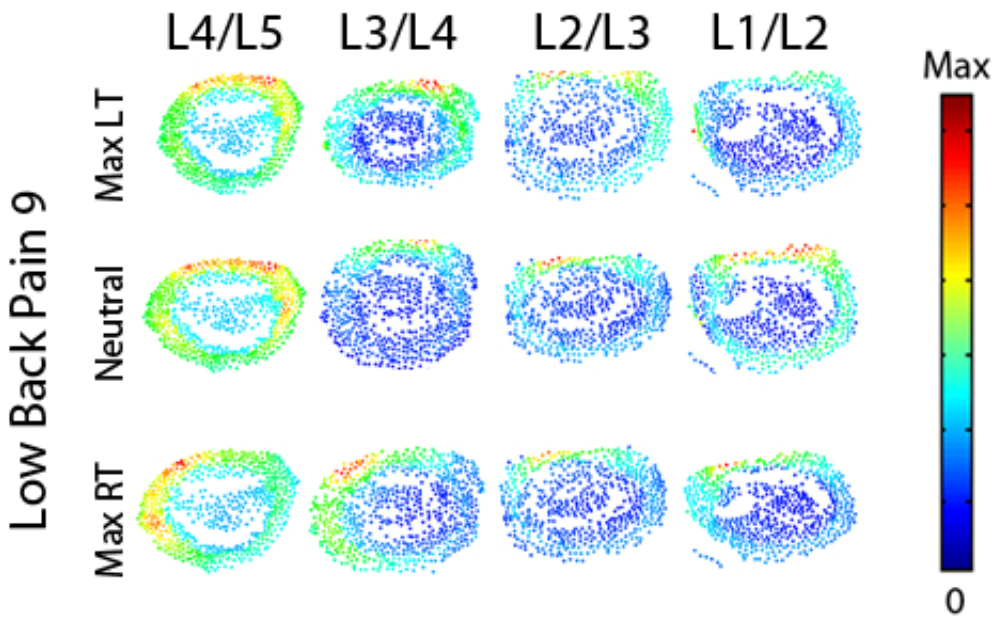

Figure 219. Magnitude stress at each atlas vertex for all levels at each major frame for Low Back Pain 9.

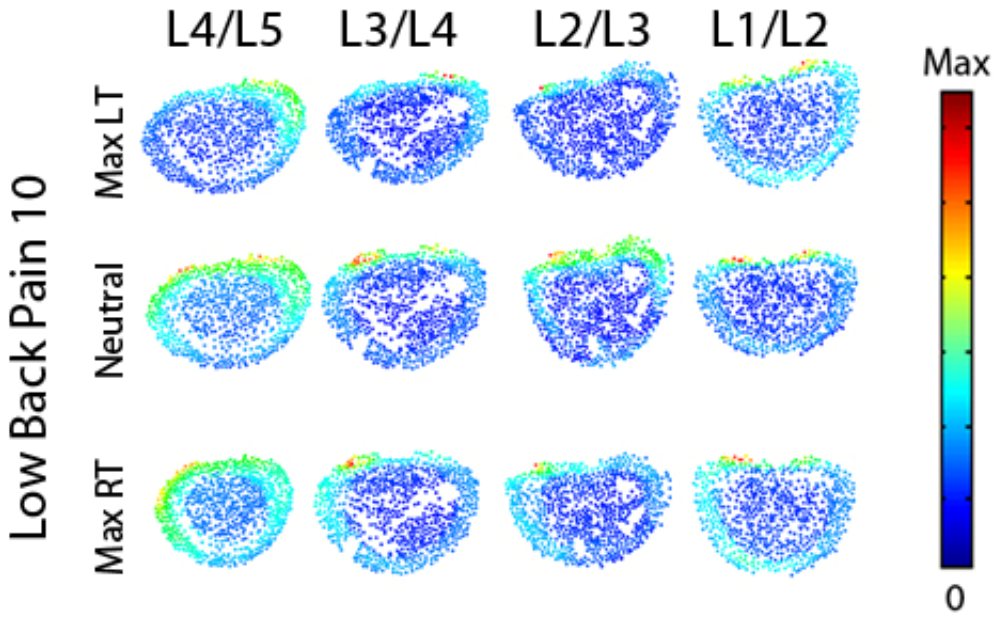

Figure 220. Magnitude stress at each atlas vertex for all levels at each major frame for Low Back Pain 10.

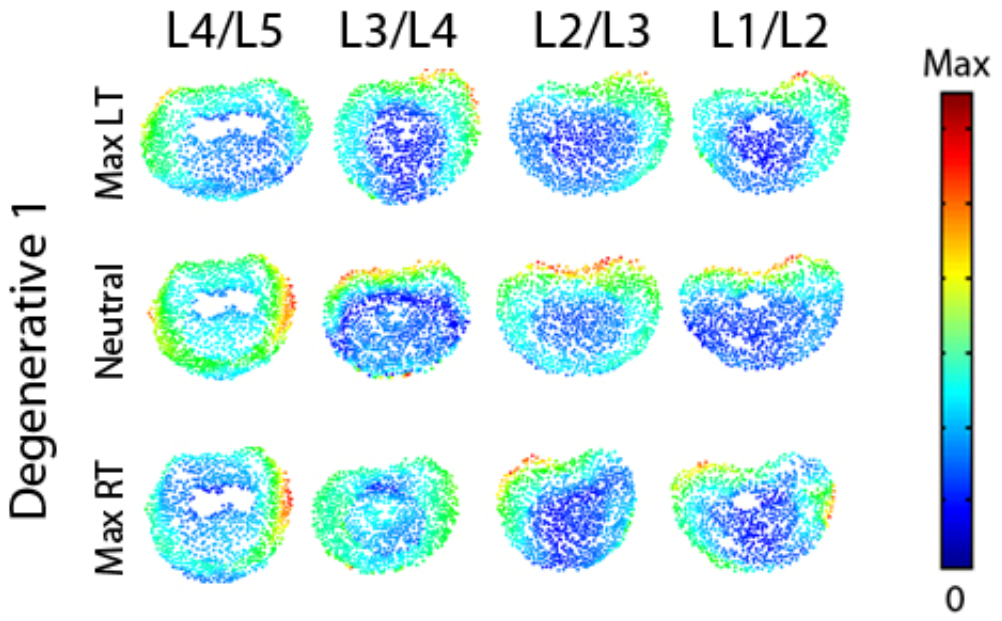

Figure 221. Magnitude stress at each atlas vertex for all levels at each major frame for Degenerative 1.

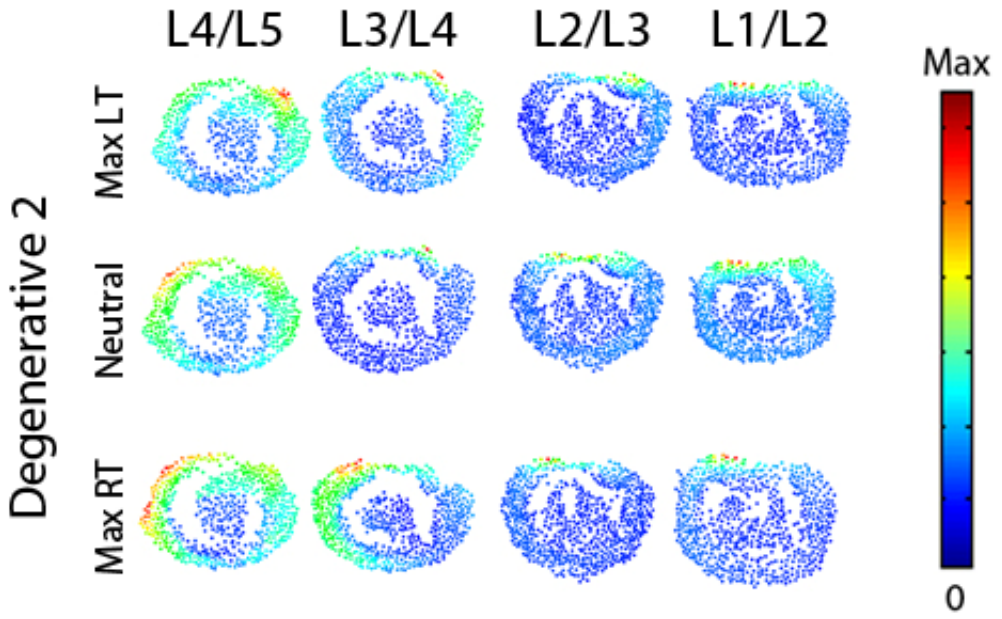

Figure 222. Magnitude stress at each atlas vertex for all levels at each major frame for Degenerative 2.

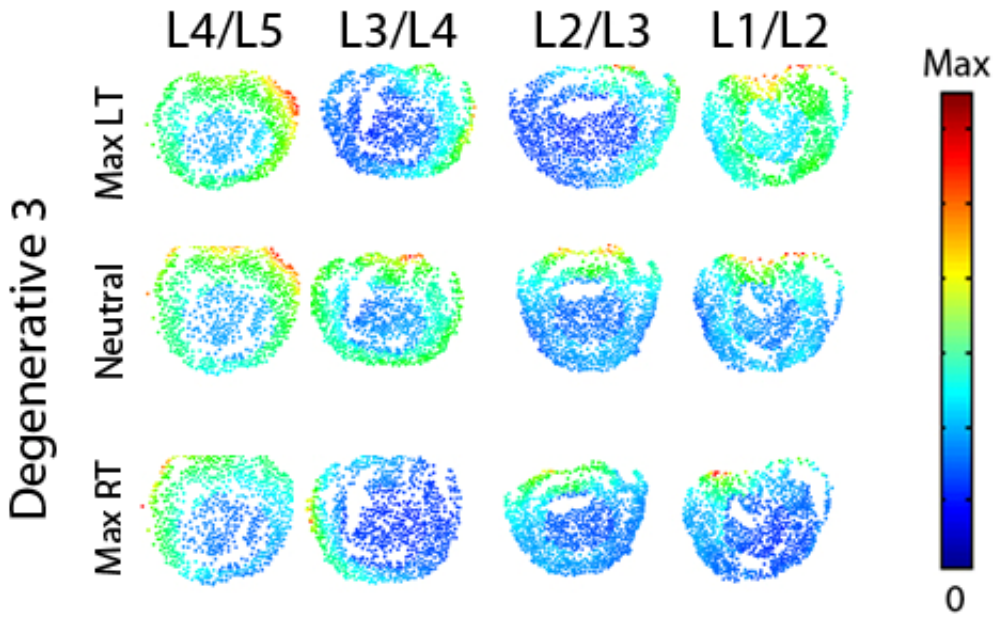

Figure 223. Magnitude stress at each atlas vertex for all levels at each major frame for Degenerative 3.

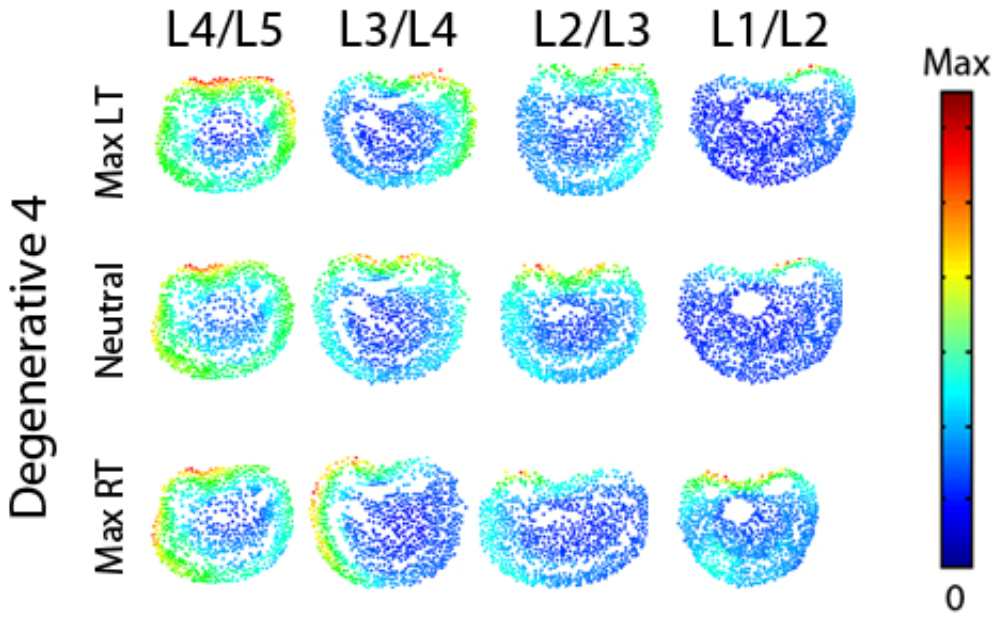

Figure 224. Magnitude stress at each atlas vertex for all levels at each major frame for Degenerative 4.

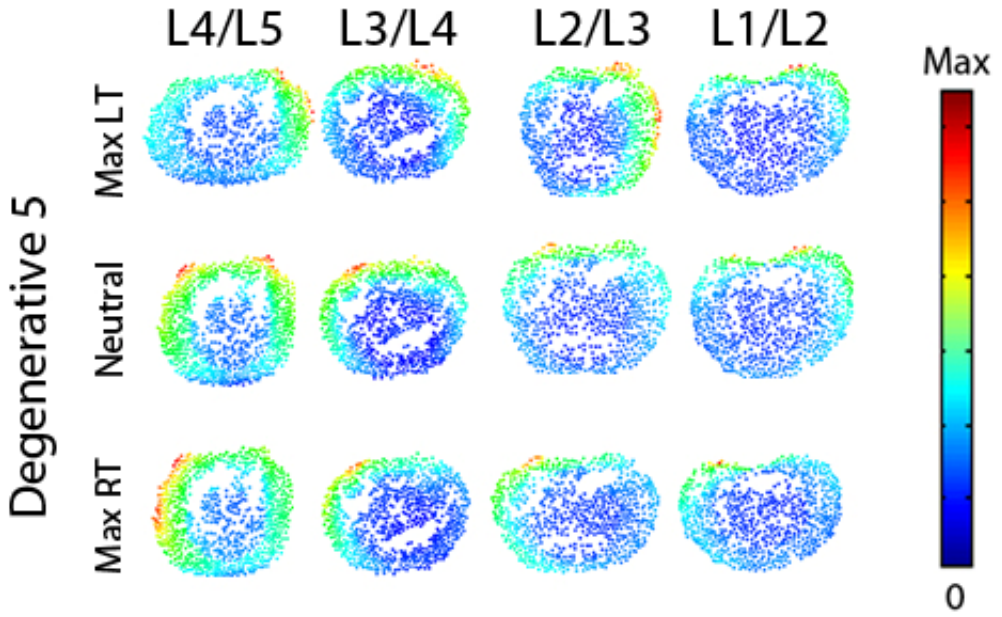

Figure 225. Magnitude stress at each atlas vertex for all levels at each major frame for Degenerative 5.

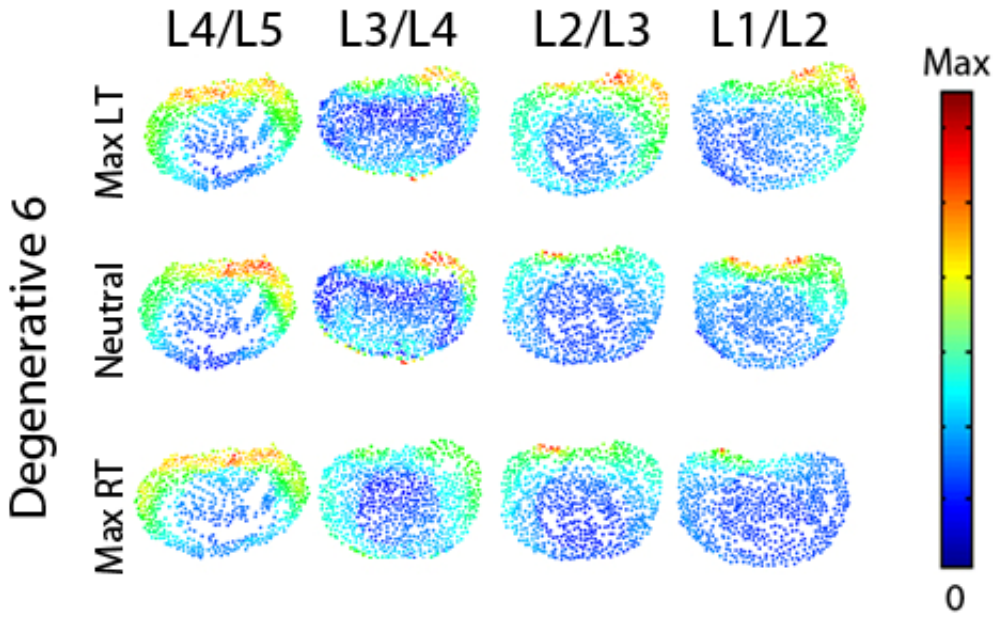

Figure 226. Magnitude stress at each atlas vertex for all levels at each major frame for Degenerative 6.

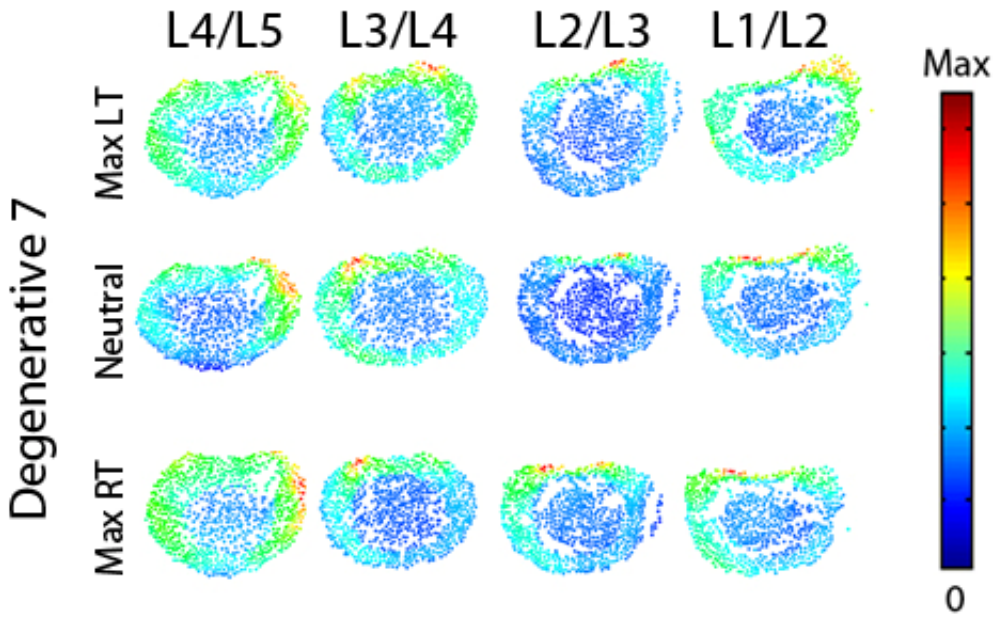

Figure 227. Magnitude stress at each atlas vertex for all levels at each major frame for Degenerative 7.

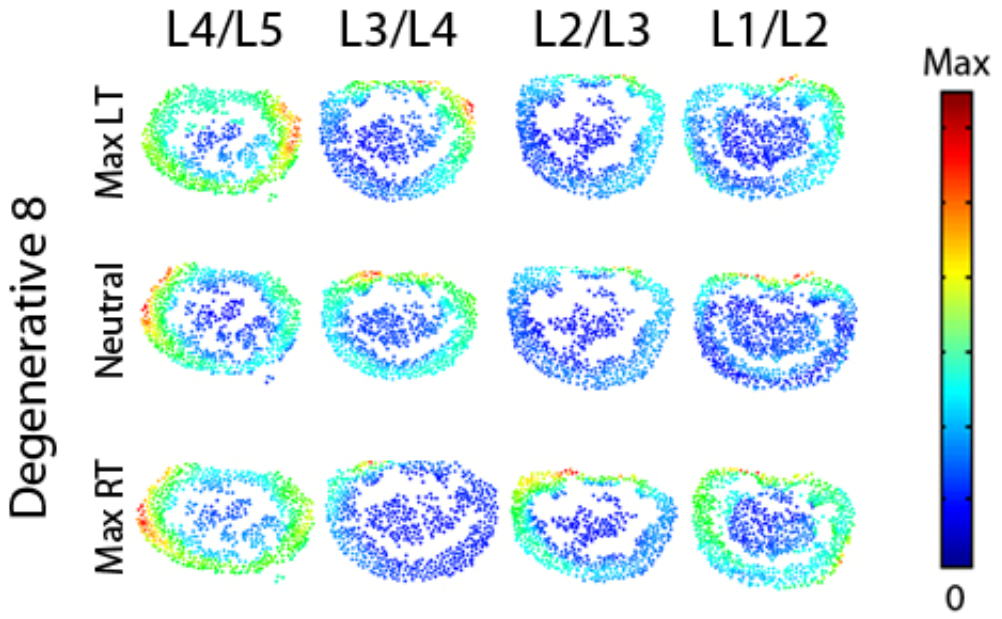

Figure 228. Magnitude stress at each atlas vertex for all levels at each major frame for Degenerative 8.

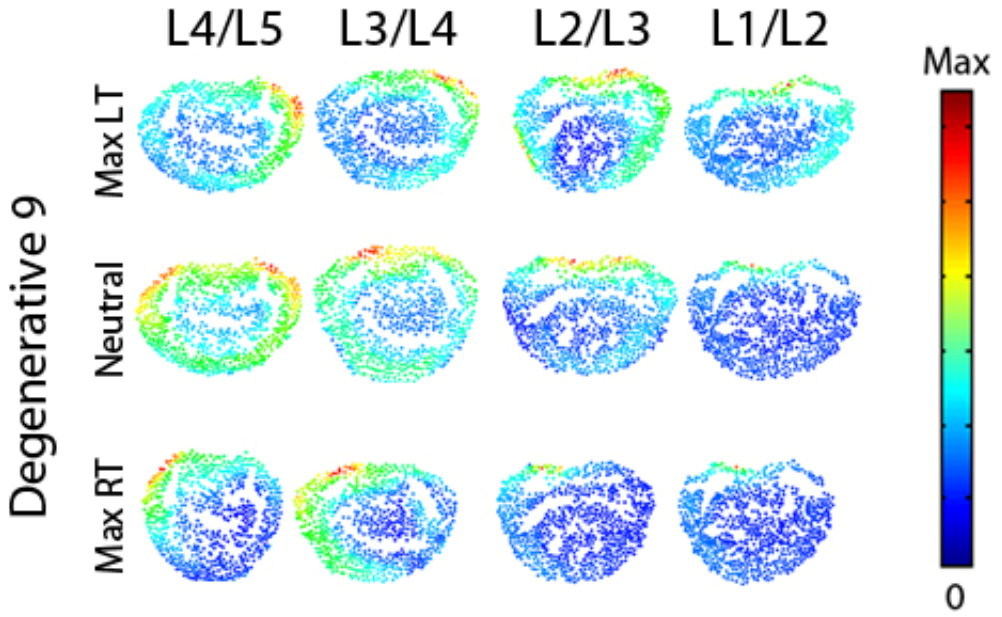

Figure 229. Magnitude stress at each atlas vertex for all levels at each major frame for Degenerative 9.

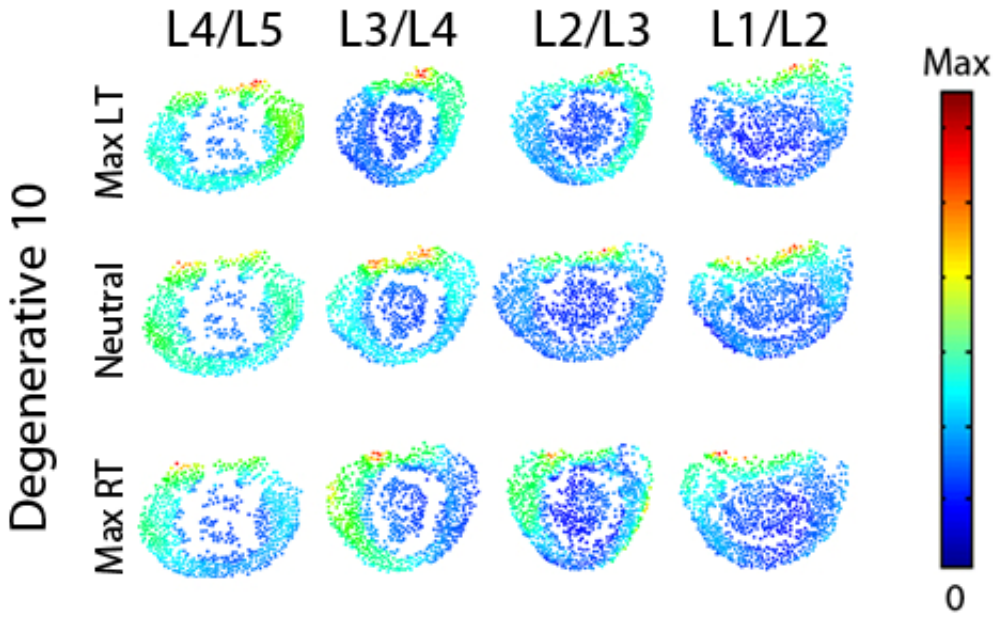

Figure 230. Magnitude stress at each atlas vertex for all levels at each major frame for Degenerative 10.

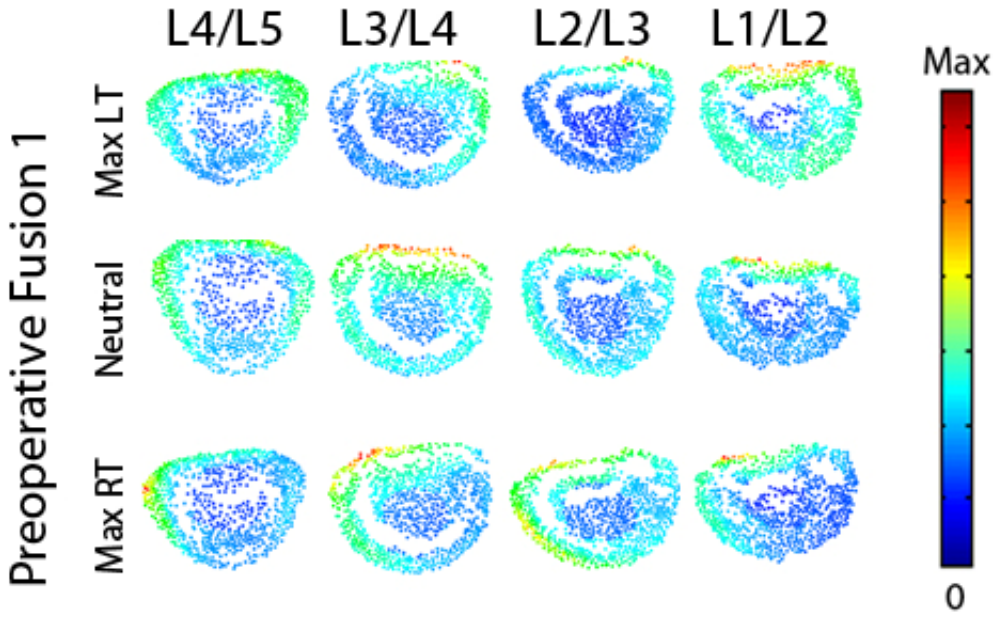

Figure 231. Magnitude stress at each atlas vertex for all levels at each major frame for Preoperative Fusion 1.

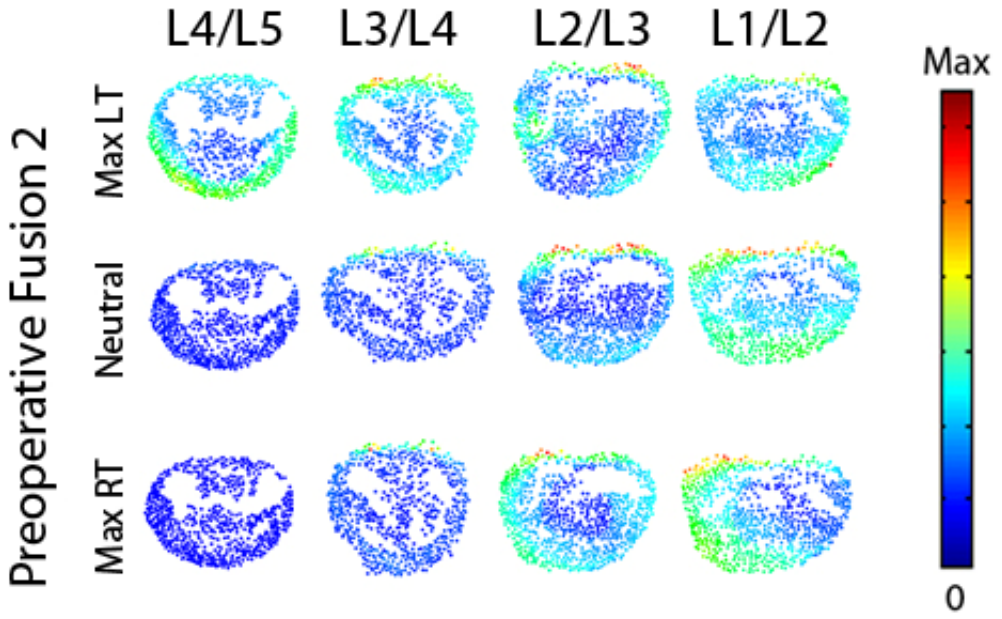

Figure 232. Magnitude stress at each atlas vertex for all levels at each major frame for Preoperative Fusion 2.

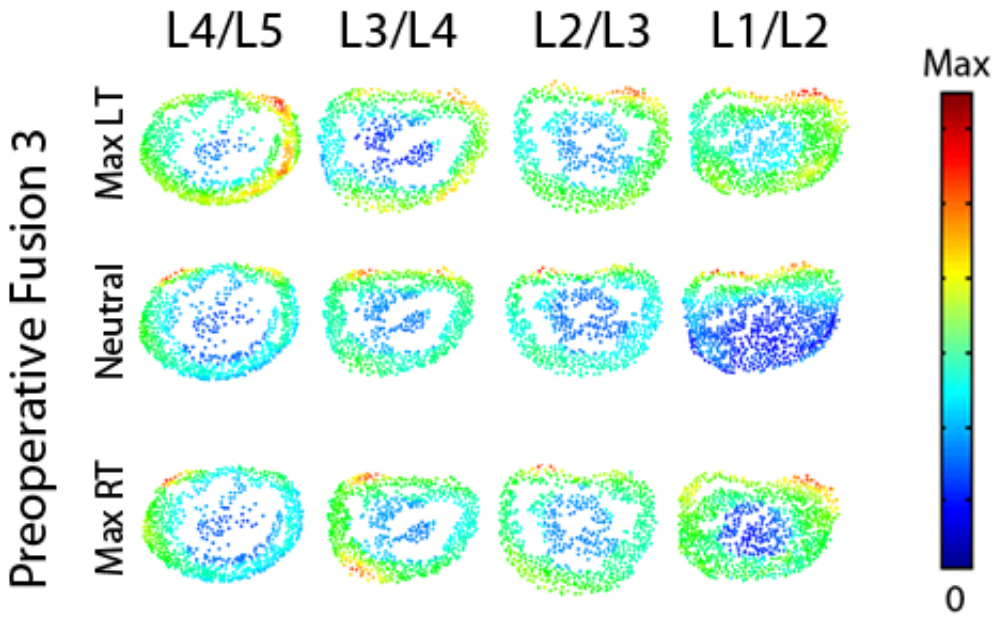

Figure 233. Magnitude stress at each atlas vertex for all levels at each major frame for Preoperative Fusion 3.

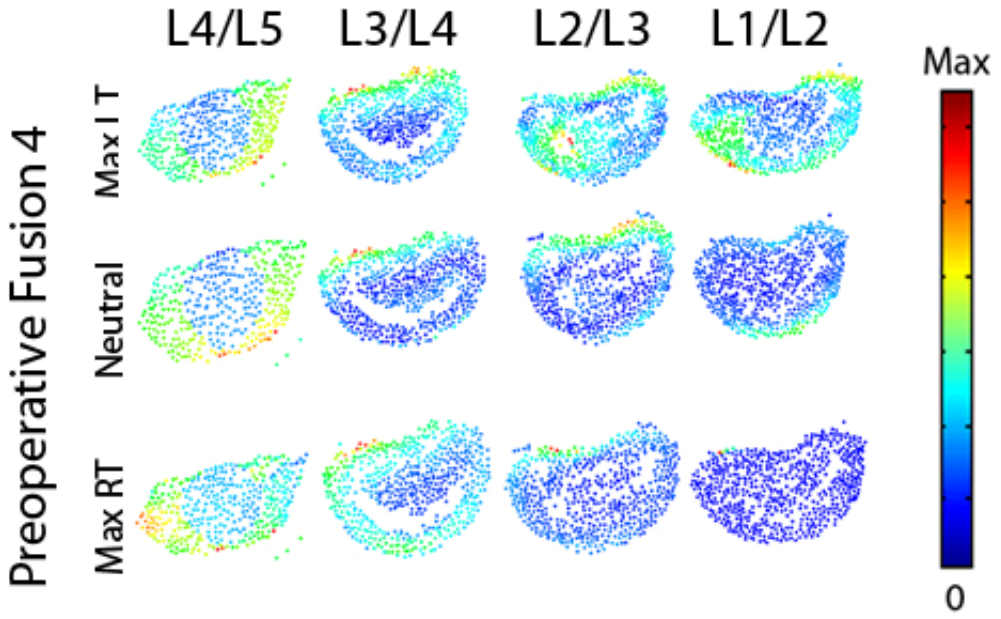

Figure 234. Magnitude stress at each atlas vertex for all levels at each major frame for Preoperative Fusion 4.

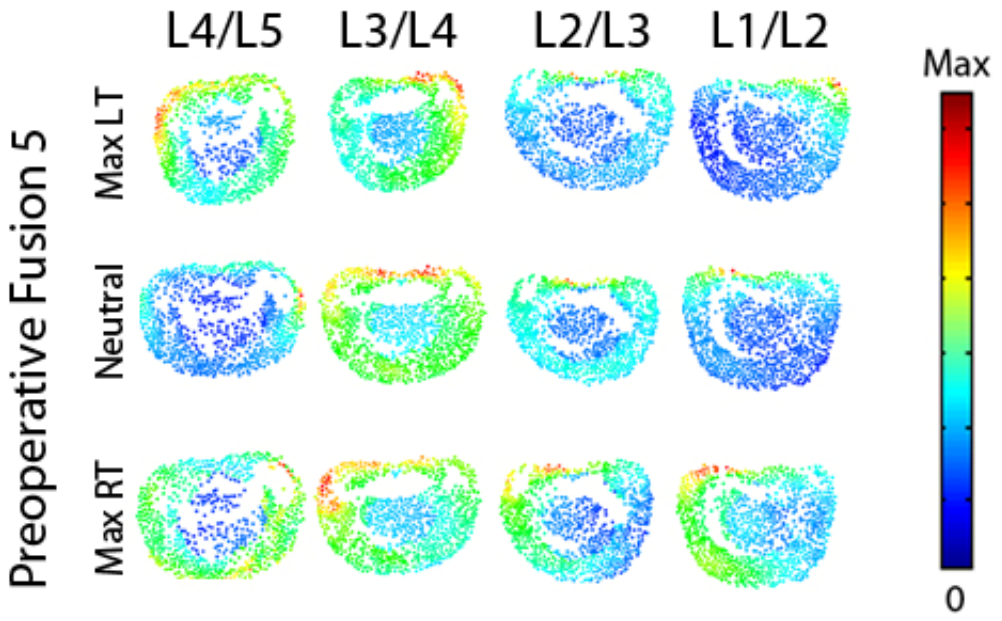

Figure 235. Magnitude stress at each atlas vertex for all levels at each major frame for Preoperative Fusion 5.

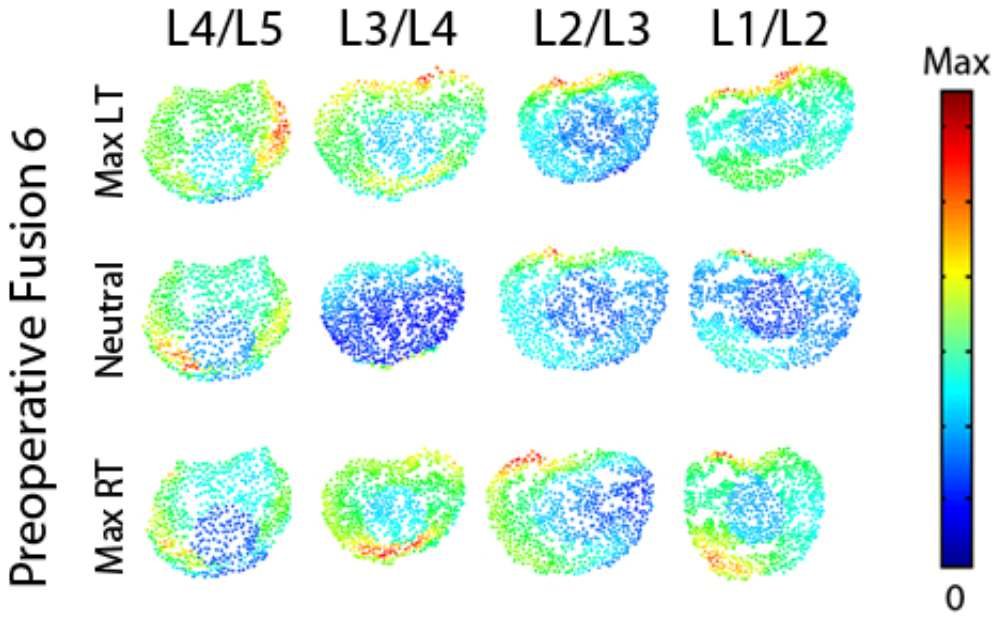

Figure 236. Magnitude stress at each atlas vertex for all levels at each major frame for Preoperative Fusion 6.

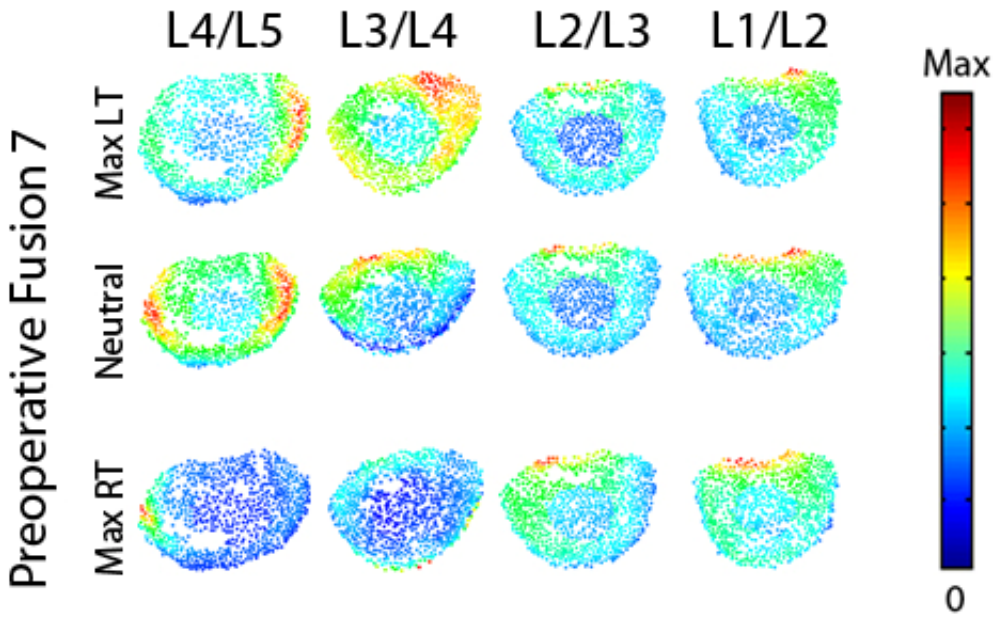

Figure 237. Magnitude stress at each atlas vertex for all levels at each major frame for Preoperative Fusion 7.

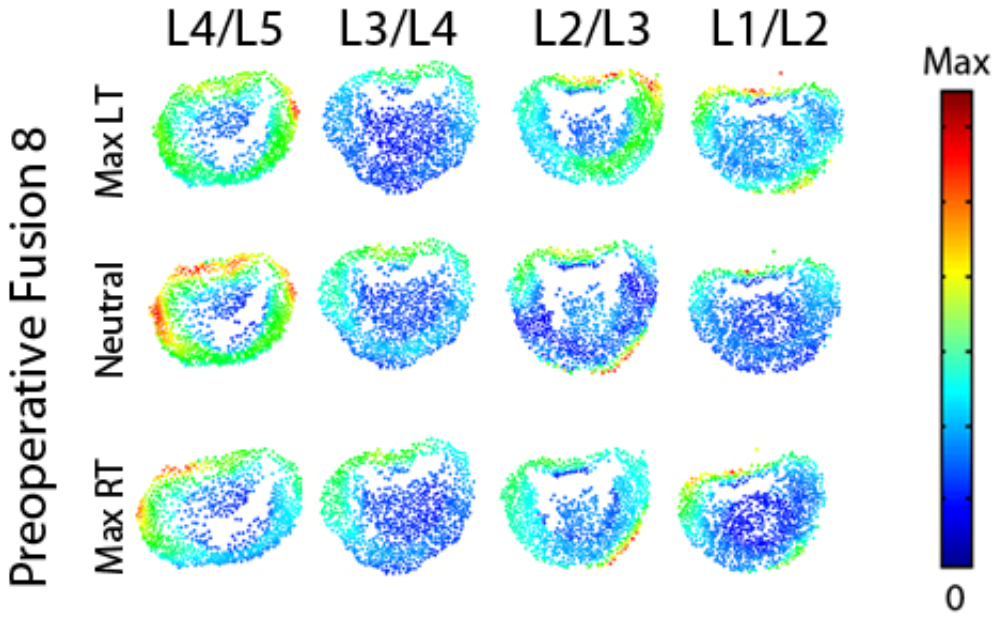

Figure 238. Magnitude stress at each atlas vertex for all levels at each major frame for Preoperative Fusion 8.

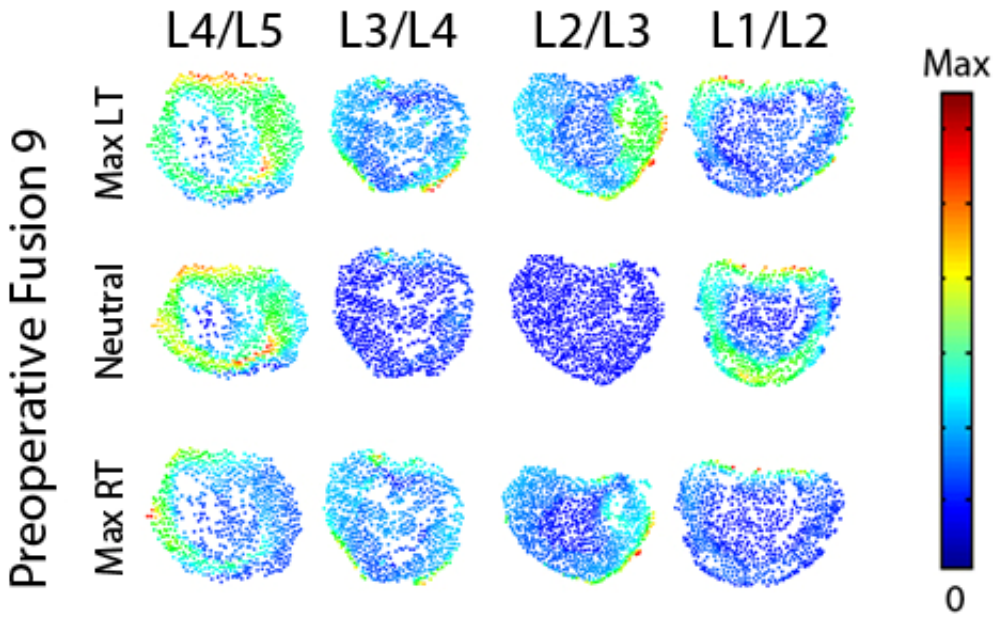

Figure 239. Magnitude stress at each atlas vertex for all levels at each major frame for Preoperative Fusion 9.

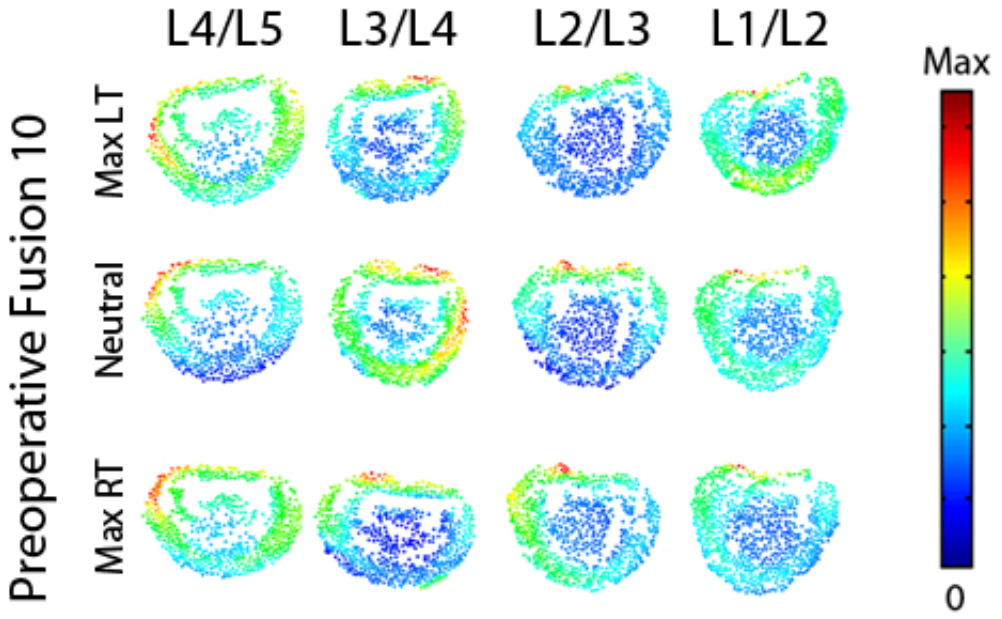

Figure 240. Magnitude stress at each atlas vertex for all levels at each major frame for Preoperative Fusion 10.

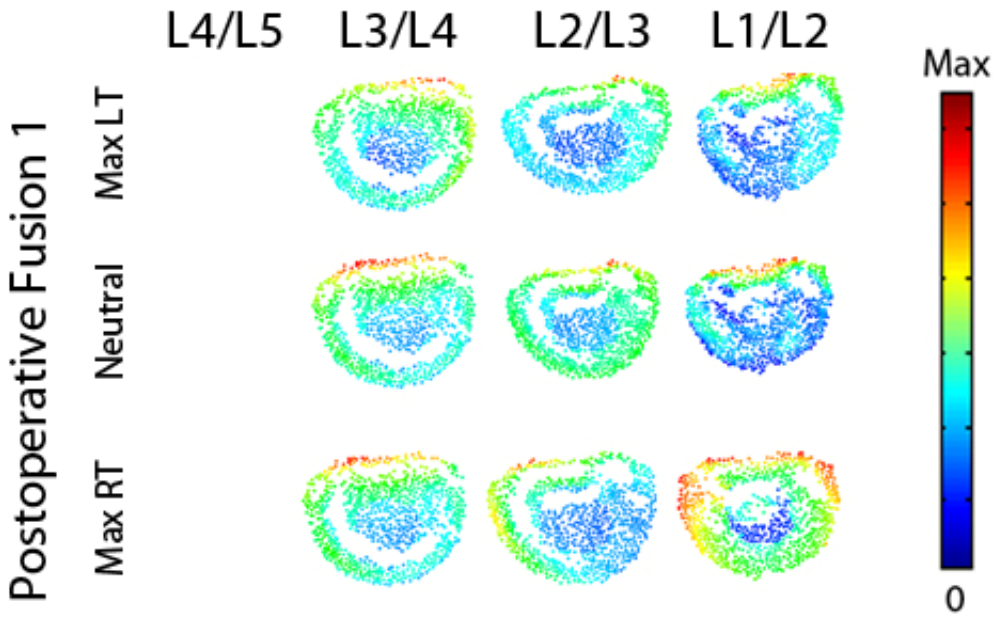

Figure 241. Magnitude stress at each atlas vertex for all levels at each major frame for Postoperative Fusion 1.

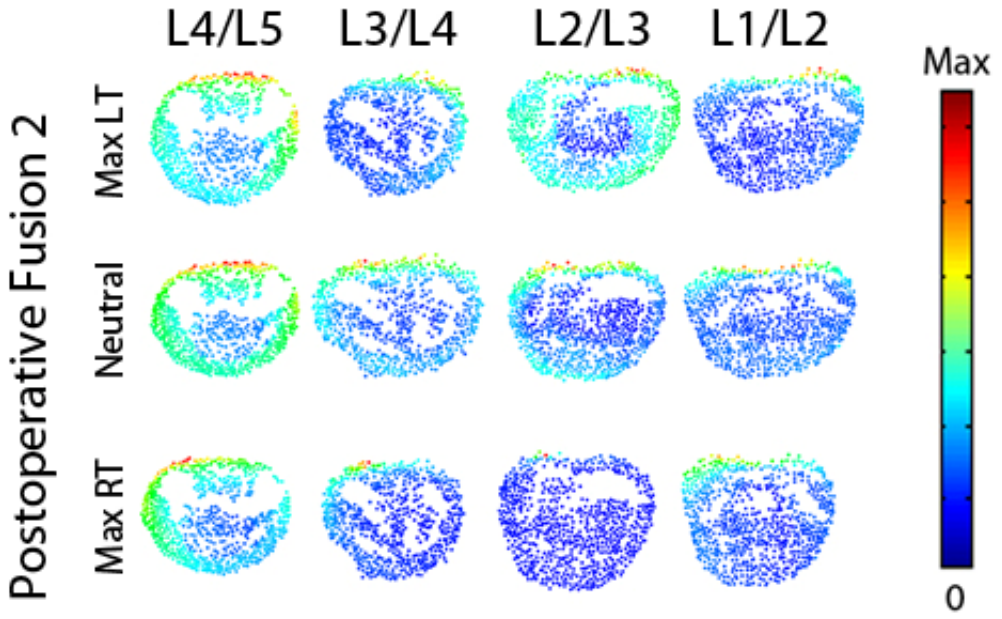

Figure 242. Magnitude stress at each atlas vertex for all levels at each major frame for Postoperative Fusion 2.

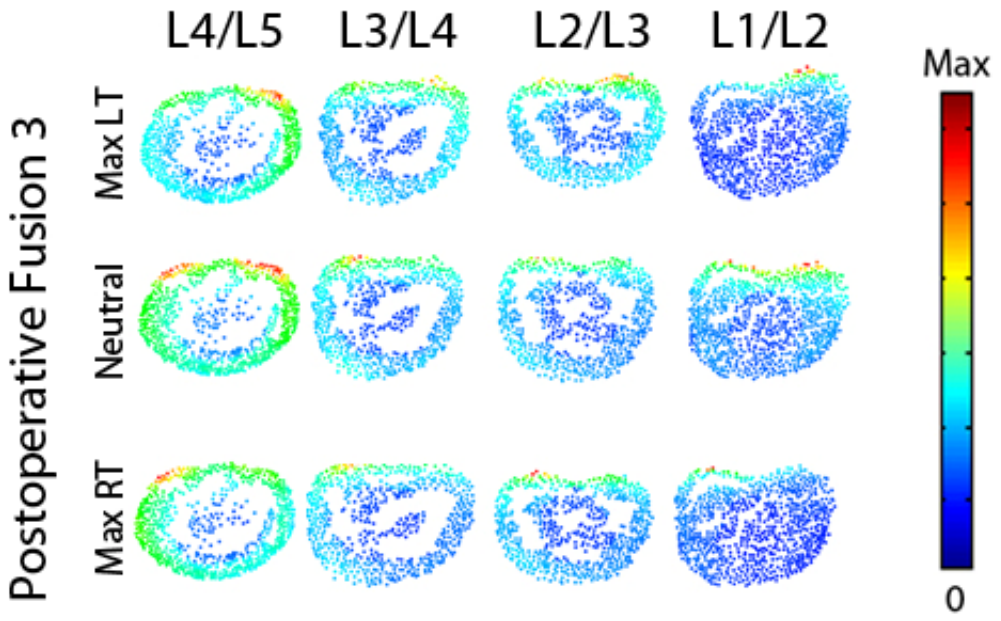

Figure 243. Magnitude stress at each atlas vertex for all levels at each major frame for Postoperative Fusion 3.

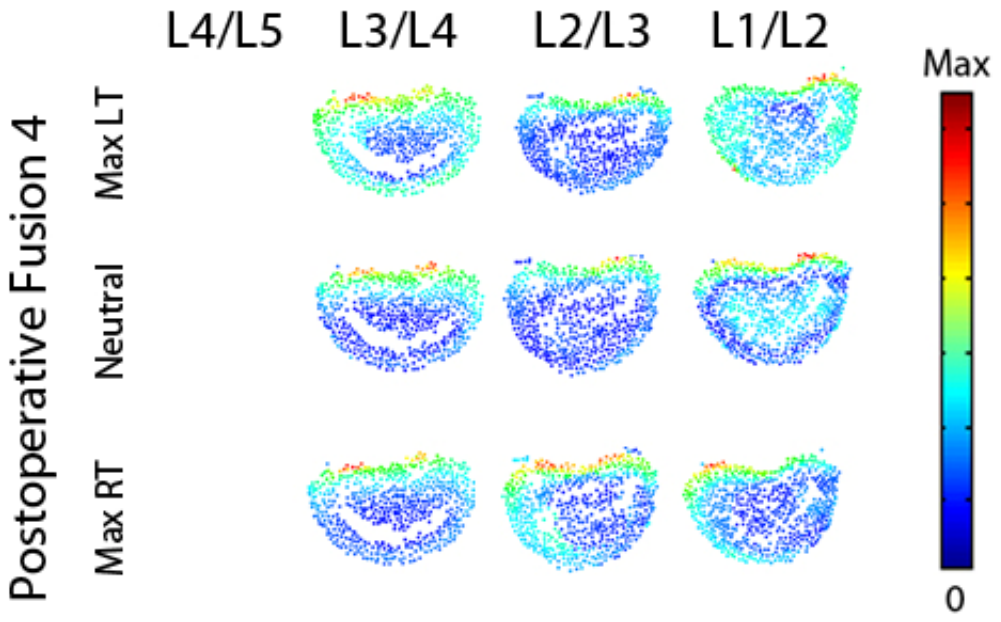

Figure 244. Magnitude stress at each atlas vertex for all levels at each major frame for Postoperative Fusion 4.

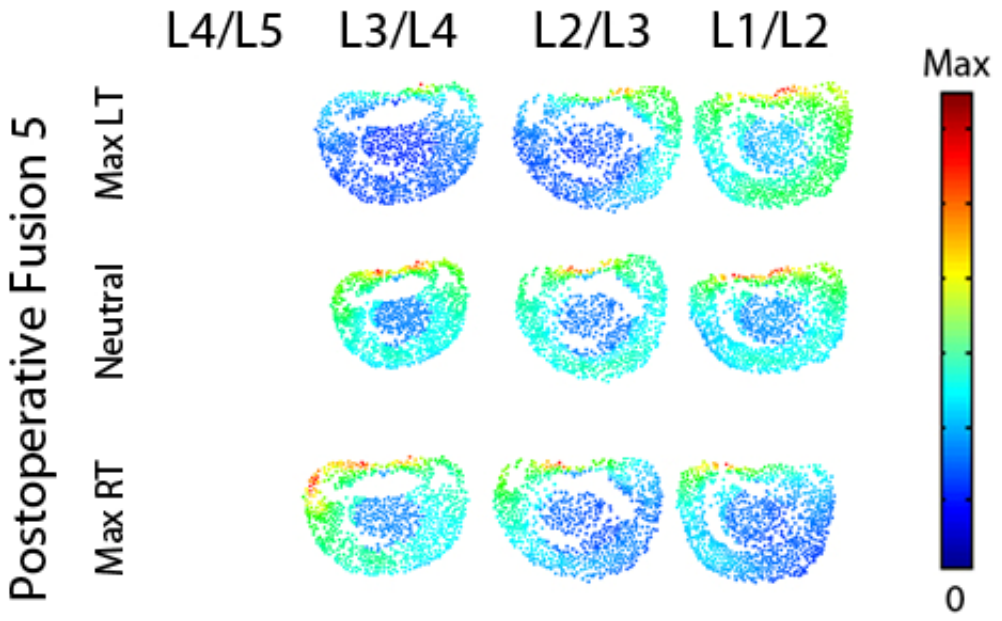

Figure 245. Magnitude stress at each atlas vertex for all levels at each major frame for Postoperative Fusion 5.

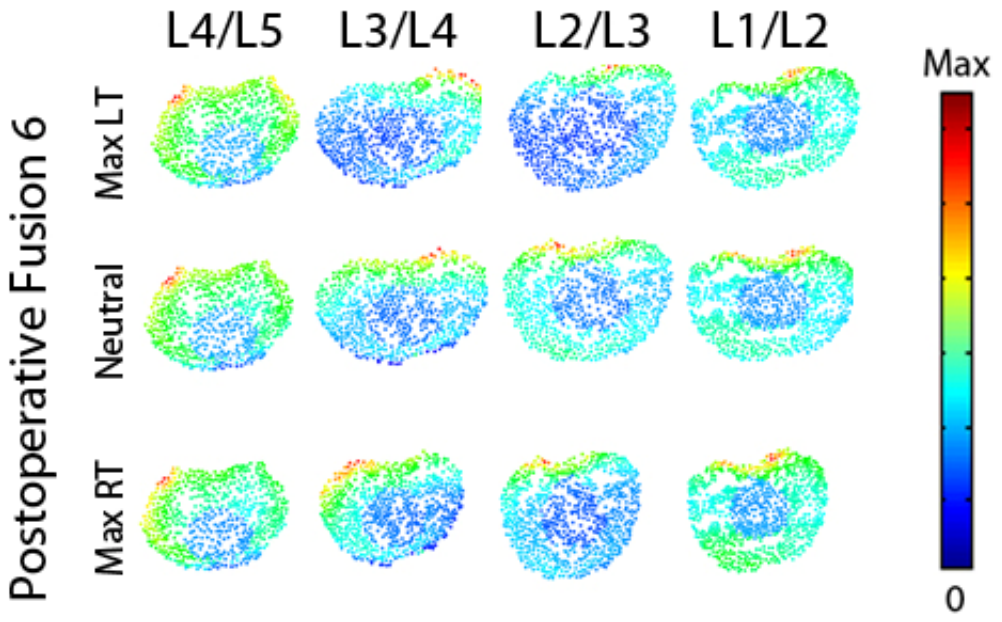

Figure 246. Magnitude stress at each atlas vertex for all levels at each major frame for Postoperative Fusion 6.

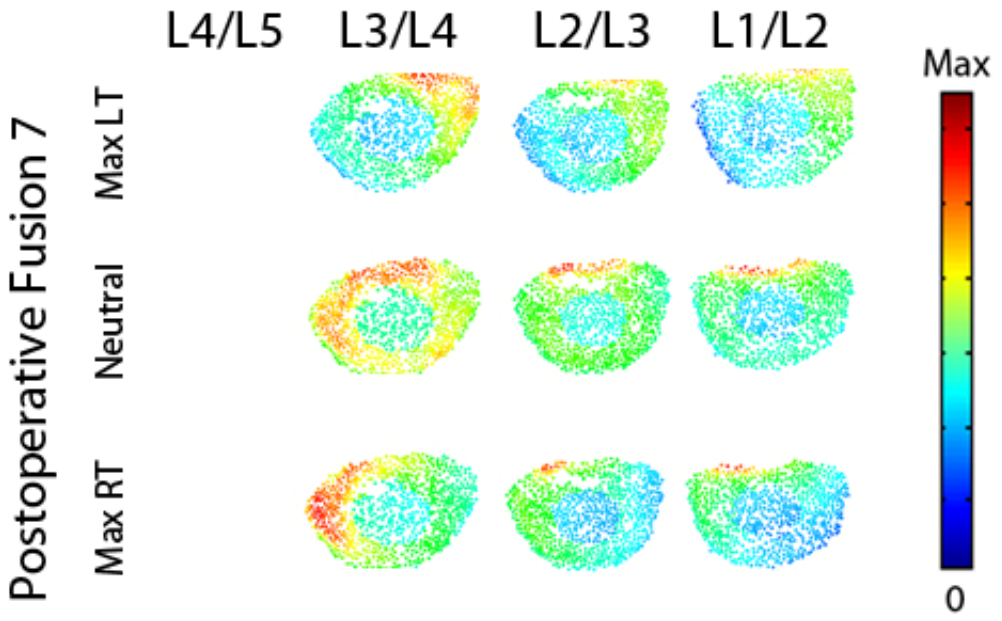

Figure 247. Magnitude stress at each atlas vertex for all levels at each major frame for Postoperative Fusion 7.

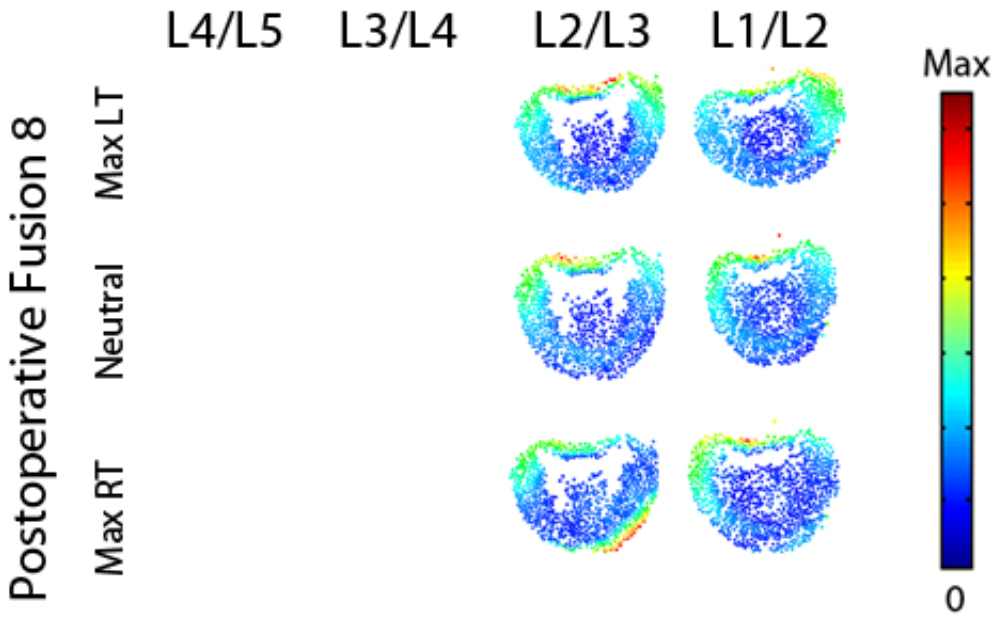

Figure 248. Magnitude stress at each atlas vertex for all levels at each major frame for Postoperative Fusion 8.

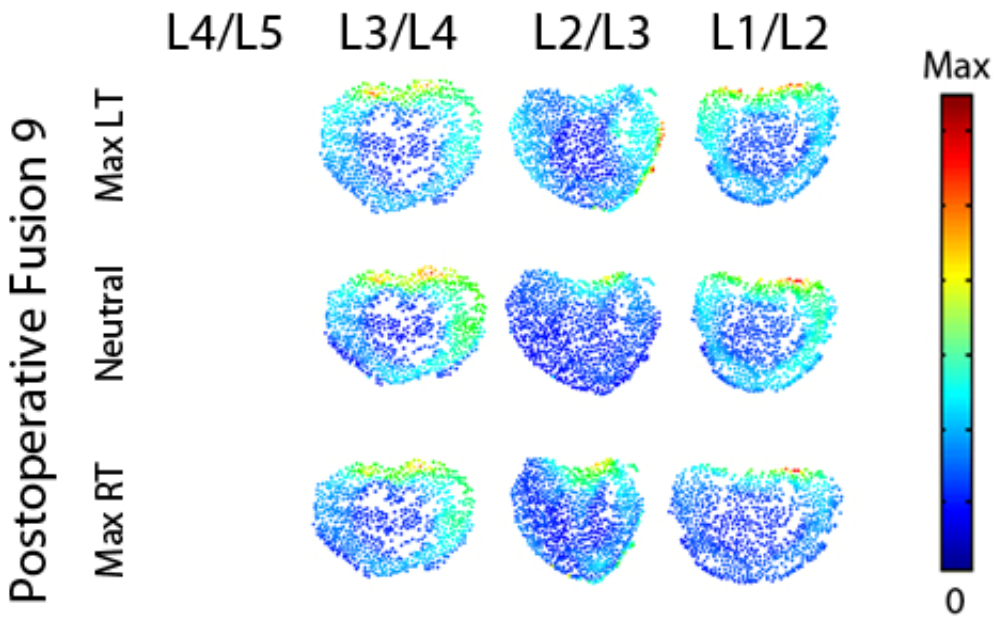

Figure 249. Magnitude stress at each atlas vertex for all levels at each major frame for Postoperative Fusion 9.

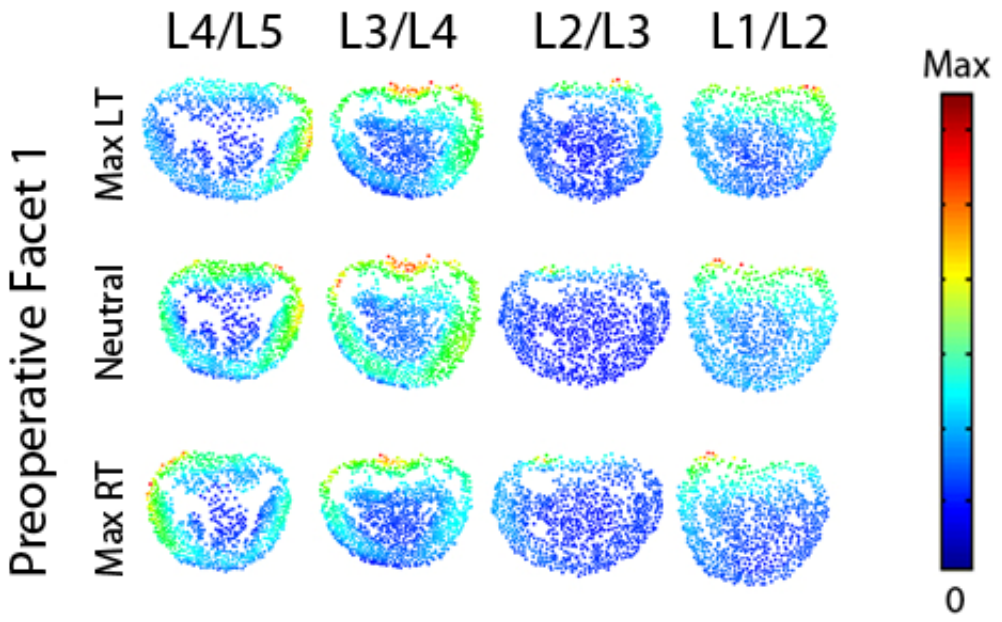

Figure 250. Magnitude stress at each atlas vertex for all levels at each major frame for Preoperative Facet 1.

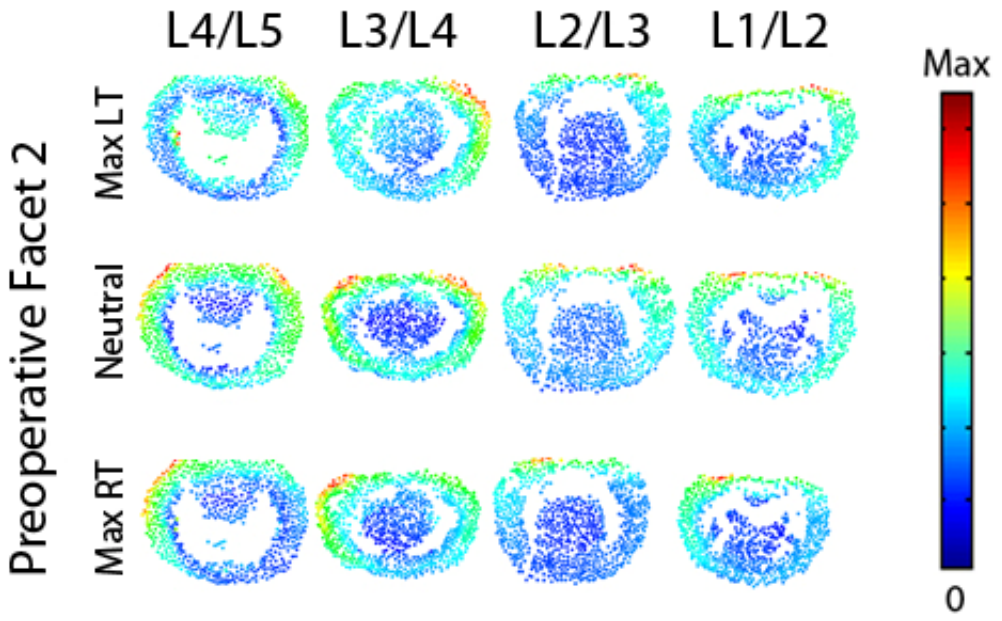

Figure 251. Magnitude stress at each atlas vertex for all levels at each major frame for Preoperative Facet 2.

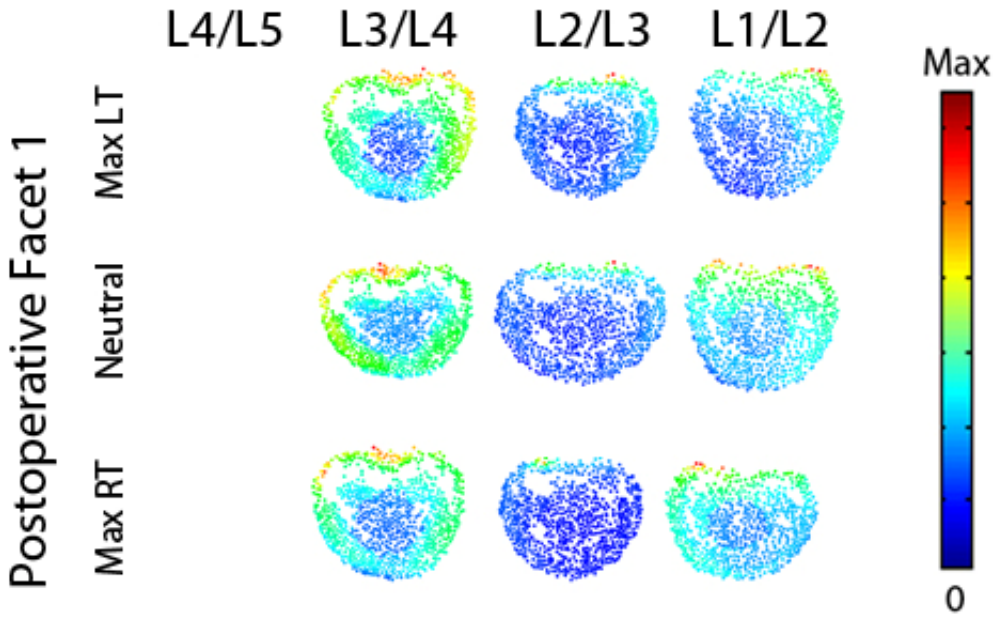

Figure 252. Magnitude stress at each atlas vertex for all levels at each major frame for Postoperative Facet 1.

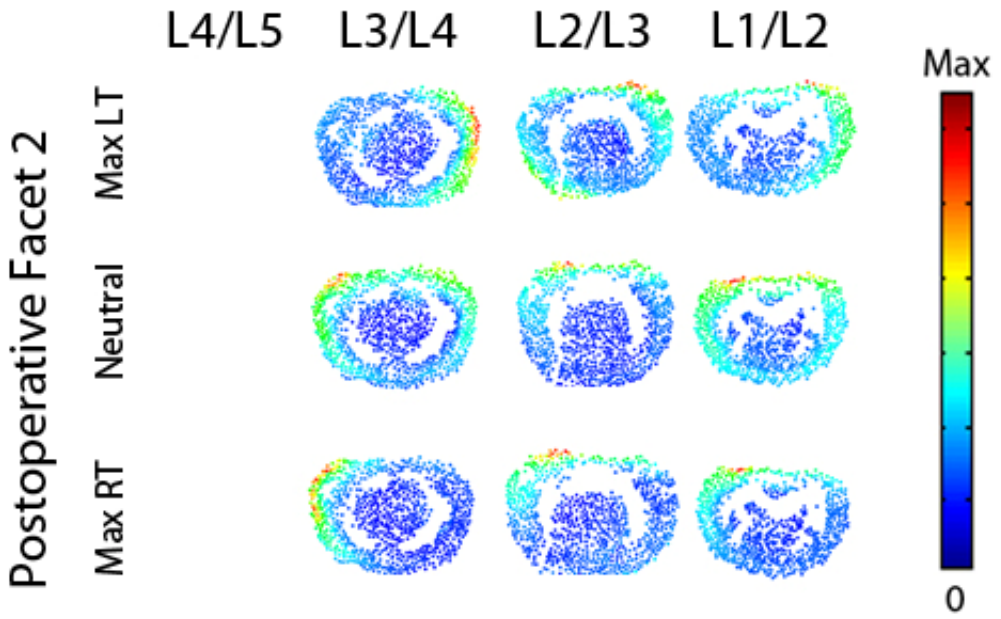

Figure 253. Magnitude stress at each atlas vertex for all levels at each major frame for Postoperative Facet 2.

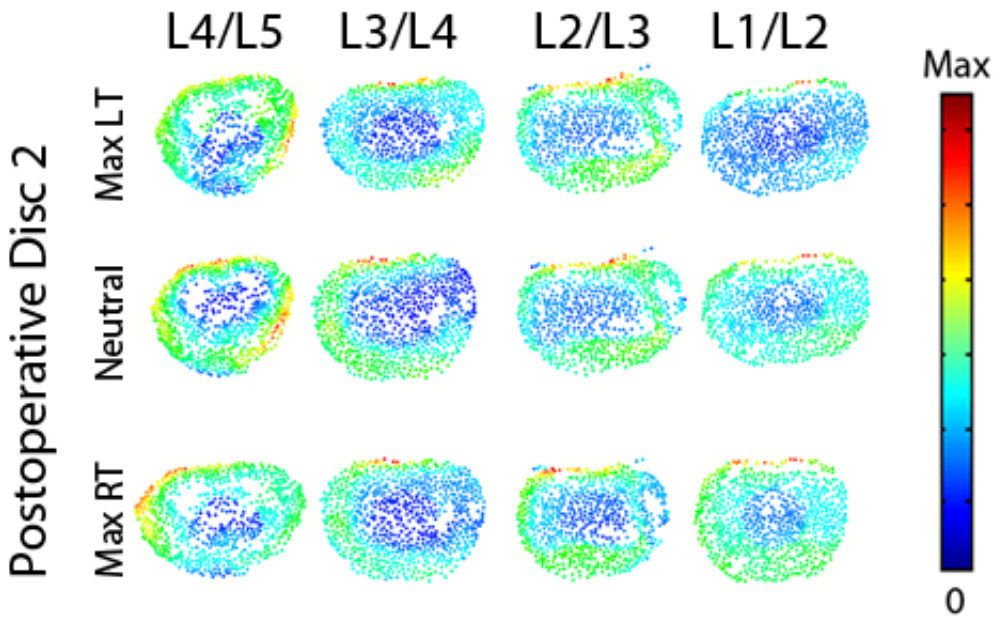

Figure 254. Magnitude stress at each atlas vertex for all levels at each major frame for Postoperative Disc 2.

VITA

Joseph Warren Mitchell was born in New Jersey, to the parents of Renee and Raymond Mitchell. He has one older sister, Aimee. He attended West Morris Mendham High School in Mendham, NJ. After graduating in 2001, he headed south to Virginia Polytechnic Institute and State University to study Mechanical Engineering. During his senior year he was introduced to Biomechanics and Human Anatomy. After graduating in 2005 from Virginia Tech he continued his journey south to continue his education at The University of Tennessee in the Biomedical Engineering joining up with the Center for Musculoskeletal Research in 2007. During this time he has had the opportunity to use his Mechanical Engineering degree and interest in the human body to form a career in orthopedic research. After graduation he is moving back to the Northeast to start his career and move forward.